STRATIGRAPHIC VARIATION OF SEDIMENTARY FACIES AND ARCHITECTUAL ELEMENTS WITHIN CHANNEL COMPLEXES OF THE MOUNT MESSENGER FORMATION, TARANAKI, NEW ZEALAND

by

Nathan Andrew Corbin

A thesis submitted in partial fulfillment
of the requirements for the degree

of

Master of Science

in

Earth Sciences

MONTANA STATE UNIVERSITY
Bozeman, Montana

April 2015

©COPYRIGHT

by

Nathan Andrew Corbin

2015

All Rights Reserved

ACKNOWLEDGEMENTS

First and foremost, I would like to thank my co-advisor, Dr. Michael H. Gardner for giving me the opportunity and framework to study deep-water outcrops around the world. His passion for sedimentology and stratigraphy greatly influenced my understanding of the science and always kept me pushing for more. I also want to thank my committee, Dr. James G. Schmitt, Dr. David W. Bowen, and Dr. David R. Lageson. Their encouragement and guidance during the last year have helped me reach my goals and continue onto the next path in my career.

I am grateful for all of my family and friends who have stood by my side and supported me throughout my education. Without your words of encouragement and insight, the last three years would have been much more difficult. To my parents, thank you for your constant support and for teaching me the value of hard work and perseverance. I want to thank Nick Atwood, Rosalba Queirolo, Ryan Hillier, Tyler Appleyard, Casey Reid, Jacob Thacker, Julian Stahl, Christine Maday, Melanie Baldwin, and the sedimentary research group. Thank you for inspiring me to stay focused and achieve my goals.

None of this work would have been possible without funding from the Slope and Basin Consortium. I want to thank BHP Billiton, BP, Statoil, and Petrobras for their financial support. I also want to thank landowners Steve and Kathy Mackenzie, and Russell and Parani Gibbs for their hospitality during my field work.

TABLE OF CONTENTS

1. INTRODUCTION 1

Purpose and Scope 1
Objectives and Research Questions 2
Study Area 4
Geologic Setting 4
Data and Methods 11
Field Data 11
Methods 11
Geologic Map 11
Sedimentological Measured Profiles 13
Facies and Event Bed Analysis 15
Architectural Element Analysis 15
Previous Work 16

2. SEDIMENTOLOGY 20

Subaqueous Flows 20
Turbidity Currents 20
Low-Density Turbidity Current 22
High-Density Turbidity Current 22
Density Flows 23
Concentrated Density Flow 23
Hyperconcentrated Density Flow 24
Cohesive Debris Flows 25
Flow Transformation 25
Hydrodynamic Facies of the Mount Messenger Formation 27
Mudstone-Clast Conglomerate Facies 27
Clast-Supported 27
Matrix-Supported 28
Thick- to Medium-Bedded Sandstone Facies 29
Horizontally Stratified or Spaced-Stratified 29
Cross-Stratified 30
Wavy-Laminated 30
Structureless 31
Secondary Structures 32
Structureless with Floating Mudstone-Clasts 32
Plane-Parallel Laminated 33
Medium- to Thin-Bedded Sandstone Facies 34
Asymmetric Ripple Cross-Laminated 34
Climbing Ripple Cross-Laminated 34

TABLE OF CONTENTS – CONTINUED

Medium- to Thin-Bedded Muddy Sandstone Facies 35
Muddy Sandstone....35
Mudstone-Clasts at Bed Tops 36
Silty Sandstone....37
Poorly-Sorted Mudstone-Rich Facies 37
Poorly-Sorted Mudstone 37
Mudstone-Clasts Dispersed 38
Siltstone Facies 39
Concentrated Bands of Organic Carbon 39
Plane-Parallel Laminated....39
Ripple-Laminated to Wavy-Laminated 40
Normal Graded....40
Mudstone Facies 41
Silty Mudstone....41
Clay Dominated 41
Claystone....42
Calcareous Facies....42
Calcareous-Rich....42
Post-Depositional Facies....43
Deformed; Mass-Transport Deposit 43
Concretions, Cementation....43
Bioturbated and Burrowed Sandstone 44
Bioturbated and Burrowed Siltstone....45
Tuffaceous Facies 45
Volcaniclastic Sandstone 45
Volcaniclastic Mudstone....46
Thin Section Analysis....47

3. ARCHITECTURAL ELEMENT ANALYSIS....54

Definition and Terminology 54
Sedimentary Bodies 56
Mass-Transport Deposits 56
Channel Complexes 60
Channel Complex 1A....60
Channel Complex 1B....63
Channel Complex 2....66
Channel Complex 2A....73
Channel Complex 3....76
Channel Complex 4....80
Wedgeforms/Levees 83

TABLE OF CONTENTS – CONTINUED

Drapes 86
Laminated Thin Beds 86

4. STRATIGRAPHIC EVOLUTION DISCUSSION 88

Stratigraphic Variation within Channel Complexes 88
Channel Complex 1A 88
Sedimentary Facies 88
Paleoflow Analysis 92
Event Bed Thickness Analysis 92
Flow Transformations 95
Channel Complex 1B 96
Sedimentary Facies 96
Paleoflow Analysis 101
Event Bed Thickness Analysis 101
Flow Transformations 102
Channel Complex 2 106
Sedimentary Facies 106
Paleoflow Analysis 108
Event Bed Thickness Analysis 109
Flow Transformations 109
Channel Complex 3 111
Sedimentary Facies 111
Paleoflow Analysis 114
Event Bed Thickness Analysis 115
Flow Transformations 115
Channel Complex 4 118
Sedimentary Facies 118
Paleoflow Analysis 120
Event Bed Thickness Analysis 120
Flow Transformations 122
Channel Stacking Patterns 122
Paleogeography 124
Influence from Mass-Transport Deposits 124
Sediment Provenance Analysis 127
Southern: Long Distance Transport 127
Northern: Mohakatino Volcanic Arc 128
Eastern: Shelf/Slope 129

5. CONCLUSIONS 130

TABLE OF CONTENTS – CONTINUED

Sedimentology 130
Architectural Elements and Stratigraphic Evolution 131

REFERENCES CITED.....135

APPENDICES 143

APPENDIX A: Measured Sedimentological Profiles.....144
APPENDIX B: Thin Section Analysis 167

LIST OF TABLES

Table Page

1. List of Sedimentological Measured Sections.....14

2. Stratigraphic Comparison of Nomenclature to Previous Studies 19

3. Channel Dimensions and Aspect Ratios.....84

LIST OF FIGURES

Figure Page

1. Study area, regional geologic map, and paleogeographic framework 5
2. Regional photo-panel of the study area with stratigraphic correlations of the coastal and inland outcrops.....6
3. Chronostratigraphic Framework of the eastern Taranaki Basin and a generalized stratigraphic section of the Lower Mount Messenger Formation from this study.....9
4. Geologic map of the study area 12
5. Overview of subaqueous flow types 21
6. Hydrodynamic facies identified in the study area.....49
7. Overview of architectural element analysis 55
8. Summary photos of the North Waikiekie mass-transport deposit and correlations to inland outcrops.....58
9. Summary photos of the Waikiekie Stream mass-transport deposit and correlations to inland outcrops.....59
10. Architectural element analysis for CC1A 62
11. Architectural element analysis for CC1B 64
12. Architectural element analysis for CC2 within the inland outcrops 68
13. Architectural element analysis for CC2 north of Waikiekie Stream 69
14. Photo-panel correlations south of Waikiekie Stream.....70
15. Photo-panel correlations south of Waikiekie Stream (continued) 71
16. Photo-panel correlations of CC2A south of Waikiekie Stream 74
17. Photo-panel correlations of CC2A south of Waikiekie Stream (continued).....75

LIST OF FIGURES - CONTINUED

Figure Page

18. Architectural element analysis for CC3 and CC4 78

19. Architectural element analysis for CC4 82

20. Quantitative analysis of sedimentary facies proportions for the LMMF 89

21. Cross-section of CC1A from measured sedimentological profiles 90

22. Event bed analysis for CC1A 94

23. Cross-section of CC1B from measured sedimentological profiles 98

24. Event bed analysis for CC1B 103

25. Cross-section for CC2 from measured sedimentological profiles 107

26. Event bed analysis for CC2 110

27. Cross-section for CC3/ CC4 from measured sedimentological profiles 113

28. Event bed analysis for CC3 116

29. Event bed analysis for CC4 121

30. Paleo-channel trends 123

31. Stacked channel complex trends 125

32. Simplified cross-section of the channel belt 126

ABSTRACT

This study establishes an architectural framework of sedimentary facies, event beds, and sedimentary bodies for channelized deep-water sandstone and siltstone deposits within the Lower Mount Messenger Formation (LMMF). Well exposed outcrops of the Late Miocene Mount Messenger Formation are present along the Taranaki coast of the North Island, New Zealand. These exposures provide an opportunity to study submarine channel complexes deposited within an inner basin-floor fan to base of slope setting. Sedimentary facies and architectural elements are described from the axis to the margin and overbank of channel complexes to show spatial and temporal variation of subaqueous flow properties operating at the time of deposition. Facies were placed into an architectural framework to show organized changes in the diversity and abundance of bodies across the LMMF. Thirty hydrodynamic facies were described from outcrop exposures. Each facies represents varying hydrodynamic processes and sediment sources present during deposition. Sediments in the LMMF are interpreted to represent deposition by high- and low-density turbidity currents, concentrated and hyperconcentrated density flows, en masse movements, and debris flows. Six channel complexes described from coastal and inland outcrops record the variation of sedimentary facies spatially and temporally throughout their evolution. Analysis of architectural elements and sedimentary facies across the LMMF indicates flows were weakly confined within the basal interval, and progressively became more confined up-dip. This is reflected by multilateral channels near the base, and multistory channels up-section. Minor flow transformations within subaqueous flows are inferred. The sediments within the LMMF reflect an overall temporal decrease in flow strength, flow frequency, and event bed thickness, and a temporal increase in flow variability up-section from the base. Channels were deposited within a 3.5 km wide channel belt with the uppermost channels confined to a 1.7 km wide master erosional channel south of the lowermost channels. Paleoflow was directed to the northwest with little variation between each successive channel complex.

INTRODUCTION

Purpose and Scope

This study focuses on Late Miocene deep-water channelized sandstone and mudstone deposits of the Mount Messenger Formation (MMF). Situated along the Taranaki coast on the North Island of New Zealand, the MMF is characterized by fining-upward successions of sandstone and siltstone. Divided into upper and lower stratigraphic intervals, the MMF reflects a progradational and aggradational submarine channel-lobe depositional system (King et al., 1993, King et al., 2011, Masalimova, 2013). The Lower Mount Messenger Formation (LMMF) is characterized by fining-upward sandstone and siltstone deposits with sheetlike geometries representing lobe complexes, and increasing amounts of channelization are present up-section. The Upper Mount Messenger Formation (UMMF) is characterized by thin-bedded sandstone and siltstone deposits with interleaved channel and channel-levee geometries (King et al., 2011). This study focuses on the channelized stratigraphy of the LMMF stratigraphic interval.

The objective of this study is to increase the understanding of the Mount Messenger deep-water depositional system by establishing an architectural framework of sedimentary facies, event beds, and sedimentary bodies for channelized sandstone deposits. Analysis is accomplished through detailed and integrated analysis of the sedimentology and stratigraphy from well-exposed outcrops along coastal cliffs and inland ridgelines. A 6 km transect between Tongaporutu and the Whitecliffs provides

excellent two-dimensional longitudinal views of the lower-slope to basin-floor channel-lobe deep-water system.

To date, little work has been completed analyzing the spatial and temporal variation of sedimentary facies and architectural elements within channel complexes of the LMMF. Expanding upon previous work, this study analyzes sedimentary facies and architectural elements to understand how subaqueous flows transformed from the axis of a channel to the margin and overbank of a channel. Sedimentary facies are placed into an architectural framework to assist with correlation and show organized changes in the diversity and abundance of bodies.

Deposited into the Taranaki Basin, the MMF represents a potential reservoir target for oil and gas. The Taranaki Basin covers approximately 100,000 square km along the central west coast of New Zealand's North Island (Hart, 2001). Eocene to Miocene age turbidite fan deposits have proven to be hydrocarbon reservoirs, with the Kaimiro and Ngatoro fields, and the Windsor-1 and Goldie-1 wells producing from the Mount Messenger Formation (Hart, 2001). Developing a stratigraphic framework of sedimentary facies and architectural elements for the channelized interval of the LMMF highlights changes in reservoir heterogeneity within sandstone-rich deposits and their associated levee deposits. The framework presented by this study introduces a high-resolution approach to understanding the building blocks of these potential reservoir targets.

Objectives and Research Questions

Channel complexes present within the LMMF exhibit a variety of sedimentary

facies and architectural elements. Spatial and temporal variation of these attributes record changes in subaqueous flow properties related to gradient, confinement, flow size or duration, and subaqueous flow type.

Objectives for this study include analyzing the sedimentology and architectural elements present within and bounding submarine channel complexes in the LMMF to gain a further understanding about the evolution of this deep-water depositional system. Research questions pertaining to this study are evaluated to explain variation within subaqueous flows and architectural elements within and bounding the channel complexes of the LMMF.

1. Sedimentology: How do sedimentary facies present within outcrops reflect transformations within subaqueous flows from the axis of a channel to the margin and overbank of a channel?
2. Sedimentary bodies: How do varying body types within the LMMF reflect changes in confinement within the depositional system?
3. Paleogeography: Does the distribution and stacking pattern of channel complexes within the LMMF represent changes in confinement related to depositional topography created by mass-transport deposits?
4. Sediment Provenance: How do the three sediment sources inferred for the LMMF populate sedimentary bodies?

Study Area

The study area is located in the Taranaki coastal region of New Zealand on the North Island, overlooking the Tasman Sea (northern extent: latitude 38°49'S, longitude 174°35'E; southern extent: latitude 38°52'S, longitude 174°33'E) (Figure 1). This is approximately 50 km northeast from the city of New Plymouth and approximately 14 km south from the town of Mokau. Situated between the Tongaporutu River and the Whitecliffs, coastal cliffs and inland ridgelines extend approximately 6 km north-south and correlation lengths inland are approximately 1.5 km to the east (Figure 2). The 9 km^2 study area is populated by near vertical, vegetation free coastal cliffs approximately 30 meters in elevation, and inland ridges approximately 150-175 meters in elevation with moderate to heavy vegetation covering their slopes. Strata within the study area dip 4 to 10 degrees southwest and strike southeast.

Geologic Setting

Located along the west coast of New Zealand's North Island, the Taranaki Basin reflects a complex tectonic and sedimentary history associated with the evolving Pacific and Australian convergent plate boundary (King and Thrasher, 1996). Early basin development reflects initial rifting during the mid-Cretaceous and gradual evolution to a passive margin that persisted through much of the Paleogene. During the mid-Oligocene, renewed subsidence was prevalent across the basin. The highest rates of subsidence occurred adjacent to the Taranaki Fault, and are hypothesized to reflect shortening and transpression within a foreland basin setting (King and Thrasher, 1996). During the

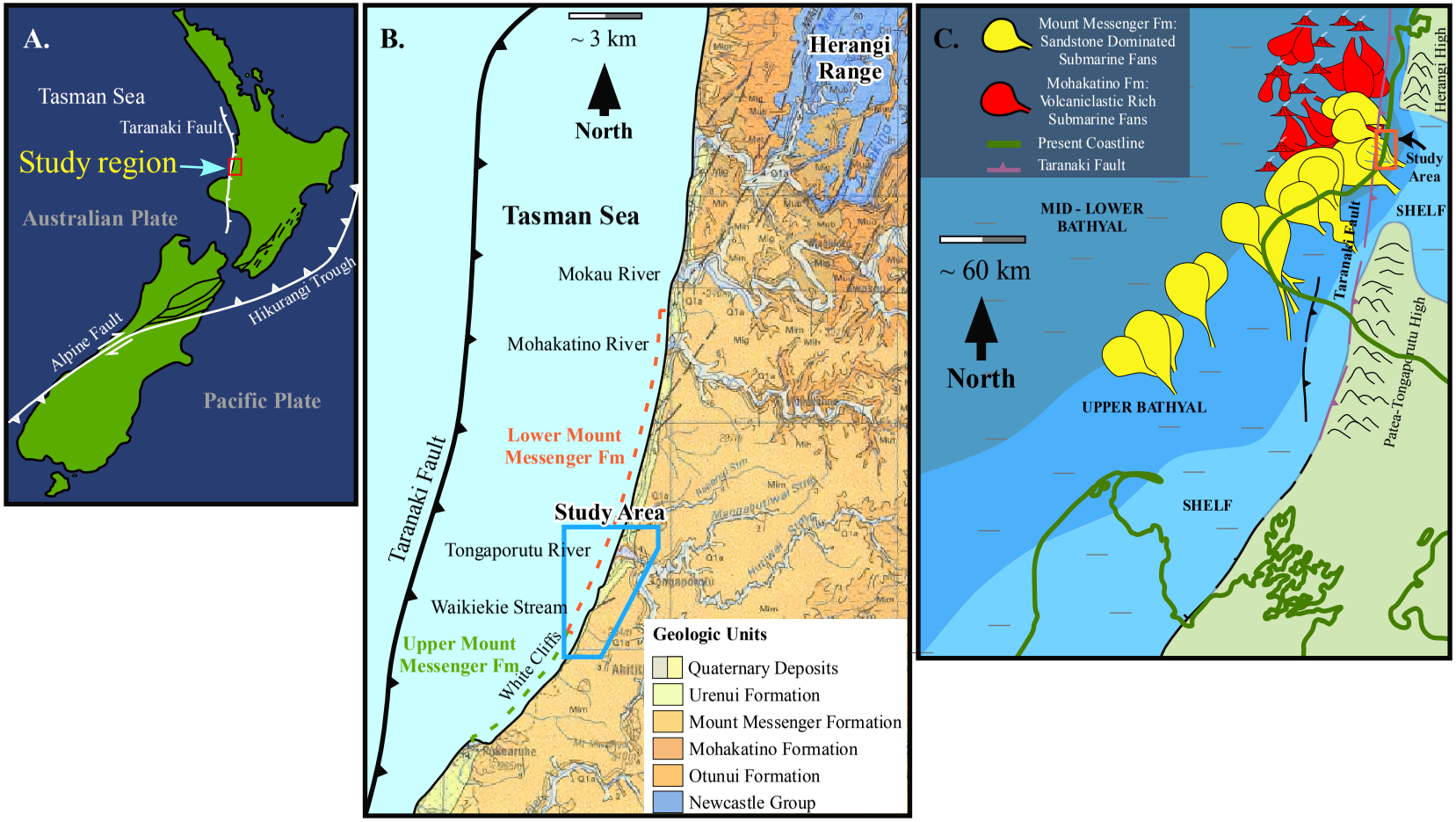


Figure 1. A) Location of the study area on the North Island of New Zealand showing the regional plate boundaries and the location of the Alpine and Taranaki Faults. B) Regional geologic map showing the general extent of geologic units and the location of the study area (modified from Edbrooke, 2005). C) Generalized paleogeographic reconstruction of the Taranaki Basin during the Late Miocene showing submarine fan deposition within the study area and the structural highs influencing sediment transport and deposition (modified from King et al., 2007).

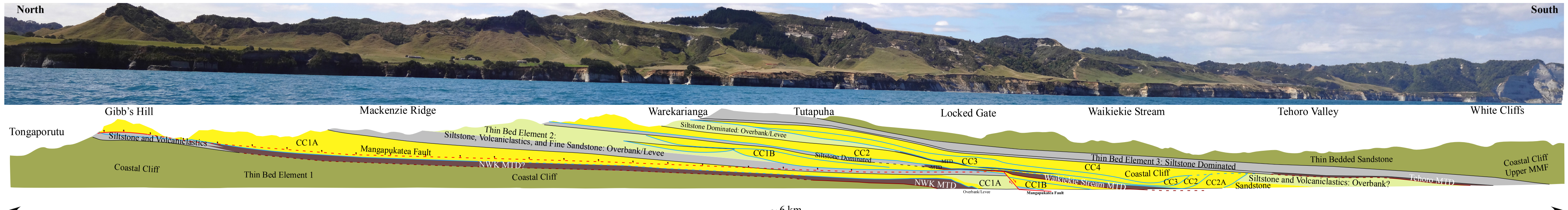


Figure 2. Overview photo-panel of the study area showing the general relationships of channel complexes present within coastal and inland ridge outcrops. Names of localities and stratigraphic units are placed above their location within the study area. Sandstone is yellow, thin-bedded siltstone and sandstone is gray, and mass-transport deposits are brown. The two green thin-bedded intervals were studied for their stratigraphic context but are not present within the channel belt.

earliest Miocene, westward overthrusting and compression of the Taranaki Fault marked the beginning of a new tectonic episode coinciding with the inception of the modern Alpine Fault transform boundary (King and Thrasher, 1996). Tectonic activity slowed during the early to mid-Miocene and subsidence ensued; however, the hinterland to the south began to rise. This allowed large quantities of sediment to reach the basin (King and Thrasher, 1996).

The Miocene strata present within the Taranaki region of New Zealand represents sediment accumulation in a foredeep trough close to the fault bounded eastern margin of the Taranaki Basin (King et al., 2011). This was an active-margin basin during the Late Miocene with the Taranaki Fault dislocating older stratigraphic successions and influencing the sedimentation style and accumulation rate through time (King and Thrasher, 1992; King and Thrasher, 1996; King et al., 2011). Major episodes of movement on this basement-cored thrust occurred during the Early to Middle Miocene and ceased during the Late Miocene. It strikes roughly north-south and is subparallel and west of the current coastline (King et al., 2011).

Representing one of the largest known thrust faults in New Zealand, the Taranaki Fault extends from the Alpine Fault on the South Island. It accommodated westward displacement during the Miocene resulting in the uplift and emplacement of a wedge of Mesozoic basement rocks over Late Cretaceous and Tertiary strata of the Taranaki Basin (King and Thrasher, 1992; King and Thrasher, 1996). Present within the wedge is Late Permian to Late Jurassic greywacke and argillite of the Murihiku Terrane (Raine et al., 2004). Basement rocks west of the fault represent Permian age terrane blocks and

batholith rocks accreted to the Gondwana margin in the Mesozoic. This relationship may indicate that the Taranaki Fault plays a significant role as a tectonic boundary with movement initiating as early as the Late Eocene (Stagpoole and Nicol, 2008). Evidence for this hypothesis is inconclusive due to the lack of preserved sedimentary rocks on the upthrown side of the fault. Even so, studies have inferred basement terrane accretion events as early as the Late Cretaceous with the Taranaki Fault propagating along terrane boundaries at later times (Stagpoole and Nicol, 2008).

With an oblique extensional transform system (West Coast-Taranaki Rift) through continental basement, and a zone of active seafloor spreading in the Tasman Sea, the tilting, uplift, and erosion of the Murihiku basement along the central-western North Island coincides with the emplacement of the (proto-) Taranaki Fault marking the eastern margin of the basin (Kamp et al., 2004). Persistent structural highs, the Patea-Tongaporutu High to the south, and the Herangi High to the north, influenced sedimentation throughout the region, although Miocene sediments overtop the Patea-Tongaporutu High in the study area (King et al., 1993). Inversion of the depocenter and tilting of the high coincided with rapid subsidence along the eastern Taranaki Basin (Kamp et al., 2004). This continued until earliest Miocene time when a dramatic change from carbonate to siliciclastic sedimentation occurred reflecting the uplift and erosion of basement rocks in response to formation of the Australia-Pacific plate boundary, and associated reverse movement on the Taranaki Fault (Kamp et al., 2004) (Figure 3).

By the Middle to Late Miocene, the eastern Taranaki Basin reflected an intra-arc to hybrid back-arc tectonic setting with discrete, overlapping and superimposed structural

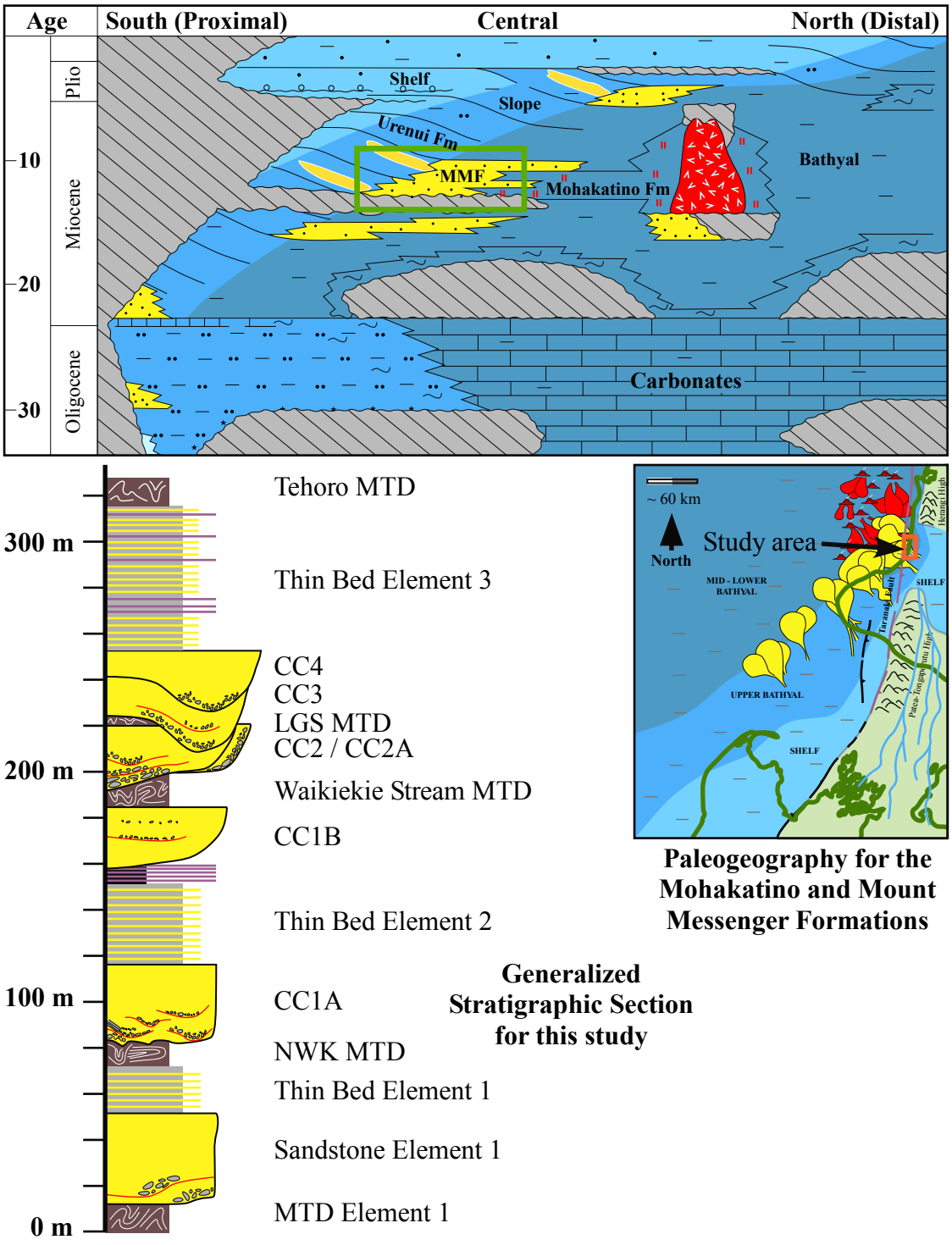


Figure 3. Chronostratigraphic framework for the Taranaki Basin showing changes in sedimention style from the Oligocene-Pliocene paired with a paleogeographic map representing sediment transport from the north, east, and south during deposition of the Mount Messenger Formation (modified from King et al., 2007; King et al., 2011). A generalized stratigraphic section represents the stratigraphy analyzed in this study.

styles associated with the Australian-Pacific plate boundary (King et al., 1993). Siliciclastic sedimentation continued into the Middle to Late Miocene with the deposition of the Mohakatino Formation which underlies the Mount Messenger Formation. Comprised of volcaniclastic sandstone sourced from andesitic volcanoes in the northern Taranaki Basin and an increasing amount of mass-transport slumping, the Mohakatino Formation indicates that the Taranaki Fault marks the eastern margin of the basin, as deep-water sediments are not present east of the fault (Kamp et al., 2004).

Above the Mohakatino Formation, the Mount Messenger Formation represents higher rates of uplift and erosion along the plate boundary. It has been suggested that sediments within the Mount Messenger Formation represent a high sediment flux sourced mainly from the Torlesse Terrane and Apline Schist eroded from the Southern Alps (Jordan et al., 1994; Kamp et al., 2004). Sediment was fed via northward flowing rivers across basement topography and toward the eastern Taranaki and Wanganui Basins where they were transported across the shelf by longshore currents, and captured by slope feeder channels draining the narrow shelf (King et al., 1993; Kamp et al., 2004) (Figure 3).

Sediment accumulation of the Late Miocene Mount Messenger Formation represents an aggradational and progradational sequence with an increased percentage of fine-grained sandstone units dominating lower-slope to basin-floor submarine fans (King et al., 1993). Fine-grained sandstones were mixed with volcaniclastic ash from northern submarine volcanoes, bioclastic debris from an eastern shelf or slope, and local and regional mass-transport deposits (King and Thrasher, 1996; King et al., 2011) (Figure 3).

Total thickness for the Mount Messenger Formation is estimated between 600-800 meters and represents deposition over a 1-2 m.y. span (King et al., 1993; King et al., 1994; Helle, 2003; Browne et al., 2005; Masalimova, 2013). Thickness of the LMMF is estimated between 500-650 meters within the study area by previous authors (Helle, 2003; Masalimova, 2013). This study measured approximately 325 meters of the LMMF south of the Tongaporutu River to the Whitecliffs (Figure 3).

Data and Methods

Field Data

Under the direction of Dr. Michael Gardner, field data was collected over a 58 day time frame in 2013 with help from one field assistant. Data collected during previous field sessions in 2011 and 2012 by Dr. Gardner and the Slope and Basin Consortium was incorporated into the analysis during the 2013 field session. Data gathered reflects centimeter-scale sedimentological information (lithology and facies) from 20 measured sedimentological profiles totaling 552 meters, correlated photo-panels with architectural element analysis for each channel complex, and a geologic map of the described lithostratigraphic units.

Methods

Geologic Map Mapping different rock units across the study area required identifying each body and the units that bound them. The geology was mapped at a 1:2,000 scale to capture a detailed spatial framework for the channel bodies (Figure 4).

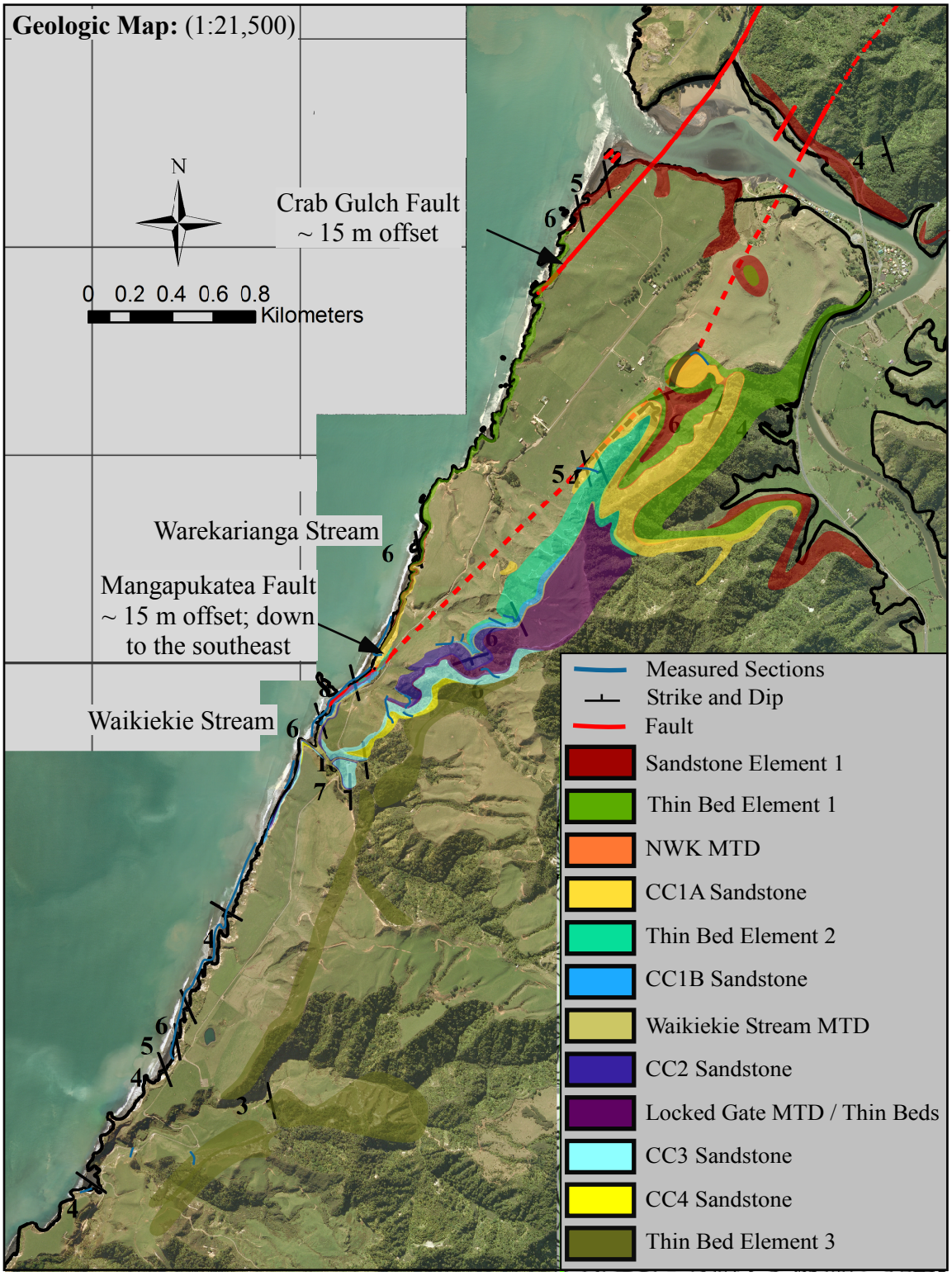


Figure 4. Geologic map of lithostratigraphic units in the Lower Mount Messenger Formation within the study area.

Channelized lithosomes consist of thick-bedded, fine- to medium-grained amalgamated sandstone, mudstone conglomerate, and thin-bedded sandstone, and siltstone. Units that bound the channelized lithosomes are composed of thin- to medium-bedded, very fine-grained sandstone with increasing siltstone, and very thin-bedded volcaniclastic sandstone. These units reflect overbank-levee deposits and mass-transport deposits within the field area. Documented within the geologic map are lithostratigraphic units, measured sedimentological profiles, bedding attitudes, and faults.

Sedimentological Measured Profiles Sedimentological profiles measured from outcrops gather a number of attributes with centimeter-scale resolution to interpret hydrodynamic facies and formative processes at the time of deposition. These include bed thickness, grain size and sorting, sedimentary structures, and bed contact relationships. Other attributes analyzed include color, texture, grading, clast composition, size, and shape, paleoflow direction, bioturbation index, stratigraphic position, and lateral bed relationships.

Twenty sedimentological profiles represent 552 meters of measured stratigraphy from deposits within and bounding channel complexes (Table 1). Measured profiles document sedimentary facies, event beds, and channel elements present at each locality. GPS waypoints were used to document each sedimentological profile at five meter intervals to assist with spatial correlation on the geologic map. Photo-panels also document measured section locations and bed meterage for each locality.

Inland Ridge Sections	Latitude	Longitude	Thickness (m)
Gibbs Hill	-38.824648	174.588556	18.0
Mackenzie Ridge	-38.829653	174.582518	60.73
Warekarianga North	-38.836169	174.578769	24.3
Warekarianga	-38.836345	174.577733	29.76
Tutapuha North	-38.837272	174.576088	27.1
Tutapuha	-38.837654	174.575751	2.76
Tutapuha East	-38.838164	174.576481	13.98
Tutapuha South	-38.837102	174.575534	37.58
Tutapuha Upper	-38.838476	174.577249	39.6
Locked Gate	-38.839697	174.573100	48.55
Locked Gate Upper	-38.840388	174.572894	19.06
Locked Gate South	-38.839820	174.572007	50.58
Tehoro Valley	-38.859578	174.561814	36.04
Tehoro Valley Overlap	-38.859449	174.558353	7.5
Coastal Cliff Sections			
North Waikiekie North	-38.837677	174.571312	26.45
North Waikiekie Fault	-38.839215	174.569947	7.17
North Waikiekie	-38.839286	174.570094	18.03
South Waikiekie	-38.842687	174.566963	18.03
South Waikiekie South	-38.846542	174.564959	52.7
Tehoro Beach	-38.861230	174.556128	14.3

Table 1. Sedimentological profiles measured from this study with latitude and longitude location, and thickness in meters.

Measured profile locations were chosen to reflect changes from the axis of channels to the margin and overbank of channels. Along coastal sections, measured profiles were gathered where continuous exposure was present up-section. This limited the number of profiles that could be measured south of Waikiekie Stream due to truncation at channel margins and the inaccessibility to measure 30 meter high cliff faces. Photo-panel analysis assisted with facies analysis where measured profiles were not able to be collected along the coastal cliffs south of Waikiekie Stream.

Facies and Event Bed Analysis Facies analysis was completed using observations from outcrops that are documented on sedimentological profiles and photo-panels measured in the field. Distinct changes in lithology were divided to reflect varying hydrodynamic properties in subaqueous flows. Thirty sedimentary facies are documented within the LMMF from 20 measured profiles.

Descriptions of the 30 sedimentary facies and a hydrodynamic interpretation of the formative processes at the time of deposition are presented in chapter 2. Facies proportions were calculated from each measured profile and compared across the channel belt for each body. They are presented in chapter 4.

Event beds were also documented on sedimentological profiles from observations collected in the field. Event beds reflect the sediments accumulated during individual subaqueous flow events (Figure 5). Event bed thickness trends and correlations are also presented in chapter 4. Subaqueous flow transformations from the axis of each channel to the margin and overbank of each channel are inferred with assistance from event bed analysis.

Architectural Element Analysis Sedimentological profiles were tied in the field to 21 photo-panels to assist with the correlation of surfaces and bodies within the depositional system, and to help document an architectural framework of facies, event beds, elementary channels, composite channels, and channel complexes across the LMMF. Photo-panels document the locations of measured sedimentological profiles tied to distinct identifiable beds, mudstone conglomerate, mass-transport deposits, elementary

channels, composite channels, and channel complexes. Channel widths were measured using GPS units, topographic maps, and a tape measure.

Bodies were traced throughout the outcrops using a number of observations. These include stratal surfaces (erosional, depositional, and inclined), cross-cutting relationships, geometry (width and thickness), internal bedding attributes (thickness, inclination, and irregularity), stacking patterns (horizontal and vertical offset), and facies associations (spatial relationships, thickness, and proportion). Correlation from the coastal cliff outcrops to the inland ridge outcrops was completed using observations of these attributes and later verified through event bed analysis.

Previous Work

Continuous outcrops along coastal cliffs and inland ridgelines have historically provided insight into the sedimentology, stratigraphy, and architectural building blocks of the MMF. Datasets gathered by previous authors describe lithofacies, facies associations, and architectural elements, as well as grain-size characteristics, biostratigraphic correlations, depositional processes, and the overall stratigraphic evolution of the progradational system (King et al., 1993; King et al., 1994; Jordan et al., 1994; Browne et al., 1996; Browne and Slatt, 2002; Helle, 2003; Browne et al., 2005; King et al., 2007; King et al., 2011; Jobe et al., 2011; Masalimova, 2013).

Early research by GNS outlines a comprehensive analysis of the physiography, structure, stratigraphy, historical background, detailed lithology, biostratigraphy, and the

depositional and tectonic history of Miocene sediments that outcrop along the North Taranaki coast (King et al., 1993). Research that followed built upon their framework.

Architectural element analysis of the MMF has been completed by multiple authors with different methods. A sequence stratigraphic approach completed in 1994 recognized 5 sequence boundaries interpreted to represent separate lowstand systems tracts. The 3 lowermost sequences are present within the LMMF. These describe basin-floor fans that overlie relatively unchannelized sediments (SB1), increasing channelized sediments with erosional relief around 20 meters (SB2), and a heterolithic association comprising a series of nested channelized sediments with erosional relief around 30 meters (SB3) (King et al., 1994). Bed morphology within individual sequences is inferred to reflect proximity to the slope and position within each respective lowstand systems tract.

An allostratigraphic approach completed in 2003 recognized 3 allostratigraphic units divided into sandstone elements, heterolithic elements, and deformed elements for the LMMF. These units reflect deposition from the mid-fan to lower-fan capped by a slope failure (Unit 2), deposition from the channel-lobe transition to overbank deposits capped by a slope failure (Unit 3), and channel abandonment with deposition on the lower-fan capped by a slope failure (Unit 4) (Helle, 2003). Each allostratigraphic unit is defined by their bounding discontinuities, typically at the erosive base of sandstone elements. Descriptions and interpretations of bedding geometry were presented for each element within allostratigraphic units.

Research presented in 2007 recognized the gross architecture of the LMMF, characterized by a hierarchy of channel forms. Six main channel elements were identified, 4 within the inland outcrops, and 2 within coastal outcrops (Arnot et al., 2007). It was hypothesized that a larger-scale 1.7 km wide and 60 meter thick channel feature bounds the smaller channels. Variability of the channel-fill architecture is documented with typical facies successions, aspect ratios, and average paleocurrent direction for each channel element.

Recent work by Masalimova in 2013 expanded upon the previous research to systematically identify a vertical succession of hierarchical architectural units for the LMMF. Her analysis described lithofacies, sedimentation units, and facies associations. This approach links the main sedimentary processes responsible for deposition of the LMMF to the larger-scale architecture of fan lobes, and channel-levee complexes (Masalimova, 2013). Architectural elements are divided into third-order lithofacies and fourth-order facies associations for the channel-lobe depositional system. In all, 5 lithofacies and 12 facies associations were identified and divided into 5 major groups. These include 5 lobe complexes (FA1), 2 crevasse or overbank splays (FA2), 3 channel fill units (FA3), levees (FA4), and mass-transport deposits (FA5) (Masalimova, 2013). Her research infers a small channel-lobe complex that was fed by a single, levee-bounded master channel belt 2-3 km wide with 5 main stages of development outlined by each facies association.

This study expands upon the previous research with new observations and correlations within the channel complexes of the LMMF. The architectural framework

presented above and the nomenclature of units compiled from the 2003, 2007, and 2013 studies are compared to this study to outline the similarities and differences between authors (Table 2).

Helle, 2003	**Arnot et al., 2007**	**Masalimova, 2013**	**This Study, 2015**
Rapanui Deformed Sub Element? / Deformed Element 1	N/A	MTD	MTD Element 1
Sandstone Element 2	N/A	FA2a	Sandstone Element 1
Heterolithic Element 2	N/A	FA4	Thin Bed Element 1
Deformed Element 2	N/A	MTD	NWK MTD
FLSA Sub-Element / Sandstone Element 3	N/A	FA2b / FA3a	CC1A
N/A	N/A	FA4	Thin Bed Element 2
MSA Sub-Element / Sandstone Element 3 and Heterolithic Element 3	C1	FA3b	CC1B
Deformed Element 3	Slumped Unit	MTD	Waikiekie Stream MTD
Sandstone Element 4	C2	FA3b / FA3c	CC2
N/A	Mudstone Deformed	MTD	Locked Gate MTD
Sandstone Element 4	C3	FA3c	CC3
Sandstone Element 4	C4	FA3c	CC4
Sandstone Element 4	C5	FA3c	CC2/CC3/CC4
Sandstone Element 4	C6	FA3c	CC2A
Heterolithic Element 4	Thin Beds	FA4	Thin Bed Element 3

Table 2: A stratigraphic framework comparison of architectural elements compiled from Helle, 2003, Arnot et al., 2007, Masalimova, 2013, and this study. The various nomenclature reflects different methods by each study. Helle's 2003 study focused on an allostratigraphic approach, the 2007 study by Arnot et al., recognized the gross architecture characterized by a hierarchy of channel forms, and the 2013 study by Masalimova identified a vertical succession of hierarchical units that are divided between facies associations. The nomenclature from this study is similar to that of the Arnot et al. study, dividing channel complexes and the bounding stratigraphy by a hierarchy of bodies and the gross architecture.

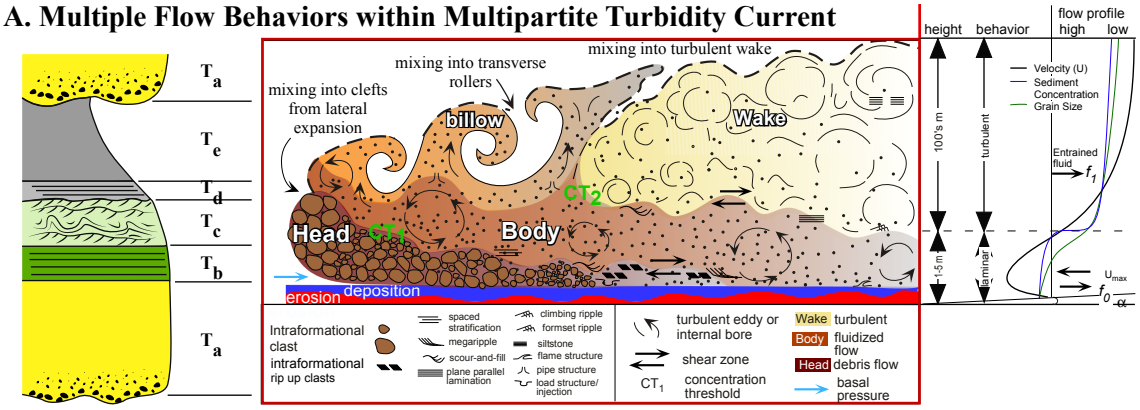
SEDIMENTOLOGY

Subaqueous Flows

Multiple subaqueous processes deliver sediment to deep-water settings. These include sediment gravity flows or turbidity currents (e.g., low-density and high-density turbidity currents), concentrated and hyperconcentrated density flows, cohesive debris flows, and *en masse* movements (e.g., slumps and slides) (Lowe, 1982; Middleton, 1993; Mulder and Alexander, 2001) (Figure 5). Processes governing these flow types record various properties within the flow and reflect characteristically different sedimentary attributes that are preserved in the sedimentary record. Inferences into the hydrodynamic processes responsible for deposition reflect an understanding of these attributes, recording variation between flows.

Turbidity Currents

Turbidity currents exhibit laminar and turbulent regimes subdivided into three parts: the head, body, and tail (Middleton, 1967; Middleton, 1993; Meiburg and Kneller, 2009) (Figure 5). The head displaces ambient fluid, which accelerates downslope, creating a resistance to the flow that is larger than the friction at the bed or upper interface (Middleton, 1993). This causes the head of the current to be thicker than the current behind the head, resulting in frictional resistance that produces an overhanging "nose", allowing the head to override lighter ambient fluid (Middleton, 1993). Ambient fluid mixing and viscous shear at the upper surface of the head leads to turbulent mixing at the back of the head, resulting in a turbulent wake (Middleton, 1993). Sediment is



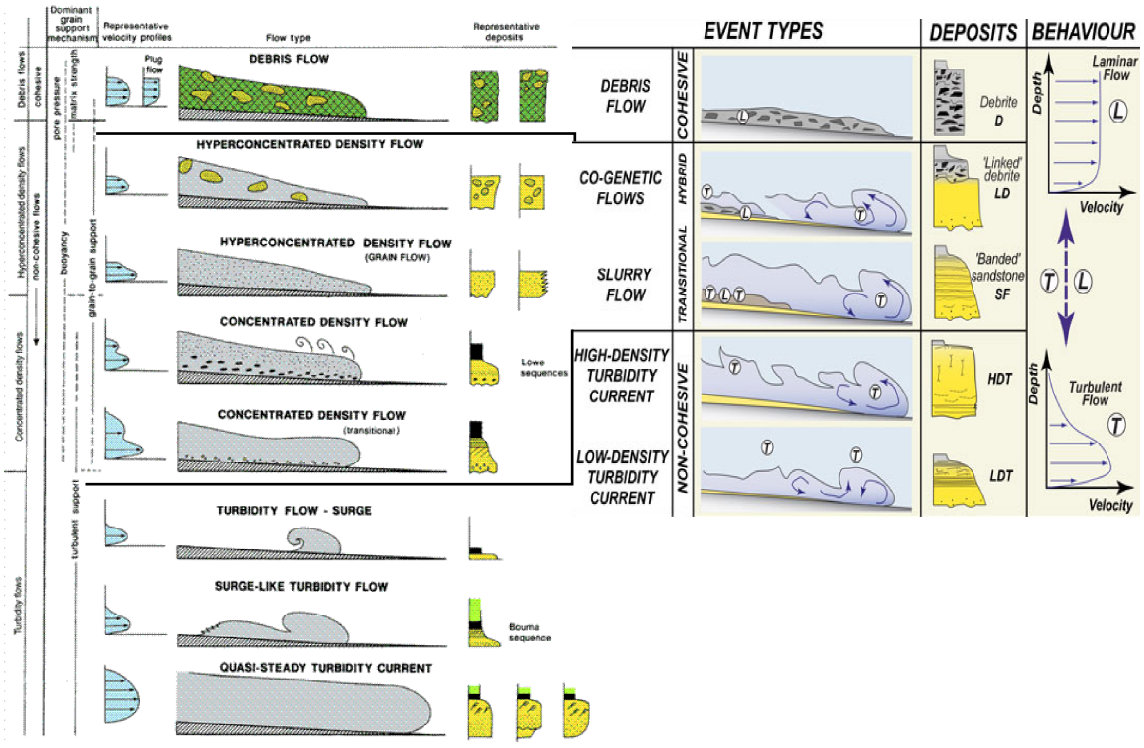


Figure 5. A) Schematic digram of an idealized sediment gravity flow showing the flow behavior and possible origination points for hydrodynamic facies transformations from the head, body, and wake of a subaqueous flow, and an idealized Bouma sequence (modified from Bouma, 1962; Gardner et al., 2003). B) Diagram for various idealized event types within subaqueous flows (Mulder and Alexander, 2001; Haughton, 2006).

suspended within the flow by fluid turbulence typically generated by the forward motion of the current, which is mainly driven by gravity (Meiburg and Kneller, 2009).

Low-Density Turbidity Current Low-density turbidity currents reflect the deceleration of a subaqueous turbidity current marked by the passage of sediment from suspended loads to bed loads with subsequent deposition, suspension sedimentation with minor traction, and direct suspension sedimentation (Lowe, 1982). These variations form the Bouma T_b-T_e divisions. The T_b division reflects upper flow regime plane-parallel laminae. The T_c division reflects lower flow regime ripple cross-laminations and wavy or convoluted laminae. The T_{de} divisions reflect fine grain deposition of upper parallel laminae and laminated to homogeneous mud (Bouma, 1962) (Figure 5).

High-Density Turbidity Current High-density turbidity currents reflect high-density turbulent flows of essentially cohesionless grains suspended by fluid turbulence generated by the forward motion of the current (Lowe, 1982). Three main stages of deposition are inferred for high-density turbidity currents (S_1-S_3).

The first stage represents slightly unsteady but fully turbulent currents that may deposit some of their load with plane beds and dune-like features (Lowe, 1982). Traction-sedimentation structures and local erosion may be present at this stage, and deposits typically show lenticularity, amalgamation, and scours (Walker, 1978; Lowe, 1982).

The second stage of deposition reflects an increase in flow unsteadiness with suspended sediment becoming more concentrated toward the bed (Lowe, 1982). As the concentration of coarse particles near the bed rises, bed-load transport in this layer

becomes increasingly dominated by grain collisions (Lowe, 1982). The basal particle layer formed is maintained by dispersive pressure and may be dominated by falling coarse-grained material from above, forming a traction carpet if turbulence is suppressed (Lowe, 1982). The collapsing and freezing of sediment and the formation of successive new carpets causes the bedform to aggrade (Lowe, 1982).

The third stage of deposition reflects higher suspended-load fallout rates with insufficient development of a bed-load layer or organized traction carpets (Lowe, 1982). Direct suspension sedimentation dominates with settling grains accumulating until the rising surface of the static bed coincides with the top of the falling cloud (Lowe, 1982). Grain supported deposits that lack traction structures may show grading with primary water-escape structures caused by mass settling (Lowe, 1982). Water-escape structures typically include dish and pillar structures.

High-density turbidity currents may record a flow transformation to low-density flows from the residual currents in the water column. The subsequent currents may make their way downslope, and deposit their sediments above the high-density division. This results in a bed that reflects both the S_1-S_3 stages, and T_{bcde} stages of the low-density turbidity current, including large-scale cross-stratification, which is commonly absent in an idealized Bouma sequence (Lowe, 1982).

Density Flows

Concentrated Density Flows

Concentrated density flows reflect a variety of operating particle-support mechanisms that vary in space and time (Mulder and

Alexander, 2001). Gravity acts as the primary driving force with grain-to-grain interactions generating dispersive pressure. This allows suspension to be maintained within a non-cohesive flow (Mulder and Alexander, 2001). Concentrated flows are more dilute than hyperconcentrated flows reflecting higher fluid turbulence within a flow, and the progressive replacement of grain-to-grain interaction as the main particle support mechanism (Mulder and Alexander, 2001). Concentrated flows may have erosional features at their base, and subsequent sand deposition showing grading and sorting trends, and bedforms. They can be distinguished from turbidity current deposits by the following features: the presence of large clasts, thick massive structureless sandstone (T_a) proportions within beds, and perhaps differences in bedform character, and other sedimentary structures (Mulder and Alexander, 2001).

Hyperconcentrated Density Flows Hyperconcentrated density flows represent a medium between concentrated density flows and cohesive flows (Mulder and Alexander, 2001) (Figure 5). They include deposits previously defined in the literature as sandy debris flows and slurry flows, as well as various other deposits not discussed (Lowe and Guy, 2000; Mulder and Alexander, 2001). The proportion of cohesive and non-cohesive particles are not well defined, and it has been suggested that debris flows may transform to non-cohesive flows with no change in water content or clay fraction when velocity is high enough (Fisher, 1983; Mulder and Alexander, 2001). The main driving force of hyperconcentrated density flows is gravity, and deposition is by frictional freezing resulting from grain-to-grain interaction (Mulder and Alexander, 2001). Deposits may

include large sediment clasts, rafted blocks of strata, and fluid escape, or collapse and deformation structures (Mulder and Alexander, 2001).

Cohesive Debris Flows

Cohesive flows have sufficient cohesive material (mud) to impart a pseudoplastic rheology (Mulder and Alexander, 2001) (Figure 5). Matrix strength acts as the main grain-support mechanism within flows, with buoyancy and pore pressure also playing a role (Mulder and Alexander, 2001). Large clasts may be present and locally supported by high pore pressures within the flow (Ineson, 1985; Mulder and Alexander, 2001). The main process for deposition within a debris flow is frictional freezing or *en masse* resulting in a chaotic arrangement of the deposits, and the presence of large grain size populations (Lowe, 1982; Mulder and Alexander, 2001).

Flow Transformation

Subaqueous flow transformations reflect changes in flow behavior (Fisher, 1983). They are influenced chiefly by particle concentration, thickness of the flow, and flow velocity, allowing laminar-turbulent transformations to occur (Fisher, 1983). At least four kinds of flow transformations have been identified from field, experimental, and theoretical descriptions (Fisher, 1983). These include body transformations, gravity transformations, surface transformations, and fluidization transformations.

Several authors have proposed flow transformations within subaqueous environments (Kuenen, 1952; Middleton, 1970; Hampton, 1972; Lowe, 1982; Fisher, 1983; Talling, 2012). These transformations reflect extensive changes in the density of

the flow, leading to longitudinal variation in the velocity structure, composition, and sediment support mechanisms (Hampton, 1972; Fisher, 1983).

Body transformations occur with no change in water content when flow velocity reaches the point to produce internal turbulence (Fisher, 1983). Gravity transformations occur when gravity segregation is present at the base of an initially turbulent, high concentration turbidity current (Fisher, 1983). They represent the deposition of a high-density suspended load, and subsequent formation of a residual low-density turbidity current that travels downslope, and possibly accelerates as a discrete turbidity current (Lowe, 1982).

Surface transformations reflect the transition from subaqueous debris flows to turbidity currents through extensive stripping of sediment at the front of the flow, and ejection of material into the overlying water column to form a dilute turbulent cloud (Hampton, 1972; Fisher, 1983). The possibility for turbidity currents to form by direct mixing of water within the body of the debris flow causing flow instability has also been proposed (Hampton, 1972).

Fluidization transformations reflect the change from a laminar-dense phase to a turbulent-dilute phase, although they have not been adequately described within subaqueous environments (Lowe, 1982; Fisher, 1983).

These transformations reflect the complex nature of subaqueous flows and their deposits. Hydrodynamic facies analysis and inferences about the conditions present at the time of deposition provide only a glimpse into the dynamics of individual flows, and do not necessarily reflect the up-dip transition between flows. Although up-dip

transformations may not be known, it may be possible to infer lateral flow transformations within deposits from the axis to margin of channels. Transformations related to the effects of confinement, flow strength, flow duration, flow variability, frequency of events, and sediment concentration are proposed. This analysis is discussed in chapter 4.

Hydrodynamic Facies of the Mount Messenger Formation

Thirty sedimentary facies divisions are described from the sedimentology documented within channel complexes and bounding channel complexes of the Lower Mount Messenger Formation. Facies described from outcrop exposures are grouped to divide mudstone-clast conglomerate, sandstone, siltstone, mudstone, post-depositionally modified sediments, and tuffaceous sediments (Figure 6). Detailed descriptions of each sedimentary facies are presented with a hydrodynamic interpretation of the formative process during deposition. Sedimentary facies proportions are documented across the channel belt for each measured sedimentological profile with the interpreted spatial position noted. These are presented in chapter 4. Sedimentary facies were analyzed from the interpreted axis to the margin of each channel complex and also outside each channel complex. Photos of each sedimentary facies are presented in figure 6.

Mudstone-Clast Conglomerate Facies

Clast Supported (1A) Clast supported mudstone-clast conglomerate deposits are exposed at the base of large erosional contacts, most notably south of Waikiekie Stream

and at Gibb's Hill localities within the LMMF. Beds up to 2 meters thick are composed of light gray mudstone clasts that are generally sub-angular to sub-rounded, elongated, and weakly imbricated. Average clast size varies upon locality, but range in scale from centimeters up to one meter wide along their longest apparent axis. Clasts are generally oriented with their longest axis parallel to sub-parallel to bedding. When present, the matrix consists of fine- to very fine-grained sandstone, and often contains bioclastic shell debris at the Waikiekie Stream locality.

Interpretation: Deposition of clast supported mudstone-clast conglomerate is inferred to represent a medium between debris flows and hyperconcentrated density flows where clasts are supported due to cohesion between mud-clasts, the shear strength of matrix, high clast concentration, and hindered settling (Mulder and Alexander, 2001). Variation in clast size is high, and clasts are oriented parallel to sub-parallel to bedding reflecting shear within the flow. Clasts were likely ripped up or slumped from the margin of the channel or mud-rich slope up dip, and carried short distances by successive flows before the flow was deposited from frictional freezing.

Matrix Supported (1B) Matrix supported mudstone-clast conglomerate deposits are present within each channel complex of the LMMF and are exposed at the base of erosional contacts, and internally along erosional scours. Beds up to 50 centimeters thick are composed of light gray mudstone clasts that are generally sub-rounded to well-rounded, elongated, and weakly imbricated. Average clast size is 5 centimeters, but range in scale from millimeters up to 20 centimeters wide along their longest apparent axis. Clasts are generally oriented with their longest axis parallel to sub-parallel to bedding. The matrix

consists of clean, fine- to very fine-grained sandstone. Minor bioclastic shell debris may accompany the clasts, but typically is not present in the inland outcrops. Shell debris becomes more abundant in the coastal outcrops north and south of Waikiekie Stream.

Interpretation: Matrix supported mudstone-clast conglomerate is inferred to represent deposition by concentrated density flows or turbidity currents with clasts ripped up from underlying strata and carried short distances within the head to body of the flow (Mulder and Alexander, 2001). Clasts are supported due to the shear strength of the matrix and fluid turbulence within the flow and subsequently deposited due to traction at the base of the bed (Mulder and Alexander, 2001).

Thick- to Medium-Bedded Sandstone Facies

Horizontally-Stratified or Spaced-Stratified (2) Horizontally-stratified or spaced-stratified sandstone deposits are present within each channel complex of the LMMF and typically occur within the base to middle half of the bed if present. Facies contacts are sharp in nature. Spaced horizontal laminations range from two to eight centimeters thick and sometimes show a coarsening upward sequence, although it is difficult to examine due to the consistent fine-grained nature of the MMF. Sandstones consist of fine- to very fine-grained angular quartz framework grains that are moderately- to well-sorted with few lithic fragments and mica. Horizontally-stratified or spaced-stratified facies thickness within event beds range from 10 centimeters to 1.5 meters, and average 40 centimeters.

Interpretation: Deposition by high-density turbidity currents is inferred due to the presence of spaced laminations commonly occurring in two to eight centimeter intervals

near the base of the bed. Coarsening upward sequences within these represent traction carpets or the S_2 division within a flow (Lowe, 1982; Hiscott, 1994). The inverse grading is a consequence of an upward velocity gradient within the flow and a laminar regime (Mulder and Alexander, 2001).

Cross-Stratified (3A) Cross-stratified sandstone deposits are present throughout the LMMF, and are generally associated with thick amalgamated beds. Plane-parallel laminated and massive structureless sandstone facies may bound cross-stratified sandstone. Cross-stratified sandstone facies reflects low angle cross-stratification with aggradational, concave, trough-shaped scours and wavy laminations. The presence of shell hash above scours is common south of Waikiekie Stream. Sandstones consist of very fine- to medium-grained angular quartz framework grains that are moderately- to well-sorted with few lithic fragments and mica. Facies thickness within event beds range from 10 centimeters up to 3.1 meters when sandstone beds are amalgamated. Average thickness measured is 68 centimeters.

Interpretation: Deposition is inferred to reflect high-density turbidity currents. Cross-stratified sandstone facies is thought to represent dune-like bedforms deposited by slightly unsteady, fully turbulent flows with traction sedimentation near the base to middle of beds (Lowe, 1982). Local erosional scours and amalgamation within beds reflects flow unsteadiness within the S_1 division of high-density flows (Lowe, 1982).

Wavy-Laminated (3B) Wavy-laminated sandstone facies is less common than cross-stratified sandstone facies, and generally thinner. Facies thickness within event

beds range from 5 centimeters to 70 centimeters, and average 17 centimeters within the study area. Wavy laminations sometimes show thickening or thinning trends laterally. Wavy-laminated stratification is occasionally the only facies present within a bed, however, it is more common at bed tops. Sandstones are very fine- to fine-grained and may have a siltstone matrix. Facies contacts are generally sharp to wavy in nature.

Interpretation: Wavy-laminated sandstone is inferred to represent deposition by low-density turbidity currents. Waning flow velocity is marked by traction sedimentation producing planar laminations followed by wavy laminae correlating to the T_c division in a Bouma sequence (Bouma, 1962). Wavy shearing within the flow reflects changes related to variations in bedform relief (Bouma, 1962).

Structureless (4A) Structureless sandstone deposits are present across the LMMF and generally are massive in nature, though they also are found in thin beds. They do not exhibit any sedimentary structures. Sandstones are composed of very fine- to medium-grained quartz that is moderately- to well-sorted with few lithic fragments and mica. Facies contacts are typically sharp, but also can be wavy, irregular, erosional, or gradational. Facies thickness within event beds range from <5 centimeters up to 3 or more meters in amalgamated sandstone beds. Average thickness is 45 to 50 centimeters within the study area.

Interpretation: Deposition is inferred to reflect rapid deposition from high-density turbidity currents or deposition from quasi-steady flow for thick-bedded deposits (Lowe, 1982; Kneller and Branney, 1995). Deposition from high-density turbidity currents would occur from suspension with no subsequent bedload transport, and correlate to the S_3

division with a flow (Lowe, 1982). Deposition from quasi-steady flows would reflect progressive aggradation during sustained flows (Kneller and Branney, 1995). Massive graded structureless sandstone correlates to the T_a division within a Bouma sequence. Medium- to thin-bedded structureless sandstone may reflect deposition by low-density turbidity currents or steady currents that carried less sediment downslope (Lowe, 1982; Kneller and Branney, 1995).

Secondary Structures (4B) Secondary structures in sandstone include convoluted bedding, dish structures, flame structures, injections, and rarely mudstone-clasts. Sandstones are generally fine- to very fine-grained and moderately- to poorly-sorted. Facies thickness within event beds range from 2 centimeters to 70 centimeters, and average 20 centimeters. Secondary structures are commonly found at the top or base of beds, and may be bounded by structureless or wavy-laminated sandstone.

Interpretation: Secondary structures in sandstone reflect deposition from high-density turbidity currents representing the S_3 division within a flow, or from low-density turbidity currents with the original primary structures destroyed by fluidization or liquefaction (Lowe, 1982). Fluidization and liquefaction may occur from loading and changes in pore pressure causing the upward flow of escaping pore fluids. The S_3 division commonly forms dish and pillar water-escape structures related to the mass settling of grains (Lowe, 1982).

Structureless with Floating Mudstone-Clasts (4C) Structureless sandstone deposits with floating mudstone-clasts are commonly found at bed tops with sharp or

wavy contacts within channel bodies. Light gray mudstone-clasts float freely in fine- to very fine-grained sandstone that is moderately-sorted. Millimeter- to centimeter-scale mudstone-clasts generally compose 10% or less of the bed. Facies thickness range from <5 centimeters up to 95 centimeters, and average 26 centimeters.

Interpretation: Deposition is inferred to reflect hyperconcentrated flows, high-density turbidity currents, or quasi-steady flows due to the lack of bedforms and the presence of mudstone-clasts (Lowe, 1982; Kneller and Branney, 1995; Mulder and Alexander, 2001). The main mechanism for deposition was frictional freezing resulting from the grain-to-grain interaction or progressive aggradation with clasts deposited along unrecognizable depositional boundaries that migrated upward during sedimentation (Kneller and Branney, 1995; Mulder and Alexander, 2001). Mud-clasts were carried in a non-cohesive matrix and deposited floating within the bed.

Plane-Parallel Laminated (5) Plane-parallel laminated sandstone deposits are abundant across the LMMF and exhibit millimeter- to centimeter-scale horizontal laminations. Plane-parallel laminated sandstone is occasionally the only facies present within a bed, however, it is commonly found within the top and base of beds, and may overlie structureless sandstone. Facies thickness range from <5 cm up to 2.5 meters, and average 22 centimeters. Sandstones are very fine- to medium-grained and moderately- to well-sorted with sharp or gradational contacts.

Interpretation: Plane-parallel laminated sandstone reflects deposition by traction within low-density turbidity currents (Lowe, 1982). Flows are marked by deceleration and a change from sediment held in suspension to bed loads, and subsequent deposition

by traction (Lowe, 1982). Plane-parallel laminated sandstone correlates to the T_b division within a Bouma sequence.

Medium- to Thin-Bedded Sandstone Facies

Asymmetric Ripple Cross-Laminated (6A) Asymmetric cross-laminated sandstone is common across the LMMF within and bounding channel bodies, and is generally found above plane-parallel laminated sandstones near bed tops. Asymmetric ripple cross-laminated sandstones are moderately- to well-sorted with grain size variation from very fine- to medium-grained. Facies thickness range from <2 centimeters to 25 centimeters, and average 9 centimeters in event beds. Contacts are gradational to sharp, and can be wavy.

Interpretation: Asymmetric ripple cross-laminations represent bedload transport by lower flow regime unidirectional currents and traction deposition within low-density turbidity currents (Bouma, 1962; Allen, 1968; Lowe, 1982). Velocity within the flow was waning and reflects traction at the transition within the body to wake of the turbidity current (Bouma, 1962; Lowe, 1982).

Climbing Ripple Cross-Laminated (6B) Climbing ripple cross-laminations are found along channel margins and within channel bodies. They generally represent thicker packages that are more aggradational than asymmetric ripple cross-laminations and commonly overlie plane-parallel laminated sandstones. Climbing ripple cross-laminations vary from subcritically climbing to supercritically climbing and occur in sandstone that is moderately- to well-sorted with grain size variation from very fine- to fine-grained.

Contacts are generally gradational to sharp, and may be wavy. Facies thickness range from 5 centimeters to 67 centimeters, and average 25 centimeters in event beds.

Interpretation: Climbing ripple cross-laminations represent bedload transport and concurrent rapid suspended fallout rates within the lower flow regime of low-density turbidity currents (Sorby, 1859; Jobe et al., 2011). Sediment fell rapidly onto a bed with active bedload transport in the ripple-stability field, and upstream ripples climbed over the next downstream ripple (Jobe et al., 2011). The angle of climb reflects the interplay of suspended-load fallout rate and bedload transport (Jobe et al., 2011). Climbing ripple cross-laminations are commonly developed on levees and along channel margins, at channel mouths and associated lobe and splay settings, and in areas where slope gradient abruptly decreases (Jobe et al., 2011).

Medium- to Thin-Bedded Muddy Sandstone Facies

Muddy Sandstone (7A) Muddy sandstone facies is not common within the LMMF. The facies consists of poorly-sorted sediments that are grain supported, but with a high concentration of mudstone matrix. They may include centimeter-scale mudstone-clasts, bioclastic shell debris, and volcaniclastic minerals in addition to the mudstone-rich sandstone matrix. They also may exhibit plane-parallel laminated or convoluted bedding. Muddy sandstone beds are typically normal graded. Facies thickness range from 7 centimeters to 27 centimeters, and average 19 centimeters. The facies is present within axial channel deposits within CC1B north of Waikiekie Stream, and also off-axis near the base of CC2 at Tutapuha Stream.

Interpretation: Deposition of muddy sandstone beds was likely by hyperconcentrated or concentrated density flows reflected by normal grading, grain-to-grain interaction, presence of bedforms, and erosion at the base (Mulder and Alexander, 2001). The principle driving force was gravity. The high mud content within the flow describes a mix between a cohesive debris flow and a non-cohesive density flow, and is similar to a "slurry bed" (Lowe and Guy., 2000). They may represent a flow transformation from a debris flow up-dip (Mulder and Alexander, 2001).

Mudstone-Clasts at Bed Tops (7B) The occurrence of mudstone-clasts dispersed in a mudstone-rich sandstone matrix at bed tops is not common within the LMMF, but only occurs within channels. Millimeter- to centimeter-scale clasts are composed of light gray mudstone. Clasts typically show elongation oriented parallel to sub-parallel to bedding. Facies contacts are gradational and may be wavy or irregular. Mica-rich lenses, volcaniclastic minerals, and bioclastic shell debris also may be present. The facies can exhibit horizontal laminations, wavy laminations, or be structureless and gradational. The facies is generally poorly- to moderately-sorted. Facies thickness range from 4 centimeters to 20 centimeters, and average 8 centimeters.

Interpretation: Deposition of mudstone-clasts dispersed at bed tops was likely by low-density turbidity currents where clasts were ripped up from underlying strata and suspended in the flow by fluid turbulence (Lowe, 1982; Mulder and Alexander, 2001). It also may reflect a flow transformation and subsequent deposition of the head, body, and wake of a turbidity flow.

Silty Sandstone (7C) Silty sandstone facies is characterized by very fine-grained sandstone with siltstone dominated matrix. It is generally finely laminated, moderately-sorted, and may contain sparse organics and mica. It is commonly found at bed tops above sandstones with a gradational contact to overlying mudstone. Facies thickness range from <1 centimeter to 1.2 meters, however, it can be difficult to break out individual event beds. Average thickness is 12.5 centimeters.

Interpretation: Silty sandstone was likely deposited at the tail of low-density turbidity flows. It represents a common deposit reflecting the longest run-out lengths, flow transformation, and hydraulic fractionation within low-density turbidity currents (Haughton et al., 2003). Its common occurrence at event bed tops indicates longer flow durations with sedimentation occurring predominantly by traction from dilute, turbulent flows and changes in capacity within the flow (Gardner et al., 2003).

Poorly-Sorted Mudstone-Rich Facies

Poorly-Sorted Mudstone (8A) Poorly-sorted mudstones are not common in the LMMF. They consist of poorly-sorted sediments that are matrix supported and rich in mudstone. They may consist of light gray mudstone-clasts up to 5 centimeters in diameter, bioclastic shell debris, a high concentration of volcaniclastic minerals, and sandstone with grain size up to pebbles. Poorly-sorted mudstones may be bounded by cross-stratification, convoluted bedding, or show no stratification. Facies thickness range from 9 centimeters to 1.1 meters, and average 42.5 centimeters. The facies is present within CC1B north of Waikiekie Stream, CC2 at Tutapuha Stream, and within siltstone

deposits that bound the channel belt at Tehoro Beach. The pebble size grains are only present north of Waikiekie Stream and represent the coarsest sediment found within the LMMF.

Interpretation: Deposition of poorly-sorted mudstone was likely by cohesive debris flows inferred by the high mudstone content and *en masse* deposition. *En masse* deposition explains the chaotic arrangement of the deposits, the presence of intact fossils, and the grain size variation from pebbles to mudstone (Mulder and Alexander, 2001). Flow transformation to a hyperconcentrated density flow may be responsible for the presence of cross-stratification.

Mudstone-Clasts Dispersed (8B) Matrix-rich siltstone deposits with dispersed mudstone-clasts are not common in the LMMF. When present, they frequently occur at bed tops within the transition from sandstone to siltstone. Millimeter- to centimeter-scale light gray mudstone-clasts are common, and bioclastic shell debris, volcaniclastics, and organics are present in some localities. Siltstone is the dominant grain size, although floating very fine grains of sandstone are typically present. Facies thickness range from 3 centimeters to 10 centimeters, and average 6 centimeters.

Interpretation: Deposition of mudstone-clasts dispersed within a matrix-rich siltstone represents deposition at the tail of a low-density turbidity current where minimal bed traction is still occurring. Mudstone-clasts were suspended by fluid turbulence and deposited through bed traction (Lowe, 1982; Mulder and Alexander, 2001).

Siltstone Facies

Concentrated Bands of Organic Carbon (8C) Matrix-rich siltstones with concentrated bands of organic carbon within beds are not common within the LMMF, although organic sediments are seldomly dispersed within a variety of other facies. This facies is dominated by siltstone with floating very fine sandstone grains and organic-rich lenses that are iron-rich. Facies thickness range from 3 centimeters to 11 centimeters, and average 7 centimeters when present.

Interpretation: Deposition was likely at the tail of low-density turbidity currents where subsequent pelagic suspension fallout of organic-rich sediments was able to accumulate at the bed tops above sand bearing siltstone. Shear velocity was likely low enough to prevent the stripping of organic material during subsequent flows (Mulder and Alexander, 2001).

Plane-Parallel Laminated (9A) Plane-parallel laminated siltstone is found across the LMMF, both within and bounding the channel belt, but not in abundance. It is commonly light gray or light tan and occurs above sandstone at the top of fining-upward successions. Horizontal laminations vary from millimeters to centimeters thick. Facies thickness range from 2 centimeters to 54 centimeters, and average 17.5 centimeters across the LMMF.

Interpretation: Plane-parallel laminated siltstone was likely deposited by traction and suspension sedimentation from low-density turbidity currents and represents the T_d division within a Bouma sequence (Lowe, 1982; Gardner et al., 2003).

Ripple-Laminated to Wavy-Laminated (9B) Ripple-laminated to wavy-laminated siltstone is found within and bounding the channel belt across the LMMF, but not in abundance. Commonly, it is light gray or light tan and occurs above sandstone at the top of fining-upward successions. Wavy laminations are more prevalent. Wavy- to ripple-laminated siltstone occur in beds that range in thickness from 2 centimeters to 55 centimeters, and average 8 centimeters. Thicker beds typically reflect more than one event bed, although it is difficult to distinguish their true thickness. Ripple- to wavy-laminated siltstone beds generally occur above ripple-laminated sandstone beds.

Interpretation: Ripple- to wavy-laminated siltstone was likely deposited by traction sedimentation at the tail of low-density turbidity currents where flow velocity was high enough to produce fine wavy laminations and ripple laminations reflecting textural sorting (Lowe, 1982). It represents a transition between the T_c and T_d divisions within a Bouma sequence.

Normal Graded (9C) Normal graded siltstone is common across the LMMF, both within and bounding the channel belt. It is typically found above fining-upward successions with sandstone below. The color varies from light gray to light tan or brown. No distinguishable sedimentary structures are seen in outcrop. It may have concretion horizons and interlamination with millimeter thick very fine-grained sandstone. Normal graded siltstones range in thickness from 1 centimeter to 55 centimeters, and average 11 centimeters.

Interpretation: Normal graded siltstone is inferred to represent flow stripping at the tail of flows and suspension sedimentation from low-density turbidity currents. It

likely reflects the T_d division within a Bouma sequence (Lowe, 1982; Gardner et al., 2003).

Mudstone Facies

Silty Mudstone (10A) Silty mudstone is light gray to dark gray in color and may be fissile. Moderate clay amounts are present. The presence of volcaniclastic minerals and silt sized volcaniclastic ash is also seen at multiple localities, although in low quantities. Beds may be interlaminated with very fine-grained sandstone beds that are less than 1 centimeter thick. Silty mudstones range in thickness from 2 centimeters to 1.05 meters, and average 29 centimeters.

Interpretation: Silty mudstone was likely deposited by low-density turbidity currents and may represent the tail of the flow (Middleton, 1993; Lowe, 1982). The flow was likely losing its competence and capacity to carry sediments and may reflect suspension settling (Hiscott, 1994). It likely represents the T_e division within a Bouma sequence.

Clay Dominated (10B) Clay dominated mudstone is dark gray to brown in color and may be fissile. Laminated to interlaminated beds range in thickness from 2 centimeters to 1 meter, and average 17.5 centimeters. Clay size grains are most prevalent, but a mixture of silt to very fine sandstone grains are present in low quantities. Beds may have a greasy appearance.

Interpretation: Deposition of clay dominated mudstone is inferred to be by low-density turbidity currents where flows nearly lost their capacity and competence to carry

sediments (Hiscott, 1994). It likely represents the T_e division within a Bouma sequence with suspension settling at the tail of the flow.

Claystone (11A) Claystone is typically found bounding channelized intervals. Deposits are dark brown to light gray in color and are dominated by clay size particles. Claystone generally occurs above volcaniclastic sandstones and may have fine grain mineral crystals dispersed throughout. Rarely, organic-rich intervals and fossils may be present. These intervals can be bioturbated. Facies thickness range from 2 centimeters to 65 centimeters, and average 6.5 centimeters.

Interpretation: Sedimentation by pelagic and hemipelagic suspension fallout is inferred. The presence of volcaniclastic minerals, organic-rich intervals, and fossils likely indicates a decrease in clastic sedimentation. Suspension settling likely dominated mud deposition with low shear velocity (Middleton et al., 1984).

Calcareous Facies

Calcareous-Rich (11B) Calcareous-rich facies are found within the axis of channel deposits and within mudstone-rich intervals above the channels. Bioclastic shell debris is common. Rarely, large intact fossils are present. The largest fossils were found within poorly-sorted mudstone-rich beds north of Waikiekie Stream in CC1B. Calcareous facies in mudstone-rich deposits may include concretions, volcaniclastic-rich siltstone intervals, and bioturbation. Calcareous facies in sandstone-rich deposits typically coincide with scouring or large erosional contacts. Facies thickness in event beds range from 1 centimeter to 23 centimeters, and average 6.5 centimeters.

Interpretation: Calcareous mudstone-rich intervals with bioclastic shell debris likely represent small slumps originating along channel margins or updip on the slope. Flows may have transitioned from matrix-supported debris flows to muddy hyperconcentrated density flows or turbidity currents downslope (Lowe and Guy, 2000). Sandstone-rich intervals with bioclastic shell debris within small scours or scattered throughout likely represent deposition by high-density turbidity currents (Lowe, 1982).

Post-Depositional Facies

Deformed; Mass-Transport Deposit (MTD) (12) Mass-transport deposits vary in thickness and lithology. They generally are mudstone-rich with varying amounts of volcaniclastics, shell debris, and sandstone, although one sandstone-rich mass-transport deposit was documented. The thickness of beds and degree of deformation or folding changes between localities across the LMMF. Mass-transport deposits seemingly transition from undeformed intervals to deformed intervals from one locality to another. Sandstone injections and rafting of large blocks is also common. Mass-transport deposits generally have steeper bedding attitudes than the surrounding stratigraphy and vary in thickness from 1 meter to up to 15 meters.

Interpretation: Deposition was by mass-transport or slumping of sediment. Slumping may have been triggered by oversteepening, sediment loading, release of gas hydrate, overpressure of pore fluids, or fluid venting (King et al., 2011).

Concretions, Cementation (13) Concretions are common within mudstone-rich deposits, but also are present within sandstones and near faulted intervals. They are often

ovoid or spherical in shape and range in size from a few centimeters up to 50 centimeters wide. The largest concretions are present north of Waikiekie Stream near the Mangapukatea Fault. Concretions most commonly occur along bedding contacts, but also can be present where large concentrations of bioclastic shell debris is found. Facies thickness range from 3 centimeters to 32 centimeters, and average 8 centimeters.

Interpretation: Concretions reflect post-depositional modification after burial. Fluids likely moved along bedding planes and also along faults, precipitating cement around various nuclei. Concretions also may be associated with bioclastic shell debris at some localities. Multiple studies have analyzed concretions within the MMF and the overlying Urenui Formation. Tubular carbonate concretions sometimes reflect the escape of subsurface fluids and/or hydrocarbon gases (Pearson et al., 2010; Nyman et al., 2006).

Burrowed and Bioturbated Sandstone (14A) Burrowed and bioturbated sandstone is common throughout the LMMF in thinning-upward successions near the top of channel bodies and outside channel bodies. Sandstones are generally very fine-grained and poorly- to moderately-sorted. Structureless sandstone or plane-parallel lamination may be present, although original sedimentary attributes are typically overprinted by intense bioturbation. Vertical escape burrows and horizontal infill traces are common. Facies thickness range from 1 centimeter to 60 centimeters, and average 8.5 centimeters.

Interpretation: Bioturbated and burrowed sandstone reflects post-depositional modification by organisms present on the sea floor. Sedimentation of sandstone was likely due to low-density turbidity currents (Lowe, 1982). Changes in the type of traces,

frequency, and density are related to nutrient supply, oxygenation, sediment supply, and depositional environment (Manley and Lewis, 1998).

Burrowed and Bioturbated Siltstone (14B) Burrowed and bioturbated siltstone is common throughout the LMMF in thinning-upward successions. It commonly is present above bioturbated sandstone. Beds are generally intensely bioturbated throughout, and horizontal burrows are found at bed tops. Burrows typically crosscut one another, and tend to be filled with silty sandstone. Facies thickness range from 1 centimeter to 1.75 meters thick, and average 23 centimeters.

Interpretation: Bioturbated and burrowed siltstone reflects post-depositional modification by organisms present on the sea floor. Sedimentation of siltstone was likely due to hemipelagic settling of sediments or deposition of sediments that were in suspension from low-density turbidity currents. Suspension sediments from low-density turbidity currents would be classified as the T_e division in a Bouma sequence (Middleton and Hampton, 1973; Lowe, 1982).

Tuffaceous Facies

Volcaniclastic Sandstone (15) Volcaniclastic sandstone deposits are predominantly found outside channel margins within the LMMF, but also occur less frequently within the channel fill. Volcaniclastic minerals consist of plagioclase, hornblende, oxides, and a low percentage of clino- and orthopyroxene described from thin section analysis. Mineral crystals range from fine- to coarse-grained and may be accompanied by very fine- to fine-grained sandstone matrix. Angular white plagioclase

minerals are most recognizable in outcrop. Beds are typically dark brown to tan in color. Facies thickness range from <1 centimeter to 45 centimeters in more sandstone-rich beds, and average 3 centimeters. Within channel bodies, volcaniclastic sandstone is commonly found at the base of massive sandstone beds.

Interpretation: Volcaniclastic sandstone likely represents fall-out of coarse-grained suspended volcaniclastic deposits after a volcanic eruption and resedimentation by low-density turbidity currents (Schneider et al., 2001; Lowe, 1982).

Volcaniclastic Mudstone (16) Volcaniclastic mudstone deposits are predominantly found outside channel margins within the LMMF. Thin section analysis identifies siltstone size angular volcaniclastics in a siltstone to mudstone matrix. Pockets of coarse-grained volcaniclastic mineral crystals and biotite mica are also common throughout. Minerals consist of plagioclase, hornblende, oxides, and a low percentage of clino- and orthopyroxene described from thin section analysis. Bioclastic shell debris is also present in thin sections from multiple localities. Facies thickness range from <1 centimeter to 110 centimeters in beds with discontinuous coarse-grained lenses. Average thickness is 28 centimeters.

Interpretation: Volcaniclastic mudstone likely represents hemipelagic fall-out very fine-grained suspended volcaniclastic ash deposits following a volcanic eruption. Resedimentation by low-density turbidity currents also may contribute to the deposition of gradational volcaniclastic mudstone beds that overlie volcaniclastic sandstone (Schneider et al., 2001; Lowe, 1982).

Thin Section Analysis

Thin section analysis was completed for 7 samples collected within the LMMF. Thin section photos are presented in Appendix 2. The 7 samples are characterized by volcaniclastic-rich sandstone, poorly-sorted mudstone-rich beds, and volcaniclastic mudstone. Collected samples reflect sediments that showed characteristic changes within the outcrop, but their origin was not completely understood.

Sample 1 was collected from volcaniclastic siltstone at Locked Gate. It shows silt sized grains that dominate within a mudstone matrix. Small pockets of coarse-grained volcaniclastic minerals and fossils are also present. Minerals consist primarily of quartz and plagioclase, although smaller amounts of biotite, hornblende, and oxides are present.

Sample 2 was collected within a bioclastic and volcaniclastic-rich interval at Locked Gate within the upper composite of CC1B. It shows a wide range of grain size, mineralogy, and bioclastic input. Grain size varies from mudstone up to coarse-grained, and the presence of large fossils is common. Volcaniclastic minerals consist of plagioclase, hornblende, and oxides, as well as low percentages of clino- and orthopyroxene. Biotite mica is also common throughout.

Sample 3 was collected north of Waikiekie Stream in CC1B from a poorly-sorted mudstone-rich bed. Grain size variation is represented by mudstone, fine- to medium-grained sandstone, and coarse-grained volcaniclastic minerals. Large fossils are common. Volcaniclastic minerals consists of plagioclase, hornblende, and oxides, as well as low percentages of clino- and orthopyroxene.

Sample 4 was collected north of Waikiekie Stream in CC1B from a poorly-sorted muddy sandstone. Less mudstone is seen within this sample compared to sample 3. Grain size varies from fine-grained sandstone to very coarse-grained volcaniclastic minerals. Large fossils are also present within this sample. Volcaniclastic minerals consists of plagioclase, hornblende, and oxides, as well as low percentages of clino- and orthopyroxene.

Sample 5 was collected south of Waikiekie Stream in a siltstone dominated volcaniclastic mudstone. Silt size grains dominate within a mudstone matrix. Sharp and angular volcaniclastic silt size grains are inferred to represent volcaniclastic ash. Pockets of very fine-grained volcaniclastic mineral crystals and small fossils are also present.

Sample 6 was collected south of Waikiekie Stream within a siltstone bearing volcaniclastic sandstone with millimeter-scale mudstone-clasts. The sample is poorly-sorted with grain size from mudstone up to fine- to medium-grained quartz and volcaniclastic minerals. Volcaniclastic mineral crystals are angular to sharp, and quartz is sub-angular. Millimeter-scale mudstone-clasts that are well rounded and show little to no shearing.

Sample 7 was collected below CC1B at Tutapuha Stream in an organic bearing volcaniclastic mudstone. Within the outcrop, this sample had a fully articulated very small leaf fossil preserved. The sample is poorly-sorted with grain size from mudstone up to coarse-grained volcaniclastic minerals. The sample shows high amounts of alteration, likely reflected by the precipitation of iron between grains.

Mudstone-Clast Conglomerate Facies

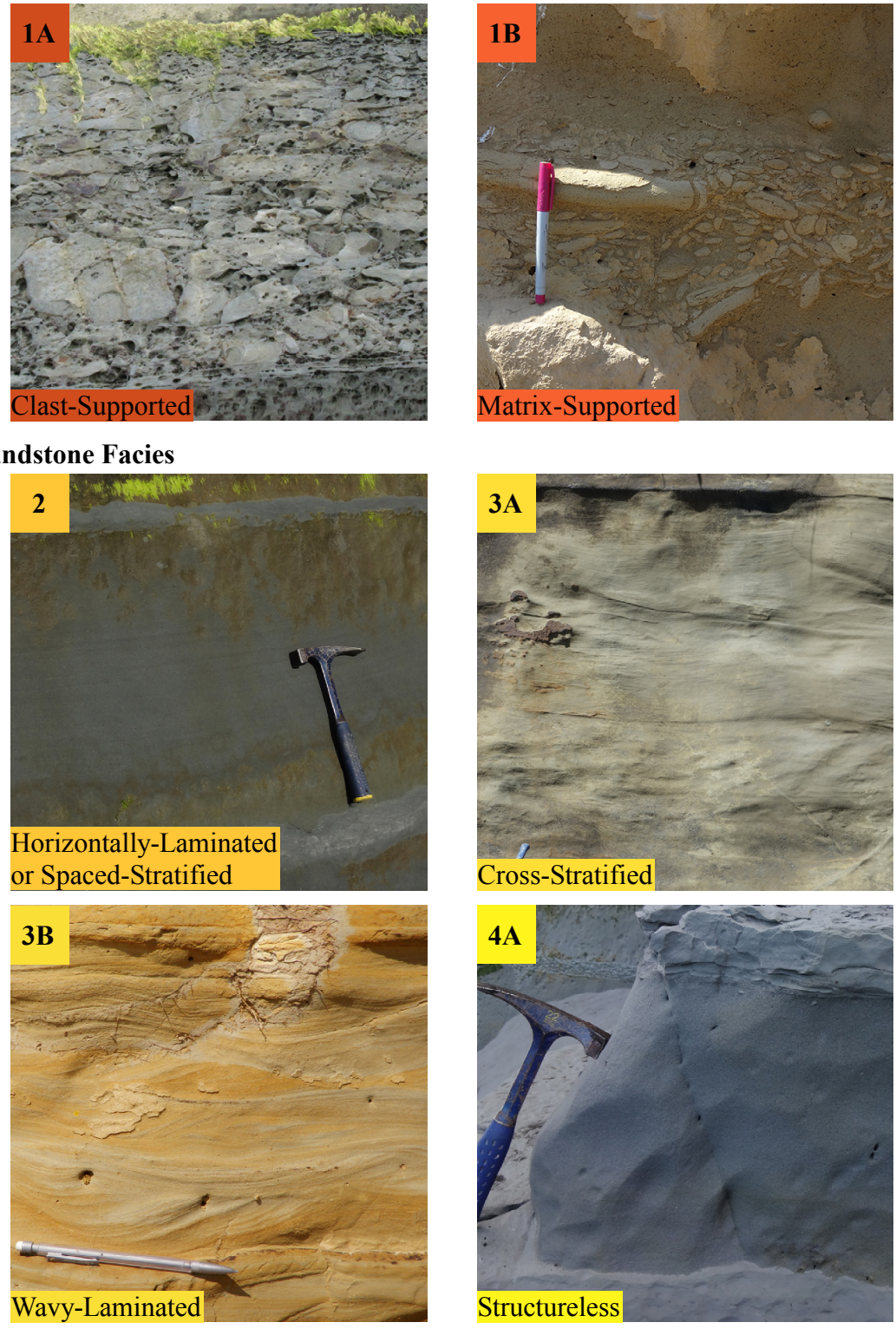


Figure 6. Photos of sedimentary facies documented within the Lower Mount Messenger Formation.

Sandstone Facies continued

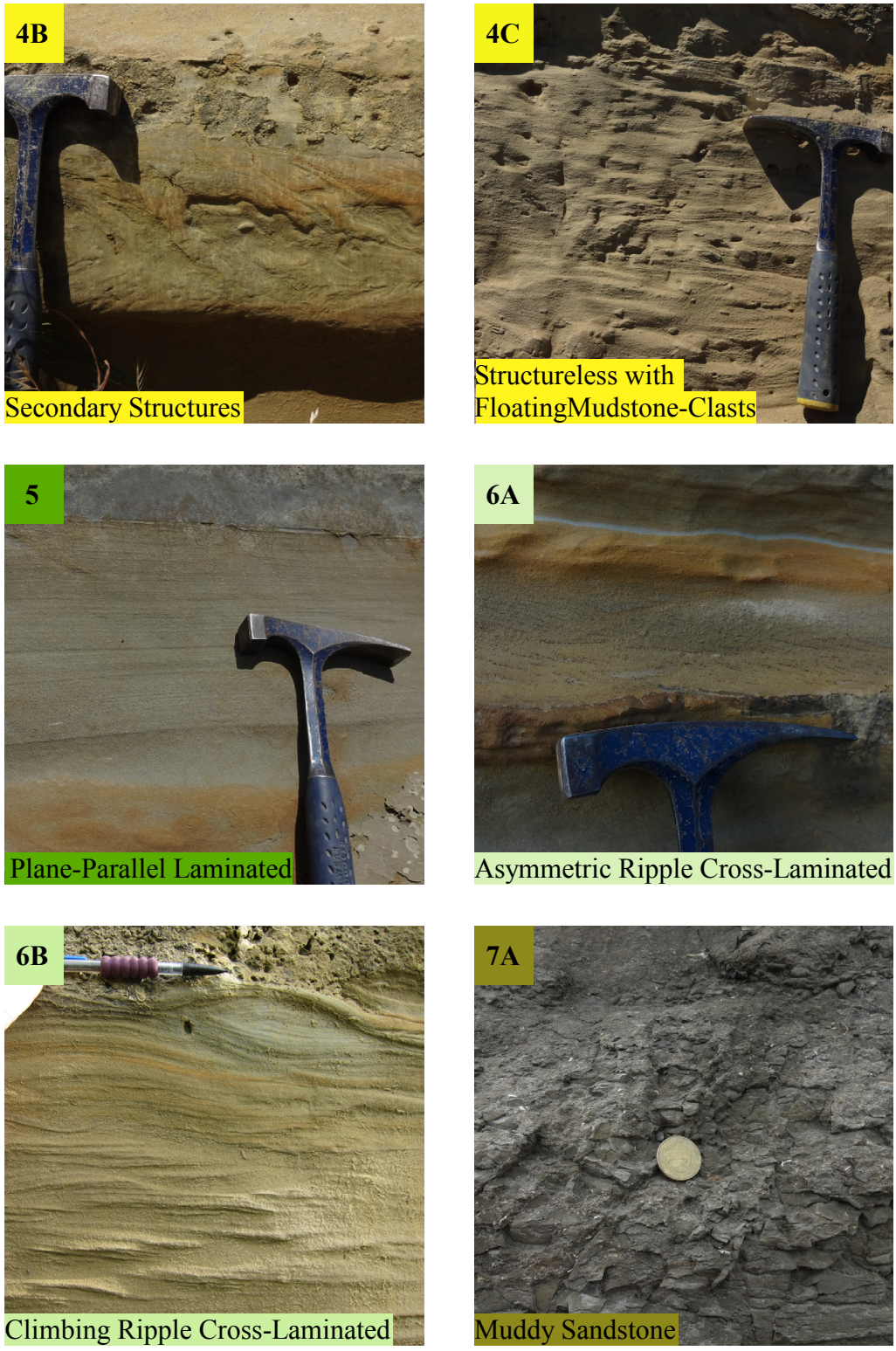


Figure 6. (Continued) Photos of sedimentary facies documented within the Lower Mount Messenger Formation.

Sandstone Facies continued

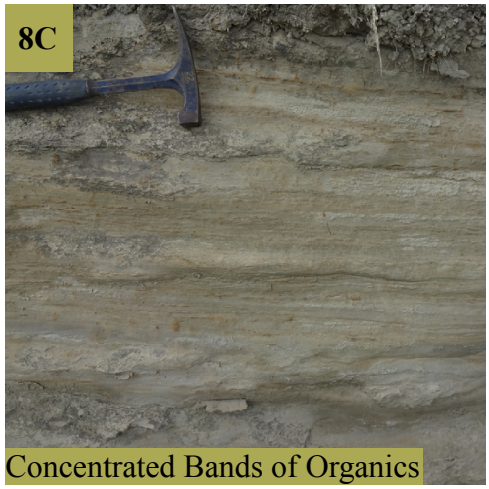




Siltstone and Mudstone Facies







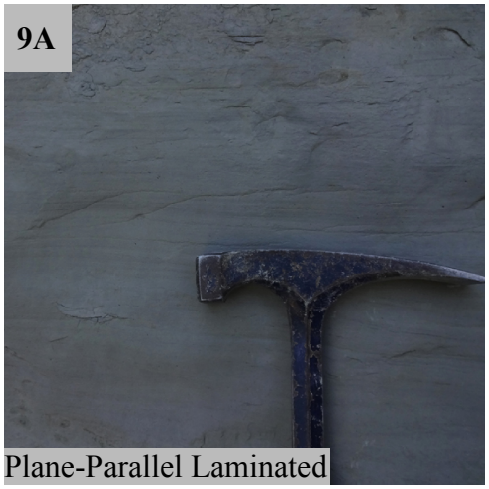


Figure 6. (Continued) Photos of sedimentary facies documented within the Lower Mount Messenger Formation.

Siltstone and Mudstone Facies continued

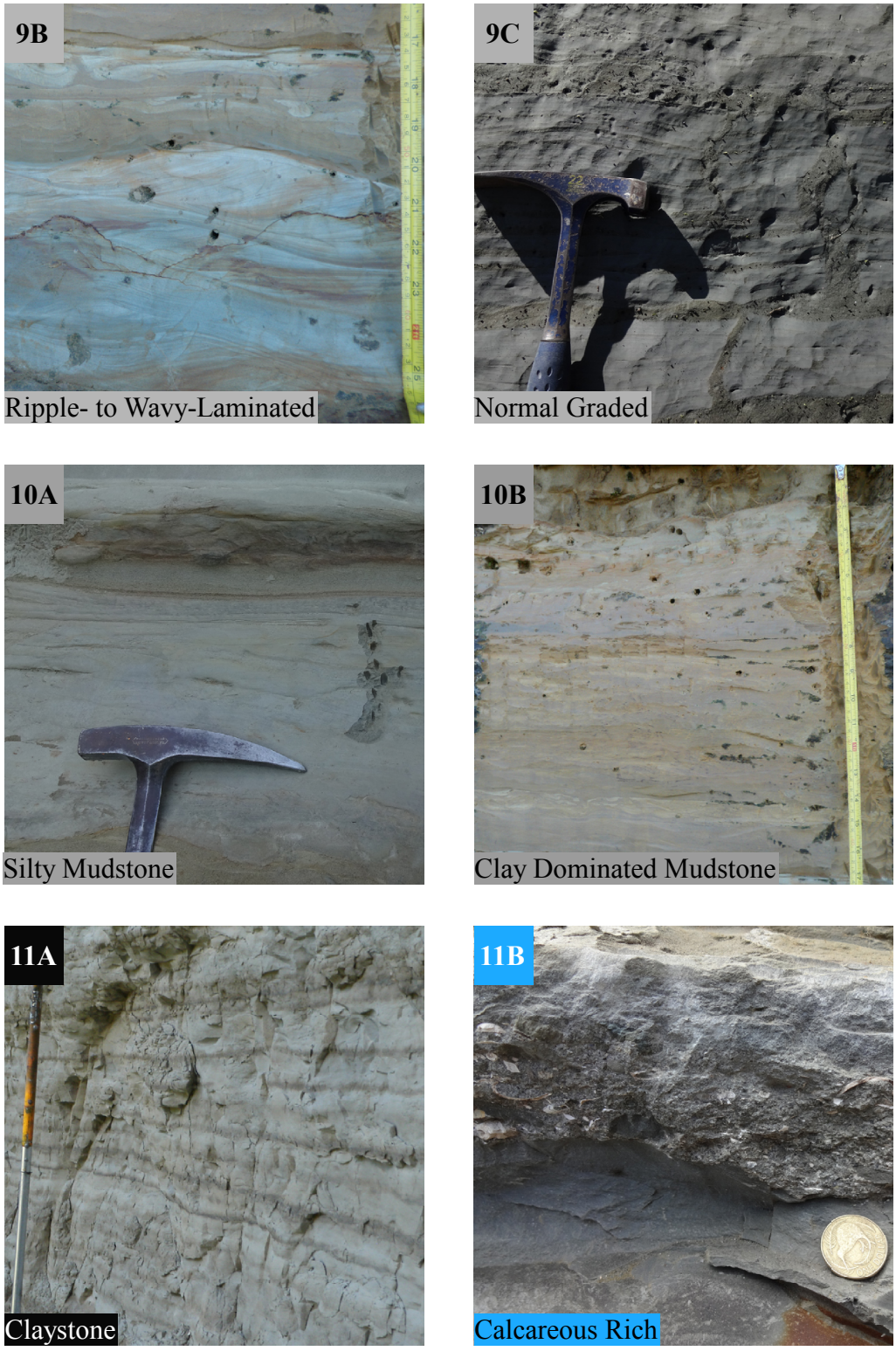
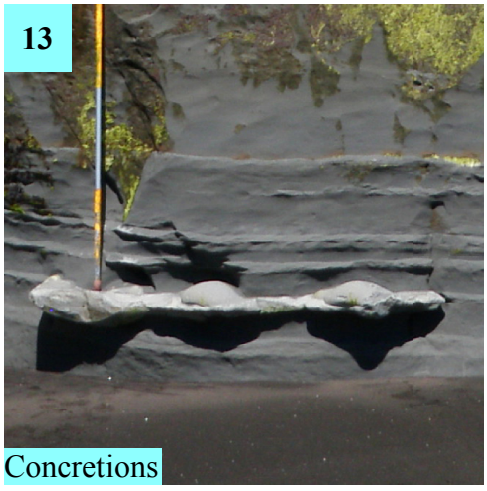
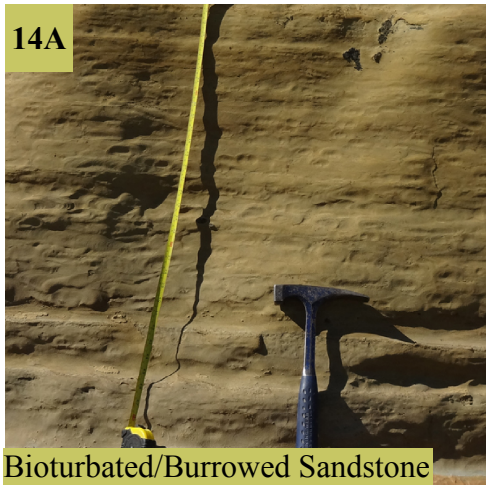


Figure 6. (Continued) Photos of sedimentary facies documented within the Lower Mount Messenger Formation.

Post-depositional Facies









Tuffaceous Sandstone and Siltstone Facies

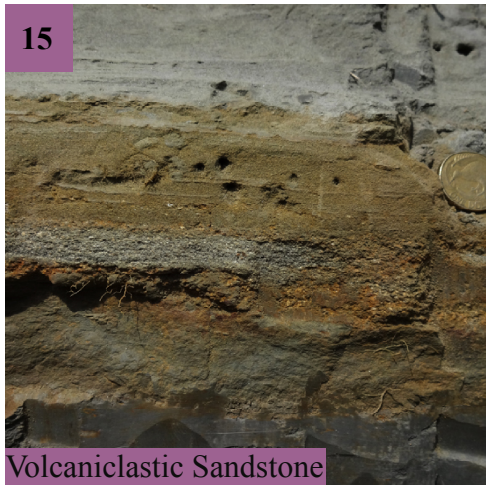




Figure 6. (Continued) Photos of sedimentary facies documented within the Lower Mount Messenger Formation.

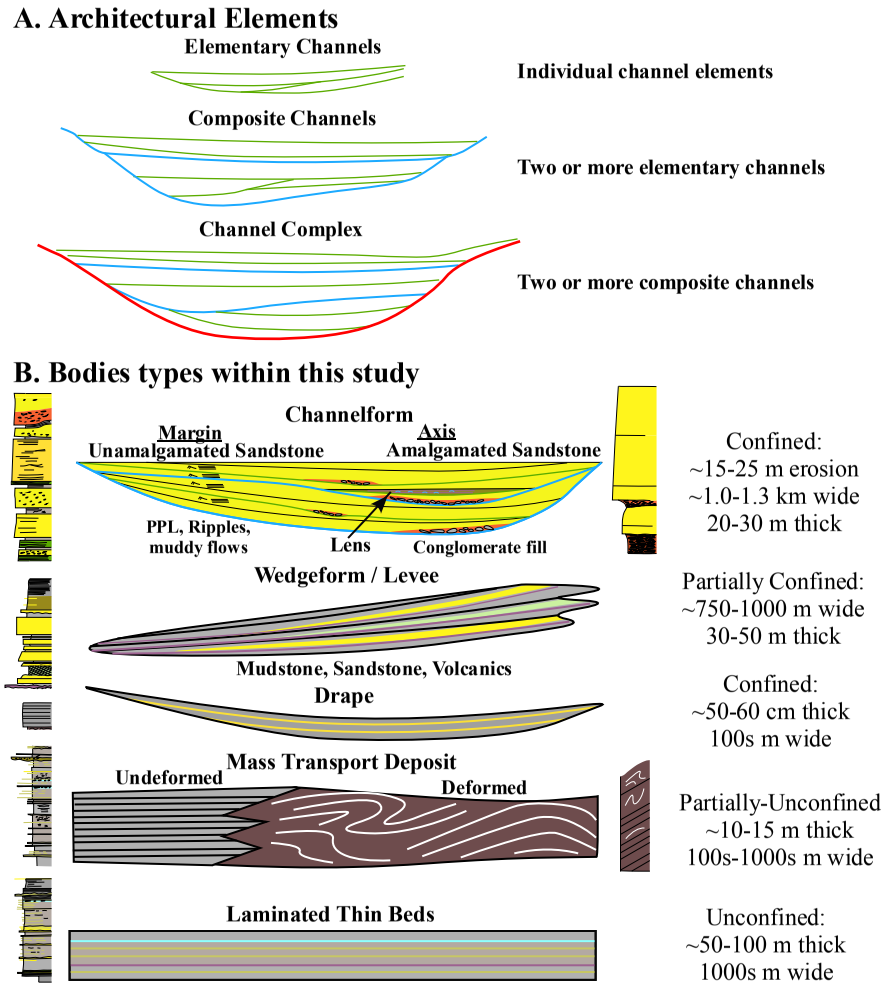
ARCHITECTURAL ELEMENT ANALYSIS

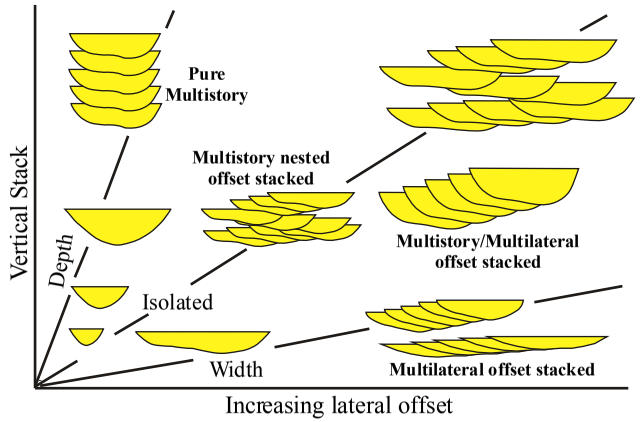
Definition and Terminology

Sedimentary bodies, also known as architectural elements, are three-dimensional mesoscale shapes defined by their external geometry, internal geometry, lithofacies assemblage, and their bounding surfaces (Allen, 1983; Miall, 1985; Clark and Pickering, 1996). Architectural elements in this study are defined by multiple recognition criteria. These include the shape, lithology, cross-cutting relationships, facies associations, and lateral correlation of bodies across the study area.

Architectural elements vary in scale and complexity, with smaller elements stacking to form larger elements (Allen, 1983; Sprague et al., 2005). First order contacts are defined by the bounding of individual cross-bedding sets and cross-strata (Allen, 1983). Contacts typically reflect erosion, and are planar or concave up (Allen, 1983). These are defined as elementary channels in this study. Second order contacts reflect sedimentation units that are genetically related by facies (Allen, 1983). These are termed composite channels by this study. Third order contacts divide groupings of composite channels, or "complexes" defined by Allen, from each other by major erosional surfaces (1983). These are termed channel complexes within this study (Figure 7).

This stacking forms a hierarchy of scales, recognized by bedding contacts of variable significance (Allen, 1983; Miall, 1985; Sprague et al., 2005). Within subaqueous flows, alternating phases of deposition and erosion create various sedimentary bodies, which are fundamental building blocks of deep-water systems (Mutti





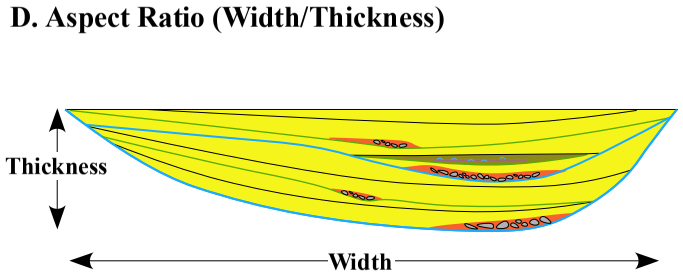


Figure 7. A) Architectural element stacking of elementary channels representing individual channel elements, composite channels with two or more elementary channels, and channel complexes with two or more composite channels. B) Body types and their associated geometry within the study area shown with example sedimentological profiles. C) Channel stacking patterns (horizontal and vertical offset) for channel complexes (modified from Clark and Pickering, 1996). D) Channelform aspect ratio (width/thickness).

and Normark, 1987). Variation of sedimentary bodies reflect changes related to the depositional system that include confinement, sediment accumulation rate, and gradient (Gardner et al., 2003, 2008).

Sedimentary Bodies

Sedimentary bodies within the study area include channelforms, wedgeforms, lobeforms, drapes, mass-transport deposits, and laminated thin beds (Figure 7). Lobeforms are inferred to be present near the base of the LMMF from previous studies (King et al., 1993; Helle, 2003; Masalimova, 2013). They are not discussed here, but were referenced for their spatial context within the stratigraphy during field work. Mass-transport deposits are found below the base of channelforms within the study area, and are thought to influence the subsequent influx of sand (King et al., 2011). They are discussed first due to their importance to the overlying channelized intervals.

Mass-Transport Deposits

Mass-transport deposits (MTDs) consistently occur at or near the tops of individual inner-fan depositional cycles (King et al., 2011). Outcrop exposures vary in scale from 1 meter up to 15 meters, and are observed with sharp, planar basal surfaces. The main lithology in MTDs is siltstone with minor sandstone, although one sandstone-rich mass-transport deposit is observed at the Locked Gate locality (Figure 19). Volcaniclastic mineral crystals and shell debris are commonly found scattered throughout the strata. Channelized intervals within the study area typically overlie MTDs.

MTDs consist of folded thin-bedded strata, and in some localities large rafted blocks of sandstone. They typically show an angular discordance to the surrounding stratigraphy, with beds dipping up to 10 degrees compared to the average dip of 5-6 degrees in the study area. At the North Waikiekie locality, the NWK MTD shows isoclinal folding and the presence of a slump detachment surface (King et al., 2011) (Figure 2, 3, 8). The thickness of this interval is up to 15 meters, with rafted sandstone blocks from the overlying CC1A body incorporated into the flow (Figure 8). The mass-transport deposit seemingly transforms from undeformed mudstone deposits east of Gibb's Hill, locally deformed mudstone to the south, and fully deformed strata at the North Waikiekie locality (Figure 8).

The Waikiekie Stream MTD is present north and south of Waikiekie Stream (Figure 9). It is approximately 13 meters thick, and shows internal deformation and folding of siltstone and sandstone deposits. Moderate amounts of volcaniclastic minerals and bioclastic shell debris are also present. The top of the MTD is planar, reflecting erosion by subsequent flows, and the deposition of a fine-grained drape above (Figure 9). Similar to the NWK MTD, the Waikiekie Stream MTD reflects a transformation from undeformed mudstone deposits at Tutapuha Stream, to partially deformed mudstone and sandstone at Locked Gate, and fully deformed strata at Waikiekie Stream (Figure 9). Channelized sandstones of CC2 to CC4 are present above the Waikiekie Stream MTD within coastal outcrops.

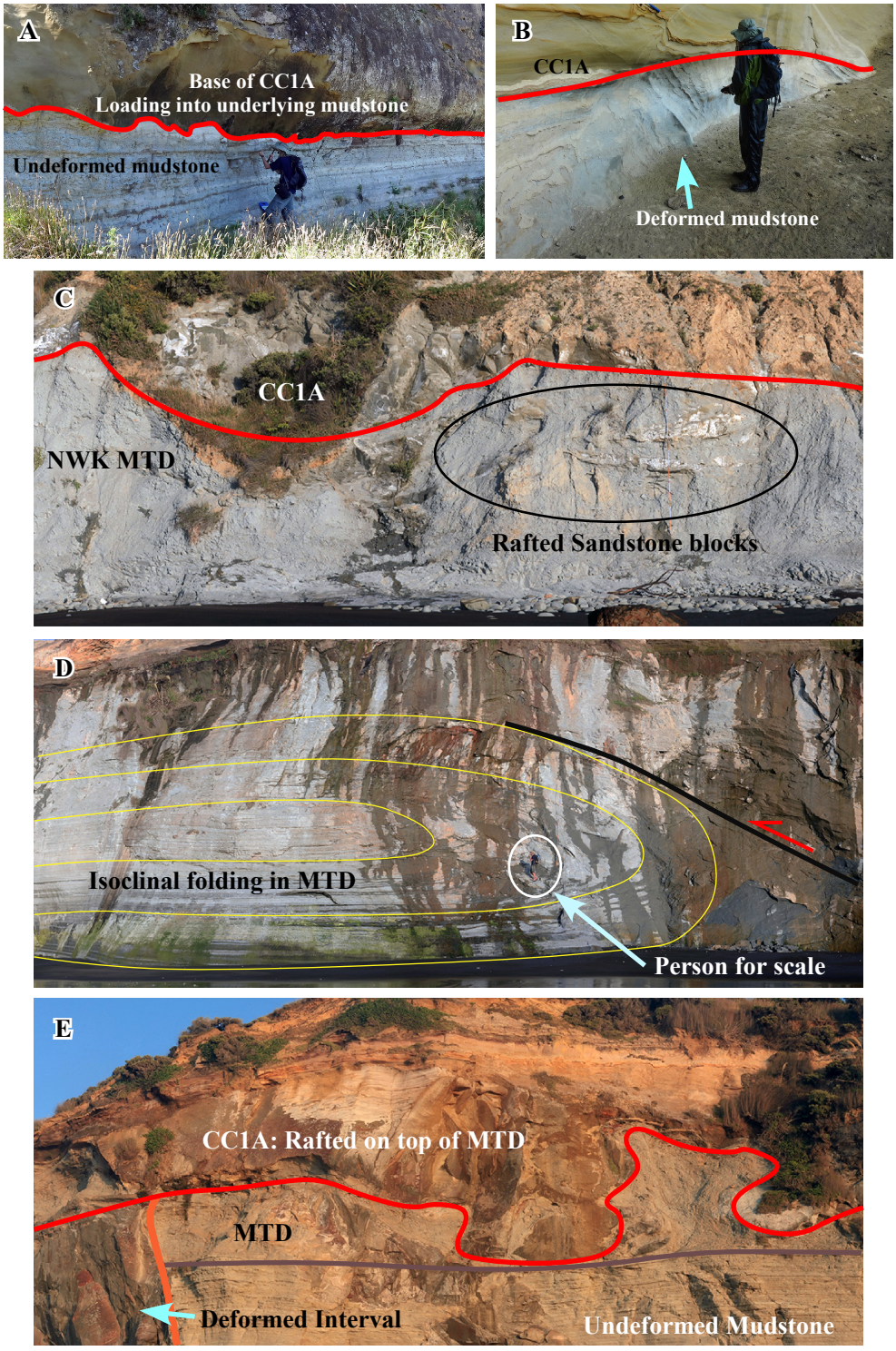


Figure 8. Photos of deformation in the NWK MTD. A) Undeformed mudstone below CC1A east of Gibb's Hill. B) Locally deformed mudstone below CC1A east and south of Gibb's Hill. C) NWK MTD in coastal outcrops north of Waikiekie Stream with rafted sandstone blocks. D) Isoclinal fold below inferred slump detachment surface. E) CC1A rafted by the NWK MTD above undeformed mudstone.

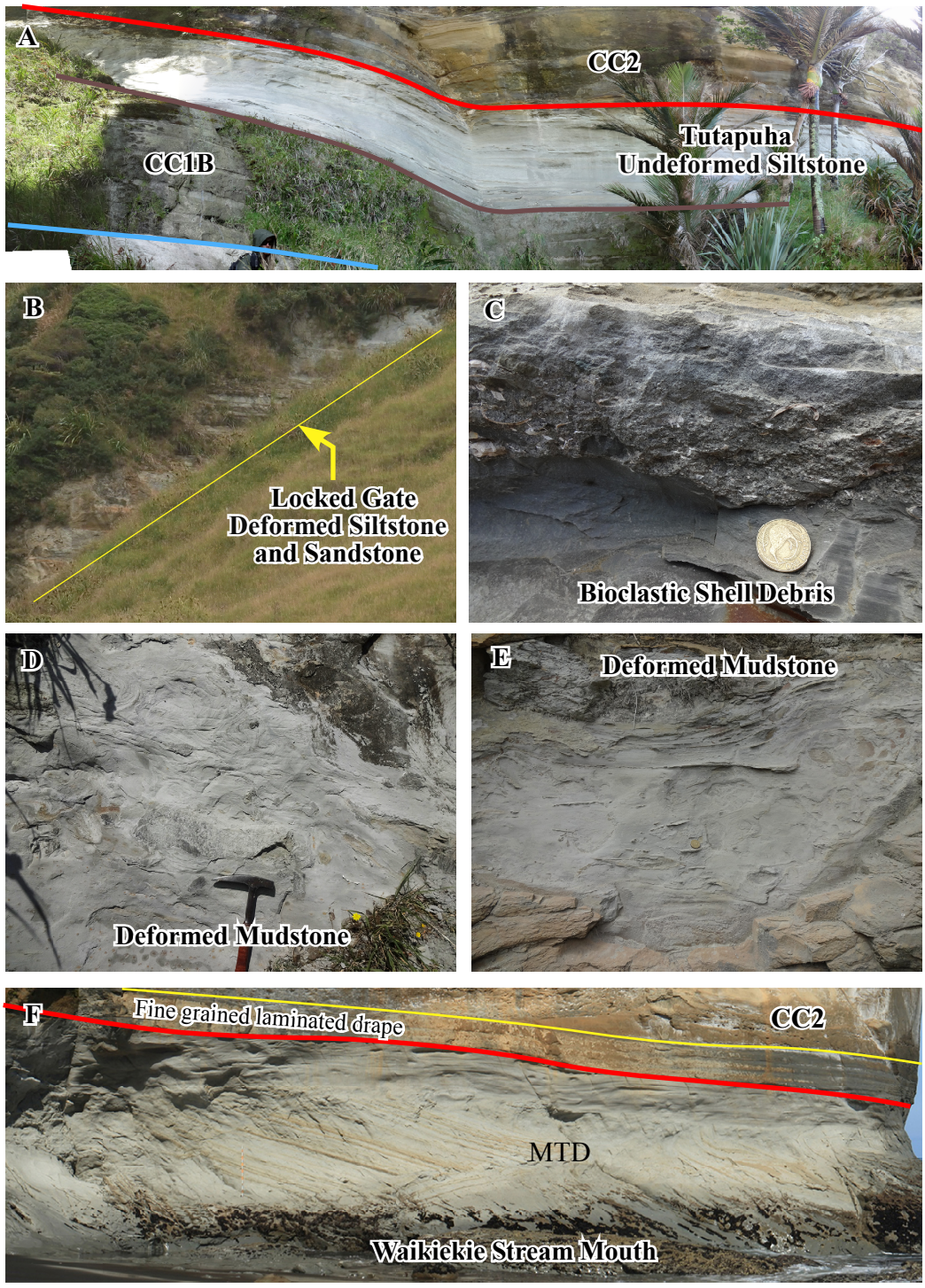


Figure 9. Photos of deformation in the Waikiekie Stream MTD. A) Undeformed mudstone below CC2 east of Tutapuha Stream. B) Locally deformed mudstone below CC2 at the Locked Gate locality. C) Bioclastic shell debris within deformed beds at Locked Gate. D) Deformed mudstone at Locked Gate. E) Deformed mudstone and thin sandstone beds at Locked Gate. F) Waikiekie MTD at Waikiekie Stream mouth overlain by CC2 with a fine grained laminated drape.

The Locked Gate MTD is approximately 1.5 meters thick and consists of folded mudstone. It is present above CC2 within the inland outcrops. To the west of Locked Gate, this MTD changes to folded sandstone with thin beds of siltstone (Figure 18, 19). This is inferred to represent cannibalization of the MTD by the overlying CC3 channel, which is seen down-cutting and eroding through the stratigraphy immediately to the east. Multiple erosional surfaces with mudstone-clast conglomerate are present above and below the folded interval. The Locked Gate MTD is not present within the coastal exposures.

Channel Complexes

Channel complexes within the LMMF are the preserved remnants of ancient channels. As the main conduits for sediment transport, channels serve as the principle deep-water sedimentary body type (Barnes and Normark, 1985; Clark and Pickering, 1996; Gardner and Borer, 2000). Their sediment-fill and bounding surfaces provide insight into the evolution of a channel and the subaqueous flow processes that were present as the channel filled (Gardner and Borer, 2000). Six sandstone-filled channel complexes are locally recognized in the study area.

Channel Complex 1A The lowermost channel complex (1A) is present within inland outcrops at the Gibb's Hill and Mackenzie Ridge localities, and north of Waikiekie Stream (Figure 2). Erosion present at the base of CC1A is less than the overlying channel complexes with approximately 10 meters relief. It commonly shows massive sandstones loading into the underlying mudstone. Underlying mudstones are undeformed near the

northern exposure extent, locally deformed to the south, and fully deformed north of Waikiekie Stream where it represents the NWK mass-transport deposit (Figure 2, 8). Thickness is approximately 25 meters within the study area.

Matrix-supported and clast-supported mudstone-clast conglomerate are locally developed along multiple intervals near the base of the complex, along with occasional rafting of large ~5 meter wide sandstone blocks with convoluted bedding (Figure 10). Massive-bedded sandstones commonly have large erosional surfaces present internally, truncating the underlying stratigraphy. The highest erosion is present at Gibb's Hill, although multiple surfaces east of the locality show erosion up to 7 to 10 meters, filled with mudstone-clast conglomerate (Figure 10). To the south, beds show less erosion, occasionally scouring less than a meter into underlying strata.

Multiple elementary channels and composite channels are inferred to be present within CC1A. Correlation of bodies between localities was completed with low confidence due to high vegetation cover. Event bed analysis assisted with correlation, and is discussed in chapter 4. At least two composite channels are inferred, with at least 7 elementary channels present in the uppermost composite channel (Figure 10). Width and thickness measurements of the elementary and composite channels were not possible due to incomplete outcrop extent, and correlations between outcrops reflecting a transect that is parallel with paleoflow analysis.

The width of CC1A is difficult to determine. The north and south margins are not exposed within the study area, although thick-bedded climbing ripple cross-laminated sandstone successions present north of Waikiekie Stream are correlated to CC1A, they

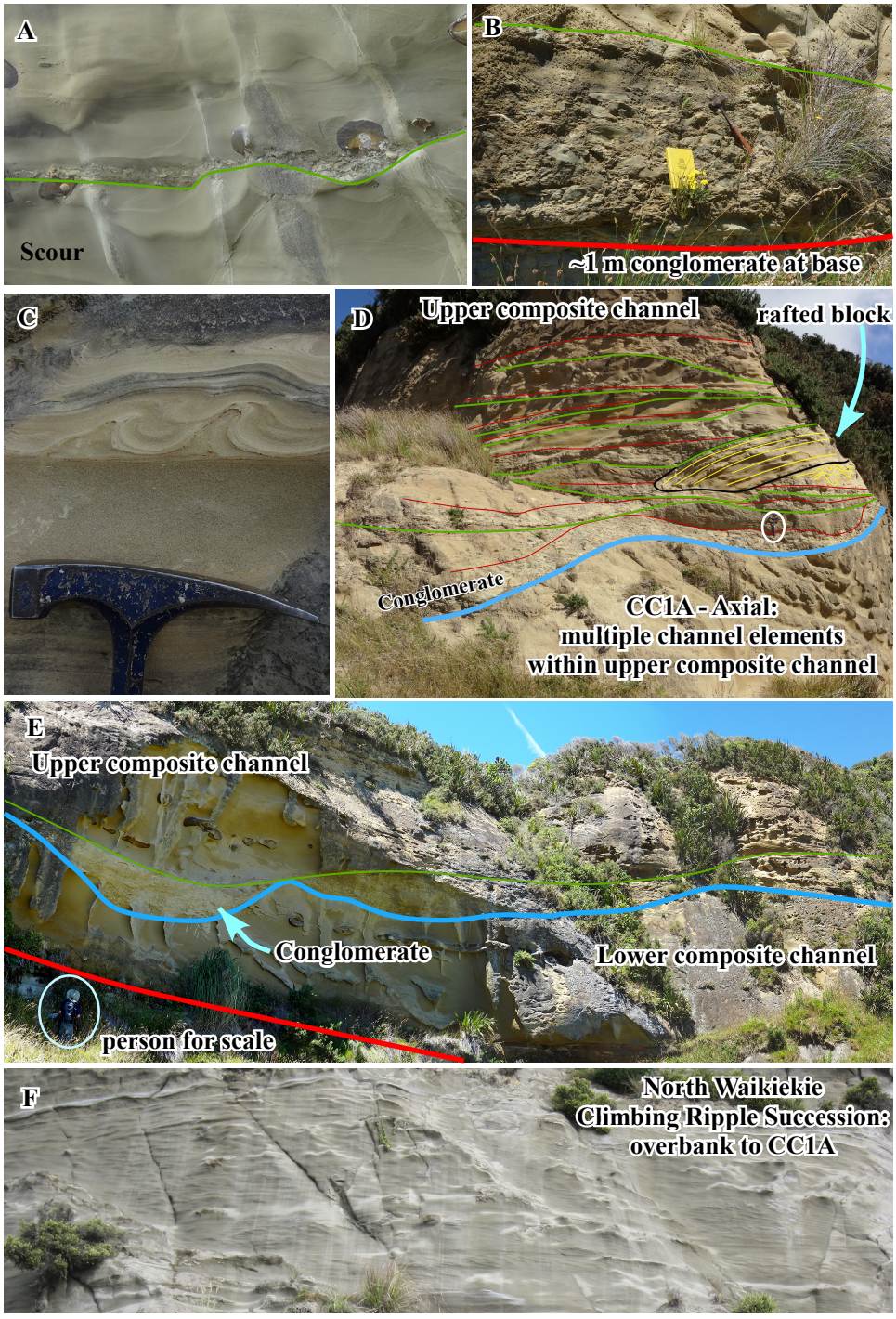


Figure 10. Photos of CC1A architectural elements A) Minor scouring with mudstone-clast conglomerate above. B) Erosion at the base of CC1A with ~1 meter of mudstone-clast conglomerate deposited above. C) Flame structure preserved east of Gibb's Hill. D) Inferred Axis of CC1A at Gibb's Hill showing multiple elementary channels and a rafted block within the upper composite channel. E) CC1A east of Gibb's Hill with exposure of the upper and lower composite channels. F) Climbing ripples within coastal outcrops north of Waikiekie Stream interpreted as overbank deposits to CC1A.

likely represent overbank deposition outside the channel margin. One exposure of massive-bedded sandstone correlated within CC1A is present immediately north of Warekarianga Stream in the inland outcrops. Estimates of channel width infer the channel margin between this locality and the climbing ripple cross-laminated sandstone succession north of Waikiekie Stream. Width/thickness measurements for CC1A reflect a minimum 1.3 km wide channel that is approximately 25 meters thick (~52:1 aspect ratio) (Table 3).

Channel Complex 1B Channel complex 1B is present within the inland outcrops from Warekarianga Stream to the Locked Gate locality, and north of Waikiekie Stream (Figure 2). One margin is fully exposed near Warekarianga Stream and shows erosional relief of approximately 15 to 20 meters into the underlying mudstone (Figure 11). Thickness is approximately 27 meters within the study area.

The base of CC1B erodes into thin-bedded mudstone and volcaniclastics that are undeformed. Exposures of the channel base are only present within the inland outcrops. The top of CC1B is marked by the presence of undeformed mudstone at Tutapuha Stream that progressively becomes more deformed near Locked Gate, and a mass-transport deposit north and south of Waikiekie Stream.

Multiple elementary channels and composite channels are inferred for CC1B. Three composite channels were identified with confidence, and the presence of a fourth may be possible. Truncation and lateral variation within the composite channels north of Waikiekie Stream complicates correlation. Elementary channels appear to dominate the

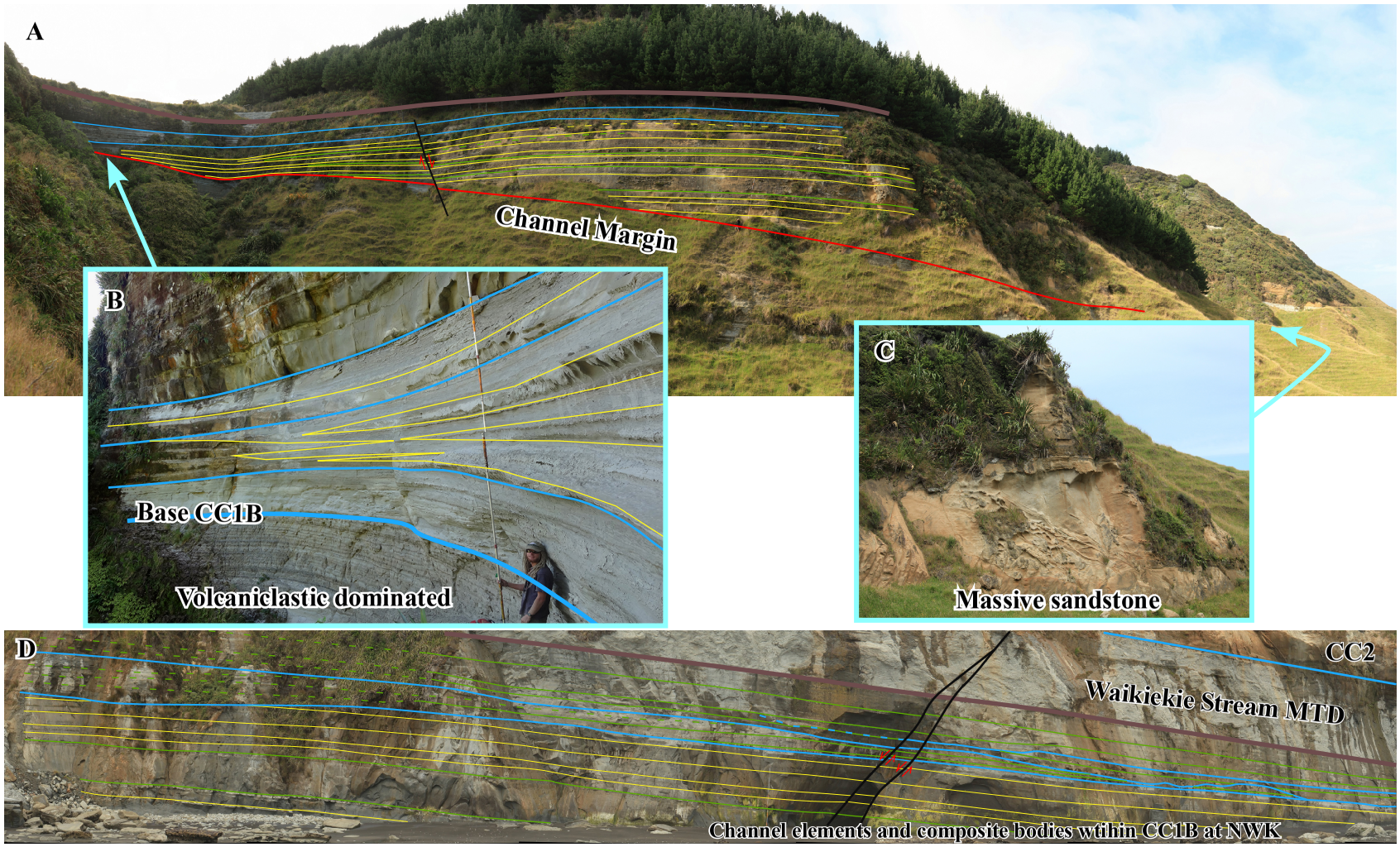


Figure 11. A) Major erosional surface of CC1B at Warekarianga Stream showing correlations along the channel margin. B) Interfingering sandstones and siltstones along the channel margin of CC1B. C) Massive amalgamated sandstone within CC1B at Tutapuha Stream. D) Lateral bed correlations north of Waikiekie Stream showing multiple composite bodies and elementary channels.

lower stratigraphy of the channel complex with little variation and truncation of beds. Minor scouring is present.

The channel fill of CC1B shows less internal erosion than the underlying CC1A, and the abundance of mudstone-clast conglomerate is significantly lower. Sandstone beds are typically massive, amalgamated, and show a variety of sedimentary structures. Erosional scours with up to 50 centimeters relief are filled with matrix-supported mudstone-clast conglomerate. The margin of the channel at Warekarianga Stream shows multiple interfingering sandstone beds that thin and subsequently thicken outside the channel margin (Figure 11). This may reflect lateral avulsion within the channel or the spilling of sandstone toward the channel levee.

North of Waikiekie Stream, massive amalgamated sandstone is prevalent, although siltstone partings between massive beds are common. Bed variation increases up-dip, and laterally changes to reflect a composite channel with a high-density of mudstone rich beds. Beds in this interval consist of a variety of sediments. Muddy sandstone and poorly-sorted mudstone have a high concentration of volcaniclastic mineral crystals, shell debris, and fossils, as well as a minor abundance of pebble size grains. The composite channel appears as a lens north of Waikiekie Stream due to truncation by successive flows in the upper sandstone-rich composite channel (Figure 11).

The lowermost composite channel reflects deposition from four or more elementary channels. Beds show sheetlike geometries at the margin and become more amalgamated to the south (Figure 11). Elementary channels are likely more than 800

meters wide, with bed correlations possible from event bed and facies analysis discussed in chapter 4. The thickness of individual elementary channels range from 2 to 5 meters.

The second composite channel represents deposition from four elementary channels comprised of mudstone-rich beds. The best exposures reflecting lateral variation are present north of Waikiekie Stream (Figure 11). These exposures show the composite channel thickens to the north and is subsequently truncated to the south. Beds appear planar with minor scours. Along the margin of the channel at Warekarianga Stream, this interval is represented by interfingering sandstone and mudstone (Figure 11). Elementary channels are likely 1 km wide with thicknesses ranging from 1 to 2 meters.

The uppermost composite channel reflects deposition of three or four elementary channels. These channels are sandstone-rich and show more variability in their sedimentary fill. Small erosional scours are present (Figure 11). At Warekarianga Stream, sandstone-rich deposits continue north beyond the major erosional surface. This likely reflects flows were less confined than those present in the lowermost composite channel. Elementary channels are likely 1 km wide with thicknesses ranging from 1 to 2.5 meters.

The CC1B channel complex reflects deposition by confined flows that became partially confined up-section. Width/thickness measurements are estimated here due to the presence of only one margin. Channel width is estimated at ~1-1.2 km and thickness is estimated at 27 meters or more (~37:1 aspect ratio) (Table 3).

Channel Complex 2 Channel complex CC2 is present from Tutapuha Stream to Locked Gate within inland outcrops, and north and south of Waikiekie Stream within coastal outcrops (Figure 2). It overlies undeformed mudstone that progressively

transitions to a mass-transport deposit at Waikiekie Stream. The northern margin is interpreted to be present at Tutapuha Stream or immediately north of the locality (Figure 12, 13). The southern margin is present approximately 400 meters south of Waikiekie Stream (Figure 14, 15). CC2 represents the highest amount of erosion within channel complexes of the LMMF. Erosional relief is approximately 30 meters, with a large abundance of clast-supported mudstone-clast conglomerate present within its base south of Waikiekie Stream where the axis is inferred (Figure 14). Thickness is approximately 25-30 meters in the study area.

Exposures of CC2 are difficult to examine due to the high-density of vegetation covering slopes within inland outcrops, and the vertical nature of 30 meter high coastal cliffs. Measured sedimentological profiles within inland outcrops primarily reflect exposures near the base of the channel complex, although two complete or nearly-complete sections at Locked Gate show lateral correlations with high confidence. To help correlate CC2 to coastal outcrops, one section was measured within the interpreted channel axis south of Waikiekie Stream.

Beds within CC2 are primarily massive and amalgamated; however, beds near the base reflect a fine-grained drape that is correlated from Tutapuha Stream to the South Waikiekie coastal section. Increasing amounts of erosion are present up-section from the channel base (Figure 14). Correlation was completed through facies and event bed analysis discussed in chapter 4.

Two composite channels are inferred for CC2, although event bed analysis indicates the possibility of a third. The lower composite channel was deposited by three

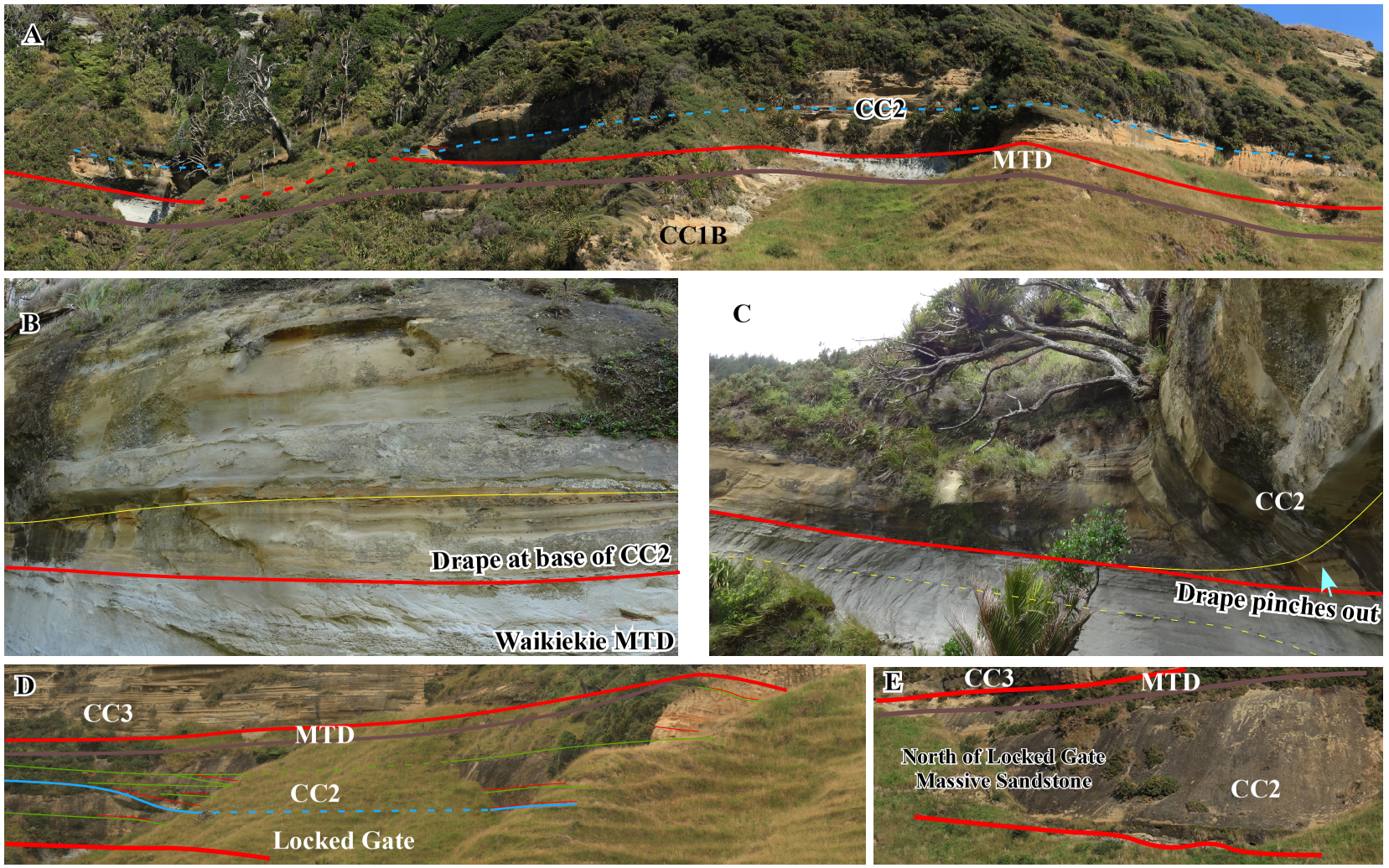


Figure 12. A) Photo of CC2 toward the channel margin at Tutapuha Stream overlying CC1B and undeformed siltstone correlated to the Waikiekie Stream MTD. B) Fine-grained drape at the base of CC2 at Tutapuha Stream. C) View looking east from (B) showing the fine-grained drape pinching out. D) Correlations of elementary channels at Locked Gate. E) Massive sandstone north of Locked Gate.

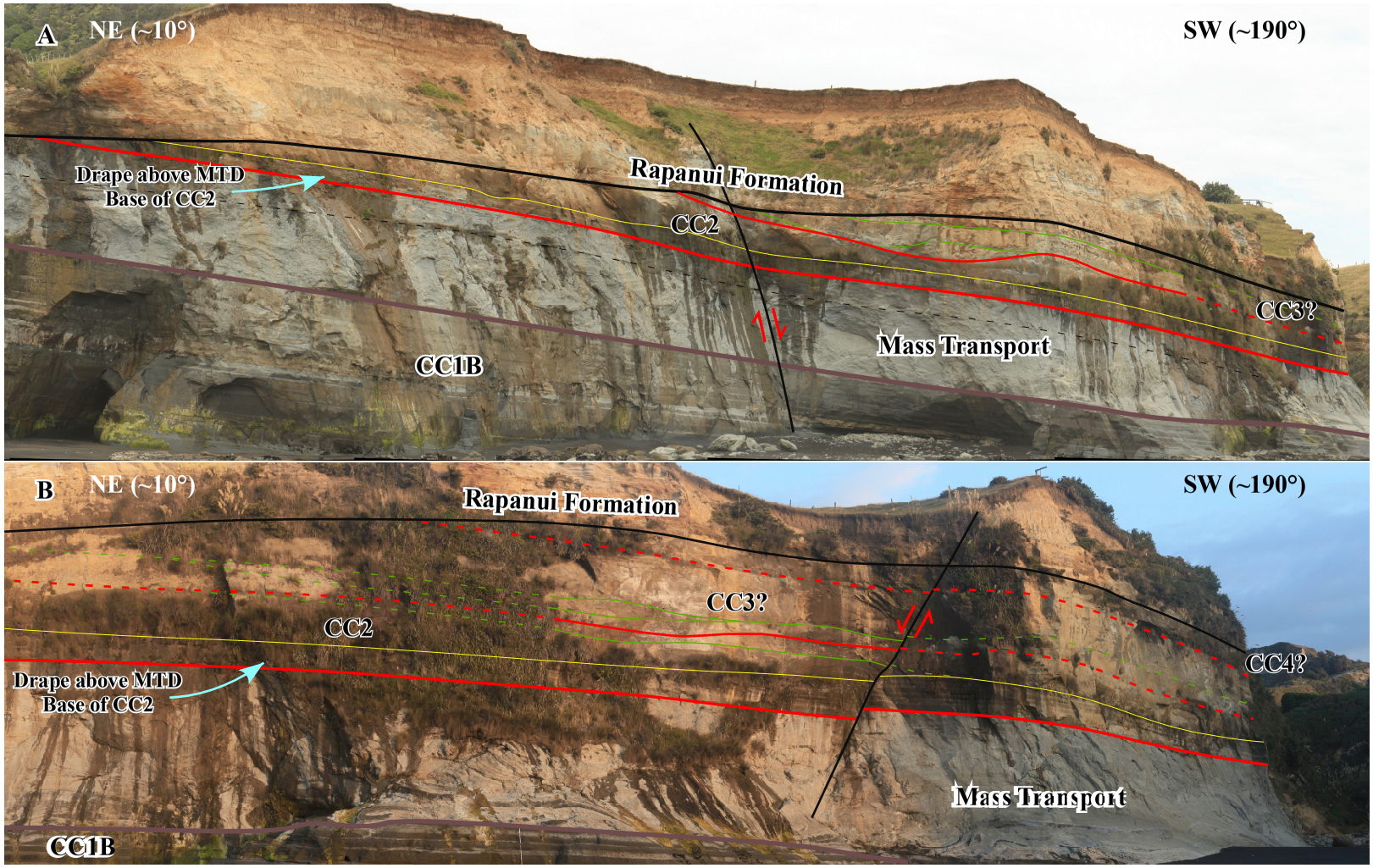


Figure 13. A) Photo north of Waikiekie of the northernmost exposures of CC2 above the Waikiekie Stream MTD. The presence of a fine-grained drape is found at the base of the channel. Inferred incision by the overlying CC3 is shown. B) Outcrop exposures immediately south from (A) showing lateral bed correlations within CC2 and the inferred incision by CC3.

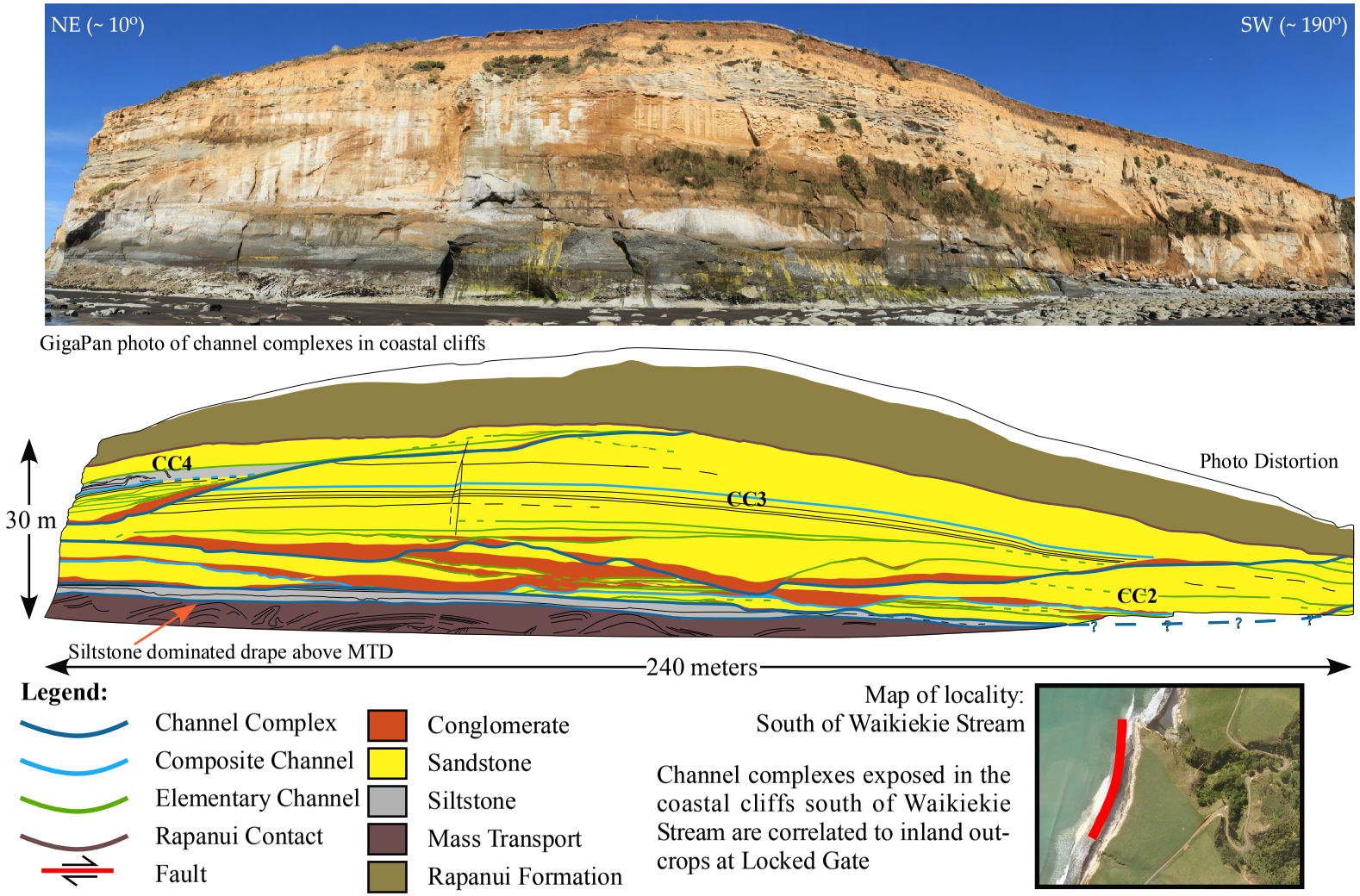


Figure 14. Photo-panel analysis of outcrop exposures south of Waikiekie Stream showing correlations of channel complexes 2, 3, and 4. The highest abundance of mudstone-clast conglomerate in the MMF is present at this locality, inferred to be the location of the channel axes. Channels are deposited above the Waikiekie Stream MTD with a high abundance of internal erosional scours.

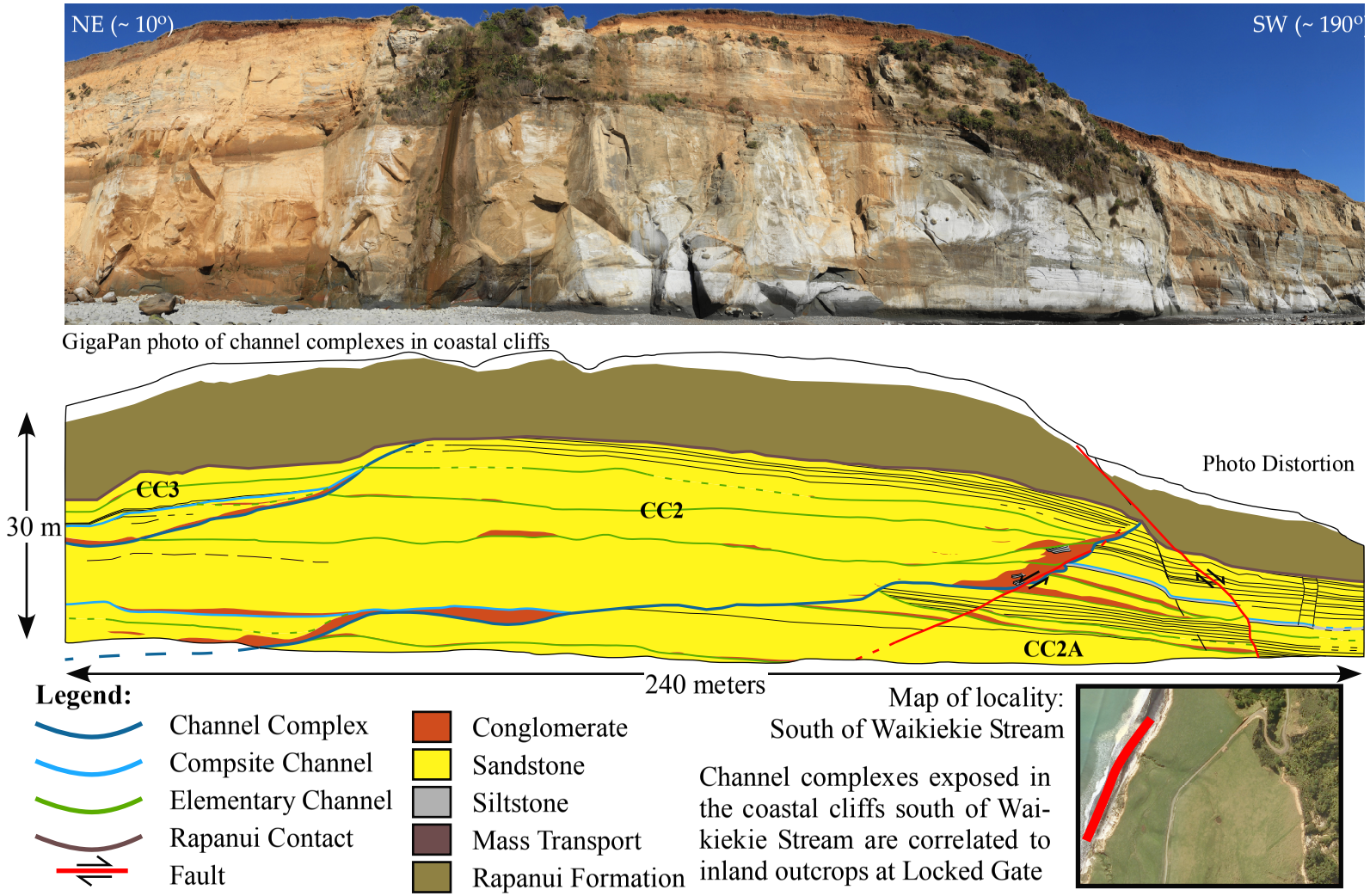


Figure 15. Photo-panel analysis of outcrop exposures south of figure 14 with correlations of channel complexes 2A, 2, and 3. The north margin of CC2A is truncated by CC2. Minor slumping and mudstone-clast conglomerate are present along the margin of CC2.

to five elementary channels. Clast-supported and matrix-supported mudstone-clast conglomerate are present at the base of each successive elementary channel within the axis, and correlate to amalgamation surfaces, and the base of sandstones within the inland outcrops. The underlying mass-transport deposit shows erosional planing by previous flows, followed by the deposition of a laminated fine-grained drape above the erosional surface (Figure 12, 13, 14, 15). Elementary channels are inferred to be ~1-1.3 km wide and approximately 0.5-1.5 meters thick.

The upper composite channel is inferred to be deposited by four or five elementary channels. The base of the upper composite channel is marked by a 1.25 meter clast-supported conglomerate at South Waikiekie and traced to inland outcrops through facies analysis. Massive amalgamated sandstone beds at South Waikiekie become less amalgamated and show more variation within their sedimentary fill toward the inland outcrops. Elementary channels within the upper composite channel are inferred to be ~1-1.3 km wide and 1.5-3.5 meters thick.

The CC2 channel complex reflects deposition primarily by confined flows. High abundances of clast-supported mudstone-clast conglomerate at the base of CC2 represent large flows that eroded mud-rich strata up-dip, possibly from the underlying mass-transport deposit, with subsequent deposition by frictional freezing. Higher within the channel, flows were sand-rich with less mudstone-clast conglomerate. Width/thickness measurements for CC2 are inferred to reflect a 1.3 km wide channel that is approximately 25-30 meters thick (~43-52:1 aspect ratio) (Table 3).

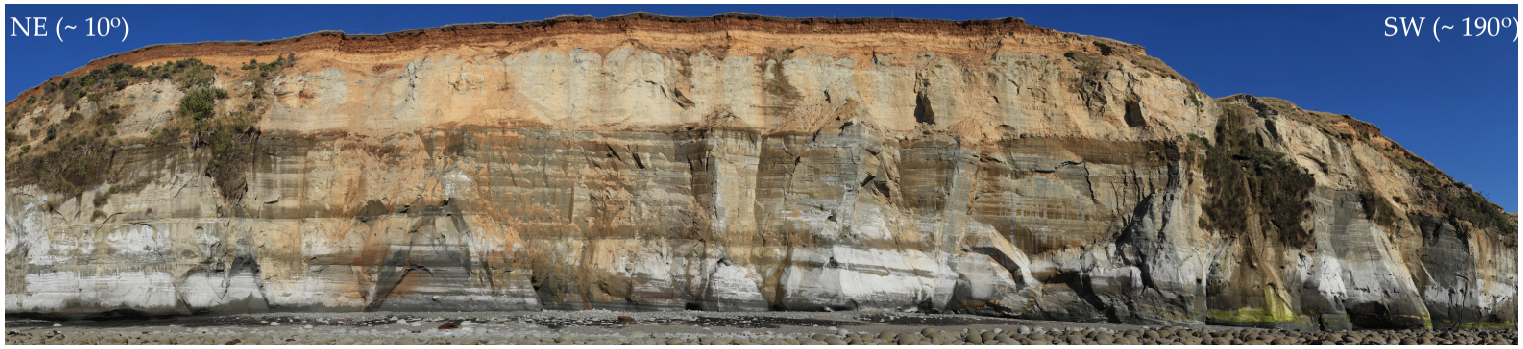
Channel Complex 2A Channel complex 2A is present south of Waikiekie Stream, and bounds the CC2 margin to the north where it is truncated by erosion (Figure 15, 16, 17). Only the southern margin of CC2A is preserved. CC2A is analyzed from photo-panel correlations completed in the field. It is inferred that CC2A's levee and overbank deposits are present south of the erosional margin. These deposits are described within one measured sedimentological profile collected along the coastal section. Erosional relief at the margin is approximately 25 meters.

Channel fill of CC2A is represented by massive sandstone, mudstone-clast conglomerate, rafted mass-transport deposits, minor siltstone, and increasing thin-bedded sandstone up-section. Erosional scouring up to 1 meter is present within some beds, and subsequently filled by mudstone-clast conglomerate. Surfaces traced along coastal outcrops are laterally continuous to the truncated margin (Figure 15, 16, 17).

Two composite channels are inferred within CC2A. The lower composite channel is filled by thick-bedded sandstone with minor erosional scours, and mudstone-clast conglomerate. Five elementary channels are present within the channel fill of the lower composite channel. Thickness of elementary channels is estimated between 0.5-2 meters.

The upper composite channel is represented by three elementary channels, each with fining- and thinning-upward successions. Minor truncation of underlying strata is seen within the uppermost elementary channels, but without the presence of mudstone-clast conglomerate. Elementary channels are estimated between 1-3 meters thick.

Channel complex 2A represents the first channel that formed after the *en masse* deposition of the Waikiekie mass-transport deposit. A large rafted block of deformed



GigaPan photo of channel complexes in coastal cliffs

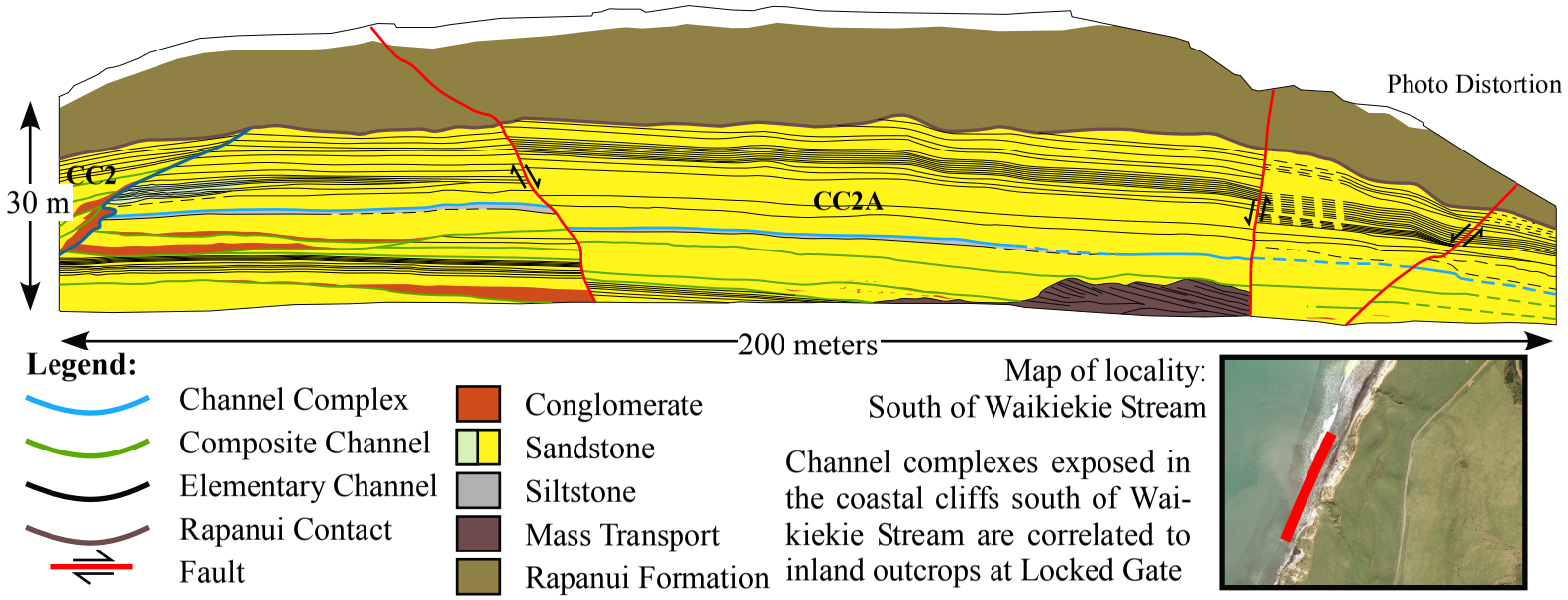


Figure 16. Photo-panel analysis of outcrop exposures south of figure 15 showing correlations of channel complex 2A. The northern margin of CC2A is truncated by CC2. Minor amounts of mudstone-clast conglomerate are present within elementary channels, and a block of mass-transport depost is found near the base. The upper composite body shows thinner beds above a thin siltstone.



GigaPan photo of channel complexes in coastal cliffs

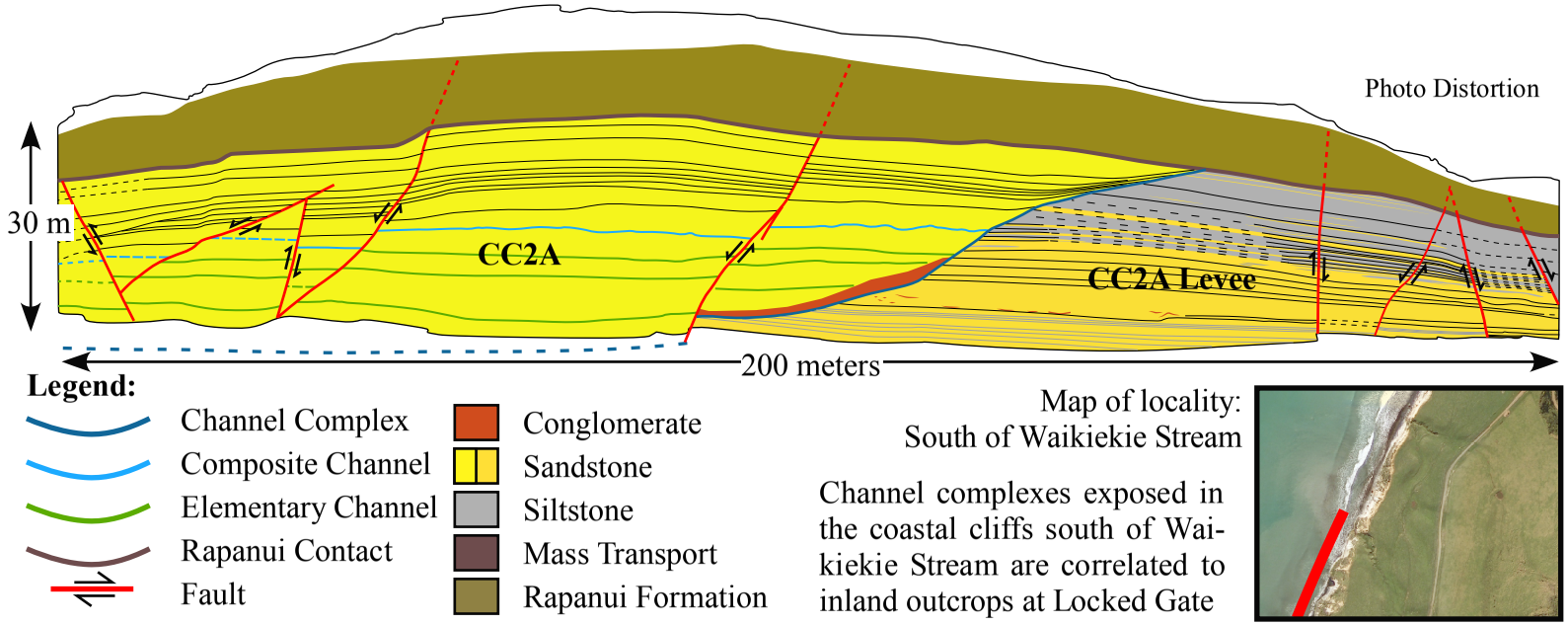


Figure 17. Photo-panel analysis of outcrop exposures south of figure 16 showing correlations of channel complex 2A. The margin of CC2A represents the southernmost channel within the LMMF. Overbank and levee deposits are interpreted to the south of the channel margin and described in one measured sedimentological profile.

mudstone present at the channel base is interpreted to reflect erosion of the underlying mass-transport deposit, followed by the deposition of sandstone-rich beds in two composite channels. Measurement of the channel's width was not possible due to truncation of the northern channel margin.

Channel Complex 3 Channel complex 3 is present from Tutapuha Stream to Locked Gate within inland outcrops, and along coastal outcrops north and south of Waikiekie Stream (Figure 2). Channel margins are present at Tutapuha Stream toward the north, and approximately 240 meters south of Waikiekie Stream. Erosional relief is approximately 20-25 meters. Analysis of CC3 was primarily through photo-panel analysis, although three measured sections represent the stratigraphy at Locked Gate and Tutapuha Stream.

Correlation of CC3 between the inland outcrops and the coastal outcrops was accomplished using a number of methods. Photo-panel analysis of elementary channels and composite channels depict most of the architectural information, although the three measured sections provide insight about major surfaces. Reflecting upon the architecture of the other channels, and the spatial and temporal position of MTDs while walking out the inland and coastal stratigraphy also helped in the correlation. The identification of large erosional surfaces within the inland outcrops at Locked Gate show the channel down-cutting toward the coastal section, and a simple math equation shows the regional dip of 6-7 degrees at Waikiekie Stream places the channel within the coastal section (Figure 23).

Near vertical cliff faces at Locked Gate provide the best views of CC3 within the inland outcrops (Figure 18). These exposures are inferred to represent beds that were deposited near the margin or slightly off-margin, and toward the axis of the channel. Beds are less amalgamated, and show minor erosion with multiple fining-upward successions. The coastal section south of Waikiekie Stream represents the inferred axis of the channel. Erosional surfaces with 1 to 4 meters of localized relief into the underlying strata are filled by moderate amounts of mudstone-clast conglomerate (Figure 14). Less erosion is present above the base of the channel. Thick-bedded sandstone and conglomerate thin upward, and are overlain by a second interval of thick-bedded sandstone.

Two composite channels are inferred for CC3, although event bed analysis may indicate a third. Changes in bed-character from the inland outcrops to the coastal section is interpreted to represent the transition from marginal to axial deposits. Inland outcrops at Locked Gate are filled by medium- to thick-bedded sandstone with fining- and thinning-upward packages (Figure 18). Multiple down-cutting erosional surfaces are present within the southern exposure, along with minor scours occurring laterally. Tracing most surfaces to the south within inland outcrops is not possible due to truncation from the overlying CC4 channel. Beds generally thicken and become more amalgamated toward the southern exposure at the Locked Gate locality.

It is inferred that four elementary channels fill the lower composite channel within inland outcrops, and five along the coastal outcrops (Figure 14, 18). The additional channel present within the coastal outcrops is truncated by successive flows and is only present along the southern margin (Figure 14). Elementary channels within the lower

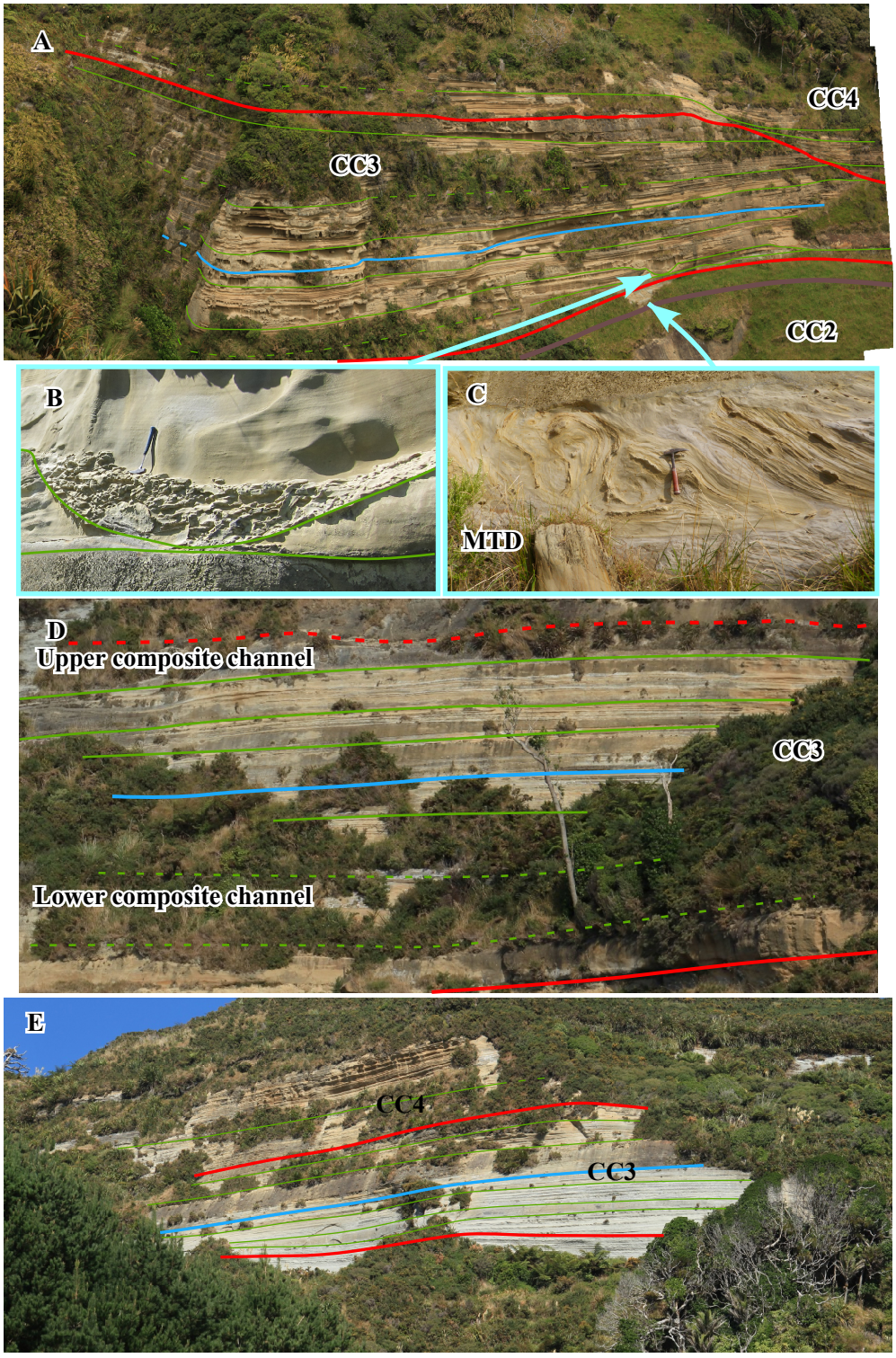


Figure 18. A) Photos of architectural elements in CC3 and CC4 at Locked Gate. B) Minor scour filled with mudstone-clast conglomerate. C) Correlation of architectural elements of CC3 to outcrops north of Locked Gate. D) Correlation of CC3 and CC4 to the margin at Tutapuha Stream where sandstone beds are seen pinching out to the east.

composite channel at Locked Gate show scours up to 1 meter or more, with multiple thinning-upward packages. The upper composite channel is also deposited by four elementary channels. The lowermost elementary channel is thick-bedded and thins to the north. The two overlying elementary channels are represented by successive thinning-upward packages of sandstone, and the uppermost elementary channel transitions back to a thick-bedded interval, which is subsequently truncated by the CC4 channel.

Within coastal outcrops, beds are more amalgamated and erosional near the base of CC3. Truncation within beds is common, represented by three left stepping elementary channels (Figure 14). Beds become more planar up-section from the base. Tracing individual elementary channels along the coast was completed with decreasing confidence up-section due to the height of the cliffs. The lower composite channel is capped by a thinning-upward package of sandstone, and the upper composite is filled by thick-bedded, amalgamated sandstone.

Elementary channels within the lower composite channel vary from 50 meters to ~1 km wide, and 1 to 5 meters thick. The smaller channel widths represent truncated channel remnants that are 50 to 150 meters wide, and 1 to 5 meters thick. Truncated channel remnants are present at the base of the channel complex and only within the axis. Elementary channels within the upper composite channel are ~800 meters to 1.3 km wide, and 3 to 6 meters thick. Width/thickness measurements for CC3 represent a ~1.3 km wide channel that is approximately 20-25 meters thick (~52-65:1 aspect ratio) (Table 3).

Channel Complex 4 Channel complex 4 is present from Tutapuha Stream to Locked Gate within inland outcrops, and south of Waikiekie Stream in coastal outcrops. The channel margins are present at Tutapuha Stream to the north and approximately 100 meters south of Waikiekie Stream. Erosional relief is approximately 20-25 meters. CC4 erodes into the underlying CC3 channel within the outcrops at Locked Gate. Analysis for CC4 was completed primarily from photo-panel analysis, although three measured sections reflect the stratigraphy at Locked Gate and Tutapuha Stream. Correlation of CC4 from the inland outcrops to the coastal outcrops followed similar methodology explained for CC3.

The best exposures of CC4 are within cliff faces at Locked Gate, and south of Waikiekie Stream (Figure 14, 18, 19). Inland exposures are interpreted to represent beds that were deposited slightly off-margin, and toward the axis of the channel. A large erosional surface truncates approximately 10 to 15 meters of underlying strata within the CC3 channel at Locked Gate. Beds dip steeply and onlap this interval, becoming more horizontal away from the margin (Figure 18). The channel fill of CC4 shows less thick-bedded sandstone than the underlying channel complexes. Minor intervals of mudstone-clast conglomerate are present within the basal erosional section, and increasing amounts of bioturbated sandstone are found up-section. Within the coastal exposures, similar abundances of mudstone-clast conglomerate are seen at the base of the channel. An interval of convoluted and slightly deformed mudstone present up-section is correlated to the inland outcrops immediately south of Locked Gate (Figure 14, 19). Outcrop character

and lithologies present within the two exposures are similar, although more deformation is seen within the coastal section.

Two composite channels are inferred to fill CC4 (Figure 14, 19). The lower composite channel is characterized by moderate erosion and the presence of mudstone-clast conglomerate at the base. Eight elementary channels are inferred for the lower composite channel with minor erosion and wavy or inclined contacts (Figure 14, 19). Width measurements of the elementary channels are difficult to determine due to the inability to walk out beds. Width estimates are inferred to be approximately 500 meters, and thicknesses range from 0.5 to 2.5 meters.

The upper composite channel is characterized by an increase in grain size and bed thickness at its base. Above a thick-bedded sandstone, higher abundances of convoluted mudstone and minor scouring correlate to the mudstone-rich interval within the coastal outcrops (Figure 14, 19). Up-section, fewer scours and increasing amounts of thin-bedded sandstone are present. At least five elementary channels are interpreted to fill the upper composite channel within CC4. Widths for elementary channels are likely 800 meters to 1.1 km, larger than those within the lower composite. As flows became partially confined above the major erosional surface, they were able to expand. This is represented by correlated sandstones within the channel margin at Tutapuha. Thickness of elementary channels within the upper composite channel range from 25 centimeters to 5 or more meters.

Channel complex 4 represents the uppermost erosional channel within the LMMF. It has characteristically different sedimentary fill, which will be discussed in the

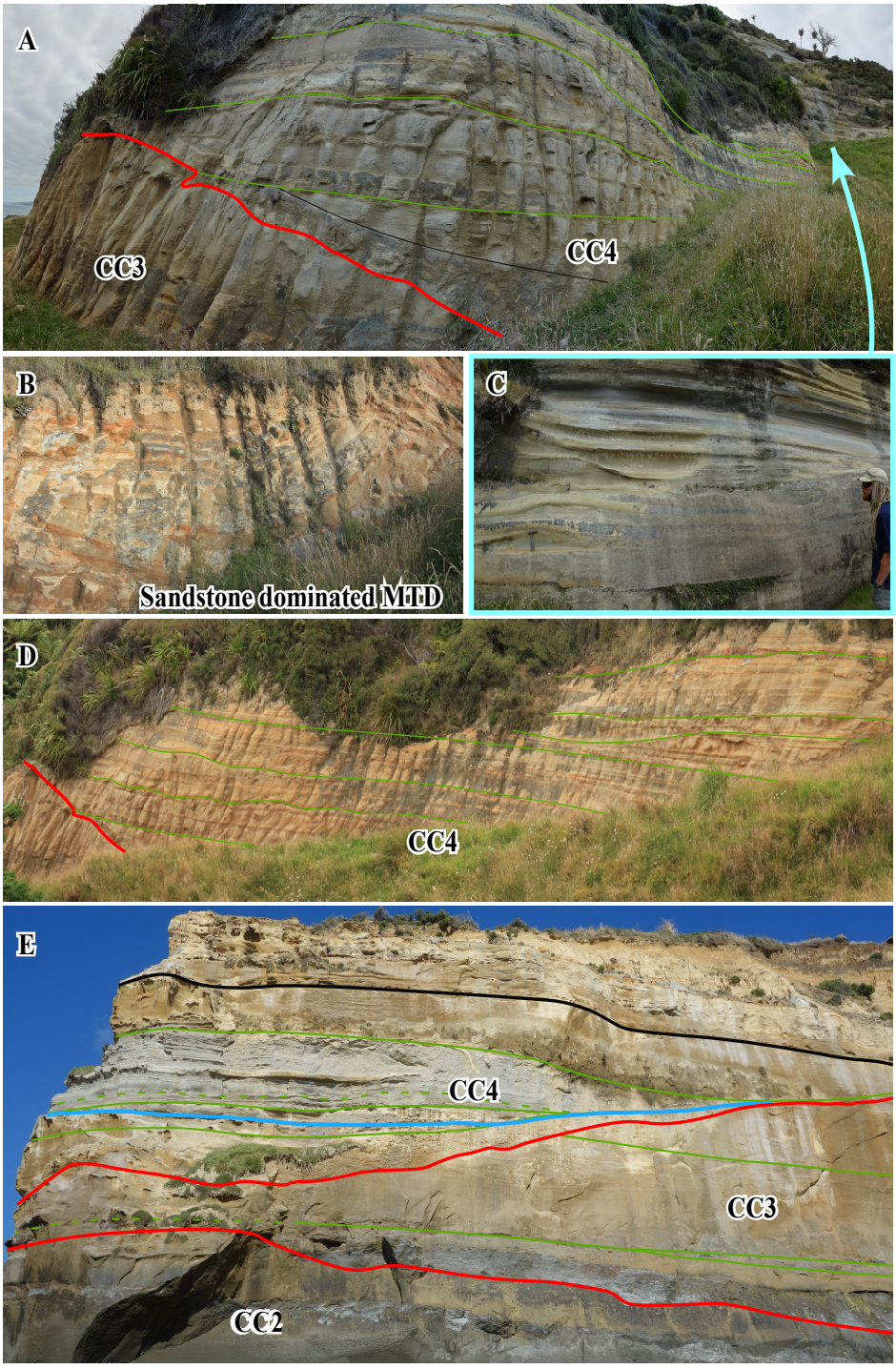


Figure 19. A) Major erosional surface of CC4 truncating the underlying CC3 channel fill south of Locked Gate. B) Folded and deformed sandstone-rich MTD at Locked Gate. It is inferred that the mass-transport deposit is cannibalized by CC3. C) Mudstone-rich unit south of Locked Gate correlated to the coastal section south of Waikiekie Stream. D) Elementary channels within the lower interval of CC4. E) Coastal exposures at South Waikiekie reflecting the correlated stratigraphy of CC4

next chapter. Flows were likely less frequent and carried less sediment to the basin. Width/thickness measurements for CC4 reflect a 1.1 km wide channel that is approximately 29 meters thick (~38:1 aspect ratio) (Table 3).

Wedgeforms/Levees

Wedgeforms or levees are depositional packages adjacent to channel complexes. They are characterized by thinning- and fining-upward deposits that record channel development and overbank deposition from the overspill of channelized turbidity currents and other subaqueous flows (Clark and Pickering, 1996).

Within the study area, two exposed wedgeform or levee deposits are inferred. The first is present above CC1A, north and adjacent to CC1B. The second bounds CC2A south of Waikiekie Stream. Beds are traced approximately 1000 meters outside the channel margins representing partially confined flows with planar beds and minor scours.

Levee deposits adjacent to CC1B are exposed north of Warekarianga Stream and overlie the CC1A complex. Medium- to thin-bedded deposits of siltstone, sandstone, and minor amounts of volcaniclastics are common. Sandstone thickness decreases up-section. Exposures are limited due to high vegetation cover. It is inferred that the levee deposits bounding CC1B are at least 750 to 1000 meters wide, and 25 to 30 meters thick.

The levee deposits adjacent to CC2A are exposed approximately 750 meters south of Waikiekie Stream (Figure 17). Sandstone deposits within the levee's basal interval are medium- to thick-bedded. Bed thickness progressively thins up-section with increasing siltstone, followed by subsequent deposition of two more sandstone dominated intervals.

A. Stratigraphic comparison of channel bodies and width/thickness measurements to the 2007 GNS study			
Stratigraphic Interval	**Stratigraphic Comparison**	**GNS, 2007 Channel Dimensions**	**This Study (Perpendicular to Paleoflow)**
CC1A	Not studied by GNS	N/A	~1.3 km Wide, ~25 m Thick: no margin
CC1B	GNS C1	C1: ~370 m Wide, >27 m Thick	~1 km Wide, ~ >27 m Thick: one margin
CC2A	GNS C6	C2: >600 m Wide, >15 m Thick	>300 m Wide, >25 m Thick: one margin
CC2	GNS C2, C5	C3: >125 m Wide, ~20 m Thick	~1.3 km Wide, ~ 20-25 m Thick: two margins
CC3	GNS C3, C5	C4: >125 m Wide, ~28 m Thick	~1.3 km Wide, ~ 20-25 m Thick: two margins
CC4	GNS C4	C5: >350 m Wide, >25 m Thick	~1.1 km Wide, ~ 29 m Thick: two margins
		C6: >300 m Wide, >25 m Thick	

B. Aspect ratio comparison of channel bodies to the 2007 GNS study			
GNS, 2007	**Channel Aspect Ratio**	**This Study**	**Channel Aspect Ratio**
C1	Only one margin	CC1A	~52:1 or more
C2	Estimated 40:1	CC1B	~37:1 or less
C3	No margins	CC2A	No margin to the north
C4	No right margin	CC2	~52:1 to 65:1
C5	Estimated 17:1	CC3	~52:1 to 65:1
C6	No left margin, top or base	CC4	~38:1

Table 3. A) Comparison of channel complexes to the 2007 GNS study showing channel width and thickness measurements. B) Aspect ratio calculations from this study compared to the 2007 GNS study.

Minor scours filled by mudstone-clast conglomerate are seen within each sandstone dominated interval.

The lowermost sandstone dominated interval is 12 meters thick, and is overlain by a 1.9 meter thick siltstone with thin-bedded sandstone. Sandstone beds within the lower interval are up to 2 meters thick. The second sandstone dominated interval is 4.5 meters thick with sandstone beds up to 75 centimeters thick. Thin-bedded sandstone with increasing amounts of bioturbated siltstone are present above the second sandstone interval. Thin beds of volcaniclastic sandstone and bioclastic shell debris increase in abundance up-section, although overall abundance is low. Siltstone-rich deposits above the second sandstone-rich interval are approximately 15 meters thick. The uppermost sandstone-rich interval is approximately 3 meters thick. This interval reflects the deposition of one sandstone bed that is 1 meter thick with minor erosion, overlain by thinning sandstone beds up to 30 centimeters thick. Minor amounts of thin-bedded sandstone are present up-section within this interval. Siltstone is the predominate lithology in the upper 15 meters.

It is inferred that the levee deposits bounding CC2A are at least 1 km wide and 50 meters thick. Deposition was by partially confined flows. Deposits near the base are interpreted to represent higher flow velocities required for deposition. Sandstone abundance decreases up-section representing waning flow velocities. Three fining- and thinning-upward sandstone-rich intervals are present within the levee, separated by siltstone dominated deposits.

Drapes

Drapes are characterized by laterally extensive fine-grained deposits at the base of channel complexes. They are generally composed of finely laminated siltstone with minor sandstone, and represent the initial sediments deposited above erosional channel contacts before subsequent sand-rich flows were initiated. Two drapes are seen within the study area. The first is present below CC1A at Warekarianga Stream. Laminated siltstone approximately 50 centimeters thick shows inclined bedding parallel to the erosional margin. It is traced approximately 100 meters to the south where it continues into the subsurface.

The second drape seen within the study area is present at the base of CC2 and overlies the Waikiekie Stream MTD. A minor abundance of mudstone-clast conglomerate at the base of the drape represents erosion into the underlying strata, and finely laminated siltstone and sandstone are present above. The 50 to 60 centimeter drape is traced from coastal outcrops north and south of Waikiekie Stream to inland outcrops at Tutapuha Stream.

Laminated Thin Beds

Laminated thin beds are present above and below the channel belt. Deposition is inferred to represent unconfined slope-fan deposits that are calcareous-rich with minor amounts of sandstone. Three sections were measured south of the channel belt within mudstone-rich laminated thin beds, and four were measured between Locked Gate and Tutapuha Stream. Laminated thin beds are commonly siltstone-rich and highly bioturbated. Sandstone beds found in laminated thin bedded intervals average 5

centimeters thick, although a low abundance of medium-bedded sandstones up to 70 centimeters thick were seen. Bioturbated siltstone represents between 40-70% of the deposits within these intervals.

STRATIGRAPHIC EVOLUTION DISCUSSION

Stratigraphic Variation within Channel Complexes

Channel Complex 1A

Sedimentary Facies The channel fill of CC1A is characterized by approximately 25 meters of thick-bedded sandstone with moderate amounts of erosion. The axis of the channel at Gibb's Hill shows the highest amounts of erosion within CC1A, indicated by a high abundance of matrix and clast-supported mudstone-clast conglomerate above numerous erosional surfaces. The overbank of CC1A is inferred north of Waikiekie Stream where increasing amounts of thick-bedded plane-parallel laminated sandstone and climbing ripple cross-laminations are present within the exposure. Sedimentary facies proportions for CC1A are shown in figure 20, and a cross-section for the channel from correlated sedimentological profiles is shown in figure 21.

The base of CC1A at Gibb's Hill is filled with thick-bedded structureless sandstone and cross-stratified sandstone above a 70 centimeter matrix supported mudstone-clast conglomerate. Four meters above the base of the channel, numerous erosional surfaces are filled with clast-supported mudstone-clast conglomerate up to 55 centimeters thick (Figure 21). Minor amounts of structureless and convoluted sandstone are present above the mudstone-clast conglomerates. A large rotated and rafted block of sandstone and siltstone is also present in this interval. Up-section, increasing amounts of plane-parallel laminated sandstone fill the channel. Minor erosional scours, and an

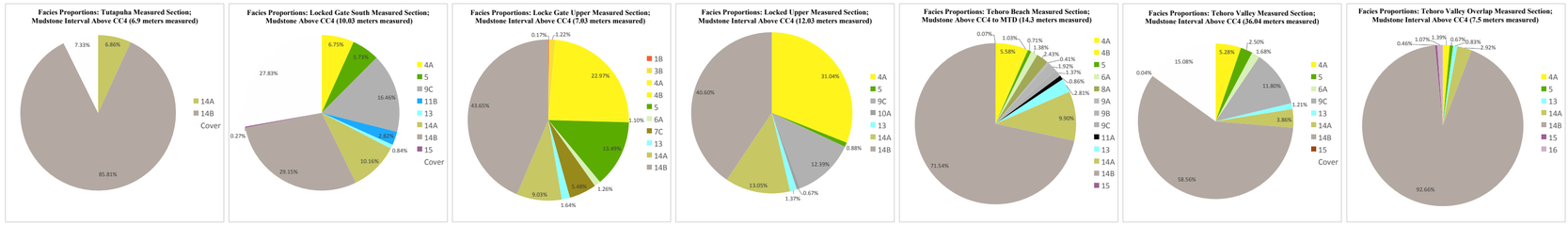
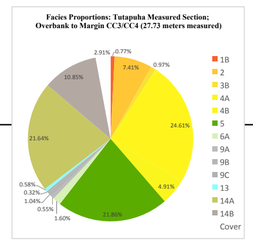
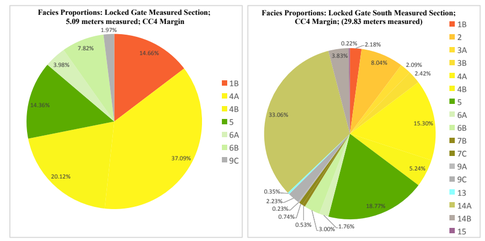
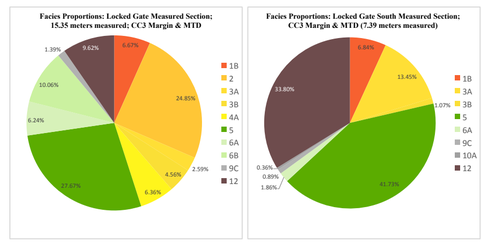
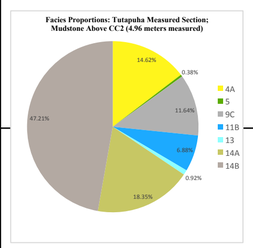
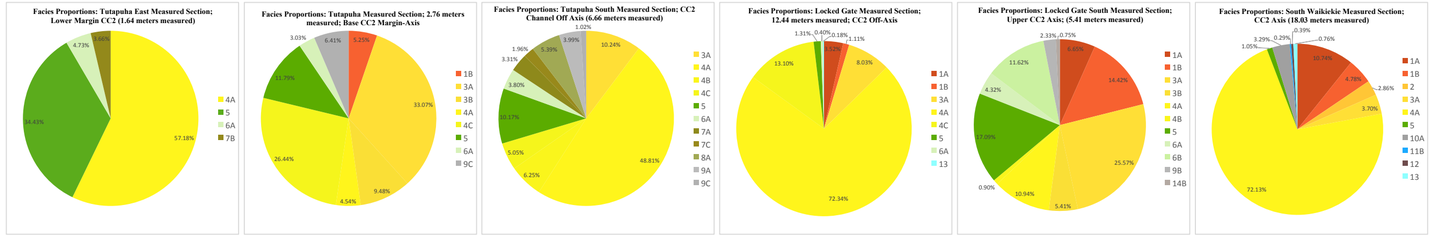
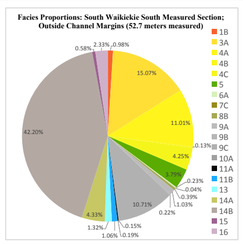
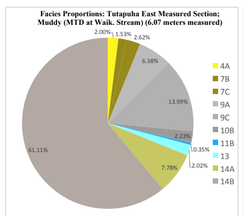
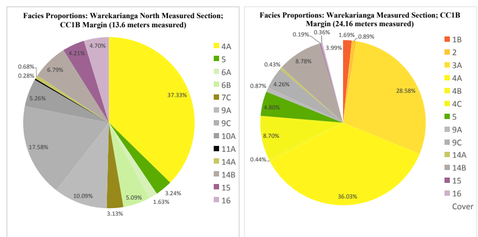
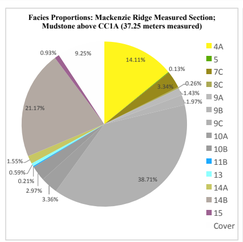
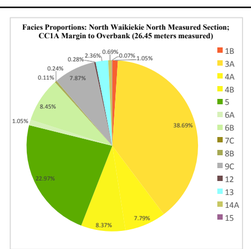
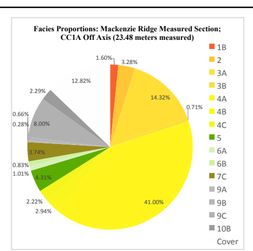
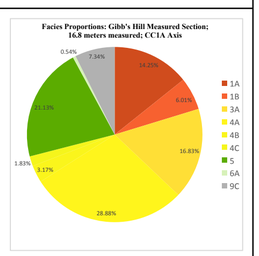
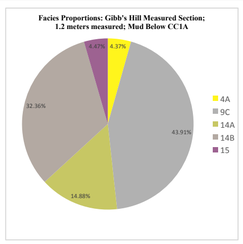
Stratigraphic Interval	Sedimentary Facies Distributions Across Channel-Belt in the Mount Messenger Formation			
Thin Bed Element 3				
	Overbank - Mudstone Dominated	**Margin**	**Margin - Off-Axis**	**Axial**
Channel Complex 4				
Channel Complex 3				
Channel Complex 2					
CC2A Levee / Overbank				
Mudstone dominated interval above Channel Complex 1B/ Waikiekie Stream MTD				
Channel Complex 1B					
Volcaniclastic interval below Channel Complex 1B and Mudstone dominated interval above Channel Complex 1A				
Channel Complex 1A					
Top of Thin Bedded Element 1				

Figure 20. Sedimentary facies proportions calculated for each measured sedimentological profile across the LMMF. Documented within the chart are each lithostratigraphic interval described in figure 3. Sedimentological profiles were spatially positioned to reflect changes from the axis to the margin of channel complexes.

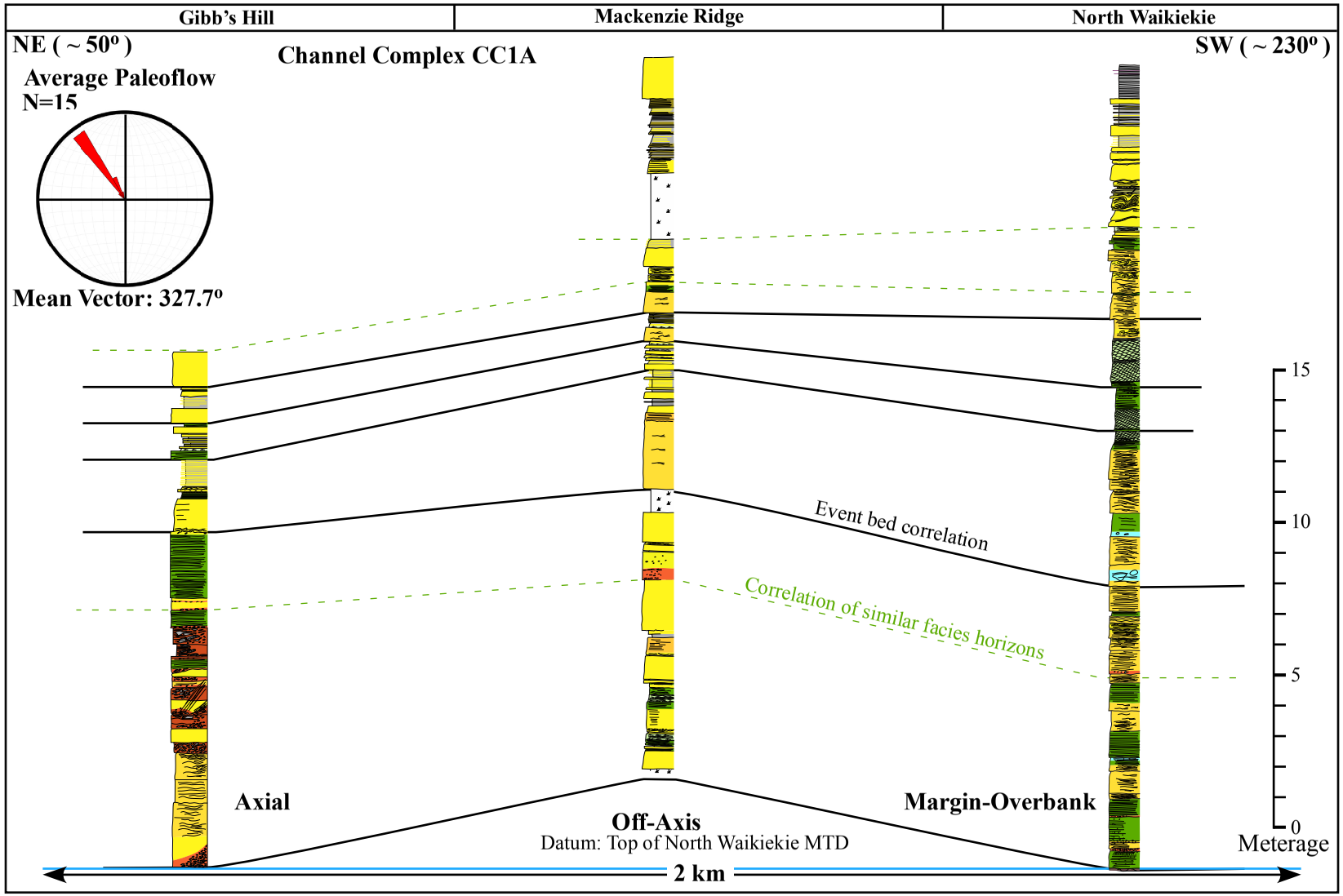


Figure 21. Cross-section of CC1A showing measured sedimentological profiles with event bed correlations between localities.

overall fining- and thinning-upward trend occur approximately 12.5 meters from the base of the channel, followed by a thickening-upward trend of structureless sandstone.

Within the Mackenzie Ridge section, fining- and thinning-upward trends of structureless sandstone are capped by plane-parallel laminated sandstone and ripple cross-laminated to convoluted sandstone (Figure 21). They reflect the deposits of a nearly complete idealized Bouma sequence (Figure 5). Massive sandstones become more prevalent away from the base. Small scours are filled by matrix supported mudstone-clast conglomerate and minor amounts of convoluted bedding. Approximately 9 meters above the base of the section, a thick-bedded sandstone with cross-stratified facies marks the start of a fining- and thinning-upward succession. Increasing amounts of siltstone and thin-bedded sandstone with ripple cross-laminated bed tops are present within a two meter thick interval above the massive bed. The overlying beds thicken and are filled by cross-stratified sandstone with ripple cross-laminated bed tops, plane-parallel laminated sandstone, and wavy-laminated to convoluted sandstone with minor amounts of siltstone. Increasing amounts of siltstone and silty sandstone are present up-section toward the top of the channel. The upper interval reflects three fining- and thinning-upward trends, marked at their base by massive structureless sandstones, each approximately 80-140 centimeters thick (Figure 21).

Along the coastal section, thick-bedded sandstones dominate the succession. The base is filled by plane-parallel laminated sandstone with minor amounts of matrix supported mudstone-clast conglomerate and shell debris (Figure 21). Up-section increasing amounts of cross-stratified sandstone and plane-parallel laminated sandstone

are present. Approximately 6.5 meters from the base, a localized interval of centimeter-scale floating mudstone-clasts is present, with increasing wavy-laminated to convoluted bedding above. The interval is capped by a 13 centimeter plane-parallel laminated sandstone. Thick-bedded cross-stratified sandstone increases up-section to thick-bedded climbing ripple cross-laminations approximately 14 meters from the base (Figure 21). Four packages of climbing ripple cross-laminations are documented, commonly occurring with plane-parallel laminated sandstone. Above the climbing ripple cross-laminated sandstone succession, increasing amounts of convoluted to wavy-laminated sandstone represent the upper five meters of the channel.

Paleoflow Analysis Paleoflow analysis for CC1A was documented from the axis of the channel at Gibb's Hill and the overbank of the channel north of Waikiekie Stream. Fifteen measurements were acquired. Two flame structures present at the Gibb's Hill locality indicate flows were directed 315° and 321°, and two climbing ripple measurements indicate flows were directed 330° and 340°. Within the overbank deposits north of Waikiekie Stream, climbing ripple measurements range from 323° to 339°. The mean vector for paleoflow is 327.7°, or to the northwest.

Event Bed Thickness Analysis Event bed analysis of CC1A reflects the presence of two or three distinct thickening-thinning trends (Figure 22). At Gibb's Hill, these packages reflect thinning-upward successions, with the lower being approximately 10 meters thick. The upper succession is represented by two ~1.25-2.25 meter event beds

with thin beds above. Three event beds near the top of the outcrop exposure show a slight thickening-upward trend (Figure 22).

At Mackenzie Ridge, the lower package shows a thickening-upward trend. The lower package at Mackenzie Ridge is also approximately 10 meters thick and marked at the top by two events beds almost 1 meter thick. Above these beds a 2.8 meter event bed with a thin-bedded interval above is correlated to the base of the upper interval at Gibb's Hill (Figure 22). Event beds show a second thickening-upward trend followed by beds that thin near the top of the channel. The uppermost event bed thickens to almost 1.5 meters.

Correlating the channel to the outcrops north of Waikiekie Stream was partially completed through event bed analysis. The exposures north of Waikiekie Stream reflect two thickening-thinning packages. Event beds present in this locality likely represent a more complete analysis of the flows that were responsible for the deposition of CC1A due to less erosion and preservation outside the margin of the channel. The lower package thickens upward to a 1.5 meter event bed followed by a thinning trend above (Figure 22). The lower package is 8.5 meters thick, likely representing the same correlation within the inland outcrops. The second package is marked by a slight upward thickening trend at its base to a 2.25 meter thick event bed that is inferred to be the same bed that marks the base of the upper trend in the inland outcrops (Figure 22). Above this bed, the overlying package show a thinning-upward trend to the top of the outcrop exposure.

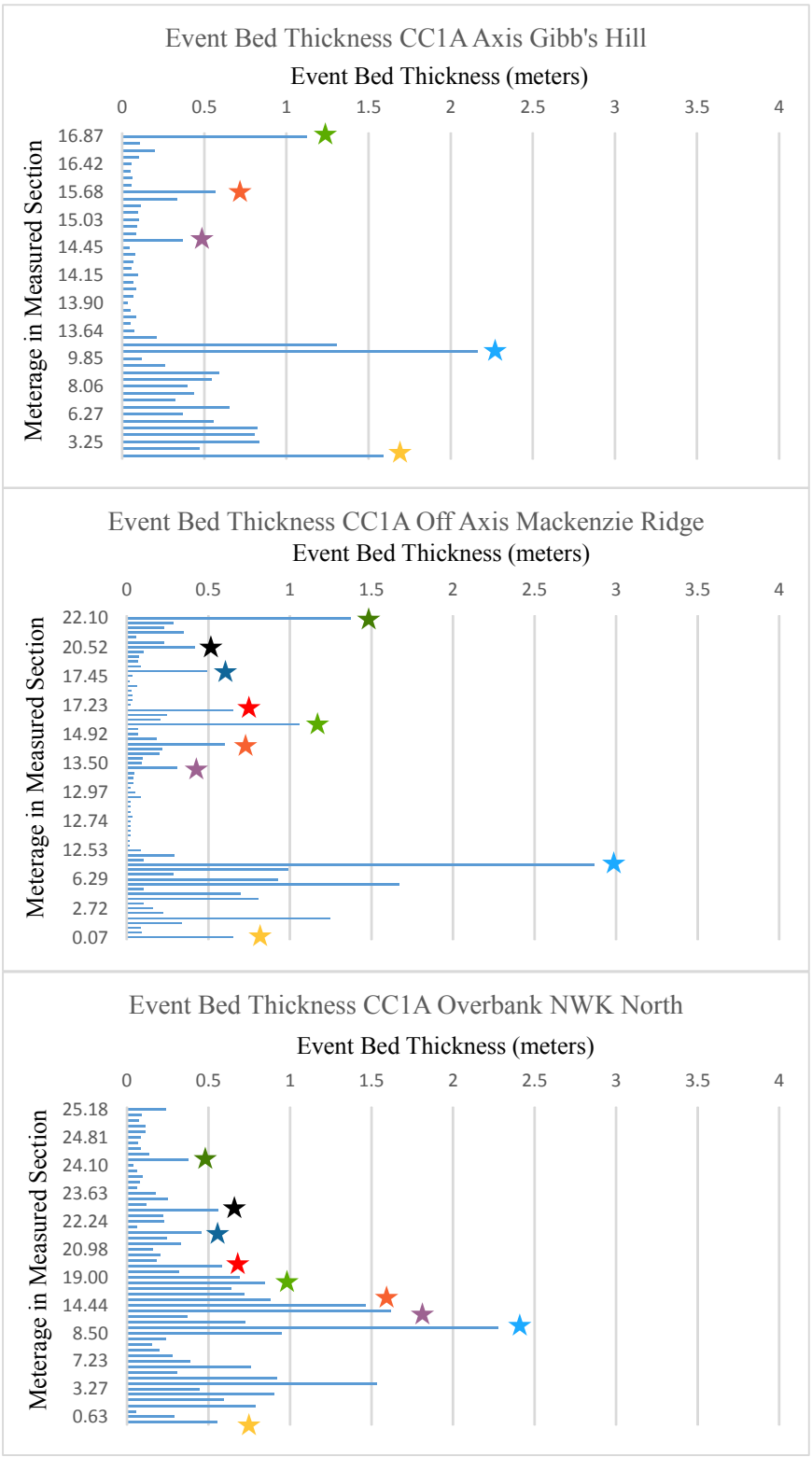


Figure 22. Event bed analysis for CC1A showing correlations between each locality where sedimentological profles were measured. Event beds reflect beds deposited by individual subaqueous flow events.

Flow Transformations Sedimentary facies within CC1A's channel fill show minor flow transformations. The base of the channel is dominated by thick-bedded sandstones at each locality. Cross-stratified sandstone is prevalent near the inferred channel axis, and plane-parallel laminated beds are common within the margin to overbank deposits. The Mackenzie Ridge section, inferred to be off-axis and toward the margin reflects higher abundances of ripple cross-laminated sandstone, structureless sandstone, and plane-parallel laminated sandstone. It is inferred that the lower interval was deposited by high-density turbidity currents within the axis of the channel that transformed to low-density turbidity currents along the margin and overbank of the channel, depositing beds with sedimentary facies that reflect lower flow velocities.

The second interval in CC1A is dominated by a high-density of erosional scours and mudstone-clast conglomerate within the interpreted channel axis, and plane-parallel laminated sandstone and cross-stratified sandstone within the channel margin to overbank. The Mackenzie Ridge section is characterized by beds dominated by structureless sandstone and horizontally-stratified or spaced-stratified sandstone. It is inferred that the second interval was deposited by hyperconcentrated density flows and low-density turbidity currents within the axis of the channel reflected by the high abundance of clast-supported mudstone-clast conglomerate, the rafting of a sandstone block, and minor amounts of convoluted bedding. The low-density flows deposited plane-parallel laminated sandstone above mudstone-clast conglomerate, and may have been associated with a flow transformation up-dip. Laterally, the margin and overbank deposits were likely deposited by high-density and low-density turbidity currents,

evidenced by structureless sandstone, horizontally-stratified or spaced-stratified sandstone, cross-stratified sandstone, and plane-parallel laminated sandstone. As flows became less confined near the margin and overbank, flow velocity decreased and deposited beds with characteristically different facies.

The upper interval within CC1A is represented by bed-thickening successions south of the interpreted channel axis. Beds within the coastal section, and Mackenzie Ridge locality are dominated by cross-stratified sandstone. The Gibb's Hill locality is dominated by structureless sandstone, minor amounts of convoluted bedding, and thick packages of interbedded sandstone and siltstone. The first occurrences of climbing ripple cross-laminated sandstone are present within the coastal section, and correlate to structureless sandstone and siltstone to the north. Up-section, cross-stratified sandstone fills the channel to the top of the exposure.

It is inferred that sediment deposition migrated to the south away from the underlying axis of sedimentation. Deposition was likely from high-density turbidity currents evidenced by the high abundance of cross-stratified sandstone, and from low-density turbidity currents inferred by the presence of climbing ripple cross-laminations and thinner-bedded sandstones and siltstone to the north.

Channel Complex 1B

Sedimentary Facies The channel fill for CC1B represents the deposition of approximately 27 meters of sandstone dominated sediments. At the margin, thick-bedded sandstones are capped by thin-bedded siltstone. Away from the margin, massive

amalgamated and thick-bedded sandstone is prevalent. Sedimentary facies proportions for CC1B are shown in figure 20, and a cross-section for the channel from correlated sedimentological profiles is shown in figure 23.

Two sections measured along the margin at Warekarianga Stream indicate the presence of a variety of sedimentary facies. The most marginal section is represented by thin- to medium-bedded plane-parallel laminated sandstone and climbing ripple cross-laminated sandstone. Minor amounts of structureless sandstone and volcaniclastic sandstone are also present. Beds increase in thickness up-section and are filled with structureless sandstone (Figure 23). Siltstone dominated sediments and moderate amounts of volcaniclastic sandstone fill the channel approximately 8 meters above the base. Medium-bedded structureless sandstone and siltstone are present at the top of the section.

Immediately to the south, the second measured profile is characterized by thick-bedded sandstone that is deposited in horizontal beds (Figure 23). Plane-parallel laminated sandstone, cross-stratified sandstone, and structureless sandstone are present at the base. Increasing amounts of cross-stratified sandstone, and minor amounts of plane-parallel laminated sandstone, horizontally-stratified or spaced-stratified sandstone, and massive sandstone with floating mudstone-clasts are present up-section to 8 meters above the channel base. Above this interval, massive sandstone with floating mudstone-clasts is more prevalent. Beds are medium- to thick-bedded and separated by siltstone partings. Plane-parallel laminated sandstone in beds up to 20 centimeters, structureless sandstone, and cross-stratified sandstone are also present, but in lower abundances than below. One 30 centimeter matrix supported conglomerate fills the channel approximately 12 meters

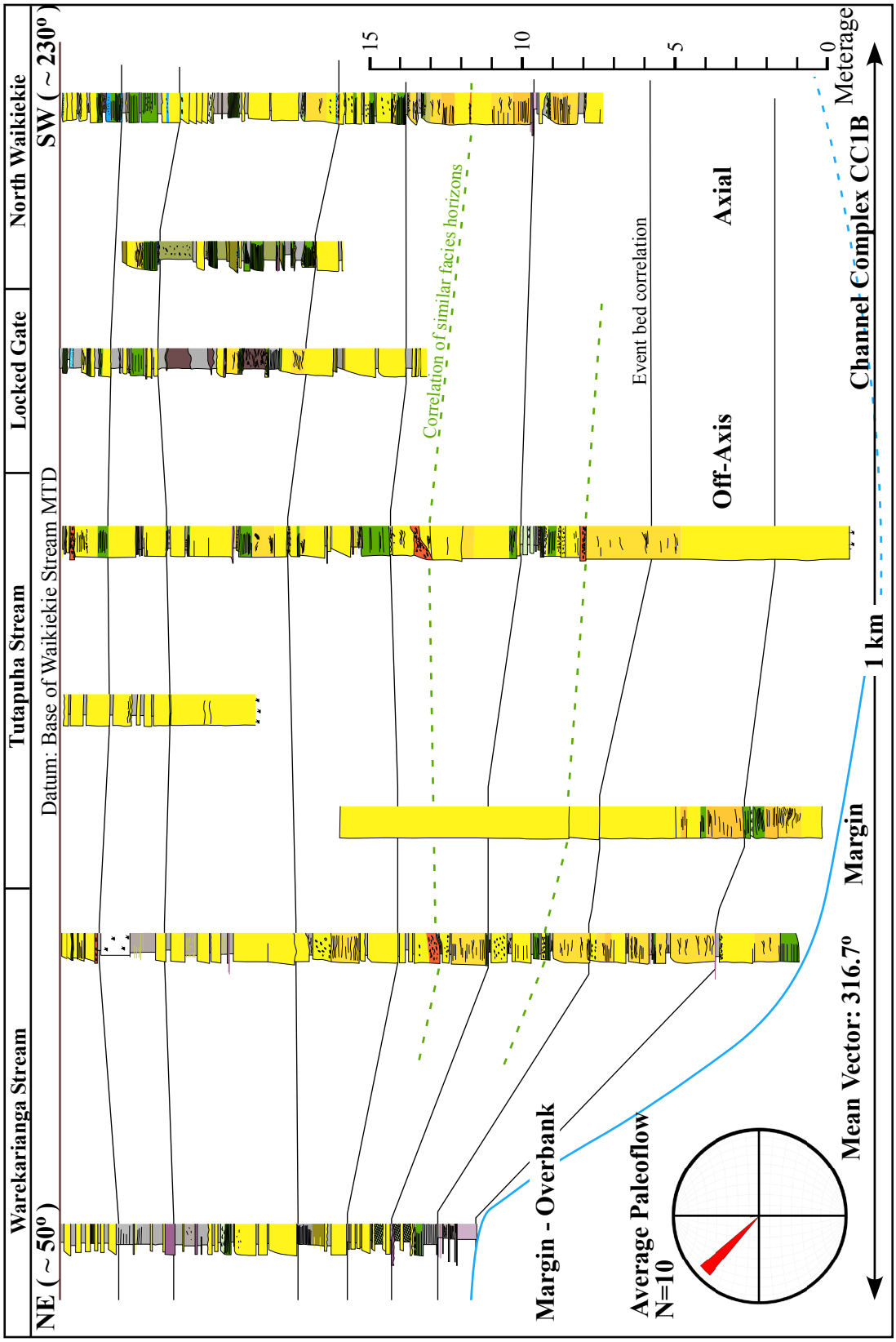


Figure 23. Cross-section of CC1B showing measured sedimentological profiles with event bed correlations between localities.

above the channel base within an erosional scour (Figure 23). Medium- to thick-bedded structureless sandstone and bioturbated siltstone are most prevalent within the upper 8 meters of the channel.

Further to south at Tutapuha Stream, sandstones near the base are massive and amalgamated. The basal interval of the channel shows an approximately 5 meter succession of sandstone with a slight fining-upward trend. This succession is filled by structureless sandstone, cross-stratified sandstone, horizontally-stratified or spaced-stratified sandstone, plane-parallel laminated sandstone, and ripple cross-laminated sandstone (Figure 23). Increasing variation is seen laterally above a massive-bedded cross-stratified sandstone. The lowermost interval shows minor erosion at its base. A small scour is filled with matrix supported mudstone-clast conglomerate 22 centimeters thick. Floating mudstone-clasts, convoluted bedding, plane-parallel laminated sandstone, ripple cross-laminated sandstone, and siltstone are present above, reflecting a fining- and thinning-upward trend two meters thick. A thickening-upward succession dominated by structureless sandstone and minor dewatering structures is deposited above the lower interval (Figure 23). A 30 centimeter scour truncates the underlying bed approximately 14 meters within the section. Thick-bedded sandstones capped by thin siltstones increase in abundance up-section. Minor amounts of volcaniclastic sandstone is deposited at the base of multiple beds above the erosional scour. Mudstone-clasts present at bed tops also become more common. Beds show minor variation internally, with structureless sandstone most prevalent, and cross-stratified sandstone and plane-parallel laminated

sandstone present in lower abundances. The massive-bedded interval is approximately 15 meters thick, capped by a 10 centimeter erosional scour at the top of the channel.

Along the coastal section, two measured profiles represent the correlation to inland outcrops. The first profile shows similar facies trends to those seen at Tutapuha Stream and Warekarianga Stream. Medium- to thick-bedded structureless sandstone, horizontally-stratified or spaced-stratified sandstone, and cross-stratified sandstone fill the channel near the base of the section, although minor abundances of plane-parallel laminated sandstone, ripple cross-laminated sandstone, and siltstone are also present (Figure 23). Volcaniclastic mineral crystals, mudstone-clasts at bed tops, and calcareous debris were also seen within the channel fill. Small erosional scours are filled by ~5 centimeters of mudstone-clast conglomerate. Beds generally decrease in thickness toward the top of the channel, with plane-parallel laminated sandstone and structureless sandstone becoming more abundant. Asymmetric ripple cross-laminations are found at the top of multiple beds within this interval. The upper 5 meters of the channel is characterized by a minor thickening-thinning trend with plane-parallel laminated beds most abundant, and an increasing amount of calcareous facies.

Laterally within the coastal outcrops, a composite channel with a high abundance of mudstone-rich beds represents characteristically different sediments than those found at the other localities (Figure 23). Mudstone-rich beds are poorly-sorted with a high-density of volcaniclastics, shell debris, fossils, and sediment grain size up to pebbles. Pebbles reflect the coarsest sediment found in the MMF, although this study does not infer where they originated. Other facies within this interval include structureless

sandstone, and plane-parallel laminated sandstone. This interval is approximately 5 meters thick. Inland at the Locked Gate locality, deformed mudstone-rich beds are interpreted to correlate to the coastal section. Laterally, similar facies are seen within the margin at Warekarianga Stream, but without the presence of deformation.

Paleoflow Analysis Paleoflow analysis for CC1B was documented from the axis to the margin of the channel by ten measurements. Along the margin of the channel at Warekarianga Stream, climbing ripple cross-laminations indicate paleoflow ranged from 310° to 319°, and one groove cast reflects a flow direction of 146°/326°. Within the axis of the channel, two measurements from ripple foresets indicate a paleoflow of 312° and 350°. The mean vector for paleoflow is 316.7°, or to the northwest.

Event Bed Thickness Analysis Event bed analysis for CC1B reflects the presence of two large-scale thickening-thinning trends, although smaller-scale thickening-thinning trends are seen within the beds present along the margin at Warekarianga Stream (Figure 24). Beds within the basal 2.5 meters show an initial thickening-upward trend along the margin of the channel. Above this interval, beds show overall thinning along the margin to approximately 16.5 meters above the base, although the most marginal section shows a slight thickening-upward trend for the same beds (Figure 24). Four packages in the lower interval reflect smaller-scale thickening-thinning trends that are 3 to 4 meters thick, likely representing the deposition of individual elementary channels (Figure 24).

The base of the second interval is marked by a 1 to 3.25 meter event bed. The variation in bed thickness represents the transition from the margin to the axis of the

channel. Beds show an overall thinning-upward signature above this bed to the top of the outcrop. Similar to the lower interval, the upper interval is characterized by smaller-scale thickening-thinning trends. Three smaller-scale trends are present along the margin of the channel in the upper interval. Each package is approximately 2-3 meters thick (Figure 24).

Correlation of CC1B to the coastal section north of Waikiekie Stream was partially completed through event bed analysis. The correlations are shown in figure 23 and 24. It is inferred that the exposures along the coastal section correlate to beds approximately 6 to 10 meters above the base of the channel. The overall event bed signature is similar to those along the margin of CC1B.

Flow Transformations Sedimentary facies present within CC1B's channel fill show minor flow transformations from the margin to the interpreted axis. The base of the channel is dominated by cross-stratified sandstone and massive structureless sandstone. These are laterally correlated to minor abundances of plane-parallel laminated sandstone, and ripple cross-laminated sandstone toward the margin. Up-section, an increasing abundance of minor erosional scours, and structureless sandstone, plane-parallel laminated sandstone, ripple cross-laminated sandstone, and siltstone are seen. The lower interval is interpreted to be deposited by high-density and low-density turbidity currents, with flows likely transforming to the latter toward the margin. High abundances of cross-stratified sandstone and massive amalgamated sandstone indicates highly turbulent flows, and ripple cross-laminated sandstone, plane-parallel laminated sandstone, and siltstone indicate lower velocity flows that were more variable in their deposits.

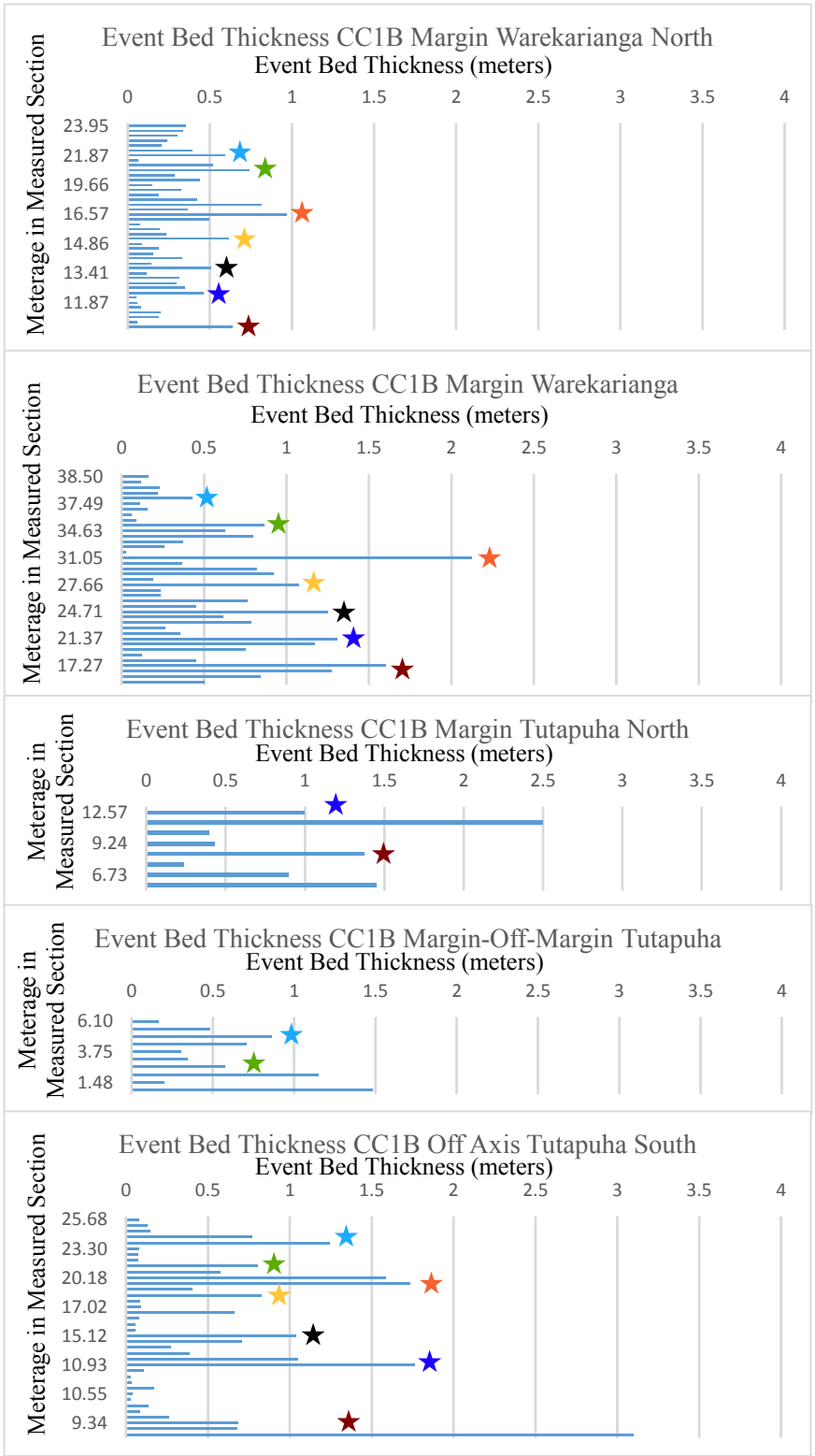
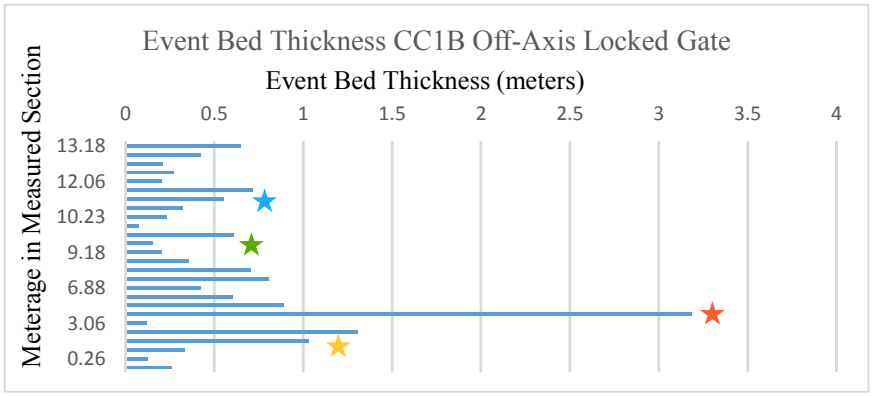
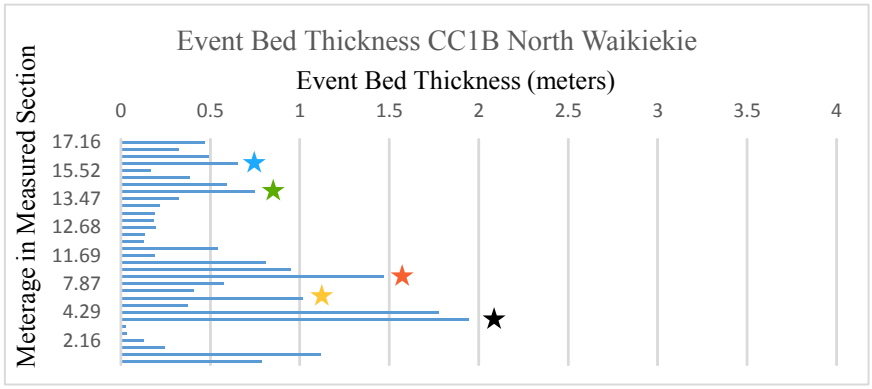


Figure 24. Event bed analysis for CC1B showing correlations between each locality where sedimentological profiles were measured.





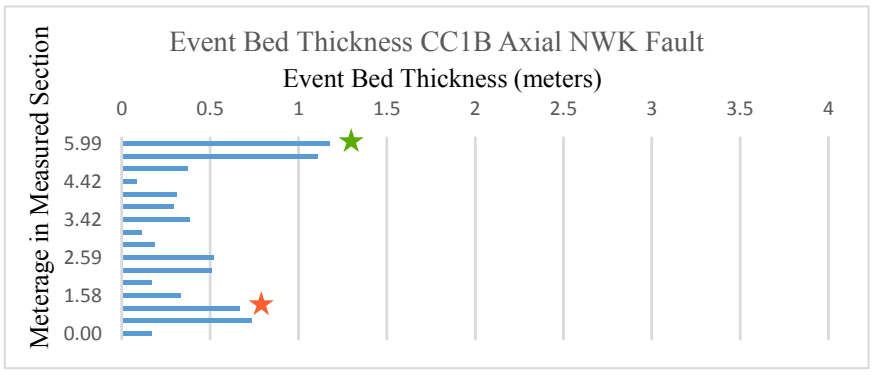


Figure 24. (Continued) Event bed analysis for CC1B showing correlations between each locality where sedimentological profiles were measured.

The middle interval is characterized by minor flow transformations from the axis to the margin of the channel. Deposits near the axis show minor erosional scours, and the presence of mudstone-clast conglomerate, cross-stratified sandstone with floating mudstone-clasts, plane-parallel laminated sandstone, and structureless sandstone. Toward the margin, facies are similar, although an increasing amount of structureless sandstone with floating mudstone-clasts dominate. Minor amounts of mudstone-clast conglomerate and cross-stratified sandstone are present. Flows were likely deposited by high- and low-density turbidity currents, with little variation laterally.

The upper interval is characterized by a variety of sedimentary facies. The presence of poorly-sorted mudstone-rich beds with a high abundance of structureless sandstone laterally represent different processes for deposition. Mudstone-rich beds were likely deposited by cohesive debris flows and hyperconcentrated density flows or concentrated density flows. This is interpreted from the chaotic assemblage of sediments, and presence of graded beds. Localized slumping was likely confined within the axis of the channel. Laterally, beds represent deposition by high- and low-density turbidity currents evidenced by thick amalgamated sandstone beds, and the presence of plane-parallel laminated sandstone and mudstone-rich caps. Low-density turbidity currents are inferred for the uppermost interval, with little variation from the axis to the margin of the channel.

Channel Complex 2

Sedimentary Facies The channel fill of CC2 is characterized by approximately 25 to 30 meters of sandstone-rich sediments. Six sedimentological profiles document the lateral variation of sedimentary facies. Sedimentary facies proportions for CC2 are shown in figure 20, and a cross-section for the channel from correlated sedimentological profiles is shown in figure 25.

Within the inland outcrops, the marginal exposures are primarily filled with plane-parallel laminated sandstone, structureless sandstone, and ripple cross-laminated sandstone at the base of the channel. Minor amounts of medium- to thick-bedded sandstone with floating mudstone-clasts and matrix supported mudstone-clast conglomerate are also present. The basal interval represents a 2.5 meter fining- and thinning-upward succession. Above this interval, massive sandstone dominates. The base of the overlying sandstone is represented by a 22 centimeter muddy sandstone with convoluted bedding and mudstone-clasts. This correlates to an amalgamation surface at Locked Gate, and a matrix-supported mudstone-clast conglomerate south of Waikiekie Stream (Figure 25). Dewatering structures, cross-stratified sandstone, and sandstone with floating mudstone-clasts are present up-section. The top of the section is marked by a 30 centimeter muddy sandstone with centimeter-scale mudstone-clasts, and convoluted bedding, or dewatering structures. This is overlain by thinner-bedded structureless sandstone capped by ripple cross-laminations.

Correlating to Locked Gate and the coastal section south of Waikiekie Stream, thick-bedded sandstone present within the channel margin records lateral variation. At

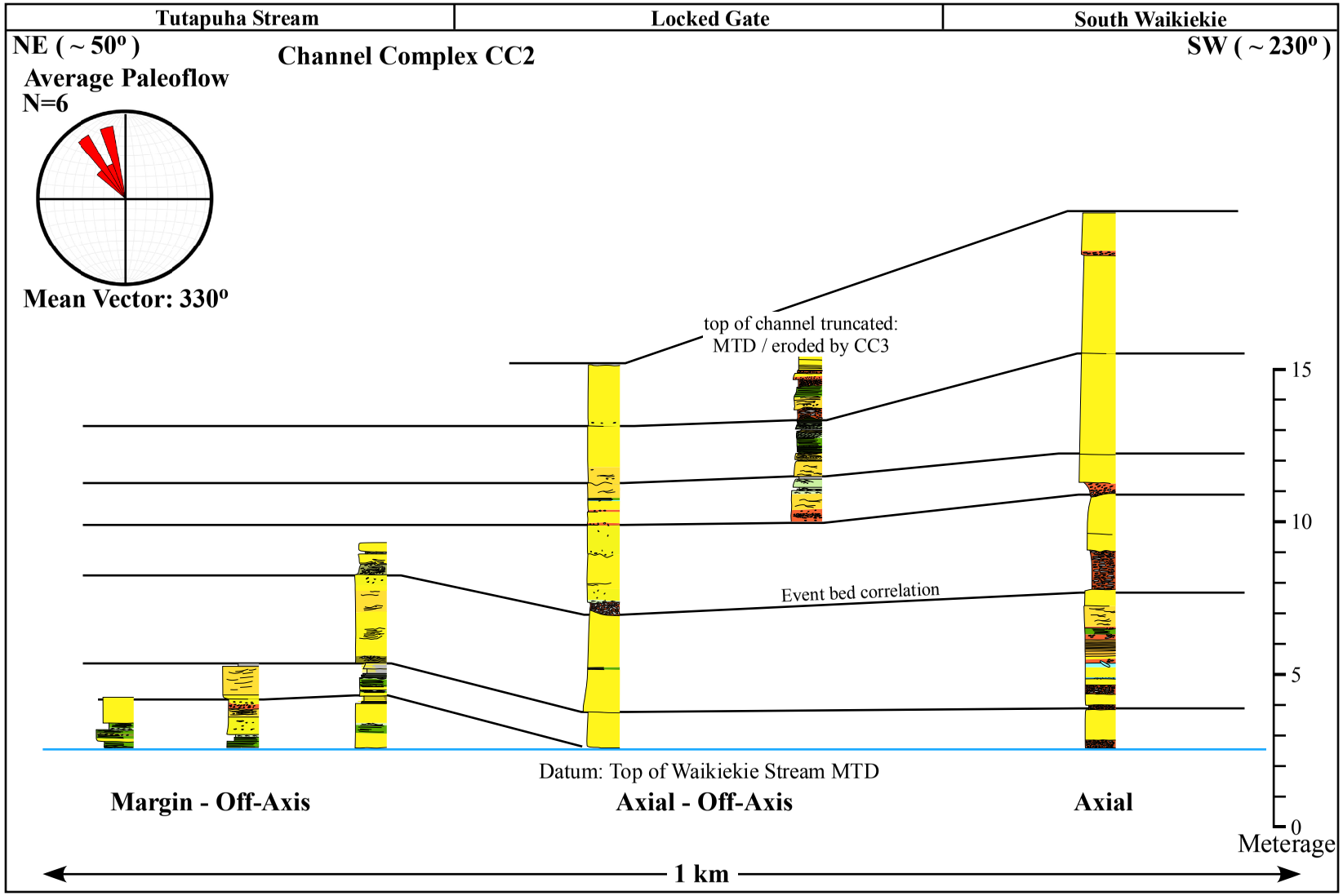


Figure 25. Cross-section of CC2 showing measured sedimentological profiles with event bed correlations between localities.

Locked Gate, it is reflected by two thick-bedded structureless sandstones separated by a thin interval of plane-parallel laminated sandstone. At Waikiekie Stream, multiple erosional scours are filled with mudstone-clast conglomerate, with structureless sandstone, horizontally-stratified or spaced-stratified sandstone, cross-stratified sandstone, and plane-parallel laminated sandstone above. Minor amounts of shell debris are also seen. The upper muddy sandstone within the margin correlates to clast-supported mudstone-clast conglomerate that significantly thickens toward the coastal outcrops (Figure 25). Thick-bedded structureless sandstone with floating mudstone-clast facies overlie the conglomerate. A second mudstone-clast conglomerate is present above this interval, with erosion decreasing toward Locked Gate from the coastal section. Lateral variability increases between the Locked Gate sections and the coastal section in the uppermost interval. At Locked Gate, massive amalgamated sandstones transition to a variety of facies approximately 100 meters to the south. Facies include mudstone-clast conglomerate, cross-stratified sandstone, wavy-laminated sandstone, plane-parallel laminated sandstone, and structureless sandstone, as well as thin siltstone partings. Within the coastal section, the same interval is represented by structureless sandstone with amalgamation surfaces.

Paleoflow Analysis Paleoflow analysis of CC2 documents six measurements from climbing ripple and asymmetric ripple foresets. Within the axis at Locked Gate, climbing ripple cross-laminations indicate paleoflow directions of 310°, 324°, 334°, 340°, and 345°. One measurement from the base of CC2 at Tutapuha Stream shows a flow direction of 327°. The mean vector for paleoflow 330°, or to the northwest.

Measurements for CC2A were acquired within levee deposits south of Waikiekie Stream outside the southern margin of the channel. A diversity of paleoflow indicators were present, including climbing ripple cross-laminations, asymmetric ripple cross-laminations, a flute cast, and the smile from a scour. CC2A's mean vector for paleoflow is 333°, or to the northwest.

Event Bed Thickness Analysis Event bed analysis for CC2 reflects the presence of three thickening-upward trends (Figure 26). These trends show beds up to 3.3 meters thick, with the thickest beds present within the axis south of Waikiekie Stream. The best outcrop exposures for CC2 are at Locked Gate and south of Waikiekie Stream, reflected by the ability to gather continuous sedimentological profiles from the base of the channel and up-section more than 10 meters. Correlations to the coastal section were inferred primarily from these localities.

Each thickening-upward trend is approximately 3 to 4 meters, and individual event beds correlated from the coastal section inland generally show minor thinning away from the axis of the channel. The uppermost beds at Locked Gate show similar thickness trends to those along the coastal section (Figure 26).

Flow Transformations Sedimentary facies present in CC2's channel fill show minor flow transformations. Facies transition from clast-supported mudstone-clast conglomerate within the channel axis, to structureless sandstone and cross-stratified sandstone toward the margin. Beds are amalgamated with an increasing presence of

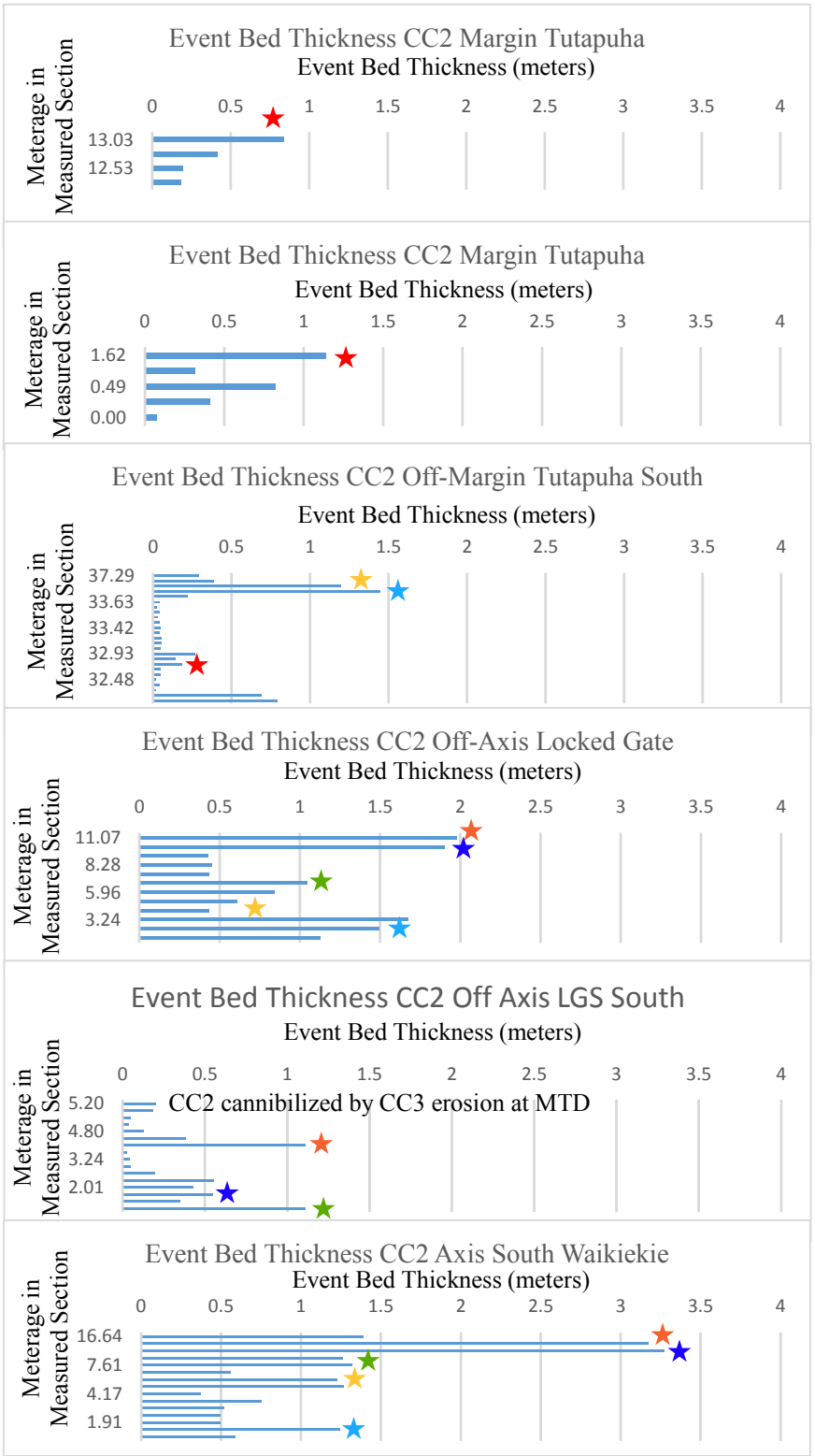


Figure 26. Event bed analysis for CC2 showing correlations between each locality where sedimentological profiles were measured.

sandstone with floating mudstone-clasts up-section from the base. The interval at Locked Gate shows high variability in the channel fill 100 meters laterally toward the south.

CC2 was likely deposited by high-density turbidity currents evidenced by cross-stratified sandstone, structureless sandstone, and the abundance of amalgamation surfaces. Flow transformations to low-density turbidity currents are inferred along the channel margin, and also south of Locked Gate where increasing amounts of plane-laminated sandstone and ripple cross-laminations are found. Correlation of the mudstone-clast conglomerate inland from the coastal section shows the flow was laterally continuous with minor variation between localities. The thick clast-supported mudstone-clast conglomerate intervals may have been deposited by hyperconcentrated density flows, and subsequently overlain by sandstone-rich sediments from high-density turbidity currents representing a flow transformation up-dip.

Channel Complex 3

Sedimentary Facies The channel fill of CC3 is characterized by approximately 20 to 25 meters of sandstone-rich sediments. Three sedimentological profiles document the lateral variation of facies, although the southernmost profile is truncated by CC4 five meters from the base of the channel. Sedimentary facies proportions for CC3 are shown in figure 20, and a cross-section for the channel from correlated sedimentological profiles is shown in figure 27.

The lowermost interval of CC3 is dominated by multiple beds of matrix supported mudstone-clast conglomerate along erosional surfaces down-cutting through the

underlying stratigraphy. Plane-parallel laminated sandstone and cross-stratified sandstone are also common, capped by ripple cross-laminated sandstone and siltstone (Figure 27). Up-section, a 2.5 meter thick sandstone shows lateral variation from plane-parallel laminated sandstone toward the south to a plane-parallel laminated sandstone, cross-stratified sandstone, and climbing ripple cross-laminated sandstone to the north. The southern exposure is subsequently truncated by erosion from CC4. Beds thin above this interval to a high abundance of plane-parallel laminated and ripple cross-laminated sandstone. Approximately 6 meters from the base of the channel, an increasing amount of horizontally-stratified or spaced-stratified sandstone dominates the section above a small erosional scour filled with mudstone-clast conglomerate (Figure 27). Thin beds of plane-parallel laminated and ripple cross-laminated sandstone are also common. The upper interval of CC3 is characterized by thinning beds filled with plane-parallel laminated sandstone capped by ripple cross-laminations. The top of CC3 is subsequently truncated by CC4.

Along the margin at Tutapuha Stream, CC3 is represented by similar facies to that at Locked Gate, although beds are thinner and show more variation. The lowermost interval is dominated by thin sandstones with a high abundance of bioturbated mudstone (Figure 27). An 80 centimeter sandstone with faint laminations is correlated to the 2.5 meter thick sandstone at Locked Gate. It shows a thinning trend to the north and east. The overlying sediments increase in facies variation. Structureless sandstone is commonly overlain by plane-parallel laminated sandstone and bioturbated sandstone present in nearly equal quantities. Minor abundances of ripple cross-laminated sandstone,

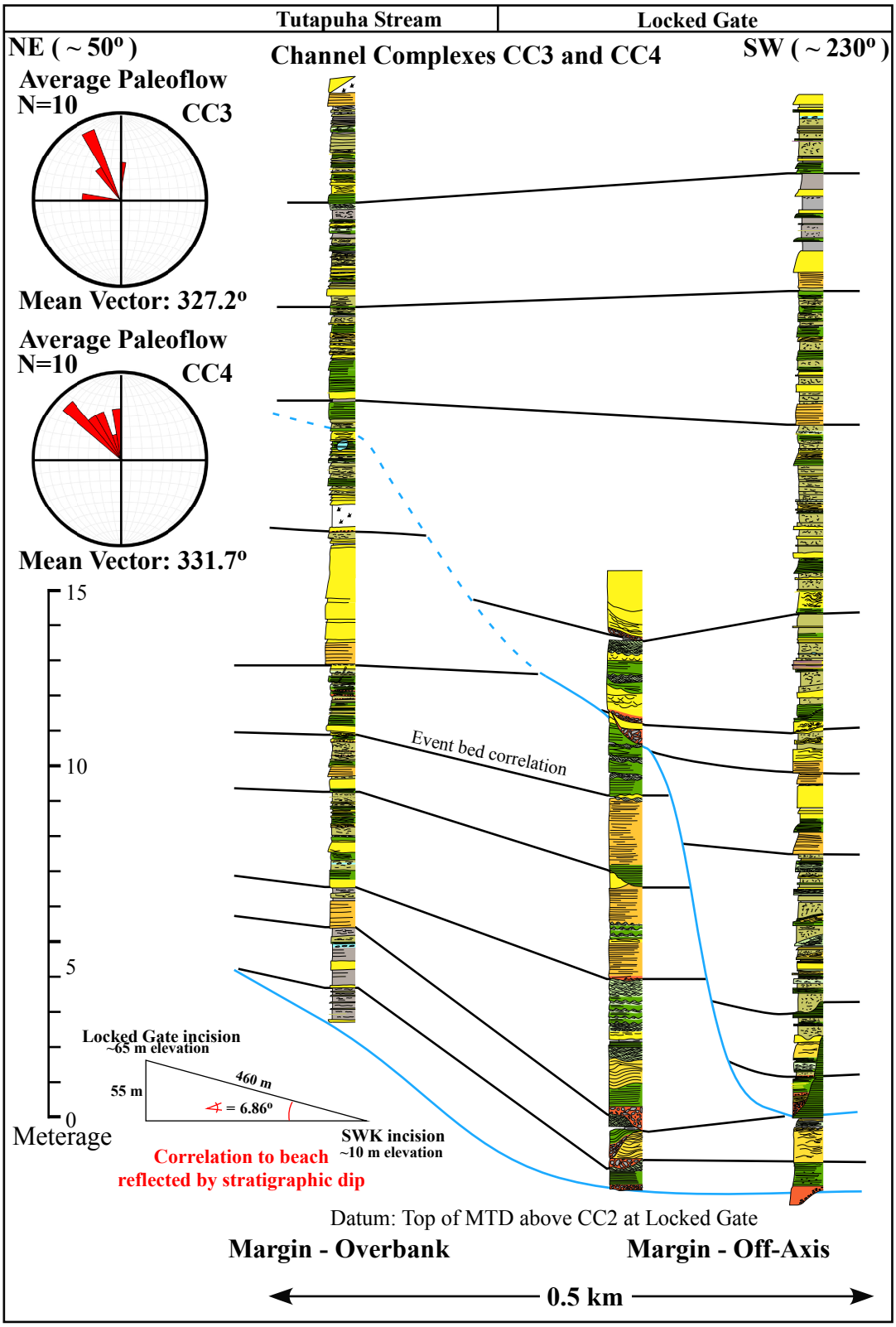


Figure 27. Cross-section for CC3 and CC4 showing measured sedimentological profiles with event bed correlations between localities.

mudstone-clasts, and horizontally-stratified or spaced-stratified sandstone are also present. The top of the Locked Gate exposure is correlated laterally to an increasing presence of plane-parallel laminated sandstone, and decreasing presence of bioturbated sandstone along the margin. Minor erosional scours and ripple cross-laminations are also present. Above this interval, a massive-bedded sandstone 4 meters thick has multiple amalgamation surfaces internally (Figure 27). At the base it is filled by horizontally-stratified or spaced-stratified sandstone, with structureless sandstone above. The uppermost bed is bioturbated, with a 4 centimeter mudstone-clast horizon. Beds thin above this interval to the top of the channel.

South of Waikiekie Stream, measured profiles were not possible due to truncation at the channel margin and the inaccessibility to climb the coastal cliffs. From photo-panel analysis, higher amounts of mudstone-clast conglomerate are present with thick-bedded sandstone above (Figure 14). Beds generally thin up-section with a second interval of thick-bedded sandstone deposited toward the top of the outcrop.

Paleoflow Analysis Paleoflow analysis for CC3 is documented from ten measurements. Measurements were acquired from asymmetric ripple cross-laminations and climbing ripple cross-laminations from Locked Gate and Tutapuha Stream. At Locked Gate, asymmetric ripple cross-laminations indicate flows were directed at 5°, 7°, and 270°. Asymmetric ripple cross-laminations along the margin at Tutapuha Stream indicate a paleoflow direction than ranges from 326° to 338°. The mean vector for paleoflow is 327.2°, or to the northwest.

Event Bed Thickness Analysis Event bed analysis for CC3 reflects the presence of two thickening-thinning upward trends, although smaller-scale thickening-thinning trends are seen within the beds present along the margin at Tutapuha Stream (Figure 28). Within exposures at Locked Gate, the lower package is represented by four smaller-scale packages, each with a thinning-upward signature (Figure 28). Each package is approximately 2 to 4 meters thick and represented by one thicker bed at their base, with significantly thinner event beds above. The upper package at Locked Gate is represented by one thinning-upward package that is 4.5 meters thick and marked at its base by a 2.4 meter event bed. The overlying stratigraphy is truncated by CC4.

Along the margin at Tutapuha Stream, four smaller-scale packages are also seen in the lower interval (Figure 28). These packages generally show a thinning-upward trend, although the lowermost interval shows a slight thickening trend. Each package is approximately 1 to 2.5 meters thick and represented by one thicker bed at their base with thinner event beds above. The upper package at Tutapuha Stream is characterized by four thickening-thinning trends upward from its base (Figure 28). Event beds thicken in the lower two meters to a bed 1.6 meters thick, followed by significant bed thinning. The overlying packages reflect event beds with nearly symmetric thickening-thinning trends, although the thickest event beds at the turnaround are generally less than 0.5 meters each (Figure 28). Each package in the upper interval is approximately 1 meter thick, although the lowermost package is 6 meters thick.

Flow Transformations Sedimentary facies present in CC3's channel fill show minor flow transformations from the channel axis to margin. At Locked Gate, the

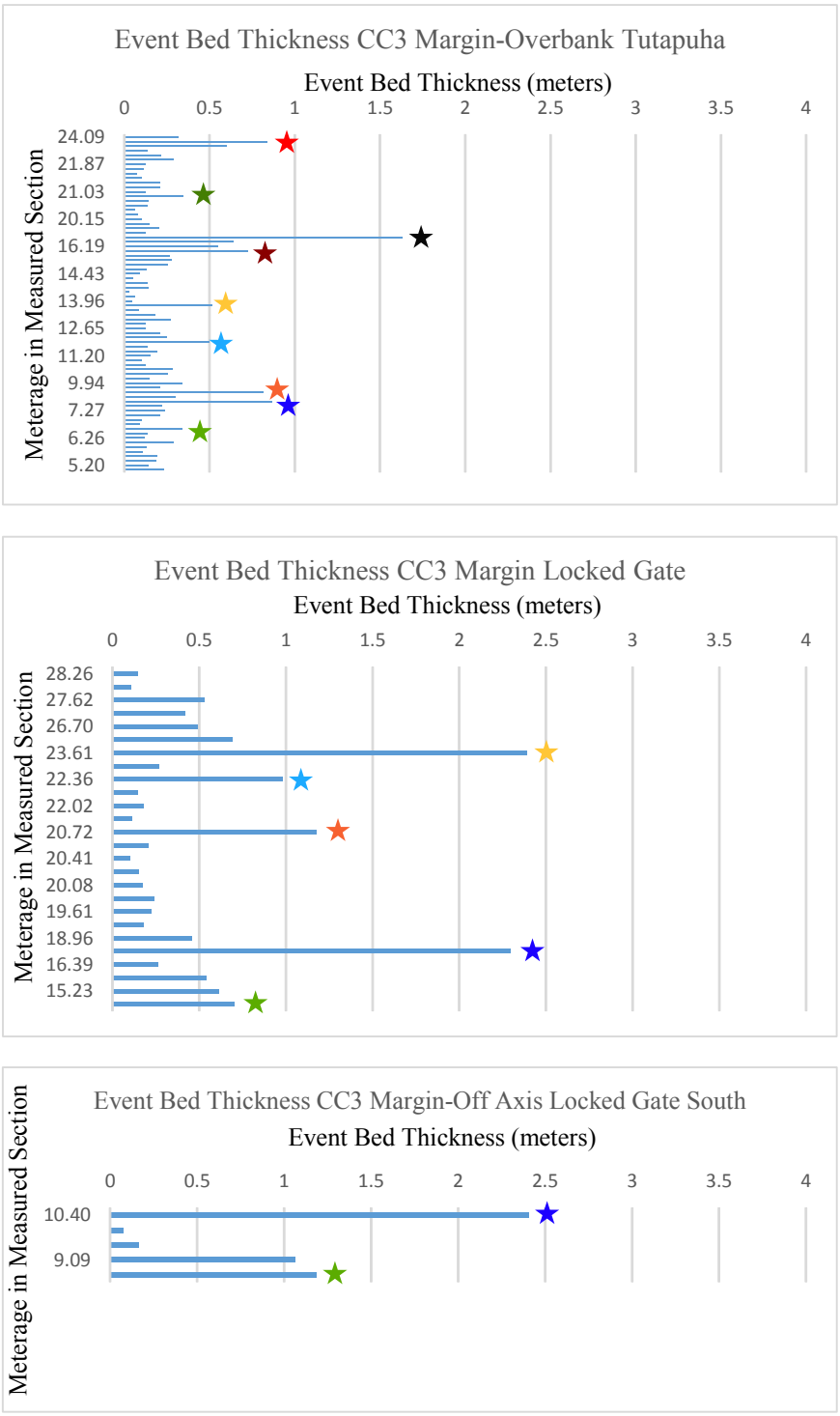


Figure 28. Event bed analysis for CC3 showing correlations between each locality where sedimentological profiles were measured.

transition from mudstone-clast conglomerate at the base to plane-parallel laminated sandstone, cross-stratified sandstone, and ripple cross-laminated sandstone correlate to a sandstone bed with faint laminations overlain by siltstone along the channel margin at Tutapuha Stream. Up-section, increasing amounts of horizontally-stratified or spaced-stratified sandstone correlate to structureless sandstone overlain by plane-parallel laminated sandstone, ripple cross-laminated sandstone, and bioturbated sandstone along the margin. The uppermost interval is represented by plane-parallel laminated and ripple cross-laminated beds at Locked Gate. Laterally at Tutapuha Stream, the same interval shows structureless sandstone overlain by plane-laminated sandstone and minor amounts of thin mudstone-clast conglomerate, bioturbated sandstone, and ripple cross-laminated sandstone.

Deposition of CC3 was likely dominated by low-density turbidity currents evidenced by the high abundance of plane-parallel laminated and ripple cross-laminated sandstone. The middle interval may represent a brief transition to high-density flows that laterally transitioned to low-density turbidity currents. This is inferred by the increased presence of horizontally-stratified or spaced-stratified sandstone at Locked Gate and the lateral correlation to plane-parallel laminated sandstone and bioturbated sandstone capped by a minor abundance of ripple cross-laminations at Tutapuha Stream. Within the interpreted axis of CC3 along the coastal section south of Waikiekie Stream, deposits likely represent high-density flows. Erosional surfaces are filled by mudstone-clast conglomerate and subsequently overlain by massive sandstone that thins up-section.

Flows likely transitioned from high-density turbidity currents at the base to low-density flows above.

Channel Complex 4

Sedimentary Facies The channel fill of CC4 is characterized by approximately 20 to 25 meters of sandstone-rich sediments. The base of CC4 truncates into the underlying strata of the CC3 channel. Sedimentary facies proportions for CC4 are shown in figure 20, and a cross-section for the channel from correlated sedimentological profiles is shown in figure 27.

Minor amounts of matrix-supported mudstone-clast conglomerate are present within the base of the channel. Up-section, sandstones are characterized by a variety of facies. Plane-parallel laminated sandstone, cross-stratified sandstone, and bioturbated sandstone are present in the most abundance, with a minor abundance of ripple cross-laminations. Bioturbated sandstone becomes the dominant lithology two meters above the channel base. Inclined elementary channels within this interval typically are filled by wavy-laminated sandstone and ripple cross-laminated sandstone. Bed tops are iron-rich and overlain by bioturbated sandstone. The bioturbated interval is approximately 5 meters thick. The overlying sandstones are thicker bedded, and filled by horizontally-stratified or spaced-stratified sandstone, plane-parallel laminated sandstone, structureless sandstone, and convoluted sandstone (Figure 27). Minor ripple cross-laminations, bioturbated sandstone, and siltstone partings are present. The interval thins up-section to a siltstone-rich interval correlated to the coastal section south of Waikiekie Stream. Beds are

bioturbated and wavy-laminated to convolute. Bioturbated sandstone increases in abundance above the siltstone-rich interval. Minor amounts of plane-parallel laminated sandstone and structureless sandstone are present. The uppermost interval of CC4 is characterized medium-bedded sandstones filled with plane-parallel laminated sandstone. Bioturbated sandstone is common at bed tops. Minor amounts of horizontally-stratified or spaced-stratified sandstone, structureless sandstone, and ripple cross-laminations also are present to the top of the channel (Figure 27).

Correlation to the margin at Tutapuha Stream shows similar facies for the upper intervals. There is some uncertainty whether the basal section at Locked Gate correlates to the thick-bedded interval along the margin, or if it represents the uppermost fill of CC3 (Figure 27). The margin of CC4 is dominated by plane-parallel laminated and wavy-laminated sandstone, with moderate amounts of bioturbated sandstone and structureless sandstone. Beds are medium- to thick-bedded at the base, and decrease in thickness up-section. Increasing amounts of bioturbated sandstone and mudstone are present toward the top of the channel.

Along the coastal outcrops, mudstone-clast conglomerate fills the base of the channel. Sandstone beds above the conglomerate thin upward to a mudstone-rich interval. The mudstone-rich interval shows minor deformation and wavy-laminated bedding (Figure 14). One ~15 centimeter sandstone bed splits the middle of the interval and pinches out laterally. The upper interval present in the coastal section is thick-bedded and shows no traceable bedding planes laterally.

Paleoflow Analysis Paleoflow analysis for CC4 was documented from ten measurements. Asymmetric ripple cross-laminations and climbing ripple cross-laminations within the outcrops at Locked Gate indicate paleoflow direction ranged between 311° to 359°. The mean vector for paleoflow is 331.7°, or to the northwest.

Event Bed Thickness Analysis Event bed analysis for CC4 reflects the presence of two large-scale thickening-thinning trends, although multiple smaller-scale thickening-thinning trends are seen within outcrops south of Locked Gate and at Tutapuha Stream (Figure 29). Within exposures at Locked Gate, the lower package is represented by eight or nine smaller-scale thickening-thinning trends. Individual packages are approximately 2 to 4 meters thick. These likely represent individual elementary channels that filled the channel complex. Event bed thickness is significantly lower than those present in the underlying channels. The thickest event bed in the lower interval is approximately 85 centimeters. The upper package at Locked Gate is represented by three to five smaller-scale thickening-thinning trends. Individual packages are approximately 1 to 3 meters thick (Figure 29).

At Tutapuha Stream, it is interpreted that only the upper package is present. This reflects the large erosional surface that is present at the Locked Gate locality. It is assumed that flows were largely confined within this erosional surface south of Locked Gate and did not extend to the Tutapuha locality, although this may be explored further. The upper interval at Tutapuha reflects three to five smaller-scale thickening-thinning packages. They are less pronounced than those in the Locked Gate locality, but still easily

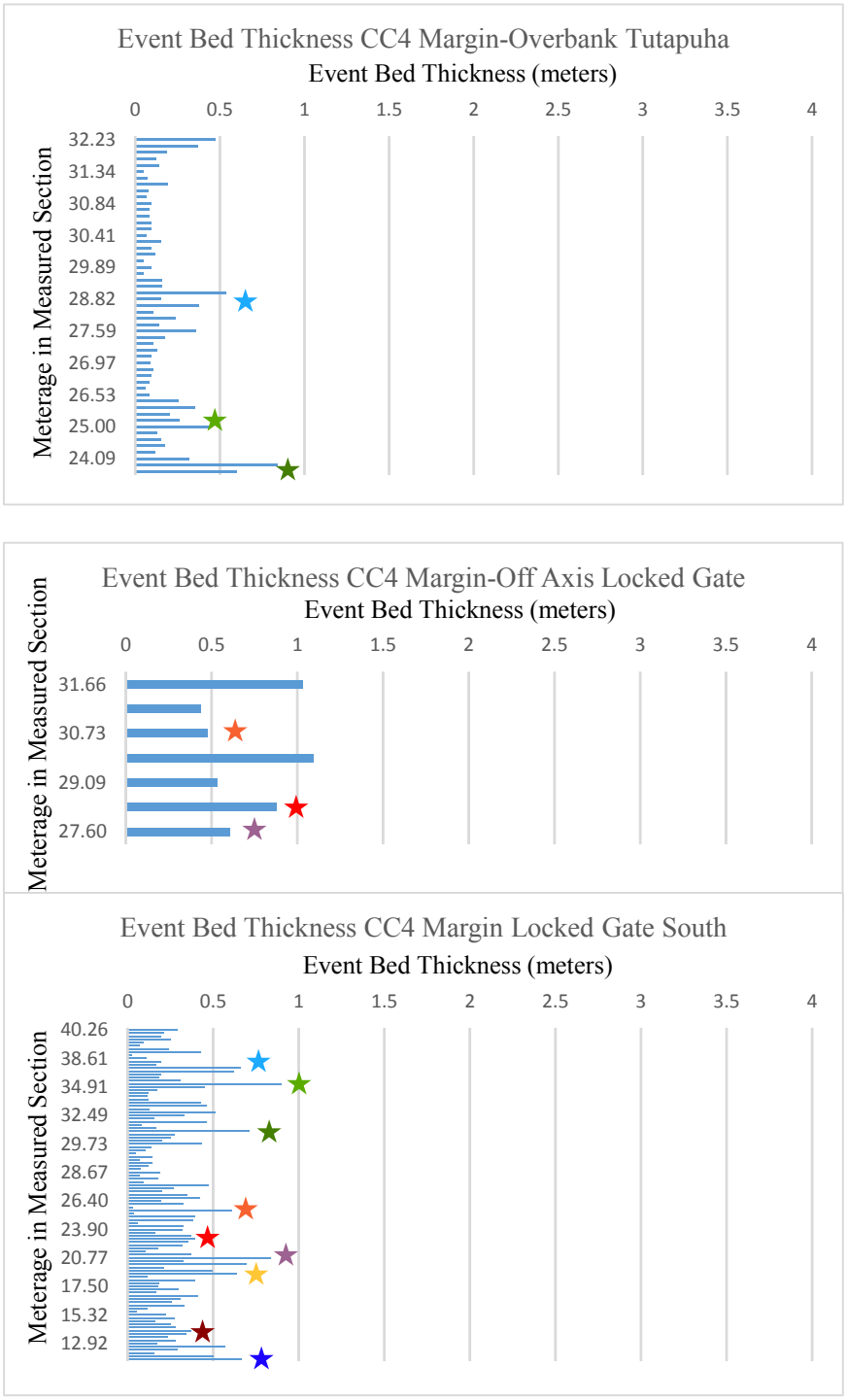


Figure 29. Event bed analysis for CC4 showing correlations between each locality where sedimentological profiles were measured.

recognizable (Figure 29). Individual thickening-thinning trends are approximately 1 to 3 meters.

Flow Transformations Lateral flow transformations are not discussed for CC4 due to insufficient data, and uncertainty in the correlation to the margin at Tutapuha Stream. Overall, the sediments present within CC4 reflect deposition by low-density turbidity currents. An increasing abundance of bioturbated sandstone represents flows were less frequent than those in the underlying channels. Event bed analysis shows they were also much smaller. Minor amounts of plane-parallel laminated sandstone and ripple cross-laminations indicate flow velocity was waning.

Channel Stacking Patterns

Exposures of six channel complexes present in the LMMF characterize a large channel belt that evolved through time. This channel belt is inferred to be approximately 3 to 3.5 km wide and 150 meters thick. The channel belt represents the evolution and stacking of smaller channel complexes through time that are approximately 800 meters to 1.3 km wide and 25 to 30 meters thick. Paleo-channel trends determined by paleoflow analysis are presented in figure 30.

Outcrop exposures show the channel belt evolved from multilateral offset at its base to channels that were more multistory above the Waikiekie Stream MTD. The large-scale stacking pattern is inferred to reflect a multistory nesting of channels migrating through time (Figure 7).

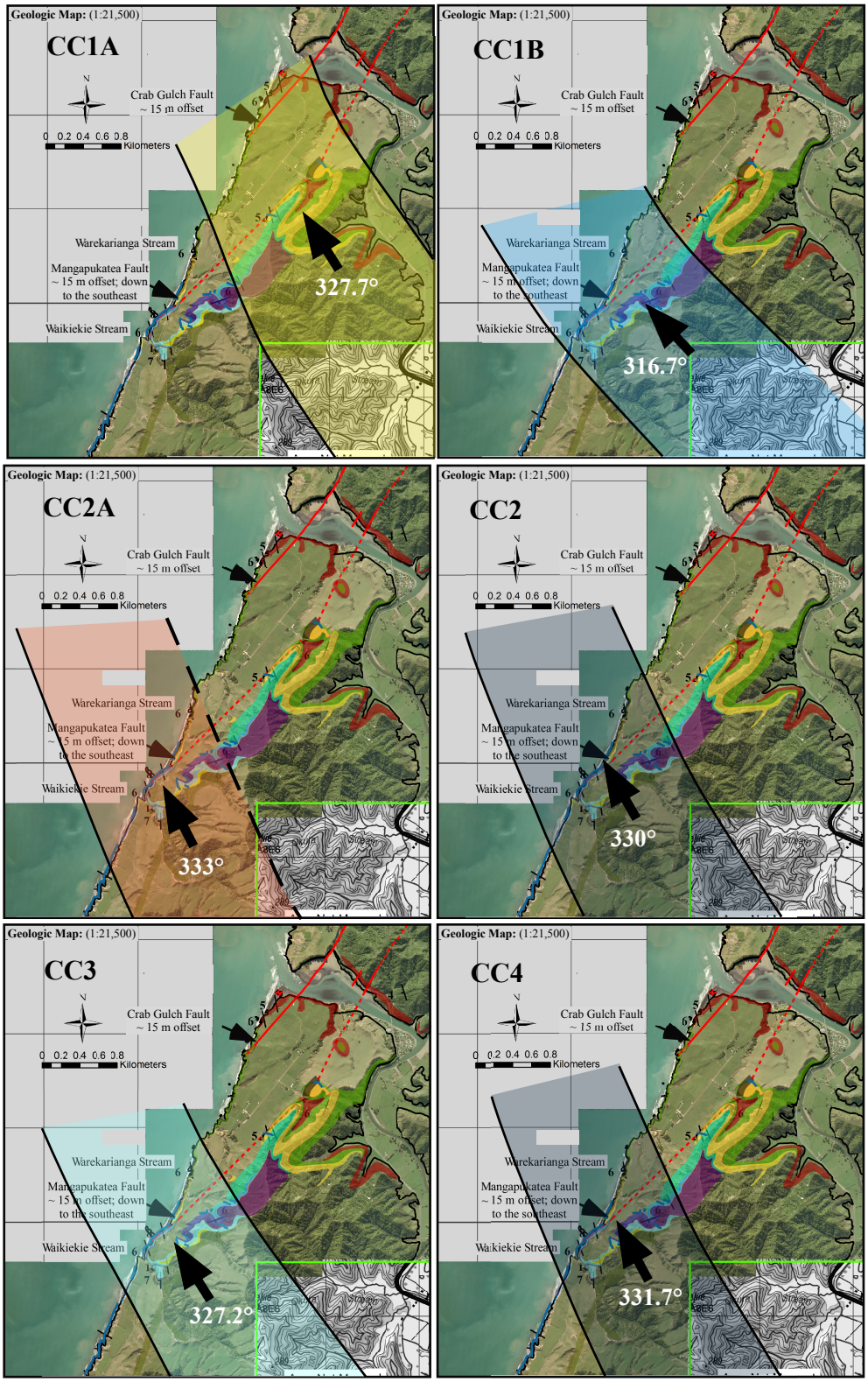


Figure 30. Paleo-channel trends from documented paleoflow analysis and correlations of channel bodies.

The basal channel shows minor scours at its base with loading into the underlying mudstone. It is interpreted that CC1A likely represents sediments that were deposited by relatively unconfined flows at the channel base, followed by an increasing amount of confinement and channelization up-section. Deposition of CC1B represents multilateral offset from CC1A with flows that were more confined at the base of the channel, reflected by the presence of a large erosional surface (Figure 31). Flows were likely able to scale to the boundary of the major erosional surface and are laterally continuous within the channel. Above CC1B, a second multilateral offsetting is represented with the deposition of CC2A. CC2A is the southernmost channel within the study area. Above CC2A, channels migrated back toward the north where CC2, CC3, and CC4 were subsequently deposited with a multistory stacking pattern (Figure 31, 32). The stacking pattern of CC2, CC3, and CC4 indicates more confinement within the depositional system.

Paleogeography

Influence from Mass-Transport Deposits

Mass-transport deposits likely influenced the deposition of channelized intervals within the LMMF. The NWK mass-transport deposit is present below CC1A. It is highly deformed north of Waikiekie Stream, but less deformed within the inland outcrops. Within the outcrops north of Waikiekie Stream, a localized section of deformation extends vertically into the mass-transport deposit (Figure 8). It is hypothesized that this localized deformation may have influenced the fluidization of overlying sediments. Large

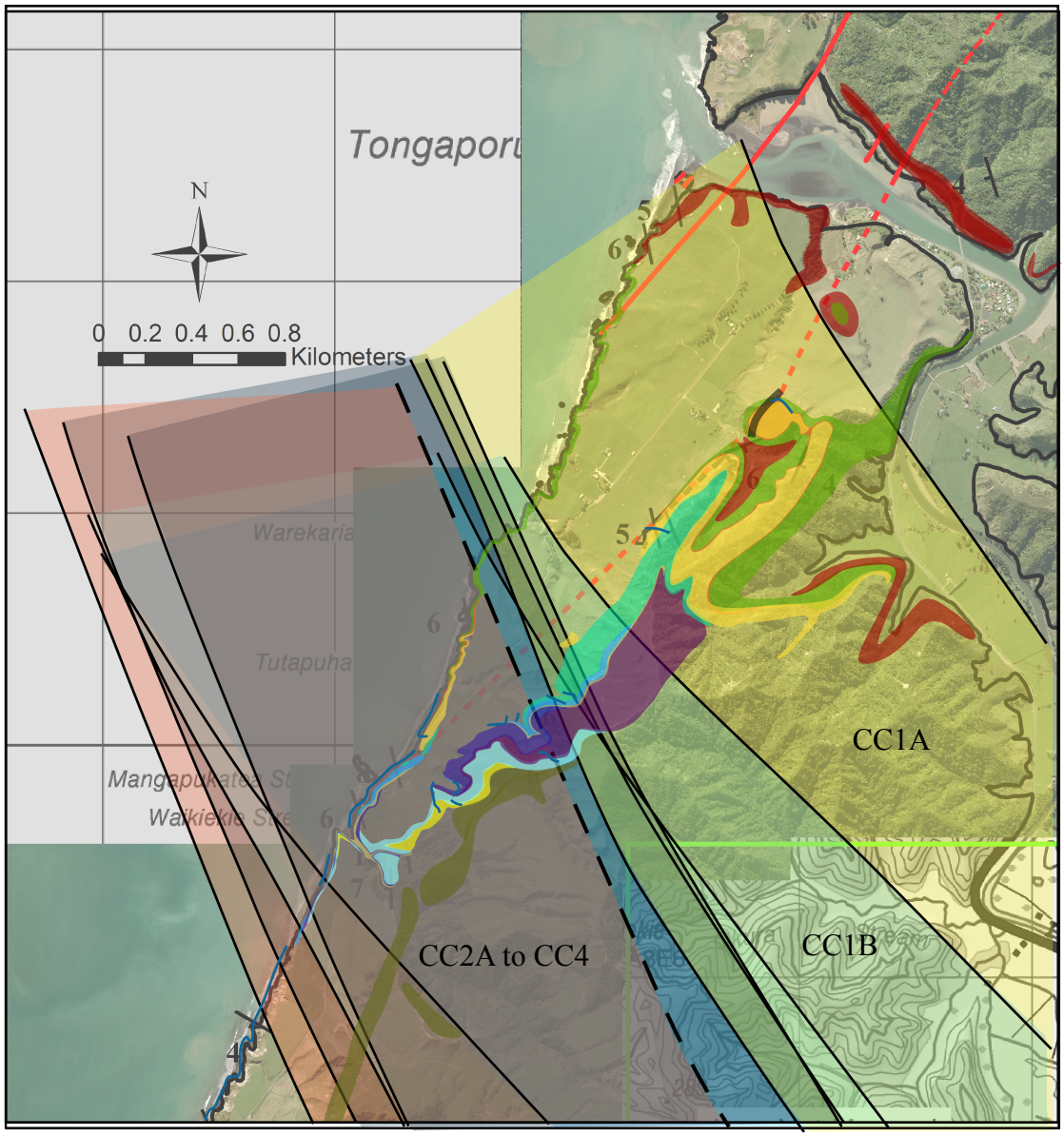


Figure 31. Stacked channel complex trends from paleoflow analysis for the LMMF showing CC1A in yellow and CC1B in light green toward the north offsetting multi-laterally to the south. CC2A through CC4 are stacked overlying one another with a multistory stacking pattern to the south above the Waikiekie MTD.

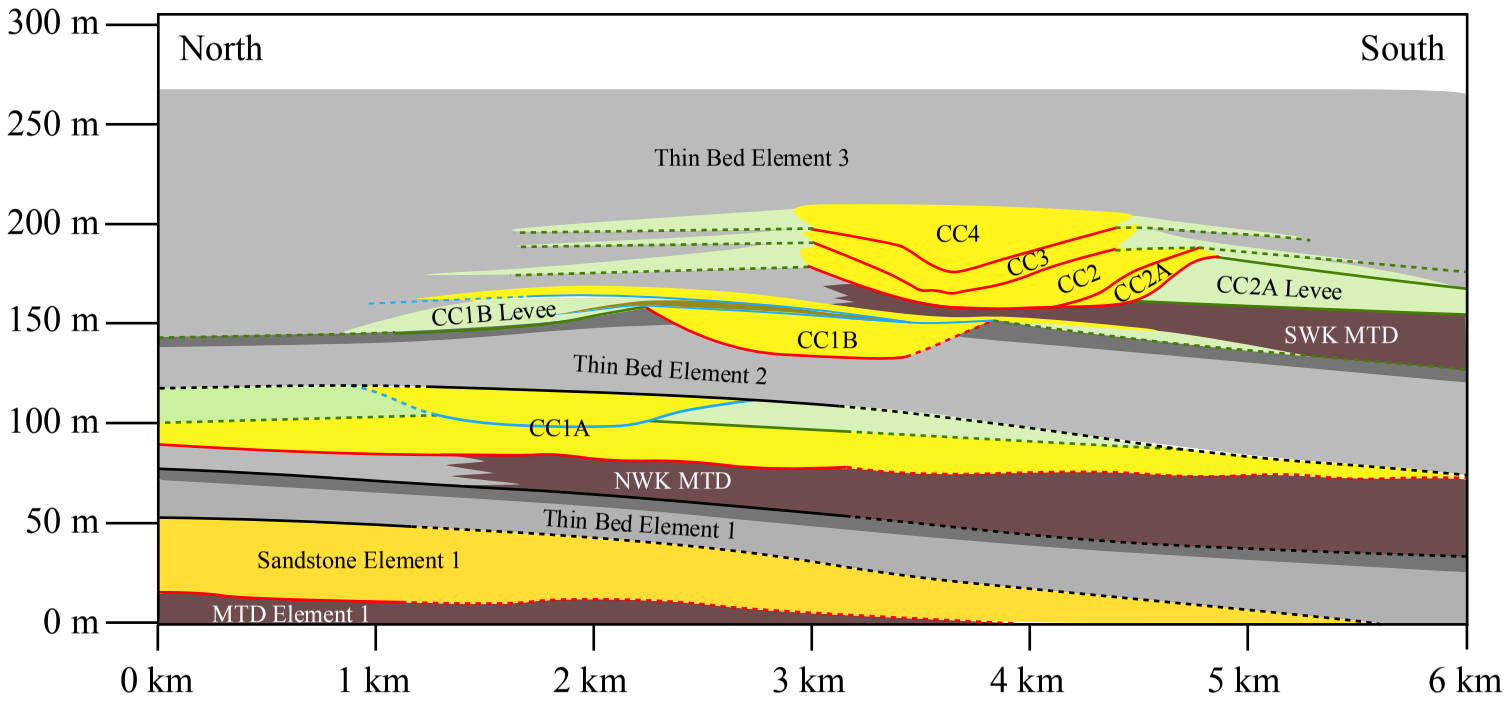


Figure 32. Simplified cross-section of the depositional system within the study area. Solid lines represent exposed stratigraphy, and dashed lines are interpretations into the subsurface. The multilateral to multistory stacking pattern is seen within CC1A to CC4. Yellow represents sandstone-rich units, light green represents levee and overbank units, brown represents mass-transport deposits, light gray represents mudstone-rich thin beds, and dark gray represents volcaniclastic-rich sediments.

deformed sandstone blocks are present immediately overlying the deformation, and the mass-transport deposit thickens to the south from the locality. It is likely that sandstone deposition within CC1A was already occurring when the mass-transport initiated, evidenced by the incorporation of large sandstone blocks into the flow. It may be possible that the second composite channel within CC1A was partially influenced by the NWK mass-transport deposit, although data is inconclusive for this hypothesis.

The Waikiekie Stream mass-transport deposit overlies CC1B, with subsequent deposition of CC2A through CC4. This mass-transport deposit is characterized by increasing deformation to the south toward Waikiekie Stream where the interpreted axes of the overlying channels are present. It is hypothesized that localized topography created from the mass-transport deposit influenced the placement of the overlying channels. CC2A steps the furthest south above the MTD and the overlying channels reflect a different stacking pattern than the underlying CC1A and CC1B. Channels are more confined and more erosional than those below, reflected by a multistory stacking pattern. Deformation of the mass-transport deposit decreases to the north within the study area.

Sediment Provenance Analysis

Southern: Long Distance Transport

Quartz-rich sediments within the MMF are interpreted from the literature to reflect long distance transport from a southern hinterland (Jordan et al., 1994; Kamp et al., 2004). Within the LMMF, channelized sandstone deposits are largely dominated by these quartz-rich sediments. Quartz-rich sandstones account for 85 to 90 percent of the

sedimentary fill of channel deposits (Figure 20). Outside the channel margins, less sandstone is present. Within these intervals, quartz-rich sandstone account for 20 to 40 percent of the sedimentary fill (Figure 20). Sandstone is less prevalent above the channel belt where increasing abundances of bioturbated mudstone are seen.

Northern: Mohakatino Volcanic Arc

Volcaniclastic-rich sediments within the MMF are interpreted from the literature to reflect transport from a northern volcanic arc (King et al., 1993). Volcaniclastic sediments are primarily found outside the channel margins, although few occurrences are seen within the channel bodies at the base of sandstones (Figure 20). Volcaniclastic sediments decrease in abundance up-section in the LMMF, with the highest percentage present outside the channel margin of CC1B. Mudstone dominated intervals along this margin are comprised of volcaniclastic-rich sandstone and claystone, accounting for 30 to 70 percent of the sedimentary fill. Within channelized deposits, volcaniclastic sediments account for less than 1 percent of the channel fill across the channel belt, although interpreted levee deposits are characterized with up to 10 percent. The mudstone-rich thin-bedded interval overlying the channel belt shows similar trends to the channelized sections, with volcaniclastic sandstone accounting for less than 1 percent of the sedimentary fill (Figure 20). The overall influence of volcaniclastic sediments within the LMMF was low.

Eastern: Shelf/Slope

Strata rich with bioclastic shell debris and organics are interpreted to represent sediments originating from the eastern shelf or slope. Shell debris is found across the LMMF, both within and bounding channel deposits, and organic-rich deposits are primarily found outside the channel, and within channel levees (Figure 20). Bioclastic shell debris accounts for less than a percent up to 7 percent of the sedimentary fill depending upon the locality. The highest abundances of shell debris are found within channel margins, channel levees, and mass-transport deposits, although one interval within the axis of CC1B represents percentages between 1 to 2 percent. Organic-rich sediments account for less than a percent up to 2 percent of the sedimentary fill across the LMMF. The overall influence from the eastern shelf or slope was low within the LMMF.

CONCLUSIONS

Sedimentology

This study analyzed outcrop exposures within the LMMF along the Taranaki coast of New Zealand to document a detailed description of sedimentary facies, event beds, and sedimentary bodies within a deep-water channelized depositional system. Measured sedimentological profiles document a number of attributes with centimeter-scale resolution to interpret hydrodynamic facies and formative processes at the time of deposition.

Sedimentological profiles totaling 552 meters reflect 30 hydrodynamic facies described from outcrop exposures and thin section analysis. Facies vary from mudstone-clast conglomerate, sandstone, siltstone, mudstone, post-depositionally modified sediments, and tuffaceous sediments. Each facies represents varying hydrodynamic processes and sediment sources present during deposition. Sediments in the LMMF are inferred to reflect deposition by high- and low-density turbidity currents, concentrated and hyperconcentrated density flows, en masse movements, and debris flows.

The sediments of the LMMF are highly variable and record multiple flow processes that represent differing flow strengths, flow frequencies, and event bed thicknesses. Through the evolution of the LMMF, deposits were dominated by high-density turbidity flows near the base that decrease in frequency toward the top of the channel belt. The uppermost intervals reflect deposition by a higher abundance of low-density turbidity flows that were less frequent, and smaller in their event size.

Architectural Elements and Stratigraphic Evolution

Architectural elements documented in the channelized interval of the LMMF exhibit a number of varying attributes. These include scale, geometry, complexity, lithology, and facies associations. This study analyzed channelforms, wedgeforms/levees, drapes, mass-transport deposits, and laminated thin beds, although lobeforms are present at the base of the LMMF.

Two mass-transport deposits, the NWK MTD and the Waikiekie Stream MTD are hypothesized to have influenced channelized intervals above. The NWK MTD shows rafting of large sandstone blocks correlated to the base of CC1A. This indicates deposition of CC1A had already begun when the slumping initiated. Higher abundances of erosional scours and mudstone-clast conglomerate increase up-section and likely represent an increase in confinement within the system. The Waikiekie Stream MTD is present below CC2A and CC2, with CC3 and CC4 up-section. These channel complexes overlie the deformed interval of the mass-transport deposit and show increased confinement reflected by a multistory stacking pattern.

Six channel complexes are inferred within the LMMF. The lowermost CC1A is represented with moderate amounts of erosion at its base, and increasing erosion up-section. It is hypothesized that CC1A was likely deposited by partially confined flows at its base followed by the slumping of the NWK MTD which increased confinement within the depositional system allowing increased channelization to occur in the upper composite channel.

CC1B is dominated largely by confined to partially confined deposits that fill a 15 to 20 meter erosional scour above undeformed mudstone. It is inferred that flows scaled to the boundary of the erosional surface reflected by bed correlations from the margin to the axis. Up-section flows became less confined than below, spilling sandstone sediments outside of the major erosional surface and toward the channel levee.

CC2A through CC4 are deposited above the Waikiekie Stream MTD. An increased abundance of large erosional scours and mudstone-clast conglomerate found within the inferred channel axes south of Waikiekie Stream likely represent channels were more confined than below. A change from multilateral stacking of channels to more multistory story stacking also reflects increased confinement within the depositional system.

The correlations presented here reflect a few key differences from previous authors. The 2007 study by GNS does not correlate the coastal section south of Waikiekie Stream to the inland outcrops (Arnot et al., 2007). The change in channel architecture is inferred to represent two channels (C5 and C6) that are younger than those inland (Arnot et al., 2007). Their study discusses the possibility of multiple channels down-cutting within a master erosion surface, subsequently depositing the coastal interval (Arnot et al., 2007). This study agrees that more confinement was present within this interval, although new data presented here shows the channels within the inland section do correlate to the beach outcrops. The change in channel architecture is inferred to primarily reflect spatial variation from the margin to the axis of the channel. Deposition of CC2A through CC4 likely represents confinement within a 1.7 km wide master channel represented by the

multistory stacking pattern. The underlying CC1A and CC1B were likely less confined, reflected by multilateral offset toward the south. This study hypothesizes a larger 3.5 km wide channel belt, initiated by the slumping of the NWK MTD that increased confinement up-section. Subsequent channels were offset to the south where the Waikiekie MTD is fully deformed. A localized topographic high created by the Waikiekie Stream MTD is hypothesized to have influenced confinement in the overlying channels.

The 2013 study by Masalimova infers CC1A represents a proximal frontal or crevasse splay setting. This study agrees with Masalimova's interpretation. Flows were more erosive up-section from the base, but the presence of a large-scale erosional surface at the base was not observed. Minor amounts of erosion, up to 7 to 10 meters into the underlying mudstone, indicate less erosional confinement than the channels present above. Her study shows similar correlations presented within this study for the upper channels, although with decreasing confidence up-section for CC2 through CC4. She describes the channels south of Waikiekie Stream as A, B, and C from youngest to oldest, but does not show how they correlate to the inland section (Masalimova, 2013).

Channel trends within the LMMF indicate little variation in their paleoflow direction. Channels were directed to the northwest during the deposition of CC1A through CC4, although minor fluctuation is seen between each locality. The stacking pattern of channel complexes records changes in confinement temporally up-section through the LMMF. CC1A and CC1B offset laterally to one another toward the south. Above CC1B, channel complexes CC2A through CC4 are spatially confined above one

another with little offsetting. This transition reflects a change from multilateral channel stacking to multistory channel stacking within the depositional system. Overall, a multistory nesting of channels is inferred for the LMMF.

The LMMF records a deep-water depositional system that transitioned from weakly confined deposits near its base, to deposits that progressively became more confined up-section. Large channels directed sediment basinward through a variety of subaqueous flow types, although high- and low-density turbidity currents are inferred to have been most common. The uppermost intervals of the LMMF recorded a temporal decrease in flow strength, with more variation in their sediments. Flows become less frequent, and event bed thickness decreased in size indicating the local depositional system was waning.

REFERENCES CITED

Allen, J.R.L., 1963, Asymmetrical ripple marks and the origin of water-laid cosets of cross-strata: Geological Journal, v. 3, p. 187-236.

Allen, J.R.L., 1968, Current ripples: Their relation to patterns of water and sediment motion: Amsterdam, North-Holland Publishing Company, 433 p.

Allen, J.R.L., 1983, Studies in fluviatile sedimentation: bars, bar-complexes and sandstone sheets (low-sinuosity braided streams) in the Brownstones (L. Devonian), Welsh Borders: Sedimentary Geology, v. 33, p. 237-293.

Arnot, M.J., King, P.R., Browne, G.H., and Helle, K., 2007, Channelized, innermost, basin-floor-fan morphologies, Mount Messenger Formation, Waikiekie South Beach and inland, New Zealand, in Nilsen, T.H., Shew, R.D., Steffens, G.S., and Sudlick, J.R.J., eds., Atlas of deep-water outcrops, American Association of Petroleum Geologists Studies in Geology, v. 56, p. 249-256.

Barnes, N.E. and W.R. Normark, 1985, Diagnostic parameters for comparing modern submarine fans and ancient turbidite systems. In Bouma, Normark, and Barnes, (Eds.) Submarine fans and related turbidite systems: New York, Springer-Verlag., p. 12-22.

Bouma, A.H., 1962, Sedimentology of some flysch deposits: Amsterdam, Elsevier Pub. Co., 168 p.

Browne, G.H., McAlpine, A., and King, P.R., 1996, An outcrop study of bed thickness, continuity and permeability in reservoir facies of the Mt Messenger formation, North Taranaki: New Zealand Petroleum Conference Proceedings, v. 1, p. 154-163.

Browne, G.H. and Slatt, R.M., 2002, Outcrop and behind-outcrop characterization of a Late Miocene slope fan (channel-levee complex), Mt Messenger Formation, New Zealand: American Association of Petroleum Geologists Bulletin, v. 86, p. 841-862.

Browne, G.H., Slatt, R.M., and P.R. King, 2000, Contrasting styles of basin-floor fan and slope fan deposition: Mount Messenger Formation, New Zealand, in A. H. Bouma and C. G. Stone, eds., Fine-grained turbidite systems: AAPG Memoir 72 /SEPM Special Publication 68, p. 143–152.

Browne, G.H., Strachan, L.J., King, P.R., and Malcolm J.A., 2006, Mass-transport complexes from a Late Miocene deep-water succession, Taranaki Basin, New Zealand: Scales, styles, and significance in relation to tectonic, eustatic, and autocyclic drivers: Search and Discovery Article #50040.

Browne, G.H., King, P.R., Higgs, K.E., and Slatt, R.M., 2005, Grain-size characteristics for distinguishing basin floor fan and slope fan depositional settings: Outcrop and subsurface examples from the late Miocene Mount Messenger Formation, New Zealand: New Zealand Journal of Geology and Geophysics, v. 48 (2), p. 213-227.

Clark, J.D., and Pickering, K.T., 1996a, Architectural elements and growth patterns of submarine channels: application to hydrocarbon exploration: American Association of Petroleum Geologists Bulletin, v. 80, no. 2, p. 194-221.

Clark, J.D., and Pickering, K.T., 1996b, Submarine Channels, 231p.

Edbrooke, S.W., 2005, Geology of the Waikato area: Institute of Geological & Nuclear Sciences 1:250,000 geological map 4: Lower Hutt, New Zealand, Institute of Geological & Nuclear Sciences Limited, 1 sheet + 68 p.

Fisher, R.V., 1983, Flow transformations in sediment gravity flows: Geology, v. 11, p. 273-274.

Gardner, M.H. and Borer, J.M., 2000, Submarine channel architecture along a slope to basin profile, Brushy Canyon Formation, West Texas. In Bouma, A.H. and Stone, C.G., (eds.), Fine-grained turbidite systems, AAPG Memoir 72/SEPM Special Publication, p. 195-214.

Gardner, M.H., Borer, J.M., Melick, J.J., Mavilla, N., Dechesne, M., and Wagerle, R.N., 2003, Stratigraphic process-response model for submarine channels and related features from studies of Permian Brushy Canyon outcrops, West Texas: Marine and Petroleum Geology, v. 20, p. 757-787.

Gardner, M.H., Borer, J.M., Romans, B.W., Baptista, N., Kling, E. K., Hanggoro, D., Melick, J.J., Wagerle, and R.M., Carr, M.M., 2008, Stratigraphic models for deep-water sedimentary systems, in GCSSEPM.

Hampton, M.A., 1972, The role of subaqueous debris flow in generating turbidity currents: Journal of Sedimentary Petrology, v. 42, no. 4, p. 775-793.

Hart, A., 2001, Taranaki basin yielding large oil and gas discoveries: Oil and Gas Journal, v. 99, no. 29, p. 38-44.

Hart, A., 2001, Numerous play types evident in Taranaki Basin: Oil and Gas Journal, v. 99, no. 30, p. 40-43.

Haughton, P.D.W., Barker, S.P., and McCaffrey, W.D., 2003, “Linked” debrites in sand-rich turbidite systems-origin and significance: Sedimentology, v. 50, p. 459-482.

Haughton, P., Davis, C., and McCaffrey., W., 2006, "Facies prediction in turbidite fan systems – nature and significance of ‘linked debrites’ in sand-rich versus mixed sand-mud systems" Recent advances in siliciclastic facies models: implications for reservoir characterization II (SEPM), AAPG Annual Convention, April 9-12, 2006 Technical Program.

Helle, K., 2003, Anatomy and allostratigraphy of deep-marine Mount Messenger Formation (Miocene), eastern-margin Taranaki Basin, New Zealand [M.Sc. thesis]: University of Bergen. 94 p.

Hiscott, R.N., 1994, Traction-carpet sedimentation in turbidites – fact or fiction?: Journal of Sedimentary Research, A64, p. 204-208

Hiscott, R.N., 1994, Loss of capacity, not competence, as the fundamental process governing deposition from turbidity currents: Journal of Sedimentary Research, A64, p. 209–214.

Ineson, J.R., 1985, Submarine glide blocks from the Lower Cretaceous of the Antarctic Peninsula: Sedimentology, v. 32, p. 657-670.

Jobe, Z.R., Lowe, D.R., Normark, W.R., 2012, Climbing-ripple successions in turbidite systems: Depositional environments, sedimentation rates and accumulation times: Sedimentology, v. 59, p. 867-898.

Jordan, D. W., Schultz, D. J., Cherng, J. A., 1994, Facies architecture and reservoir quality of Miocene Mount Messenger deep-water deposits, Taranaki Peninsula, New Zealand: GCSSEPM Foundation 15th annual research conference: submarine fans and turbidite systems, p. 151-166.

Kamp, P.J.J., Vonk, A.J., Bland, K.J., Hansen, R.J., Hendy, A.J., McIntyre, A.P., Ngatai, M., Cartwright, S.J., Hayton, S., and Nelson, C.S., 2004, Neogene stratigraphic architecture and tectonic evolution of Wanganui, King County, and eastern Taranaki Basins, New Zealand: New Zealand Journal of Geology & Geophysics, v. 47, p. 625-644.

King, P.R., Browne, G.H., Arnot, M.J., Slatt, R.M., Helle, K., and Stromsoyen, I., 2007, A 2-D oblique-dip outcrop transect through an entire third-order, progradational, deep-water clastic succession (late Miocene Mount Messenger-Urenui Formations), Taranaki Basin, New Zealand, in Nilsen, T.H., Shew, R.D., Steffens, G.S., and Sudlick, J.R.J., eds., Atlas of deep-water outcrops:

American Association of Petroleum Geologists, Studies in Geology, v. 56, p. 238-240.

King, P.R., 2000, Tectonic reconstructions of New Zealand: 40 Ma to present: New Zealand Journal of Geology and Geophysics, v. 43, p. 611-638.

King, P.R. and Thrasher, G.P., 1992, Post-Eocene development of the Taranaki Basin, New Zealand: Convergent overprint of a passive margin, In: Watkins, J.S. Watkins, F. Zhiqiang, and K.J. McMillen, eds., Geology and geophysics of continental margins: AAPG Memoir 53, p. 93-118.

King, P. R., Browne, G. H., and Slatt, R. M. 1994b: Sequence architecture of exposed Late Miocene basin floor fan and channel-levee complexes (Mount Messenger Formation), Taranaki Basin, New Zealand. GCSSEPM Foundation 15th annual research conference: submarine fans and turbidite systems, 4-7 December. Pp. 177-192.

King, P.R. and Thrasher, G.P., 1996, Cretaceous-Cenozoic geology and petroleum systems of the Taranaki Basin, New Zealand: Institute of Geological and Nuclear Sciences, Monograph 13, p. 244.

King, P.R., Browne, G.H., and Robinson, P.H., 1993, Description, correlation and depositional history of Miocene sediments outcropping along North Taranaki Coast, New Zealand: Institute of Geological and Nuclear Sciences, Monograph 5.

King, P.R., Ilg, B.R., Arnot, M., Browne, G.H., Strachan, L.J., Crundwell, M., and Helle, K., 2011, Outcrop and seismic examples of mass-transport deposits from a Late Miocene deep-water succession, Taranaki Basin, New Zealand, in Posamentier, H.W., Shipp, C., Weimer, P., eds., Submarine Slope Systems: SEPM Special Publication No. 96.

Kneller, B.C. and Branney, M.J., 1995, Sustained high-density turbidity currents and the deposition of thick massive sands: Sedimentology, v. 42, p. 607-616.

Kneller B., 2003, The influence of flow parameters on turbidite slope channel architecture: Marine and Petroleum Geology, v. 20, p. 901-910.

Kuenen, P.H., 1952, Estimated size of the Grand Banks turbidity current: American Journal of Science, v. 250, p. 874-884.

Lowe, D.R., 1982, Sediment gravity flows; II, Depositional models with special reference to the deposits of high-density turbidity currents: Journal of Sedimentary Petrology, v. 52, no. 1, p. 279-297.

Lowe, D.R. and Guy, M., 2000, Slurry-flow deposits in the Britannia Formation (Lower Cretaceous), North Sea: a new perspective on the turbidity current and debris flow problem: Sedimentology, v. 47, p. 31-70.

Manley, R., and Lewis, D.W., 1998, Ichnocoenoses of the Mount Messenger Formation, a Miocene submarine fan system, Taranaki Basin, New Zealand: New Zealand Journal of Geology and Geophysics, v. 41, p. 15-33.

Masalimova, L.U., 2013, Stratigraphic architecture and flow dynamics of deep-water turbidite deposites: the Miocene Lower Mount Messenger Formation in the Taranaki Basin in New Zealand, and the Oligocene Puchkirchen Formation in the Molasse Basin in Austria [Ph.D. thesis]: Stanford University, 213 p.

McHargue, T., Pyrcz, M.J., Sullivan, M.D., Clark, J.D., Fildani, A., Romans, B.W., Covault, J.A., Levy, M., Posamentier, H.W., and Drinkwater, N. J., 2011, Architecture of turbidite channel systems on the continental slope: patterns and predictions: Marine and Petroleum Geology, v. 28(3), p. 728-743.

Miall, A.D., 1985, Architectural-element analysis: a new method of facies analysis applied to fluvial deposits: Earth Science Review, v. 22, p. 261-308.

Meiburg, E., and Kneller, B., 2009, Turbidity currents and their deposits. Annual Review Fluid Mechanics, v. 42, p. 135-156.

Middleton, G.V., 1967, Experiments on density and turbidity currents. III, Deposition of sediment: Canadian Journal of Earth Science, v. 4, p. 475-505.

Middleton, G.V., 1970, Experimental studies related to the problems of flysch sedimentation. In: Flysch Sedimentology in North America: Geological Association of Canada Special Paper 7, p. 253-272.

Middleton, G.V., and Hampton, M.A., 1973, Sediment gravity flows: mechanics of flow and deposition, in G.V. Middleton, and A.H. Bouma, Co-chairmen, Turbidites and Deep-water Sedimentation: Society of Economic Paleontologists and Mineralogists, Pacific Section, Short Course Notes, p. 1-38.

Middleton, G.V. and Hampton, M.A., 1976, Subaqueous sediment transport and deposition by sediment gravity flows, *In*: Marine sediment transport and environmental management (Eds D.J. Stanley and D.J.P. Swift, John Wiley & Sons, New York), p. 197-218.

Middleton, G.V., and Southard, J.B., 1984, Mechanics of sediment movement: SEPM, Short course No. 3, Binghamton, New York, p. 401.

Middleton, G.V., 1993, Sediment deposition from turbidity current: Annual Review Earth Planet Science, v. 21, p. 89-114.

Mulder, T., and Alexander, J., 2001, The physical character of subaqueous sedimentary density flows and their deposits: Sedimentology, v. 48, p. 269–299.

Mutti, E., and Normark, W.R., 1987, Comparing examples of modern and ancient turbidite systems: Problems and concepts, in J.K. Leggett and G.G. Zuffa, eds., Marine Clastic Sedimentology: Concepts and case studies; Graham & Trotman, London, p. 1-38.

Normark, W.R., 1978, Fan valleys, channels, and depositional lobes on modern submarine fans: Characters for recognition of sandy turbidite environments: AAPG Bulletin, v. 62, p. 912-931.

Nyman, S.L., Nelson, C.S., Campbell, K.A., Schellenberg, F., Pearson, M.J., Kamp, P.J.J., Browne, G.H., and King, P.R., 2006, Tubular carbonate concretions as hydrocarbon migration pathways? Examples from North Island, New Zealand: In Proceedings of New Zealand Petroleum Conference 2006, 6 – 10 March.

Peakall, J., McCaffrey, W.D., and Kneller, B.C., 2000, A process model for the evolution, morphology and architecture of meandering submarine channels: Journal of Sedimentary Research, v. 70, p. 434-448.

Pearson, M.J., Grosjean, E., Nelson, C.S., Nyman, S.L., and Logan, G.A., 2010, Tubular concretions in New Zealand petroliferous basins: lipid biomarker evidence for mineralization around proposed Miocene hydrocarbon seep conduits: Journal of Petroleum Geology, v. 33, p. 205-219.

Raine, I., Cook, R., Strong, P., 2004, Eastern Taranaki boundary fault paleontology and time of thrusting: Institute of Geological & Nuclear Sciences science report 2004/12. Institue of Geological & Nuclear Sciences, Wellington, 63 p.

Schneider, J.L., Ruyet, A.L., Chanier, F., Buret, C., Ferriere, J., Proust, J.N., and Rosseel, J.B., 2001, Primary or secondary distal volcaniclastic turbidites: how to make the distinction? An example from the Miocene of New Zealand (Mahia Peninsula, North Island): Sedimentary Geology, v. 145, p. 1-22.

Sorby, H.C., 1859, On the structures produced by the currents present during the deposition of stratified rocks: Geologist, v. 2, p. 137-147.

Sprague, A.R.G., Garfield, T.R., Goulding, F.J., Beaubouef, R.T., Sulivan, M.D., Rossen, C., Campion, K.M., Sickafoose, D.K., Abreu, V., Schellpeper, M.E., Jensen, G.N., Jennette, D.C., Pirmez, C., Dixon, B.T., Ying, D., Ardill, J., Mohrig, D.C., Porter, M.L., Farrell, M.E., and Mellere, D., 2005, Integrated slope channel depositional models: the key to successful prediction of reservoir presence and quality in offshore west Africa: CIPM, cuarto E-Exitep 2005, Veracruz, Mexico, p. 1-13.

Stagpoole, V., and Nicol, A., 2008, Regional structure and kinematic history of a large subduction back thrust: Taranaki Fault, New Zealand: Journal of Geophysical Research: Solid Earth, v. 113, B01403.

Sylvester, Z., Pirmez, C., and Cantelli, A., 2011, A model of submarine channel-levee evolution based on channel trajectories: Implications for stratigraphic architecture: Marine and Petroleum Geology, v. 28(3), p. 716-727.

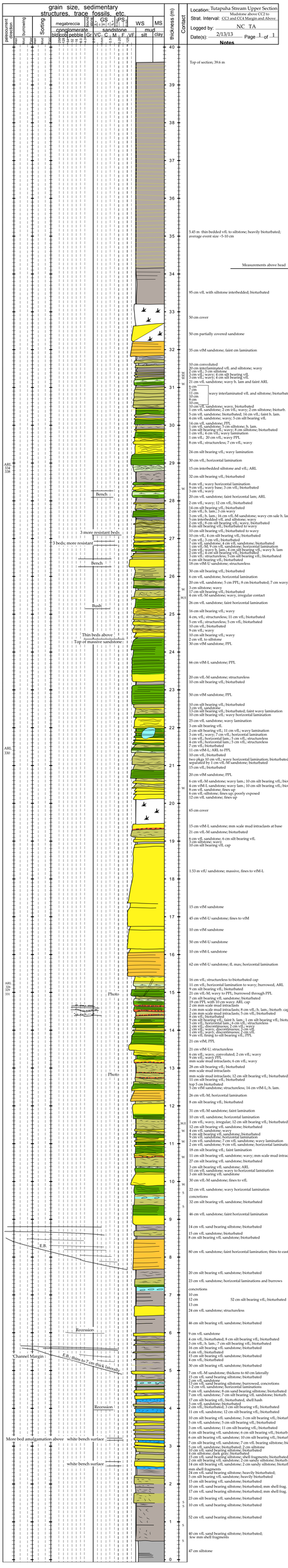
Talling, P.J., Masson, D.G., Sumner, E.J., and Malgesini, G., 2012, Subaqueous sediment density flows: depositional processes and deposit types: Sedimentology, v. 59, p. 1937-2003.

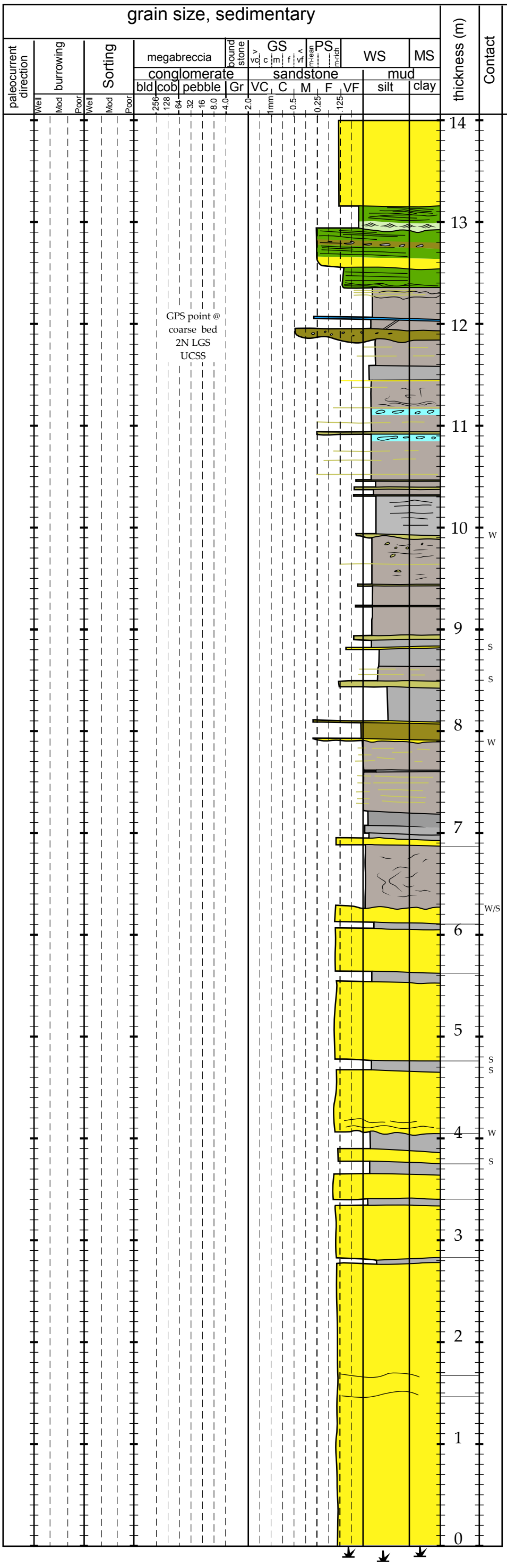
Walker, R.G., 1978, Deep-water sandstone facies and ancient submarine fans: models for exploration and stratigraphic traps: AAPG Bulletin, v. 62, p. 932-966.

APPENDICES

APPENDIX A

MEASURED SEDIMENTOLOGICAL SECTIONS


grain size, sedimentary structures, trace fossils, etc.
Location: Tutapuka Stream Upper Section
Strat. Interval: Mudstone above CC2 to CC1 and CC4 Margin and Above
Logged by: NC TA
Date(s): 2/13/13 Page 1 of 1
Notes
thickness (m)
Context
paleocurrent direction
Sorting
bioturbation
megabreccia
conglomerate
sandstone
mud
WS
MS
silt
clay
Top of section; 39.6 m
5.45 m thin bedded vfL to siltstone; heavily bioturbated; average event size ~5-10 cm
Measurements above head
95 cm vfL with siltstone interbedded; bioturbated
50 cm cover
50 cm partially covered sandstone
35 cm vfM sandstone; faint cm lamination
10 cm convoluted
20 cm interlaminated vfL and siltstone; wavy
3 cm vfL; wavy; 4 cm silt bearing vfL
3 cm vfL; wavy; 4 cm silt bearing vfL
21 cm vfL sandstone; wavy h. lam and faint ARL
6 cm
7 cm
11 cm
10 cm
9 cm
10 cm
wavy interlaminated vfL and siltstone; bioturbated
10 cm vfL sandstone; wavy, bioturbated
1 cm vfL sandstone; 3 cm vfL; wavy; 2 cm siltstone; bioturb
5 cm vfL sandstone; bioturbated; 14 cm vfL; faint h. lam.
4 cm vfL sandstone; wavy; 5 cm silt bearing vfL
14 cm vfL sandstone; PPL
1 cm vfL sandstone; 3 cm siltstone; h. lam.
3 cm silt bearing vfL; wavy; 8 cm siltstone; bioturbated
1 cm vfL; 4 cm vfL; wavy lamination
1 cm vfL; 20 cm vfL; wavy PPL
6 cm vfL; structureless; 7 cm vfL wavy
24 cm silt bearing vfL; wavy lamination
30 cm vfL; horizontal lamination
15 cm interbedded siltstone and vfL; ARL
32 cm silt bearing vfL; bioturbated
8 cm vfL; wavy horizontal lamination
9 cm vfL; wavy base; 3 cm vfL; bioturbated
3 cm vfL; wavy
6 cm vfL sandstone; faint horizontal lam; ARL
2 cm vfL; wavy; 12 cm vfL; bioturbated
14 cm silt bearing vfL; bioturbated
2 cm vfL; h. lam.; 3 cm wavy
3 cm vfL; h. lam.; 16 cm vfL-M sandstone; wavy cm sale h. lam.
5 cm interbedded vfL and siltstone; wavy
2 cm vfL; 8 cm silt bearing vfL; wavy; bioturbated
8 cm silt bearing vfL; bioturbated to wavy
10 cm silt bearing vfL; bioturbated to wavy
10 cm vfL; 4 cm silt bearing vfL; bioturbated
2 cm vfL; 3 cm vfL; bioturbated
1 cm vfL sandstone; 2 cm vfL sandstone; bioturbated
1 cm vfL; 30 cm vfL sandstone; horizontal lamination
5 cm vfL; wavy h. lam.; 4 cm silt bearing vfL; wavy h. lam
2 cm vfL; 4 cm silt bearing vfL; bioturbated
3 cm vfL sandstone; bioturbated; silt bearing vfL; bioturbated
6 cm silt bearing vfL; bioturbated
18 cm vfM-U sandstone; structureless
30 cm silt bearing vfL; bioturbated
6 cm vfL sandstone; horizontal lamination
20 cm vfL sandstone; 5 cm PPL; 8 cm bioturbated; 7 cm wavy
3 cm siltstone; wavy
17 cm silt bearing vfL; bioturbated
4 cm vfL-M sandstone; wavy, irregular contact
26 cm vfL sandstone; faint horizontal lamination
16 cm silt bearing vfL; wavy
4 cm, vfL; structureless; 11 cm vfL; bioturbated
5 cm vfL; structureless; 5 cm vfL; bioturbated
10 cm vfL; bioturbated
9 cm vfL; wavy
10 cm silt bearing vfL; wavy
2 cm vfL to siltstone
30 cm vfM sandstone; PPL
66 cm vfM-L sandstone; PPL
20 cm vfL-M sandstone; structureless
10 cm silt bearing vfL; bioturbated
50 cm vfM sandstone; PPL
10 cm silt bearing vfL; bioturbated
12 cm vfL sandstone
12 cm silt bearing vfL; bioturbated; faint wavy lamination
10 cm silt bearing vfL; wavy horizontal lamination
25 cm vfL sandstone; wavy lamination
3 cm silt bearing vfL
2 cm silt bearing vfL; 11 cm vfL; wavy lamination
3 cm vfL; wavy; 7 cm vfL; horizontal lamination
1 cm vfL; horizontal lam.; 5 cm vfL; structureless
2 cm vfL; horizontal lam.; 3 cm vfL; structureless
2 cm vfL; bioturbated
11 cm vfM-L; ARL to PPL
10 cm vfL; bioturbated
two pkgs, 0 cm vfL; wavy horizontal lamination; bioturbated; separated by 1 cm vfL-M sandstone; bioturbated
15 cm vfL; bioturbated
20 cm vfM sandstone; PPL
6 cm vfL-M sandstone; wavy lam.; 10 cm silt bearing vfL; bioturb.
4 cm vfM-L sandstone; wavy lam.; 10 cm silt bearing vfL; bioturb.
8 cm vfL sandstone; fines up
6 cm vfL-siltstone; fines up; poorly exposed
12 cm vfL sandstone; fines up
65 cm cover
15 cm vfM-L sandstone; mm scale mud intraclasts at base
21 cm vfL-M sandstone; bioturbated
6 cm vfL sandstone; 6 cm silt bearing vfL
3 cm siltstone; wavy
10 cm silt bearing vfL cap
1.53 m vfU sandstone; massive, fines to vfM-L
15 cm vfM sandstone
45 cm vfM-U sandstone; fines to vfM
10 cm vfM sandstone
50 cm vfM-U sandstone
10 cm vfM-L sandstone
62 cm vfM-U sandstone; fl. max; horizontal lamination
16 cm vfL; structureless to bioturbated cap
11 cm vfL; horizontal lamination to wavy; burrowed, ARL
9 cm silt bearing vfL; bioturbated
2 cm vfL-M; wavy to PPL; burrowed through PPL
7 cm silt bearing vfL sandstone; bioturbated
19 cm PPL with 10 cm wavy ARL cap
2 cm mm scale mud intraclasts
2 cm mm scale mud intraclasts; 6 cm vfL; h. lam.; bioturb. cap
2 cm mm scale mud intraclasts; 5 cm vfL; bioturbated
2 cm vfL; bioturbated
6 cm silt bearing vfL; faint h. lam.; 1 cm silt bearing vfL; bioturb.
5 cm vfL; horizontal lam.; 6 cm vfL; structureless
5 cm vfL; discontinuous; 2 cm vfL; wavy
1 cm vfL; wavy; discontinuous; 2 cm vfL
1 cm vfL; wavy; discontinuous; 2 cm vfL
9 cm vfL fining to silt bearing vfL; PPL
21 cm vfM; PPL
21 cm vfM-U; structureless
6 cm vfL; wavy, cgrovolated; 2 cm vfL; wavy
9 cm vfL; wavy PPL
mm scale mud intraclasts; 6 cm vfL; wavy
28 cm silt bearing vfL; bioturbated
mm scale mud intraclasts
mm scale mud intraclasts; 12 cm silt bearing vfL; bioturbated
11 cm silt bearing vfL; bioturbated
top 5 cm bioturbated
5 cm vfM sandstone; structureless; 14 cm vfM-L; h. lam.
26 cm vfL-M; horizontal lamination
8 cm silt bearing vfL; bioturbated
31 cm vfL-M sandstone; faint lamination
10 cm vfL sandstone; horizontal lamination
1 cm vfL; wavy, irregular; 12 cm silt bearing vfL; bioturbated
12 cm silt bearing vfL sandstone; bioturbated
6 cm vfL sandstone; wavy
6 cm silt bearing vfL sandstone; bioturbated
9 cm vfL sandstone; horizontal lamination
2 cm vfL sandstone; 9 cm vfL sandstone; horizontal lamination
18 cm silt bearing vfL; faint lamination
11 cm silt bearing vfL sandstone; wavy; mm scale mud intraclasts
27 cm silt bearing vfL sandstone; bioturbated
3 cm silt bearing vfL sandstone; ARL
11 cm vfL sandstone; wavy to horizontal lamination
11 cm silt bearing vfL sandstone
30 cm vfL-M sandstone; fines to vfL
22 cm vfL sandstone; wavy horizontal lamination
concretions
32 cm silt bearing vfL sandstone; bioturbated
46 cm vfL sandstone; faint horizontal lamination
14 cm vfL sand bearing siltstone; bioturbated
15 cm vfL sandstone; bioturbated
8 cm silt bearing vfL sandstone; bioturbated
80 cm vfL sandstone; faint horizontal lamination; thins to east
20 cm silt bearing vfL sandstone; bioturbated
23 cm vfL sandstone; horizontal laminations and burrows
concretions
10 cm
12 cm
52 cm silt bearing vfL; bioturbated
13 cm
24 cm vfL sandstone; structureless
46 cm silt bearing vfL sandstone; bioturbated
9 cm vfL sandstone
4 cm vfL; bioturbated; 8 cm silt bearing vfL; bioturbated
3 cm vfL; h. lam.; 7 cm silt bearing vfL; bioturbated
16 cm silt bearing vfL sandstone; bioturbated
15 cm vfL sandstone; bioturbated
13 cm silt bearing vfL sandstone; bioturbated
4 cm vfL; bioturbated
30 cm silt bearing vfL sandstone; bioturbated
7 cm vfL-M sandstone; thickens to 60 cm laterally
15 cm vfL sand bearing siltstone; bioturbated
2 cm vfL sandstone
12 cm vfL sand bearing siltstone; burrowed; concretions
3 cm vfL; wavy; 2 cm silt bearing vfL; bioturbated
9 cm vfL sandstone; 6 cm sand bearing siltstone; bioturbated
7 cm vfL sandstone; 7 cm silt bearing vfL sandstone; bioturb.
17 cm silt bearing vfL; bioturbated, shell hash
2 cm vfL sandstone; bioturbated
2 cm vfL; bioturbated; 3 cm silt bearing vfL; bioturbated
11 cm vfL sandstone; 12 cm silt bearing vfL; bioturbated
10 cm silt bearing vfL sandstone; 2 cm silt bearing vfL; bioturb.
5 cm vfL sandstone; 5 cm silt bearing vfL; bioturbated
3 cm vfL sandstone; 11 cm silt bearing vfL; bioturbated
4 cm silt bearing vfL sandstone; 6 cm silt bearing vfL; bioturb.
6 cm silt bearing vfL sandstone; 10 cm silt bearing vfL; bioturb.
7 cm silt bearing vfL sandstone; 7 cm vfL bearing siltstone; bioturbated
5 cm vfL sandstone; bioturbated; 2 cm siltstone
10 cm vfL sandstone; 4 cm silt bearing vfL; bioturbated
4 cm siltstone; dark grey; bioturbated
15 cm vfL sand bearing siltstone; shell fragments; bioturbated
2 cm silt bearing vfL sandstone; 2 cm sandy siltstone; bioturb.
14 cm silt bearing vfL sandstone; 2 cm sandy siltstone; bioturb.
mm shell fragments
24 cm vfL sand bearing siltstone; heavily bioturbated;
3 cm silt bearing vfL sandstone; heavily bioturbated
15 cm silt bearing vfL sandstone; bioturbated
10 cm vfL sand bearing siltstone; bioturbated; mm shell frag.
17 cm vfL sand bearing siltstone; bioturbated; mm shell frag.
23 cm silt bearing vfL sandstone; bioturbated
10 cm vfL sand bearing siltstone; bioturbated
52 cm vfL sand bearing siltstone; bioturbated
40 cm vfL sand bearing siltstone; bioturbated; few mm shell fragments
47 cm siltstone
Bench
3 more resistant beds
3 beds; more resistant
Bench
Thin beds above
Top of massive sandstone
Thalli
Photo
Photo
E.B.
Recession
Channel Margin
E.B. thins to 7 cm thick laterally
Recession
More bed amalgamation above
white bench surface
white bench surface
ARL 334
ARL 330
ARL 332
ARL 333



Location: Tutapuha East Composite

Strat. Interval: CC1B to Base CC2

Logged by: NC TA

Date(s): 1/9/13 Page 1 of 1

Notes

80 cm vfU-fL sandstone

10 cm ARL; wavy base; upper 12 cm PPL to wavy
cm scale PPL
40 cm fU-mL sandstone with mud intraclast rip ups
10 cm fU-mL sandstone; structureless
15 cm PPL; cm scale
10 cm wavy siltstone; interbedded with sandstone lenses; sand increases up
25 cm siltstone; little bioturbation
fU sandstone; shell hash
siltstone; escape burrow
mU-cL sandstone; bioclastic debris, cm scale intraclasts

25 cm siltstone; heavily bioturbated, sandstone lenses

1 cm vfU sandstone; 12 cm siltstone

30 cm silt dominated; cm scale sandstone lenses; heavily bioturbated at base
concretions at top

fU sandstone lenses
concretions at top

40 cm siltstone
fU-mL sandstone lenses

5 cm sandstone lenses in siltstone/silty sandstone

40 cm siltstone

3 cm vfL sandstone, wavy base; discontinuous

25 cm siltstone; mm scale sandstone intraclasts; wavy bedding

20 cm siltstone

20 cm siltstone — Thick siltstone with sand lenses; heavily bioturbated

35 cm siltstone

4 cm vfM sandstone; bioturbated
1 cm vfM sandstone; 7 cm siltstone
20 cm siltstone
15 cm siltstone; heavily bioturbated
1 cm vfL sandstone lenses
5 cm vfU-fL sandstone; discontinuous, bioturbated

35 cm siltstone

2 cm mL sandstone (marker bed)
15 cm silty sandstone
2 cm mL sandstone (marker bed)
30 cm silty sandstone lenses; heavily bioturbated
1 cm siltstone
43 cm silty sandstone; bioturbated, sands are discontinuous; bioturbation of coarser sand layers

8 cm light gray siltstone; 12 cm dark gray siltstone
5 cm fL sandstone; 5 cm siltstone

60 cm silty sandtstone; heavily bioturbated

17 cm fL sandstone
5 cm siltstone

45 cm fL sandstone

10 cm siltstone

75 cm fL sandstone

10 cm siltstone

60 cm vfU-fL sandstone

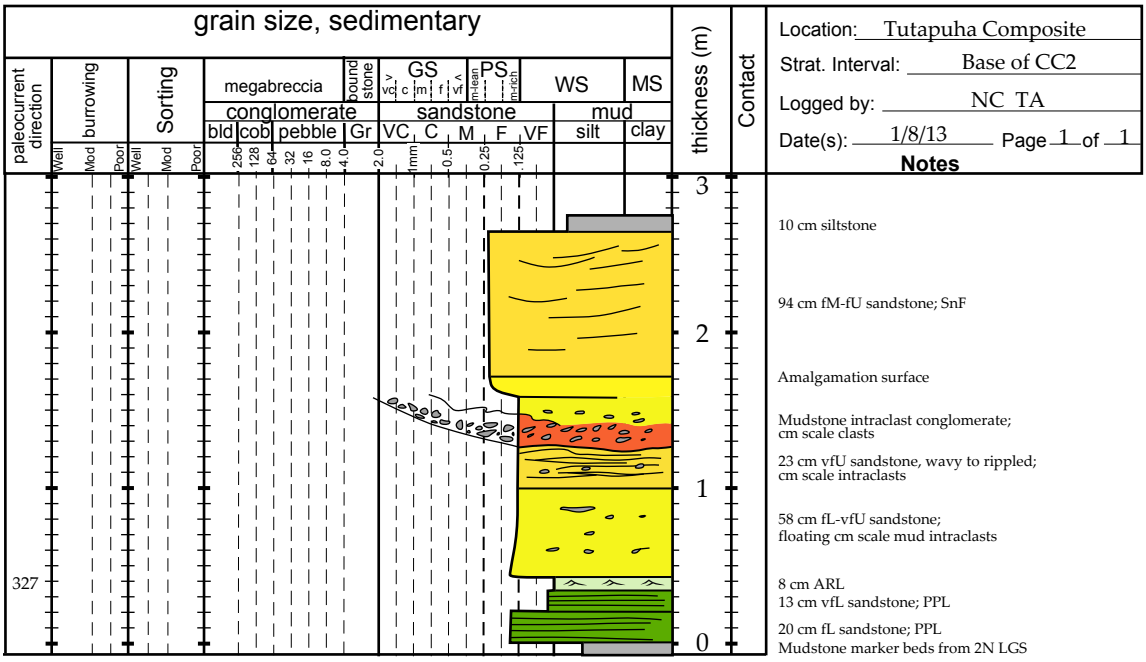
20 cm siltstone
10 cm fL sandstone
10 cm siltstone
25 cm fL sandstone
7 cm siltstone; sharp contact

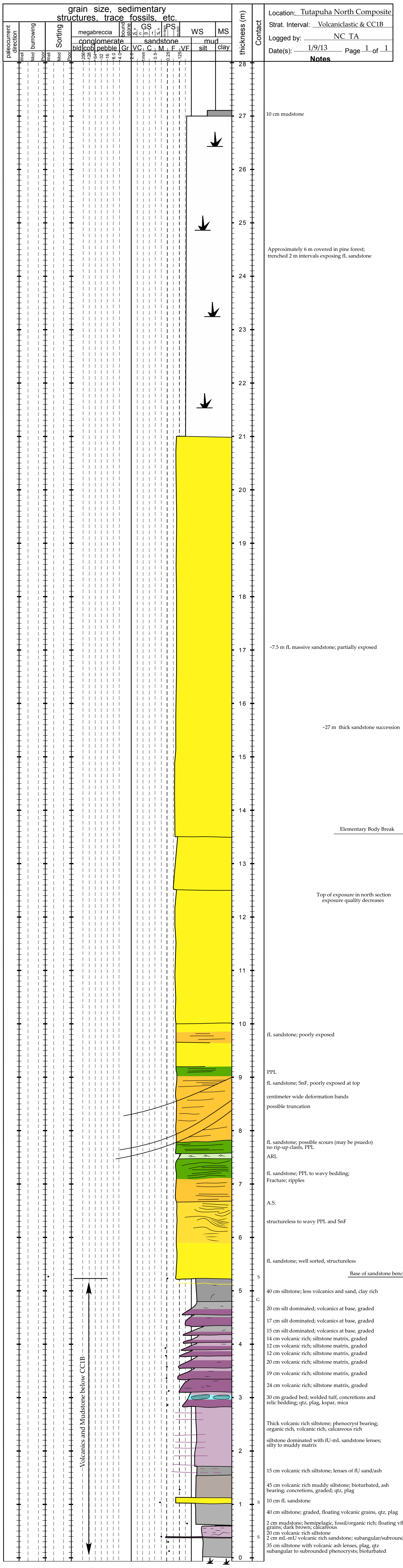
50 cm fL sandstone

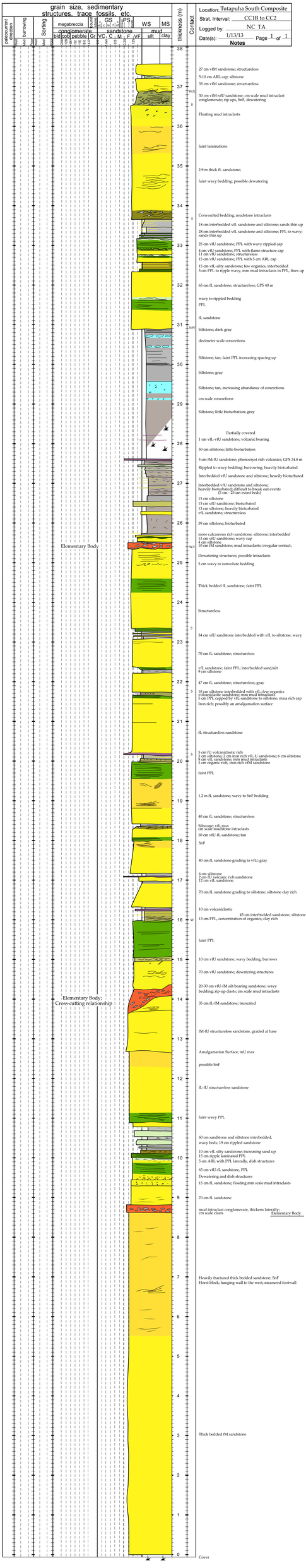
5 cm siltstone; sharp contact

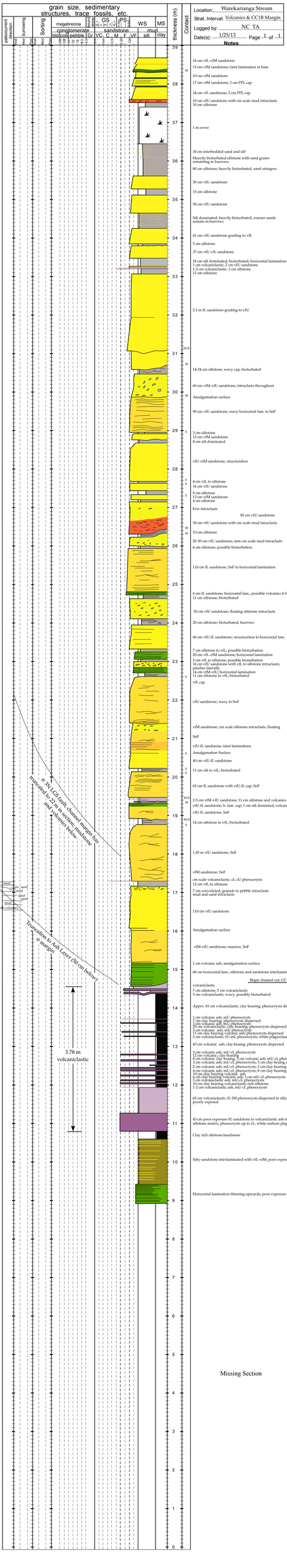
2.7 m exposed of massive fL sandstone; two wavy beds amalgamated at 1.4 m and 1.55 m

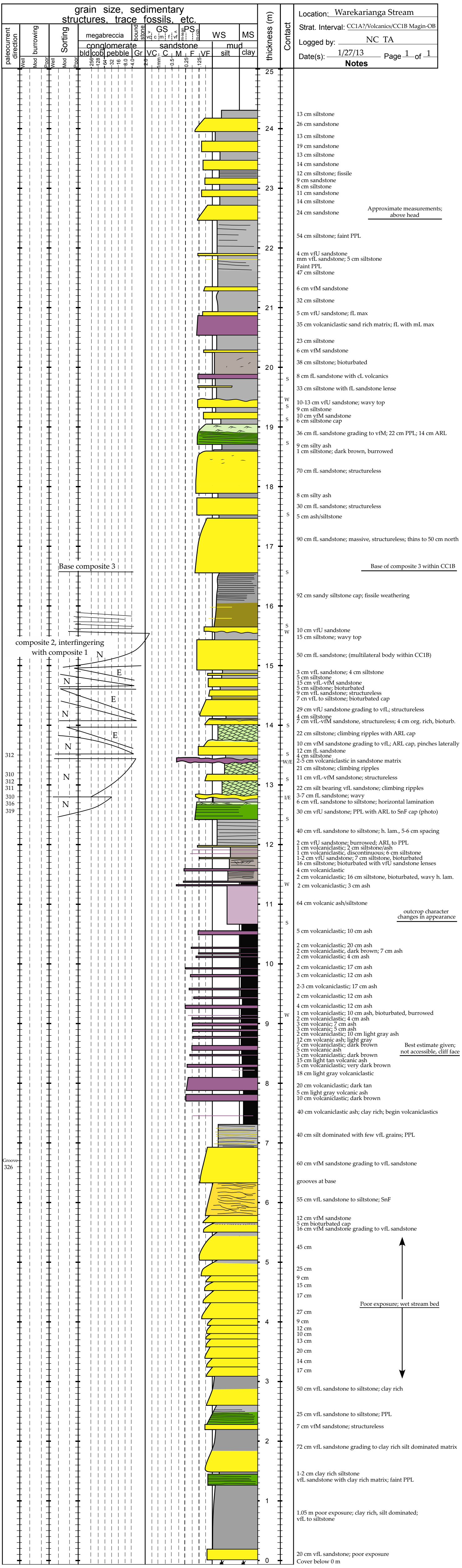
Cover (massive sandstone)

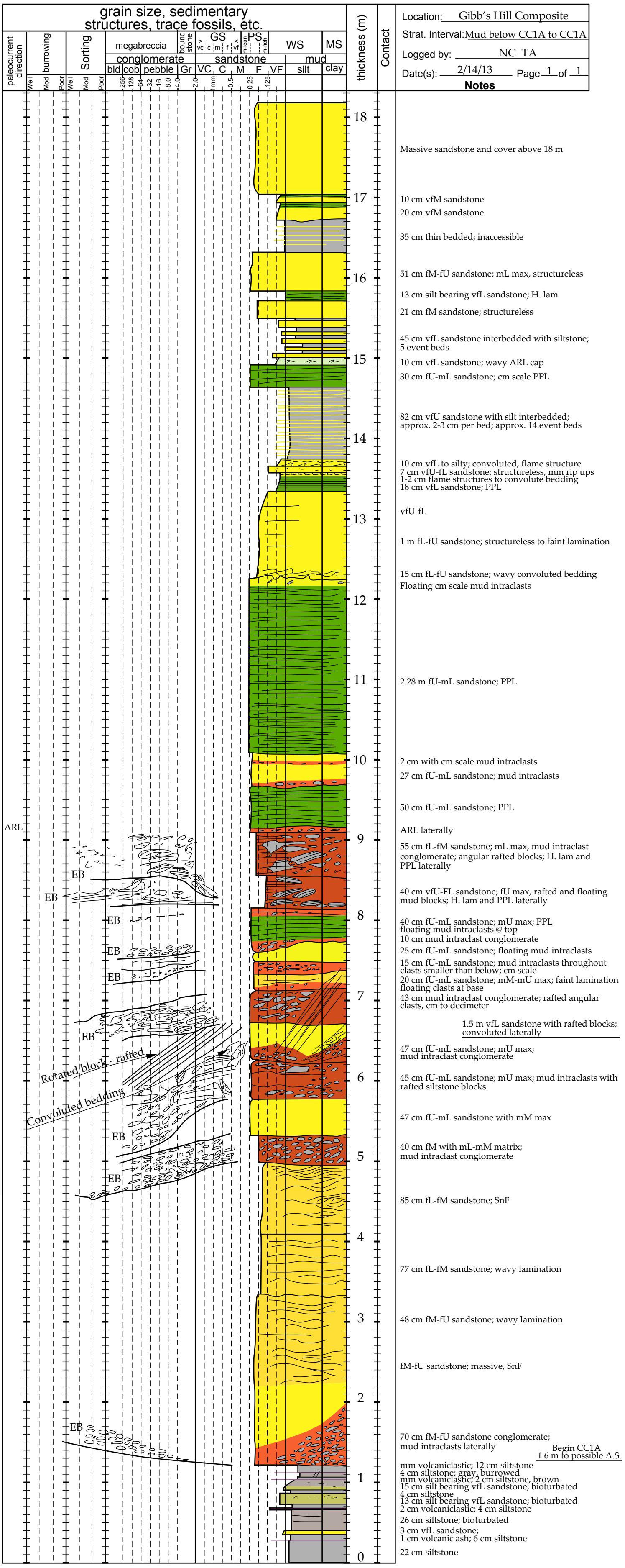

grain size, sedimentary
paleocurrent direction
burrowing
Well
Mod
Poor
Sorting
Well
Mod
Poor
megabreccia
bound stone
conglomerate
bld
cob
pebble
Gr
256
128
64
32
16
8.0
4.0
2.0
GS
vc
c
m
f
vf
sandstone
VC
C
M
F
VF
1mm
0.5
0.25
125
PS
m-lean
m-rich
WS
MS
mud
silt
clay
thickness (m)
Contact
327
3
2
1
0
Location: Tutapuha Composite
Strat. Interval: Base of CC2
Logged by: NC TA
Date(s): 1/8/13
Page 1 of 1
Notes
10 cm siltstone
94 cm fM-fU sandstone; SnF
Amalgamation surface
Mudstone intraclast conglomerate; cm scale clasts
23 cm vfU sandstone, wavy to rippled; cm scale intraclasts
58 cm fL-vfU sandstone; floating cm scale mud intraclasts
8 cm ARL
13 cm vfL sandstone; PPL
20 cm fL sandstone; PPL
Mudstone marker beds from 2N LGS

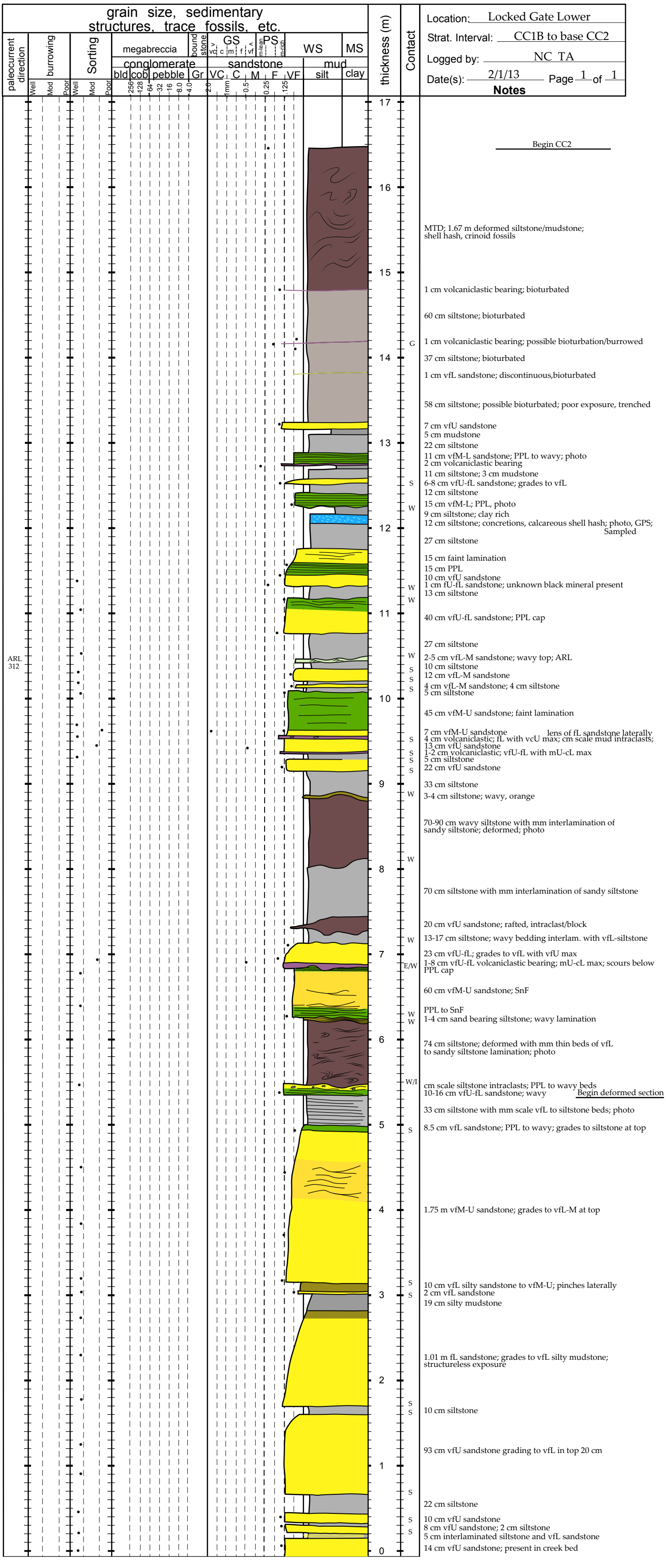

grain size, sedimentary structures, trace fossils, etc.
paleocurrent direction
bioturbation
Sorting
megabreccia
conglomerate
sandstone
mud
bld cob peb gran
VC C M F VF
GS PS
WS MS
silt clay
thickness (m)
Contact
Location: Tutapuha North Composite
Strat. Interval: Volcaniclastic & CC1B
Logged by: NC TA
Date(s): 1/9/13
Page 1 of 1
Notes
10 cm mudstone
Approximately 6 m covered in pine forest; trenched 2 m intervals exposing fL sandstone
~7.5 m fL massive sandstone; partially exposed
~27 m thick sandstone succession
Elementary Body Break
Top of exposure in north section exposure quality decreases
fL sandstone; poorly exposed
PPL
fL sandstone; SnF, poorly exposed at top
centimeter wide deformation bands
possible truncation
fL sandstone; possible scours (may be psuedo) no rip-up clasts, PPL
ARL
fL sandstone; PPL to wavy bedding; Fracture; ripples
A.S.
structureless to wavy PPL and SnF
fL sandstone; well sorted, structureless
Base of sandstone bench
40 cm siltstone; less volcanics and sand, clay rich
20 cm silt dominated; volcanics at base, graded
17 cm silt dominated; volcanics at base, graded
15 cm silt dominated; volcanics at base, graded
14 cm volcanic rich; siltstone matrix, graded
12 cm volcanic rich; siltstone matrix, graded
12 cm volcanic rich; siltstone matrix, graded
20 cm volcanic rich; siltstone matrix, graded
19 cm volcanic rich; siltstone matrix, graded
24 cm volcanic rich; siltstone matrix, graded
30 cm graded bed; welded tuff, concretions and relic bedding; qtz, plag, kspar, mica
Thick volcanic rich siltstone; phenocryst bearing; organic rich, volcanic rich, calcareous rich
siltstone dominated with fU-mL sandstone lenses; silty to muddy matrix
15 cm volcanic rich siltstone; lenses of fU sand/ash
45 cm volcanic rich muddy siltstone; bioturbated, ash bearing; concretions, graded; qtz, plag
10 cm fL sandstone
40 cm siltstone; graded, floating volcanic grains, qtz, plag
2 cm mudstone; hemipelagic, fossil/organic rich; floating vfL grains; dark brown; calcareous
20 cm volcanic rich siltstone
2 cm mL-mU volcanic rich sandstone; subangular/subrounded
35 cm siltstone with volcanic ash lenses, plag, qtz subangular to subrounded phenocrysts; bioturbated
Volcanics and Mudstone below CC1B

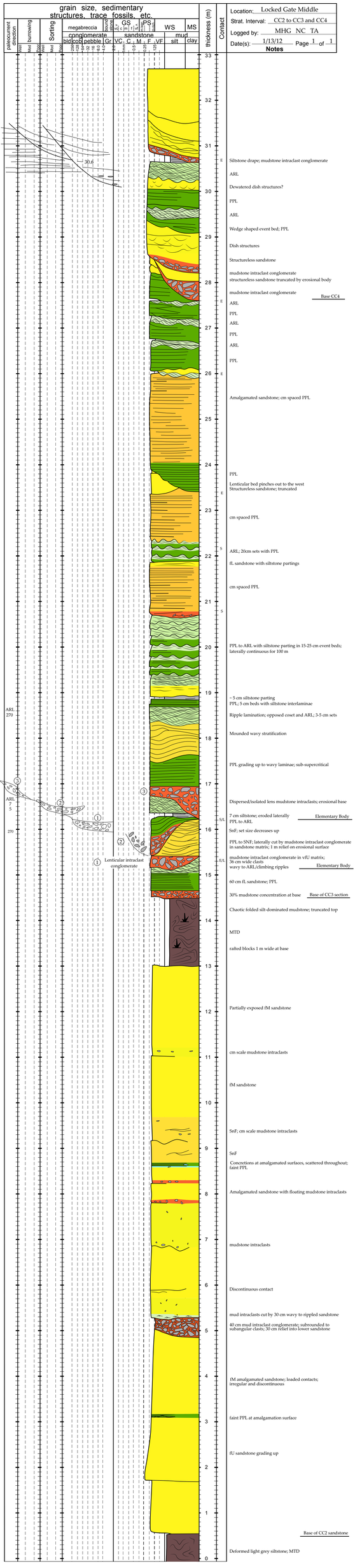

grain size, sedimentary structures, trace fossils, etc.
paleocurrent indicators
bioturbation
Sorting
megabreccia
conglomerate
sandstone
mud
boulder pebble gr VC C M F VF
GS
PS
WS
MS
silt
clay
thickness (m)
Contact
Location: Tutapuha South Composite
Strat. Interval: CC1B to CC2
Logged by: NC TA
Date(s): 1/13/13
Page 1 of 1
Notes
27 cm vfM sandstone; structureless
5-10 cm ARL cap; siltstone
35 cm vfM sandstone; structureless
30 cm vfM-vfU sandstone; cm scale mud intraclast conglomerate; rip ups, SnF, dewatering
Floating mud intraclasts
faint laminations
2.9 m thick fL sandstone;
faint wavy bedding; possible dewatering
Convoulted bedding; mudstone intraclasts
18 cm interbedded vfL sandstone and siltstone; sands thin up
28 cm interbedded vfL sandstone and siltstone; FPL to wavy; sands thin up
25 cm vfU sandstone; FPL with wavy rippled cap
4 cm vfU sandstone; FPL with flame structure cap
11 cm vfU sandstone; structureless
15 cm vfU sandstone; FPL with 5 cm ARL cap
15 cm vfL-silty sandstone; few organics, interbedded
5 cm FPL to ripple wavy, mm mud intraclasts in FPL, fines up
65 cm fL sandstone; structureless; GPS 40 m
wavy to rippled bedding
FPL
fL sandstone
Siltstone; dark gray
decimeter scale concretions
Siltstone; tan; faint FPL increasing spacing up
Siltstone; gray
Siltstone; tan, increasing abundance of concretions
cm scale concretions
Siltstone; little bioturbation; gray
Partially covered
1 cm vfL-vfU sandstone; volcanic bearing
50 cm siltstone; little bioturbation
5 cm fM-fU sandstone; phenocryst rich volcanics; GPS 34.8 m
Rippled to wavy bedding; burrowing, heavily bioturbated
Interbedded vfU sandstone and siltstone; heavily bioturbated
Interbedded vfU sandstone and siltstone; heavily bioturbated; difficult to break out events (5 cm - 25 cm event beds)
15 cm siltstone
15 cm vfU sandstone; bioturbated
13 cm siltstone; heavily bioturbated
vfL sandstone; structureless
39 cm siltstone; bioturbated
more calcareous rich sandstone, siltstone; interbedded
13 cm vfU sandstone; wavy cap
4 cm siltstone
Elementary Body
10 cm fM sandstone; mud intraclasts; irregular contact;
Dewatering structures; possible intraclasts
5 cm wavy to convolute bedding
Thick bedded fL sandstone; faint FPL
Structureless
34 cm vfU sandstone interbedded with vfL to siltstone; wavy
70 cm fL sandstone; structureless
vfL sandstone; faint FPL; interbedded sand/silt
9 cm siltstone
47 cm fL sandstone; structureless; gray
18 cm siltstone interbedded with vfL; few organics
volcaniclastic sandstone: mm mud intraclasts
5 cm FPL capped by vfL sandstone to siltstone; mica rich cap
Iron rich; possibly an amalgamation surface
fL structureless sandstone
5 cm fU volcaniclastic rich
2 cm siltstone; 2 cm iron rich vfL-U sandstone; 6 cm siltstone
2 cm vfU sandstone; mm mud intraclasts
3 cm organic rich, iron rich vfM sandstone
faint FPL
1.2 m fL sandstone; wavy to SnF bedding
40 cm fL sandstone; structureless
Siltstone; vfL max
cm scale mudstone intraclasts
30 cm vfU-fL sandstone; tan
SnF
80 cm fL sandstone grading to vfU; gray
6 cm siltstone
2 cm fU volcanic rich sandstone
12 cm vfL sandstone
70 cm fL sandstone grading to siltstone; siltstone clay rich
10 cm volcaniclastic
45 cm interbedded sandstone, siltstone
13 cm FPL, concentration of organics,clay rich
faint PPL
10 cm vfU sandstone; wavy bedding, burrows
70 cm vfU sandstone; dewatering structures
20-30 cm vfU-fM silt bearing sandstone; wavy bedding; rip-up clasts; cm scale mud intraclasts
Elementary Body;
Cross-cutting relationship
35 cm fL-fM sandstone; truncated
fM-fU structureless sandstone, graded at base
Amalgamation Surface; mU max
possible SnF
fL-fU structureless sandstone
faint wavy FPL
60 cm sandstone and siltstone interbedded, wavy beds; 19 cm rippled sandstone
10 cm vfL silty sandstone; increasing sand up
15 cm ripple laminated FPL
5 cm ARL with FPL laterally, dish structures
65 cm vfU-fL sandstone, FPL
Dewatering and dish structures
15 cm fL sandstone; floating mm scale mud intraclasts
70 cm fL sandstone
mud intraclast conglomerate, thickens laterally; cm scale clasts
Elementary Body
Heavily fractured thick bedded sandstone; SnF
Horst block; hanging wall to the west, measured footwall
Thick bedded fM sandstone
Cover


grain size, sedimentary structures, trace fossils, etc.
paleocurrent direction
bed
burrowing
Sorting
megabreccia
conglomerate
sandstone
mudstone
boulder pebble
GS
SS
PS
WS
MS
silt
clay
thickness (m)
Contact
Location: Warekarianga Stream
Strat. Interval: Volcanics & CC1B Margin
Logged by: NC TA
Date(s): 1/25/13 Page 1 of 1
Notes
16 cm vfL-vfM sandstone
15 cm vfM sandstone; faint lamination at base
10 cm vfM sandstone
17 cm vfM sandstone; 3 cm PPL cap
34 cm vfL sandstone; 2 cm PPL cap
10 cm vfU sandstone with cm scale mud intraclasts
10 cm siltstone
1 m cover
30 cm interbedded sand and silt
Heavily bioturbated siltstone with sand grains remaining in burrows
80 cm siltstone; heavily bioturbated, sand stringers
30 cm vfU sandstone
15 cm siltstone
50 cm vfU sandstone
Silt dominated; heavily bioturbated, coarser sands remain in burrows
41 cm vfU sandstone grading to vfL
5 cm siltstone
37 cm vfU-vfL sandstone
18 cm silt dominated; bioturbated, horizontal lamination
1 cm volcaniclastic; 2 cm vfU sandstone
1-2 cm volcaniclastic; 3 cm siltstone
15 cm siltstone
2.1 m fL sandstone grading to vfU
14-24 cm siltstone; wavy cap, bioturbated
60 cm vfM-vfU sandstone; intraclasts throughout
Amalgamation surface
90 cm vfU sandstone; wavy horizontal lam. to SmF
3 cm siltstone
15 cm vfM sandstone
8 cm silt dominated
vfU-vfM sandstone; structureless
4 cm vfL to siltstone
16 cm vfU sandstone
9 cm siltstone
13 cm vfM sandstone
4 cm siltstone
Few intraclasts
85 cm vfU sandstone
30 cm vfU sandstone with cm scale mud intraclasts
10 cm siltstone
20-30 cm vfU sandstone; mm-cm scale mud intraclasts
6 cm siltstone; possible bioturbation
110 cm fL sandstone; SmF to horizontal lamination
6 cm fL sandstone; horizontal lam.; possible volcanics @ base
11 cm siltstone; bioturbated
50 cm vfU sandstone; floating siltstone intraclasts
20 cm siltstone; bioturbated, burrows
60 cm vfU-fL sandstone; structureless to horizontal lam.
7 cm siltstone to vfL; possible bioturbation
20 cm vfL-vfM sandstone; horizontal lamination
5 cm vfL to siltstone; possible bioturbation
16 cm vfU sandstone with vfL to siltstone intraclasts; pinches laterally
14 cm vfM-vfU horizontal lamination
11 cm siltstone to vfL; bioturbated
vfL cap
vfU sandstone; wavy to SmF
vfM sandstone; cm scale siltstone intraclasts, floating
SmF
vfU-fL sandstone; faint laminations
Amalgamation Surface
40 cm vfU-fL sandstone
11 cm silt to vfL; bioturbated
65 cm fL sandstone with vfU-fL cap; SmF
2-5 cm vfM-vfU sandstone; 11 cm siltstone and volcanics cap
vfU-fL sandstone; h. lam. cap; 1 cm silt dominted; volcanics
vfU-fL sandstone; SmF
14 cm siltstone to vfL; bioturbated
1.45 m vfU sandstone; SmF
vfM sandstone; SmF
cm scale volcaniclastic; cL-vU phenocrysts
12 cm vfL to siltstone
7 cm convoluted; granule to pebble intraclasts mud and sand intraclasts
110 cm vfU sandstone
Amalgamation surface
vfM-vfU sandstone; massive, SmF
1 cm volcanic ash; amalgamation surface
60 cm horizontal lam.; siltstone and sandstone interlaminated
Begin channel cut; CC1B
volcaniclastic
7 cm siltstone; 5 cm volcaniclastic
5 cm volcaniclastic; wavy, possibly bioturbated
Apprx. 65 cm volcaniclastic; clay bearing; phenocrysts dispersed
1 cm volcanic ash; mU phenocrysts
1 cm clay bearing; phenocrysts dispersed
2 cm volcaniclastic; fU-mL phenocrysts
20 cm volcaniclastic; clay bearing; phenocrysts dispersed
3 cm volcanic ash; mU phenocrysts
11 cm clay bearing volcanic ash; phenocrysts dispersed
2 cm volcaniclastic; fU-mL phenocrysts; white plagioclase
45 cm volcanic ash; clay bearing; phenocrysts dispersed
3 cm volcanic ash; mU-cL phenocrysts
12 cm volcanic; clay bearing
1 cm volcanic ash; mU-cL phenocrysts; 8 cm volcanic ash; mU-cL phenocrysts
3 cm volcanic ash; mU-cL phenocrysts; 5 cm clay boaing ash
2 cm volcanic ash; mU-cL phenocrysts; 2 cm clay bearing ash
4 cm volcanic ash; mU-cL phenocrysts; 8 cm clay bearing ash
10 cm clay bearing volcanic ash
1 cm volcanic ash; mU-cL phenocrysts; 3 cm mU-cL phenocrysts
3 cm volcaniclastic ash; mU-cL phenocrysts
10 cm clay bearing volcaniclastic rich siltstone
1-2 cm volcaniclastic ash; mU-cL phenocrysts
65 cm volcaniclastic; fL-fM phenocrysts dispersed in silty matrix; poorly exposed
45 cm poor exposure fU sandstone to volcaniclastic ash in siltstone matrix; phenocrysts up to cL, white sodium plagioclase
Clay rich siltstone/mudstone
Silty sandstone interlaminated with vfL-vfM; poor exposure
Horizontal lamination thinning upwards; poor exposure
Missing Section
@ 3M, GS, multi-channel margin lag, truncated for 22 m in section, mudclasts and volcanics below
Truncation to Ash Layer (5m below) @ margin
3.78 m volcaniclastic
Ash
mud
silt
sand
with volcanics


grain size, sedimentary structures, trace fossils, etc.
paleocurrent direction
burrowing
Well
Mod
Poor
Sorting
megabreccia
bound stone
conglomerate
bld
cob
pebble
Gr
sandstone
VC
C
M
F
VF
GS
PS
m-lean
m-rich
WS
MS
mud
silt
clay
thickness (m)
Contact
Location: Warekarianga Stream
Strat. Interval: CC1A?/Volcanics/CC1B Magin-OB
Logged by: NC TA
Date(s): 1/27/13
Page 1 of 1
Notes
13 cm siltstone
26 cm sandstone
13 cm siltstone
19 cm sandstone
13 cm siltstone
14 cm sandstone
12 cm siltstone; fissile
9 cm sandstone
8 cm siltstone
11 cm sandstone
14 cm siltstone
24 cm sandstone
Approximate measurements; above head
54 cm siltstone; faint PPL
4 cm vfU sandstone
mm vfL sandstone; 5 cm siltstone
Faint PPL
47 cm siltstone
6 cm vfM sandstone
32 cm siltstone
5 cm vfU sandstone; fL max
35 cm volcaniclastic sand rich matrix; fL with mL max
23 cm siltstone
6 cm vfM sandstone
38 cm siltstone; bioturbated
8 cm fL sandstone with cL volcanics
33 cm siltstone with fL sandstone lense
10-13 cm vfU sandstone; wavy top
9 cm siltstone
10 cm vfM sandstone
6 cm siltstone cap
36 cm fL sandstone grading to vfM; 22 cm PPL; 14 cm ARL
9 cm silty ash
1 cm siltstone; dark brown, burrowed
70 cm fL sandstone; structureless
8 cm silty ash
30 cm fL sandstone; structureless
5 cm ash/siltstone
90 cm fL sandstone; massive, structureless; thins to 50 cm north
Base composite 3
Base of composite 3 within CC1B
92 cm sandy siltstone cap; fissile weathering
composite 2, interfingering with composite 1
10 cm vfU sandstone
15 cm siltstone; wavy top
50 cm fL sandstone; (multilateral body within CC1B)
3 cm vfL sandstone; 4 cm siltstone
5 cm siltstone
15 cm vfL-vfM sandstone
5 cm siltstone; bioturbated
9 cm vfL sandstone; structureless
7 cn vfL to siltstone; bioturbated cap
29 cm vfU sandstone grading to vfL; structureless
4 cm siltstone
7 cm vfL-vfM sandstone, structureless; 4 cm org. rich, bioturb.
22 cm siltstone; climbing ripples with ARL cap
10 cm vfM sandstone grading to vfL; ARL cap, pinches laterally
12 cm fL sandstone
4 cm siltstone
2-5 cm volcaniclastic in sandstone matrix
21 cm siltstone; climbing ripples
11 cm vfL-vfM sandstone; structureless
22 cm silt bearing vfL sandstone; climbing ripples
3-7 cm fL sandstone; wavy
6 cm vfL sandstone to siltstone; horizontal lamination
30 cm vfU sandstone; PPL with ARL to SnF cap (photo)
40 cm vfL sandstone to siltstone; h. lam., 5-6 cm spacing
2 cm vfU sandstone; burrowed; ARL to PPL
1 cm volcaniclastic; 2 cm siltstone/ash
1 cm volcaniclastic, discontinuous; 6 cm siltstone
1-2 cm vfU sandstone; 7 cm siltstone, bioturbated
16 cm siltstone; bioturbated with vfU sandstone lenses
4 cm volcaniclastic
2 cm volcaniclastic; 16 cm siltstone, bioturbated, wavy h. lam.
2 cm volcaniclastic; 3 cm ash
64 cm volcanic ash/siltstone
outcrop character changes in appearance
5 cm volcaniclastic; 10 cm ash
2 cm volcaniclastic; 20 cm ash
2 cm volcaniclastic, dark brown; 7 cm ash
2 cm volcaniclastic; 4 cm ash
2 cm volcaniclastic; 17 cm ash
3 cm volcaniclastic; 12 cm ash
2-3 cm volcaniclastic; 17 cm ash
2 cm volcaniclastic; 12 cm ash
4 cm volcaniclastic; 12 cm ash
1 cm volcaniclastic; 10 cm ash, bioturbated, burrowed
2 cm volcaniclastic; 4 cm ash
3 cm volcanic; 7 cm ash
3 cm volcanic; 5 cm ash
2 cm volcaniclastic; 10 cm light gray ash
12 cm volcanic ash; light gray
7 cm volcaniclastic; dark brown
5 cm volcanic ash
3 cm volcaniclastic; dark brown
15 cm light tan volcanic ash
5 cm volcaniclastic; very dark brown
Best estimate given; not accessible, cliff face
18 cm light gray volcaniclastic
20 cm volcaniclastic; dark tan
5 cm light gray volcanic ash
10 cm volcaniclastic; dark brown
40 cm volcaniclastic ash; clay rich; begin volcaniclastics
40 cm silt dominated with few vfL grains; PPL
60 cm vfM sandstone grading to vfL sandstone
grooves at base
55 cm vfL sandstone to siltstone; SnF
12 cm vfM sandstone
5 cm bioturbated cap
16 cm vfM sandstone grading to vfL sandstone
45 cm
25 cm
9 cm
15 cm
17 cm
27 cm
9 cm
12 cm
10 cm
13 cm
20 cm
14 cm
17 cm
Poor exposure; wet stream bed
50 cm vfL sandstone to siltstone; clay rich
25 cm vfL sandstone to siltstone; PPL
7 cm vfM sandstone; structureless
72 cm vfL sandstone grading to clay rich silt dominated matrix
1-2 cm clay rich siltstone
vfL sandstone with clay rich matrix; faint PPL
1.05 m poor exposure; clay rich, silt dominated; vfL to siltstone
20 cm vfL sandstone; poor exposure
Cover below 0 m
N
E
312
310
312
311
310
316
319
Groove
326


grain size, sedimentary structures, trace fossils, etc.
paleocurrent direction
burrowing
Well
Mod
Poor
Sorting
megabreccia
boundstone
conglomerate
bld
cob
pebble
Gr
GS
sandstone
VC
C
M
F
VF
PS
m-lean
m-rich
WS
MS
mud
silt
clay
thickness (m)
Contact
Location: Gibb's Hill Composite
Strat. Interval: Mud below CC1A to CC1A
Logged by: NC TA
Date(s): 2/14/13
Page 1 of 1
Notes
ARL
EB
Rotated block - rafted
Convoluted bedding
Massive sandstone and cover above 18 m
10 cm vfM sandstone
20 cm vfM sandstone
35 cm thin bedded; inaccessible
51 cm fM-fU sandstone; mL max, structureless
13 cm silt bearing vfL sandstone; H. lam
21 cm fM sandstone; structureless
45 cm vfL sandstone interbedded with siltstone; 5 event beds
10 cm vfL sandstone; wavy ARL cap
30 cm fU-mL sandstone; cm scale PPL
82 cm vfU sandstone with silt interbedded; approx. 2-3 cm per bed; approx. 14 event beds
10 cm vfL to silty; convoluted, flame structure
7 cm vfU-fL sandstone; structureless, mm rip ups
1-2 cm flame structures to convolute bedding
18 cm vfL sandstone; PPL
vfU-fL
1 m fL-fU sandstone; structureless to faint lamination
15 cm fL-fU sandstone; wavy convoluted bedding
Floating cm scale mud intraclasts
2.28 m fU-mL sandstone; PPL
2 cm with cm scale mud intraclasts
27 cm fU-mL sandstone; mud intraclasts
50 cm fU-mL sandstone; PPL
ARL laterally
55 cm fL-fM sandstone; mL max, mud intraclast conglomerate; angular rafted blocks; H. lam and PPL laterally
40 cm vfU-FL sandstone; fU max, rafted and floating mud blocks; H. lam and PPL laterally
40 cm fU-mL sandstone; mU max; PPL floating mud intraclasts @ top
10 cm mud intraclast conglomerate
25 cm fU-mL sandstone; floating mud intraclasts
15 cm fU-mL sandstone; mud intraclasts throughout clasts smaller than below; cm scale
20 cm fU-mL sandstone; mM-mU max; faint lamination floating clasts at base
43 cm mud intraclast conglomerate; rafted angular clasts, cm to decimeter
1.5 m vfL sandstone with rafted blocks; convoluted laterally
47 cm fU-mL sandstone; mU max; mud intraclast conglomerate
45 cm fU-mL sandstone; mU max; mud intraclasts with rafted siltstone blocks
47 cm fU-mL sandstone with mM max
40 cm fM with mL-mM matrix; mud intraclast conglomerate
85 cm fL-fM sandstone; SnF
77 cm fL-fM sandstone; wavy lamination
48 cm fM-fU sandstone; wavy lamination
fM-fU sandstone; massive, SnF
70 cm fM-fU sandstone conglomerate; mud intraclasts laterally
Begin CC1A
1.6 m to possible A.S.
mm volcaniclastic; 12 cm siltstone
4 cm siltstone; gray, burrowed
mm volcaniclastic; 2 cm siltstone, brown
15 cm silt bearing vfL sandstone; bioturbated
4 cm siltstone
13 cm silt bearing vfL sandstone; bioturbated
2 cm volcaniclastic; 4 cm siltstone
26 cm siltstone; bioturbated
3 cm vfL sandstone;
1 cm volcanic ash; 6 cm siltstone
22 cm siltstone


grain size, sedimentary structures, trace fossils, etc.
paleocurrent direction
burrowing
Well
Mod
Poor
Sorting
megabreccia
bound stone
conglomerate
bld
cob
pebble
Gr
GS
sandstone
VC
C
M
F
VF
PS
m-lean
m-rich
WS
MS
mud
silt
clay
thickness (m)
Contact
Location: Locked Gate Lower
Strat. Interval: CC1B to base CC2
Logged by: NC TA
Date(s): 2/1/13 Page 1 of 1
Notes
Begin CC2
MTD; 1.67 m deformed siltstone/mudstone; shell hash, crinoid fossils
1 cm volcaniclastic bearing; bioturbated
60 cm siltstone; bioturbated
1 cm volcaniclastic bearing; possible bioturbation/burrowed
37 cm siltstone; bioturbated
1 cm vfL sandstone; discontinuous,bioturbated
58 cm siltstone; possible bioturbated; poor exposure, trenched
7 cm vfU sandstone
5 cm mudstone
22 cm siltstone
11 cm vfM-L sandstone; PPL to wavy; photo
2 cm volcaniclastic bearing
11 cm siltstone; 3 cm mudstone
6-8 cm vfU-fL sandstone; grades to vfL
12 cm siltstone
15 cm vfM-L; PPL, photo
9 cm siltstone; clay rich
12 cm siltstone; concretions, calcareous shell hash; photo, GPS; Sampled
27 cm siltstone
15 cm faint lamination
15 cm PPL
10 cm vfU sandstone
1 cm fU-fL sandstone; unknown black mineral present
13 cm siltstone
40 cm vfU-fL sandstone; PPL cap
27 cm siltstone
ARL 312
2-5 cm vfL-M sandstone; wavy top; ARL
10 cm siltstone
12 cm vfL-M sandstone
4 cm vfL-M sandstone; 4 cm siltstone
5 cm siltstone
45 cm vfM-U sandstone; faint lamination
7 cm vfM-U sandstone lens of fL sandstone laterally
4 cm volcaniclastic; fL with vcU max; cm scale mud intraclasts;
13 cm vfU sandstone
1-2 cm volcaniclastic; vfU-fL with mU-cL max
5 cm siltstone
22 cm vfU sandstone
33 cm siltstone
3-4 cm siltstone; wavy, orange
70-90 cm wavy siltstone with mm interlamination of sandy siltstone; deformed; photo
70 cm siltstone with mm interlamination of sandy siltstone
20 cm vfU sandstone; rafted, intraclast/block
13-17 cm siltstone; wavy bedding interlam. with vfL-siltstone
23 cm vfU-fL; grades to vfL with vfU max
1-8 cm vfU-fL volcaniclastic bearing; mU-cL max; scours below PPL cap
60 cm vfM-U sandstone; SnF
PPL to SnF
1-4 cm sand bearing siltstone; wavy lamination
74 cm siltstone; deformed with mm thin beds of vfL to sandy siltstone lamination; photo
cm scale siltstone intraclasts; PPL to wavy beds
10-16 cm vfU-fL sandstone; wavy Begin deformed section
33 cm siltstone with mm scale vfL to siltstone beds; photo
8.5 cm vfL sandstone; PPL to wavy; grades to siltstone at top
1.75 m vfM-U sandstone; grades to vfL-M at top
10 cm vfL silty sandstone to vfM-U; pinches laterally
2 cm vfL sandstone
19 cm silty mudstone
1.01 m fL sandstone; grades to vfL silty mudstone; structureless exposure
10 cm siltstone
93 cm vfU sandstone grading to vfL in top 20 cm
22 cm siltstone
10 cm vfU sandstone
8 cm vfU sandstone; 2 cm siltstone
5 cm interlaminated siltstone and vfL sandstone
14 cm vfU sandstone; present in creek bed


grain size, sedimentary structures, trace fossils, etc.
thickness (m)
Contact
Location: Locked Gate Middle
Strat. Interval: CC2 to CC3 and CC4
Logged by: MHG NC TA
Date(s): 1/13/12 Page 1 of 1
Notes
paleocurrent
Well
Mod
burrowing
Sorting
megabreccia
conglomerate
sandstone
mud
boulder
cobble
pebble
gr
VC
C
M
F
VF
GS
PS
WS
MS
silt
clay
30.6
ARL
270
ARL
7
5
270
Lenticular intraclast conglomerate
Silstone drape; mudstone intraclast conglomerate
ARL
Dewatered dish structures
PPL
ARL
Wedge shaped event bed; PPL
Dish structures
Structureless sandstone
mudstone intraclast conglomerate
structureless sandstone truncated by erosional body
mudstone intraclast conglomerate
Base CC4
ARL
PPL
ARL
PPL
ARL
PPL
Amalgamated sandstone; cm spaced PPL
PPL
Lenticular bed pinches out to the west
Structureless sandstone; truncated
cm spaced PPL
ARL; 20cm sets with PPL
fL sandstone with sillstone partings
cm spaced PPL
PPL to ARL with siltstone parting in 15-25 cm event beds; laterally continuous for 100 m
~ 5 cm siltstone parting
PPL; 5 cm beds with sillstone interlaminae
Ripple lamination; opposed coset and ARL; 3-5 cm sets
Mounded wavy stratification
PPL grading up to wavy laminae; sub-supercritical
Dispersed/isolated lens mudstone intraclasts; erosional base
7 cm sillstone; eroded laterally
Elementary Body
PPL to ARL
SnF; set size decreases up
PPL to SNF; laterally cut by mudstone intraclast conglomerate in sandstone matrix; 1 m relief on erosional surface
mudstone intraclast conglomerate in vfU matrix; 36 cm wide clasts
wavy to ARL/climbing ripples
Elementary Body
60 cm fL sandstone; PPL
30% mudstone concentration at base
Base of CC3 section
Chaotic folded silt-dominated mudstone; truncated top
MTD
rafted blocks 1 m wide at base
Partially exposed fM sandstone
cm scale mudstone intraclasts
fM sandstone
SnF; cm scale mudstone intraclasts
SnF
Concretions at amalgamated surfaces, scattered throughout; faint PPL
Amalgamated sandstone with floating mudstone intraclasts
mudstone intraclasts
Discontinuous contact
mud intraclasts cut by 30 cm wavy to rippled sandstone
40 cm mud intraclast conglomerate; subrounded to subangular clasts; 30 cm relief into lower sandstone
fM amalgamated sandstone; loaded contacts; irregular and discontinuous
faint PPL at amalgamation surface
fU sandstone grading up
Base of CC2 sandstone
Deformed light grey sillstone; MTD

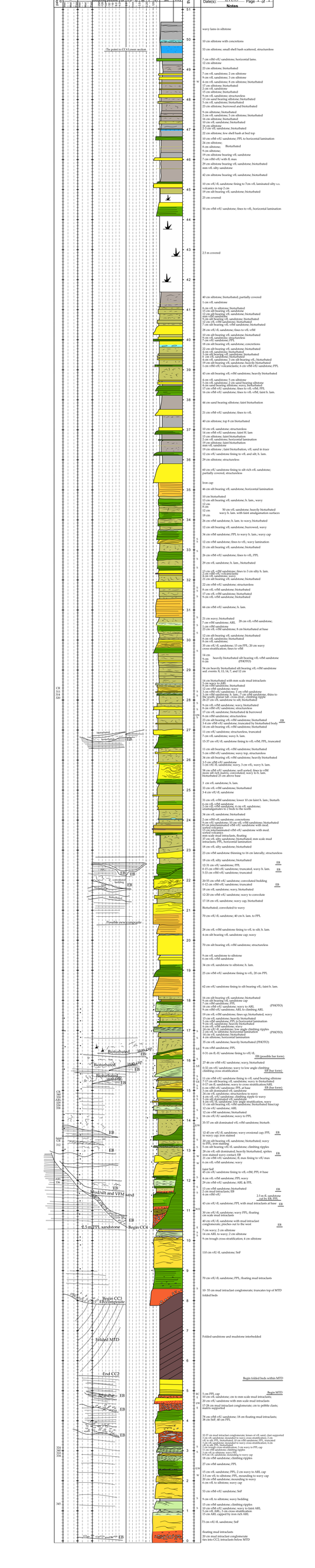
Location: Locked Gate South

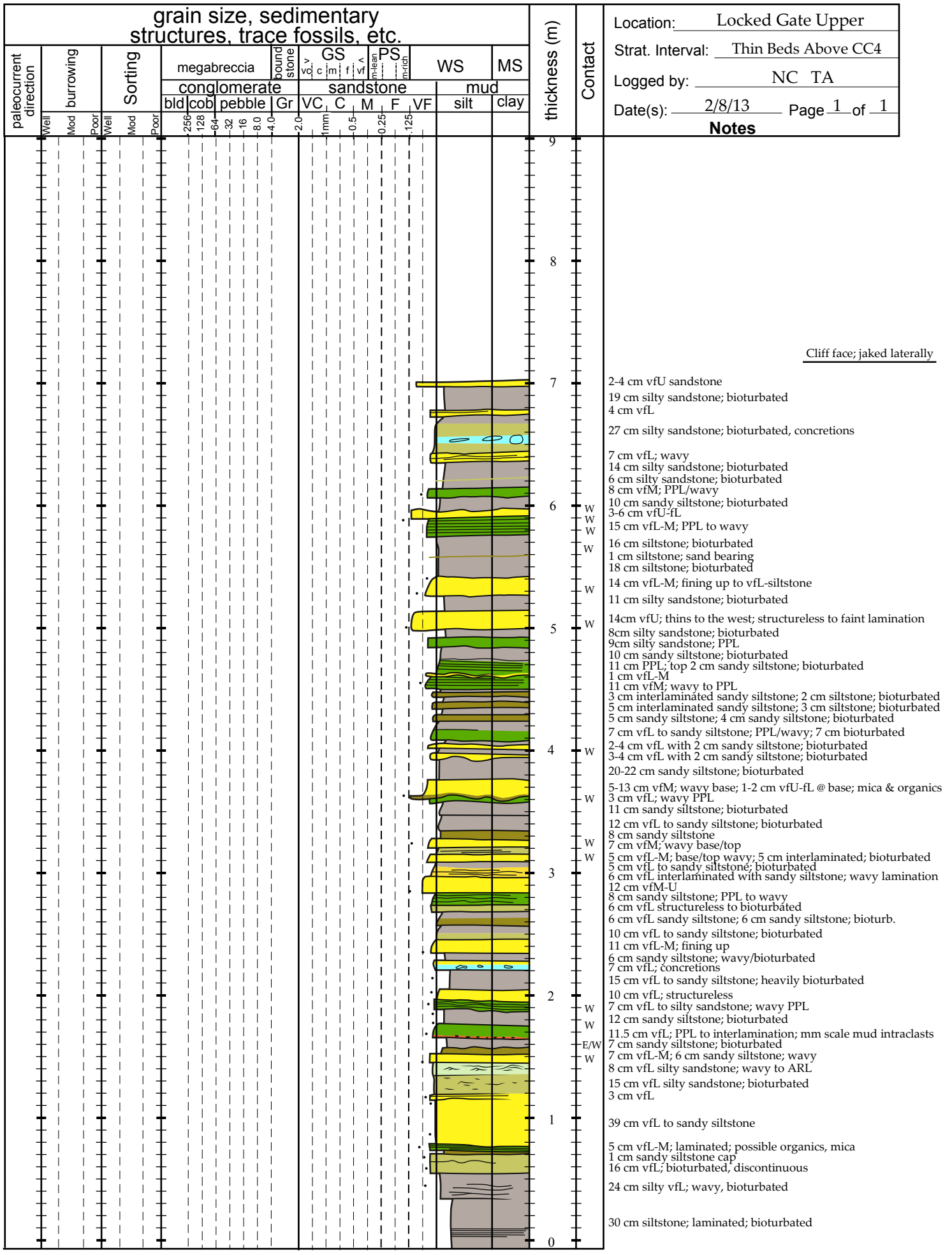
Strat. Interval: CC2 to CC3/CC4 and above

Logged by: NC TA

Date(s): 2/1/13 — Page 1 of 1

Notes





Location: Locked Gate Upper

Strat. Interval: Thin Beds Above CC4

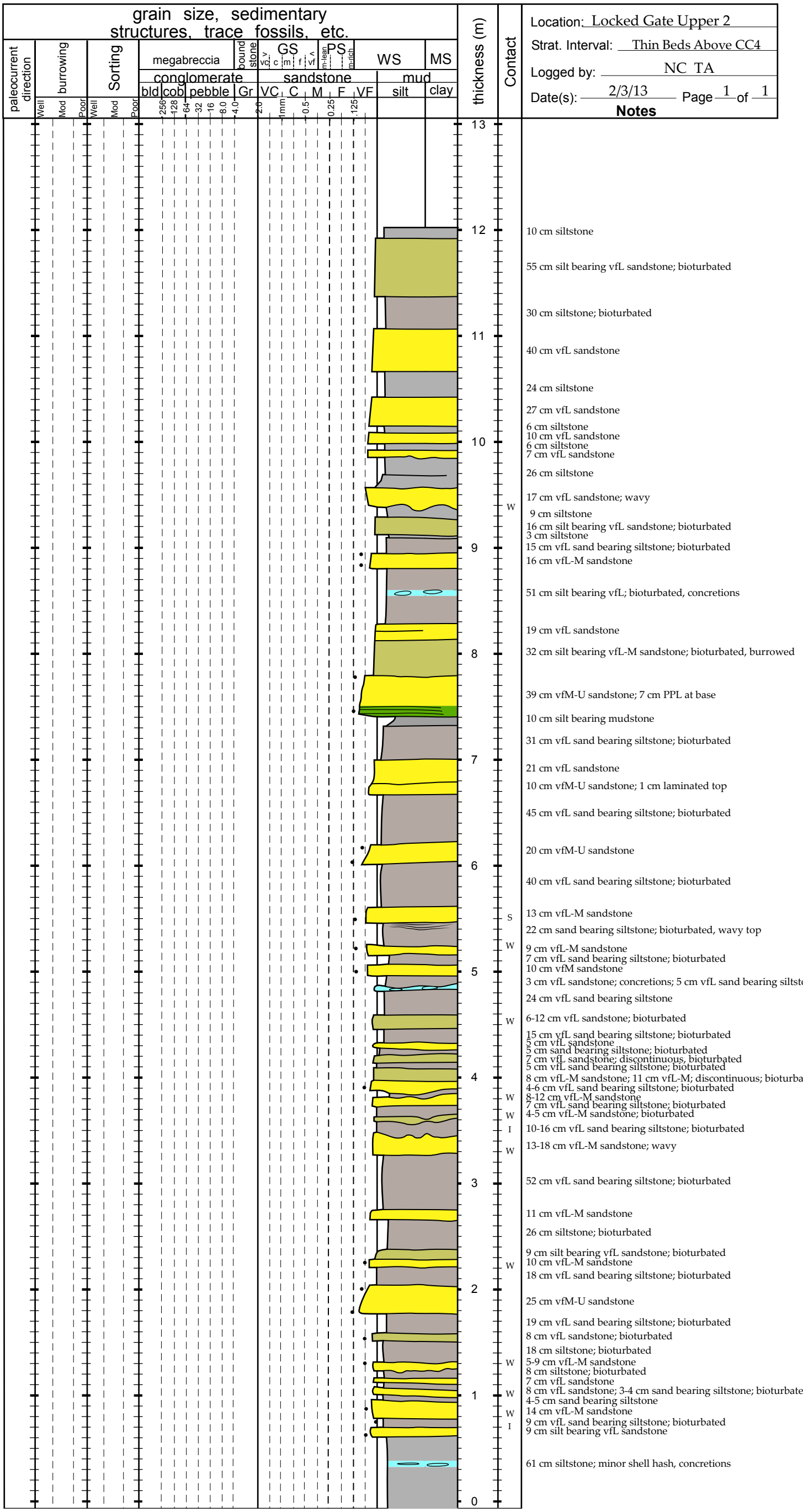
Logged by: NC TA

Date(s): 2/8/13 Page 1 of 1

Notes

Cliff face; jaked laterally

2-4 cm vfU sandstone
19 cm silty sandstone; bioturbated
4 cm vfL
27 cm silty sandstone; bioturbated, concretions
7 cm vfL; wavy
14 cm silty sandstone; bioturbated
6 cm silty sandstone; bioturbated
8 cm vfM; PPL/wavy
10 cm sandy siltstone; bioturbated
3-6 cm vfU-fL
15 cm vfL-M; PPL to wavy
16 cm siltstone; bioturbated
1 cm siltstone; sand bearing
18 cm siltstone; bioturbated
14 cm vfL-M; fining up to vfL-siltstone
11 cm silty sandstone; bioturbated
14cm vfU; thins to the west; structureless to faint lamination
8cm silty sandstone; bioturbated
9cm silty sandstone; PPL
10 cm sandy siltstone; bioturbated
11 cm PPL; top 2 cm sandy siltstone; bioturbated
1 cm vfL-M
11 cm vfM; wavy to PPL
3 cm interlaminated sandy siltstone; 2 cm siltstone; bioturbated
5 cm interlaminated sandy siltstone; 3 cm siltstone; bioturbated
5 cm sandy siltstone; 4 cm sandy siltstone; bioturbated
7 cm vfL to sandy siltstone; PPL/wavy; 7 cm bioturbated
2-4 cm vfL with 2 cm sandy siltstone; bioturbated
3-4 cm vfL with 2 cm sandy siltstone; bioturbated
20-22 cm sandy siltstone; bioturbated
5-13 cm vfM; wavy base; 1-2 cm vfU-fL @ base; mica & organics
3 cm vfL; wavy PPL
11 cm sandy siltstone; bioturbated
12 cm vfL to sandy siltstone; bioturbated
8 cm sandy siltstone
7 cm vfM; wavy base/top
5 cm vfL-M; base/top wavy; 5 cm interlaminated; bioturbated
5 cm vfL to sandy siltstone; bioturbated
6 cm vfL interlaminated with sandy siltstone; wavy lamination
12 cm vfM-U
8 cm sandy siltstone; PPL to wavy
6 cm vfL structureless to bioturbated
6 cm vfL sandy siltstone; 6 cm sandy siltstone; bioturb.
10 cm vfL to sandy siltstone; bioturbated
11 cm vfL-M; fining up
6 cm sandy siltstone; wavy/bioturbated
7 cm vfL; concretions
15 cm vfL to sandy siltstone; heavily bioturbated
10 cm vfL; structureless
7 cm vfL to silty sandstone; wavy PPL
12 cm sandy siltstone; bioturbated
11.5 cm vfL; PPL to interlamination; mm scale mud intraclasts
7 cm sandy siltstone; bioturbated
7 cm vfL-M; 6 cm sandy siltstone; wavy
8 cm vfL silty sandstone; wavy to ARL
15 cm vfL silty sandstone; bioturbated
3 cm vfL
39 cm vfL to sandy siltstone
5 cm vfL-M; laminated; possible organics, mica
1 cm sandy siltstone cap
16 cm vfL; bioturbated, discontinuous
24 cm silty vfL; wavy, bioturbated
30 cm siltstone; laminated; bioturbated


grain size, sedimentary structures, trace fossils, etc.
paleocurrent direction
burrowing
Well
Mod
Poor
Sorting
Well
Mod
Poor
megabreccia
bound stone
conglomerate
bld
cob
pebble
Gr
256
128
64
32
16
8.0
4.0
2.0
GS
vc
c
m
f
vf
PS
m-lean
m-rich
sandstone
VC
C
M
F
VF
1mm
0.5
0.25
.125
WS
MS
mud
silt
clay
thickness (m)
Contact
Location: Locked Gate Upper 2
Strat. Interval: Thin Beds Above CC4
Logged by: NC TA
Date(s): 2/3/13
Page 1 of 1
Notes
13
12
11
10
9
8
7
6
5
4
3
2
1
0
10 cm siltstone
55 cm silt bearing vfL sandstone; bioturbated
30 cm siltstone; bioturbated
40 cm vfL sandstone
24 cm siltstone
27 cm vfL sandstone
6 cm siltstone
10 cm vfL sandstone
6 cm siltstone
7 cm vfL sandstone
26 cm siltstone
17 cm vfL sandstone; wavy
W
9 cm siltstone
16 cm silt bearing vfL sandstone; bioturbated
3 cm siltstone
15 cm vfL sand bearing siltstone; bioturbated
16 cm vfL-M sandstone
51 cm silt bearing vfL; bioturbated, concretions
19 cm vfL sandstone
32 cm silt bearing vfL-M sandstone; bioturbated, burrowed
39 cm vfM-U sandstone; 7 cm PPL at base
10 cm silt bearing mudstone
31 cm vfL sand bearing siltstone; bioturbated
21 cm vfL sandstone
10 cm vfM-U sandstone; 1 cm laminated top
45 cm vfL sand bearing siltstone; bioturbated
20 cm vfM-U sandstone
40 cm vfL sand bearing siltstone; bioturbated
13 cm vfL-M sandstone
S
22 cm sand bearing siltstone; bioturbated, wavy top
W
9 cm vfL-M sandstone
7 cm vfL sand bearing siltstone; bioturbated
10 cm vfM sandstone
3 cm vfL sandstone; concretions; 5 cm vfL sand bearing siltstone
24 cm vfL sand bearing siltstone
W
6-12 cm vfL sandstone; bioturbated
15 cm vfL sand bearing siltstone; bioturbated
5 cm vfL sandstone
5 cm sand bearing siltstone; bioturbated
7 cm vfL sandstone; discontinuous, bioturbated
5 cm vfL sand bearing siltstone; bioturbated
8 cm vfL-M sandstone; 11 cm vfL-M; discontinuous; bioturbated
4-6 cm vfL sand bearing siltstone; bioturbated
W
8-12 cm vfL-M sandstone
7 cm vfL sand bearing siltstone; bioturbated
W
4-5 cm vfL-M sandstone; bioturbated
I
10-16 cm vfL sand bearing siltstone; bioturbated
W
13-18 cm vfL-M sandstone; wavy
52 cm vfL sand bearing siltstone; bioturbated
11 cm vfL-M sandstone
26 cm siltstone; bioturbated
9 cm silt bearing vfL sandstone; bioturbated
W
10 cm vfL-M sandstone
18 cm vfL sand bearing siltstone; bioturbated
25 cm vfM-U sandstone
19 cm vfL sand bearing siltstone; bioturbated
8 cm vfL sandstone; bioturbated
18 cm siltstone; bioturbated
W
5-9 cm vfL-M sandstone
8 cm siltstone; bioturbated
7 cm vfL sandstone
W
8 cm vfL sandstone; 3-4 cm sand bearing siltstone; bioturbated
4-5 cm sand bearing siltstone
W
14 cm vfL-M sandstone
I
9 cm vfL sand bearing siltstone; bioturbated
9 cm silt bearing vfL sandstone
61 cm siltstone; minor shell hash, concretions

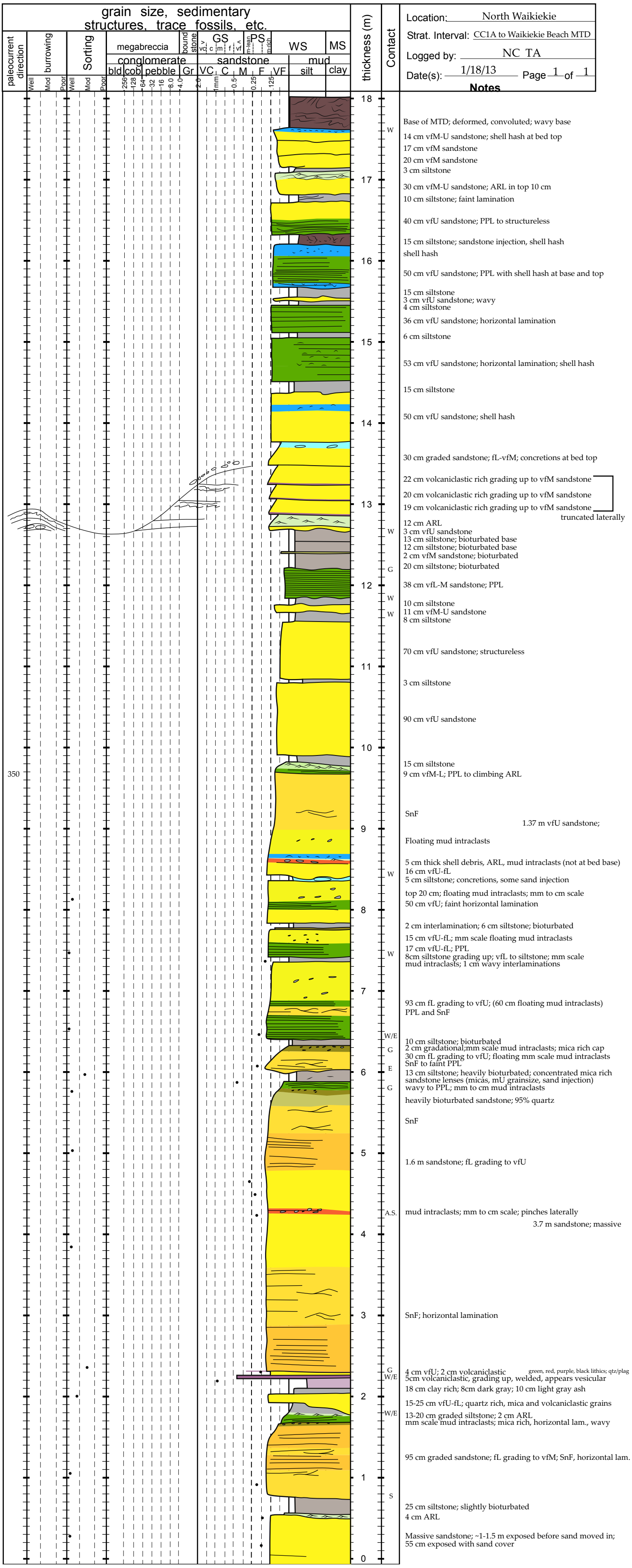
Location: Mackenzie Ridge
Strat. Interval: CCLA and mudstone above
Logged by: NC, TA
Date(s): 1/31/13 Page 1 of 1

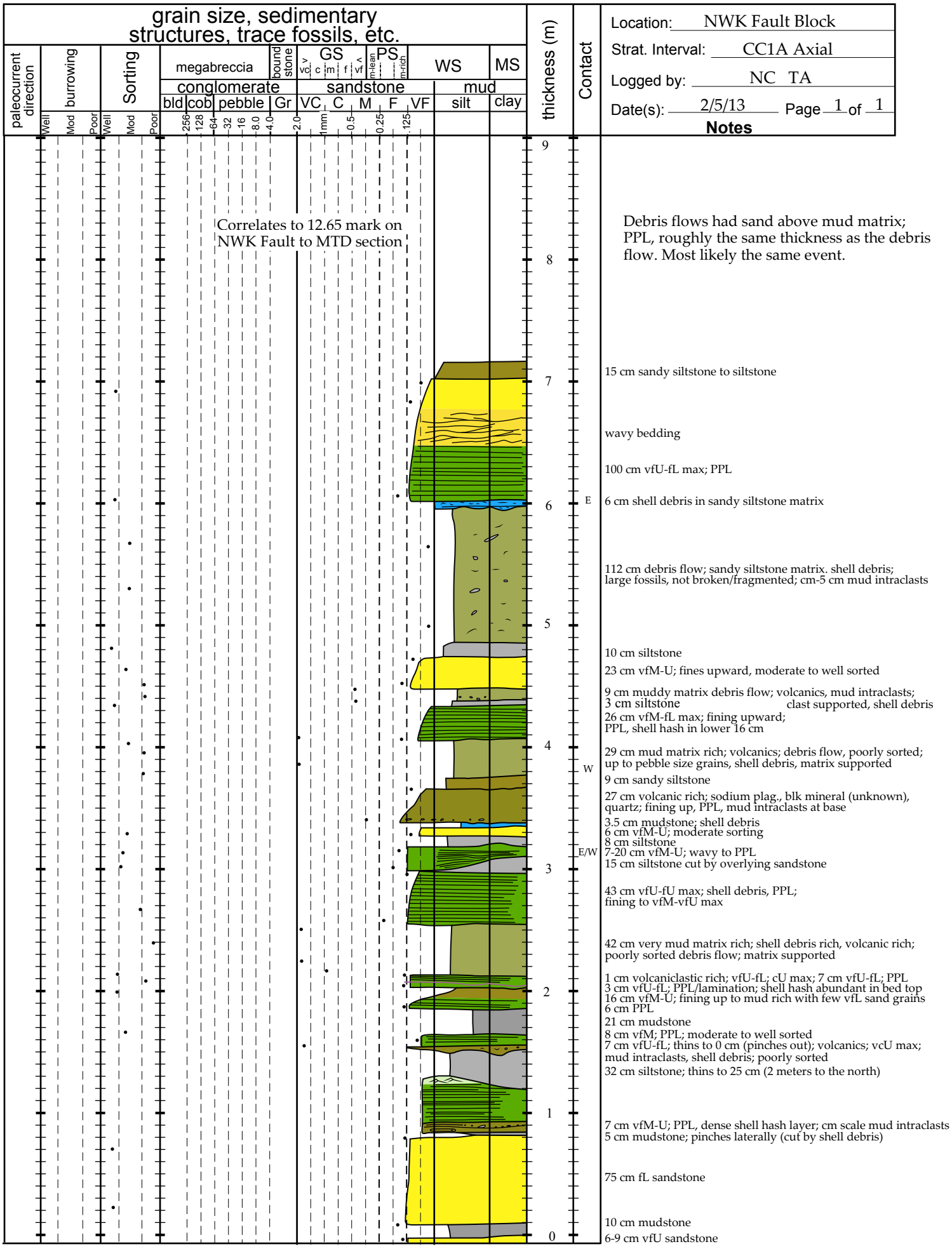
Notes

grain size, sedimentary structures, trace fossils, etc.

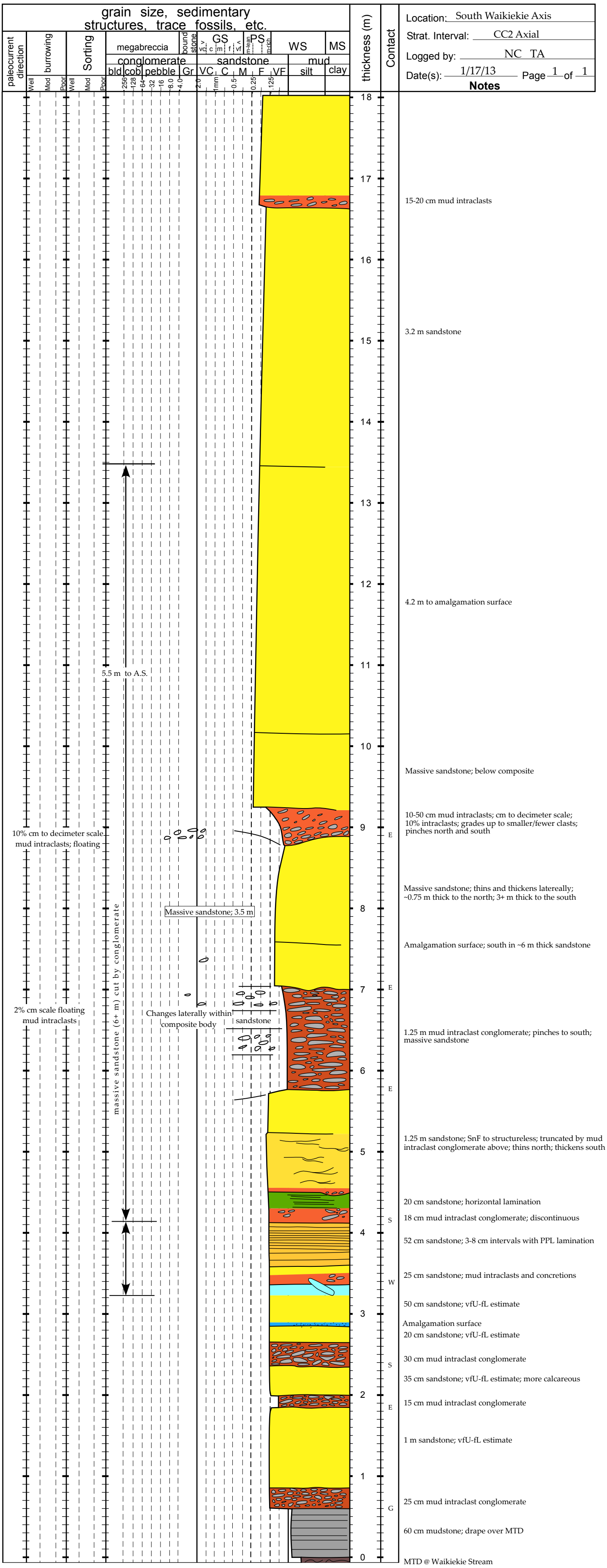
Cuttings

Sorting: megaclastic | conglomeratic | sandstone | mudstone
Grain size: GS | SS | MS
Bedding: WS | MS
Mud: SltV | SltH | SltL | SltW | SltF | SltR | SltV | SltH | SltL | SltW | SltF | SltR | SltV | SltH | SltL | SltW | SltF | SltR |


grain size, sedimentary structures, trace fossils, etc.
paleocurrent direction
burrowing
Well
Mod
Poor
Sorting
megabreccia
bound stone
conglomerate
bld
cob
pebble
Gr
256
128
64
32
16
8.0
4.0
2.0
GS
vc
c
m
f
vf
sandstone
VC
C
M
F
VF
1mm
0.5
0.25
.125
PS
m-lean
m-rich
WS
MS
mud
silt
clay
thickness (m)
Contact
Location: North Waikiekie
Strat. Interval: CC1A to Waikiekie Beach MTD
Logged by: NC TA
Date(s): 1/18/13 Page 1 of 1
Notes
18
17
16
15
14
13
12
11
10
9
8
7
6
5
4
3
2
1
0
350
W
G
E
A.S.
W/E
S
Base of MTD; deformed, convoluted; wavy base
14 cm vfM-U sandstone; shell hash at bed top
17 cm vfM sandstone
20 cm vfM sandstone
3 cm siltstone
30 cm vfM-U sandstone; ARL in top 10 cm
10 cm siltstone; faint lamination
40 cm vfU sandstone; PPL to structureless
15 cm siltstone; sandstone injection, shell hash
shell hash
50 cm vfU sandstone; PPL with shell hash at base and top
15 cm siltstone
3 cm vfU sandstone; wavy
4 cm siltstone
36 cm vfU sandstone; horizontal lamination
6 cm siltstone
53 cm vfU sandstone; horizontal lamination; shell hash
15 cm siltstone
50 cm vfU sandstone; shell hash
30 cm graded sandstone; fL-vfM; concretions at bed top
22 cm volcaniclastic rich grading up to vfM sandstone
20 cm volcaniclastic rich grading up to vfM sandstone
19 cm volcaniclastic rich grading up to vfM sandstone
truncated laterally
12 cm ARL
3 cm vfU sandstone
13 cm siltstone; bioturbated base
12 cm siltstone; bioturbated base
2 cm vfM sandstone; bioturbated
20 cm siltstone; bioturbated
38 cm vfL-M sandstone; PPL
10 cm siltstone
11 cm vfM-U sandstone
8 cm siltstone
70 cm vfU sandstone; structureless
3 cm siltstone
90 cm vfU sandstone
15 cm siltstone
9 cm vfM-L; PPL to climbing ARL
SnF
1.37 m vfU sandstone;
Floating mud intraclasts
5 cm thick shell debris, ARL, mud intraclasts (not at bed base)
16 cm vfU-fL
5 cm siltstone; concretions, some sand injection
top 20 cm; floating mud intraclasts; mm to cm scale
50 cm vfU; faint horizontal lamination
2 cm interlamination; 6 cm siltstone; bioturbated
15 cm vfU-fL; mm scale floating mud intraclasts
17 cm vfU-fL; PPL
8cm siltstone grading up; vfL to siltstone; mm scale
mud intraclasts; 1 cm wavy interlaminations
93 cm fL grading to vfU; (60 cm floating mud intraclasts)
PPL and SnF
10 cm siltstone; bioturbated
2 cm gradational;mm scale mud intraclasts; mica rich cap
30 cm fL grading to vfU; floating mm scale mud intraclasts
SnF to faint PPL
13 cm siltstone; heavily bioturbated; concentrated mica rich
sandstone lenses (micas, mU grainsize, sand injection)
wavy to PPL; mm to cm mud intraclasts
heavily bioturbated sandstone; 95% quartz
SnF
1.6 m sandstone; fL grading to vfU
mud intraclasts; mm to cm scale; pinches laterally
3.7 m sandstone; massive
SnF; horizontal lamination
4 cm vfU; 2 cm volcaniclastic
green, red, purple, black lithics; qtz/plag
5cm volcaniclastic, grading up, welded, appears vesicular
18 cm clay rich; 8cm dark gray; 10 cm light gray ash
15-25 cm vfU-fL; quartz rich, mica and volcaniclastic grains
13-20 cm graded siltstone; 2 cm ARL
mm scale mud intraclasts; mica rich, horizontal lam., wavy
95 cm graded sandstone; fL grading to vfM; SnF, horizontal lam.
25 cm siltstone; slightly bioturbated
4 cm ARL
Massive sandstone; ~1-1.5 m exposed before sand moved in;
55 cm exposed with sand cover

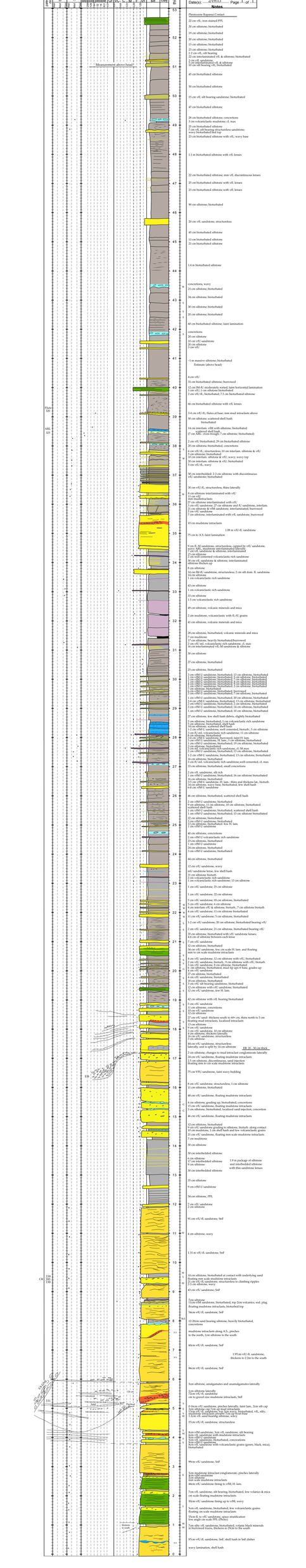

grain size, sedimentary structures, trace fossils, etc.
paleocurrent direction
burrowing
Well
Mod
Poor
Sorting
megabreccia
bound stone
conglomerate
bld
cob
pebble
Gr
sandstone
GS
PS
WS
MS
mud
silt
clay
VC
C
M
F
VF
thickness (m)
Contact
Location: NWK Fault Block
Strat. Interval: CC1A Axial
Logged by: NC TA
Date(s): 2/5/13 Page 1 of 1
Notes
Correlates to 12.65 mark on NWK Fault to MTD section
Debris flows had sand above mud matrix; PPL, roughly the same thickness as the debris flow. Most likely the same event.
15 cm sandy siltstone to siltstone
wavy bedding
100 cm vfU-fL max; PPL
6 cm shell debris in sandy siltstone matrix
112 cm debris flow; sandy siltstone matrix. shell debris; large fossils, not broken/fragmented; cm-5 cm mud intraclasts
10 cm siltstone
23 cm vfM-U; fines upward, moderate to well sorted
9 cm muddy matrix debris flow; volcanics, mud intraclasts; clast supported, shell debris
3 cm siltstone
26 cm vfM-fL max; fining upward; PPL, shell hash in lower 16 cm
29 cm mud matrix rich; volcanics; debris flow, poorly sorted; up to pebble size grains, shell debris, matrix supported
9 cm sandy siltstone
27 cm volcanic rich; sodium plag., blk mineral (unknown), quartz; fining up, PPL, mud intraclasts at base
3.5 cm mudstone; shell debris
6 cm vfM-U; moderate sorting
8 cm siltstone
7-20 cm vfM-U; wavy to PPL
15 cm siltstone cut by overlying sandstone
43 cm vfU-fU max; shell debris, PPL; fining to vfM-vfU max
42 cm very mud matrix rich; shell debris rich, volcanic rich; poorly sorted debris flow; matrix supported
1 cm volcaniclastic rich; vfU-fL; cU max; 7 cm vfU-fL; PPL
3 cm vfU-fL; PPL/lamination; shell hash abundant in bed top
16 cm vfM-U; fining up to mud rich with few vfL sand grains
6 cm PPL
21 cm mudstone
8 cm vfM; PPL; moderate to well sorted
7 cm vfU-fL; thins to 0 cm (pinches out); volcanics; vcU max; mud intraclasts, shell debris; poorly sorted
32 cm siltstone; thins to 25 cm (2 meters to the north)
7 cm vfM-U; PPL, dense shell hash layer; cm scale mud intraclasts
5 cm mudstone; pinches laterally (cut by shell debris)
75 cm fL sandstone
10 cm mudstone
6-9 cm vfU sandstone
E
W
E/W

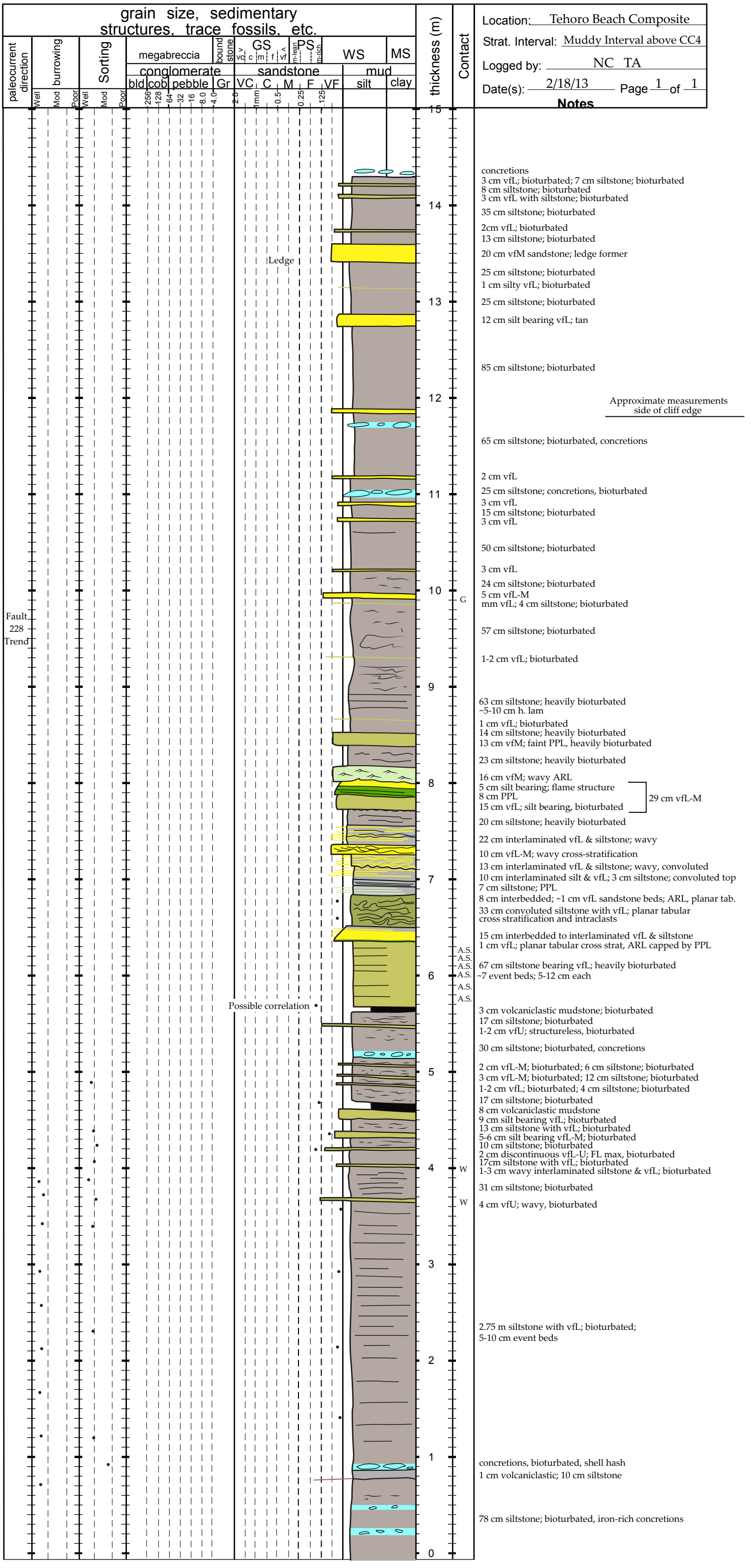
grain size, sedimentary structures, trace fossils, etc.
paleocurrent direction
burrowing
Well
Mod
Poor
Sorting
megabreccia
bound stone
GS
PS
WS
MS
conglomerate
sandstone
mud
bld
cob
pebble
Gr
VC
C
M
F
VF
silt
clay
thickness (m)
Contact
Location: North Waikiekie North
Strat. Interval: CC1A Margin to Overbank
Logged by: NC TA
Date(s): 2/6/13
Page 1 of 1
Notes
Volcanic interbedded (1 cm each)
1.1m siltstone
~1 cm sandstone beds interbedded with siltstone
Best estimate using jacob staff (cliff face)
8 cm sandstone; 3 cm interlaminated (sand/silt)
1 cm siltstone
51 cm vfU sandstone; fines to vfM
20 cm vfM; wavy bedding
Begin EB (thins laterally)
5 cm siltstone; thins to north; mudstone intraclasts
top 30 cm of convoluted interval; burrowed/bioturbated
33 cm vfM-U; convoluted, thin wavy bedding
5-10 cm vfM-U; convoluted
Convoluted bedding;
vfM sandstone; 1 cm fL-M max
Begin EB
15 cm; 2 cm vfL-M; 13 cm vfL; wavy to ARL
6 cm vfL-M; wavy PPL; 12 cm vfL wavy to ARL
9 cm vfM-U; PPL
9 cm vfU-FL; faint wavy
16 cm vfL-U; faint wavy
2 cm vfM-U
33cm fL; fU max; PPL to wavy SnF
34 cm vfU-fL; convoluted bedding to SnF @base
70 cm vfM-U; SnF to convoluted wavy bedding
85 cm vfU-fL fining to vfL-M; SnF
Begin EB; scours into underlying bed
60 cm vfL-M; SnF, convoluted
60 cm vfL-M
10 cm wavy to ARL
63 cm vfM-U; climbing ripples to wavy laterally
10 cm wavy to ARL
1.37 m vfM-U
64 cm vfM-U; climbing ripples
17 cm vfM-U; faint PPL/wavy
73 cm vfL-M; PPL to wavy/ARL
67 cm vfL-M; PPL to ARL, possible climbing ripples
4 cm vfM; wavy to PPL
43 cm vfL-M; PPL @ base, wavy to climbing ripple ARL
top 20 cm vfM-U; PPL
120 cm vfU-FL fining to vfM-U; SnF
fL-fM @ Base
37 cm SnF
SnF @ base; vfU-fL
70 cm vfU-fL fining to vfM-U; SnF
80 cm vfM-U; faint PPL
Concretions
85 cm vfU-fL; SnF
75 cm vfU-fL, fU max; SnF, concretions
85 cm vfM-U; fL max; PPL to SnF
13 cm vfM-U; faint PPL to wavy
6 cm vfU-fL wavy; 3 cm vfU-fL
9 cm vfU-fL wavy, 4 cm vfU-fL
20 cm vfU; fL max
wavy SnF at base to wavy PPL/PPL
27 cm vfU; fU max; wavy bedding
39 cm vfM-U; fU max; wavy top
wavy to SnF
78 cm vfU-fL; SnF to faint PPL
-concretions
vfU-fL- localized cm scale floating mud intraclasts
30 cm vfU; fU max; SnF (Jaked Laterally)
31 cm vfU; faint PPL; top vfM-vfU, more black minerals
62 cm vfU-fM; SnF to PPL
65cm vfM-vfU; SnF
90 cm vfU-fL; PPL; fining to vfU at top
Concretions
22 cm vfU-fL; PPL
20 cm vfU-fL; SnF
top 6 cm rich in micaceous minerals
74 cm vfU-fL; SnF
16 cm vfU-fL; wavy to SnF
60 cm vfU-fM; PPL
wavy/PPL
80 cm vfU-fM with mm scale floating
mud intraclasts throughout
1 cm floating mm scale mud intraclasts
1 cm floating mm scale mud intraclasts; 4 cm vfU-fL
17 cm vfU-fL; SnF to PPL, wavy
10 cm mud intraclast conglomerate; matrix supported with shell hash incorporated
55 cm vfU-fL; PPL; shell hash concentrated at bed top and scattered throughout
~20 m; MTD below; siltstone to vfL sandy siltstone interbedded with volcanics in MTD (sodium plag.)
-rafted sand blocks
S
W
G/W
A.S.
G
327
326
331
326
323
329
327
329
339
325
327

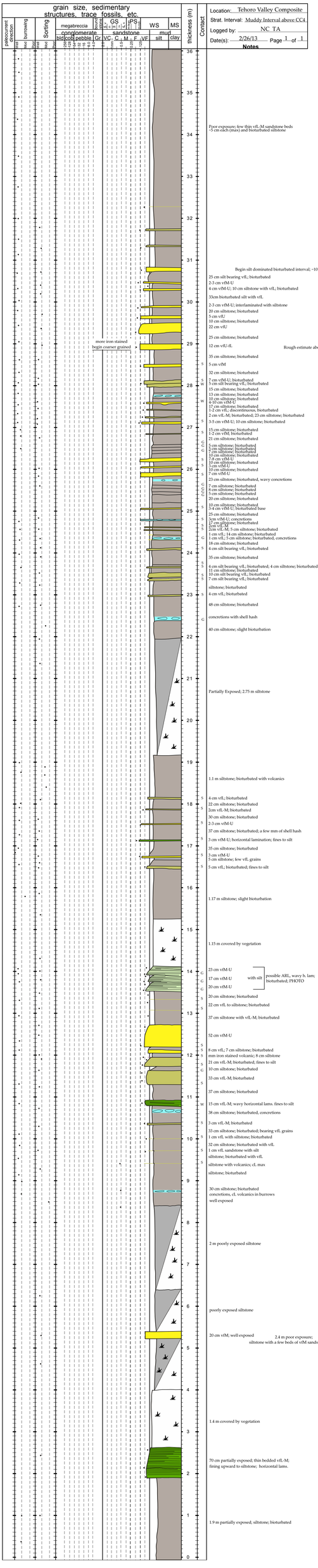

grain size, sedimentary structures, trace fossils, etc.
paleocurrent direction
burrowing
Well
Mod
Poor
Sorting
megabreccia
boundstone
conglomerate
bld
cob
pebble
Gr
sandstone
VC
C
M
F
VF
GS
PS
m-lean
m-rich
WS
MS
mud
silt
clay
thickness (m)
Contact
Location: South Waikiekie Axis
Strat. Interval: CC2 Axial
Logged by: NC TA
Date(s): 1/17/13 Page 1 of 1
Notes
5.5 m to A.S.
10% cm to decimeter scale mud intraclasts; floating
Massive sandstone; 3.5 m
2% cm scale floating mud intraclasts
massive sandstone (6+ m) cut by conglomerate
Changes laterally within composite body
sandstone
15-20 cm mud intraclasts
3.2 m sandstone
4.2 m to amalgamation surface
Massive sandstone; below composite
10-50 cm mud intraclasts; cm to decimeter scale; 10% intraclasts; grades up to smaller/fewer clasts; pinches north and south
Massive sandstone; thins and thickens latereally; ~0.75 m thick to the north; 3+ m thick to the south
Amalgamation surface; south in ~6 m thick sandstone
1.25 m mud intraclast conglomerate; pinches to south; massive sandstone
1.25 m sandstone; SnF to structureless; truncated by mud intraclast conglomerate above; thins north; thickens south
20 cm sandstone; horizontal lamination
18 cm mud intraclast conglomerate; discontinuous
52 cm sandstone; 3-8 cm intervals with PPL lamination
25 cm sandstone; mud intraclasts and concretions
50 cm sandstone; vfU-fL estimate
Amalgamation surface
20 cm sandstone; vfU-fL estimate
30 cm mud intraclast conglomerate
35 cm sandstone; vfU-fL estimate; more calcareous
15 cm mud intraclast conglomerate
1 m sandstone; vfU-fL estimate
25 cm mud intraclast conglomerate
60 cm mudstone; drape over MTD
MTD @ Waikiekie Stream

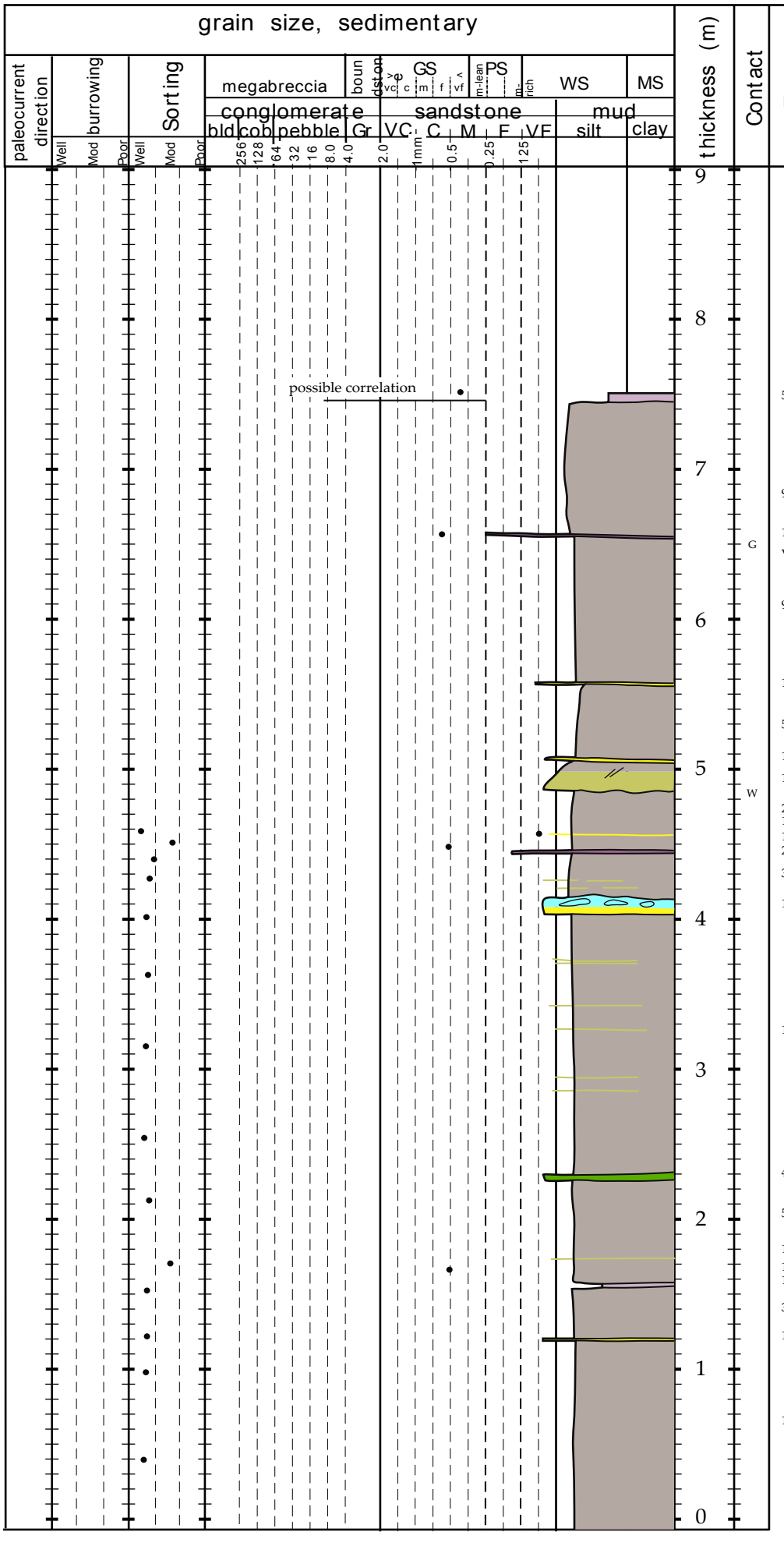
Location: SWK South Composite
Strat. Interval: Outside CA to CA2 to the south
Logged by: NC, TA
Date(s): 2/19/13 Page 1 of 1

Notes:




grain size, sedimentary structures, trace fossils, etc.
paleocurrent direction
burrowing
Well
Mod
Poor
Sorting
megabreccia
bound stone
conglomerate
bld
cob
pebble
Gr
GS
sandstone
VC
C
M
F
VF
PS
m-lean
m-rich
WS
MS
mud
silt
clay
thickness (m)
Contact
Location: Tehoro Beach Composite
Strat. Interval: Muddy Interval above CC4
Logged by: NC TA
Date(s): 2/18/13 Page 1 of 1
Notes
Ledge
Fault
228
Trend
Possible correlation
Approximate measurements
side of cliff edge
concretions
3 cm vfL; bioturbated; 7 cm siltstone; bioturbated
8 cm siltstone; bioturbated
3 cm vfL with siltstone; bioturbated
35 cm siltstone; bioturbated
2cm vfL; bioturbated
13 cm siltstone; bioturbated
20 cm vfM sandstone; ledge former
25 cm siltstone; bioturbated
1 cm silty vfL; bioturbated
25 cm siltstone; bioturbated
12 cm silt bearing vfL; tan
85 cm siltstone; bioturbated
65 cm siltstone; bioturbated, concretions
2 cm vfL
25 cm siltstone; concretions, bioturbated
3 cm vfL
15 cm siltstone; bioturbated
3 cm vfL
50 cm siltstone; bioturbated
3 cm vfL
24 cm siltstone; bioturbated
5 cm vfL-M
mm vfL; 4 cm siltstone; bioturbated
57 cm siltstone; bioturbated
1-2 cm vfL; bioturbated
63 cm siltstone; heavily bioturbated
~5-10 cm h. lam
1 cm vfL; bioturbated
14 cm siltstone; heavily bioturbated
13 cm vfM; faint PPL, heavily bioturbated
23 cm siltstone; heavily bioturbated
16 cm vfM; wavy ARL
5 cm silt bearing; flame structure
8 cm PPL
15 cm vfL; silt bearing, bioturbated
29 cm vfL-M
20 cm siltstone; heavily bioturbated
22 cm interlaminated vfL & siltstone; wavy
10 cm vfL-M; wavy cross-stratification
13 cm interlaminated vfL & siltstone; wavy, convoluted
10 cm interlaminated silt & vfL; 3 cm siltstone; convoluted top
7 cm siltstone; PPL
8 cm interbedded; ~1 cm vfL sandstone beds; ARL, planar tab.
33 cm convoluted siltstone with vfL; planar tabular cross stratification and intraclasts
15 cm interbedded to interlaminated vfL & siltstone
1 cm vfL; planar tabular cross strat, ARL capped by PPL
67 cm siltstone bearing vfL; heavily bioturbated
~7 event beds; 5-12 cm each
3 cm volcaniclastic mudstone; bioturbated
17 cm siltstone; bioturbated
1-2 cm vfU; structureless, bioturbated
30 cm siltstone; bioturbated, concretions
2 cm vfL-M; bioturbated; 6 cm siltstone; bioturbated
3 cm vfL-M; bioturbated; 12 cm siltstone; bioturbated
1-2 cm vfL; bioturbated; 4 cm siltstone; bioturbated
17 cm siltstone; bioturbated
8 cm volcaniclastic mudstone
9 cm silt bearing vfL; bioturbated
13 cm siltstone with vfL; bioturbated
5-6 cm silt bearing vfL-M; bioturbated
10 cm siltstone; bioturbated
2 cm discontinuous vfL-U; FL max, bioturbated
17cm siltstone with vfL; bioturbated
1-3 cm wavy interlaminated siltstone & vfL; bioturbated
31 cm siltstone; bioturbated
4 cm vfU; wavy, bioturbated
2.75 m siltstone with vfL; bioturbated;
5-10 cm event beds
concretions, bioturbated, shell hash
1 cm volcaniclastic; 10 cm siltstone
78 cm siltstone; bioturbated, iron-rich concretions
G
A.S.
W
W


grain size, sedimentary structures, trace fossils, etc.
paleocurrent direction
abd burrowing
Sorting
megabreccia
conglomerate
sandstone
mud
bldr cob peb gran vc c m f vf
GS
PS
WS
MS
silt
clay
thickness (m)
Contact
Location: Tehoro Valley Composite
Strat. Interval: Muddy Interval above CC4
Logged by: NC TA
Date(s): 2/26/13 Page 1 of 1
Notes
Poor exposure; few thin vfL-M sandstone beds ~5 cm each (max) and bioturbated siltstone
Begin silt dominated bioturbated interval; ~10 m
25 cm silt bearing vfL; bioturbated
2-3 cm vfM-U
4 cm vfM-U; 10 cm siltstone with vfL; bioturbated
33cm bioturbated silt with vfL
2-3 cm vfM-U; interlaminated with siltstone
20 cm siltstone; bioturbated
5 cm vfU
10 cm siltstone; bioturbated
22 cm vfU
25 cm siltstone; bioturbated
more iron stained
begin coarser grained
12 cm vfU-fL
Rough estimate above
35 cm siltstone; bioturbated
5 cm vfM
32 cm siltstone; bioturbated
7 cm vfM-U; bioturbated
5 cm silt bearing vfL; bioturbated
15 cm siltstone; bioturbated
13 cm siltstone; bioturbated
10 cm siltstone; bioturbated
4-10 cm vfM-U
17 cm siltstone; bioturbated
1-2 cm vfL; discontinuous, bioturbated
2 cm vfL-M; bioturbated; 23 cm siltstone; bioturbated
3-5 cm vfM-U; 10 cm siltstone; bioturbated
15 cm siltstone; bioturbated
1-2 cm vfM; bioturbated
21 cm siltstone; bioturbated
3 cm siltstone; bioturbated
2 cm siltstone; bioturbated
2 cm siltstone; bioturbated
10 cm siltstone; bioturbated
7-8 cm vfM-U
10 cm siltstone; bioturbated
7 cm vfM-U
10 cm siltstone; bioturbated
7 cm vfM-U
23 cm siltstone; bioturbated, wavy concretions
7 cm siltstone; bioturbated
8 cm siltstone; bioturbated
5 cm siltstone; bioturbated
20 cm siltstone; bioturbated
10 cm siltstone; bioturbated
3-4 cm vfM-U; bioturbated base
25 cm siltstone; bioturbated
3cm vfM-U; concretions
17 cm siltstone; bioturbated
2cm vfL-M
2cm vfL-M; 5 cm siltstone; bioturbated
1 cm vfL; 14 cm siltstone; bioturbated
1 cm vfL; 5 cm siltstone; bioturbated, concretions
18 cm siltstone; bioturbated
4 cm silt bearing vfL; bioturbated
35 cm siltstone; bioturbated
4 cm silt bearing vfL; bioturbated; 4 cm siltstone; bioturbated
11 cm siltstone; bioturbated
10 cm silt bearing vfL; bioturbated
7 cm silt bearing vfL; bioturbated
siltstone; bioturbated
4 cm vfL; bioturbated
48 cm siltstone; bioturbated
concretions with shell hash
40 cm siltstone; slight bioturbation
Partially Exposed; 2.75 m siltstone
1.1 m siltstone; bioturbated with volcanics
4 cm vfL; bioturbated
22 cm siltstone; bioturbated
2cm vfL-M; bioturbated
30 cm siltstone; bioturbated
2-3 cm vfM-U
37 cm siltstone; bioturbated; a few mm of shell hash
3 cm vfM-U; horizontal lamination; fines to silt
35 cm siltstone; bioturbated
3 cm vfM-U
5 cm siltstone; few vfL grains
5 cm vfL; bioturbated; fines to silt
1.17 m siltstone; slight bioturbation
1.15 m covered by vegetation
23 cm vfM-U
17 cm vfM-U
with silt
possible ARL, wavy h. lam; bioturbated; PHOTO
20 cm vfM-U
20 cm siltstone; bioturbated
22 cm vfL to siltstone; bioturbated
37 cm siltstone with vfL-M; bioturbated
52 cm vfM-U
8 cm vfL; 7 cm siltstone; bioturbated
mm iron stained volcanic; 8 cm siltstone
21 cm vfL-M; bioturbated; fines to silt
10 cm siltstone; bioturbated
33 cm vfL-M; bioturbated
37 cm siltstone; bioturbated
15 cm vfL-M; wavy horizontal lams. fines to silt
38 cm siltstone; bioturbated, concretions
3 cm vfL-M; bioturbated
33 cm siltstone; bioturbated; bearing vfL grains
1 cm vfL with siltstone; bioturbated
32 cm siltstone; bioturbated with vfL
1 cm vfL sandstone with silt
siltstone; bioturbated with vfL
siltstone with volcanics; cL max
siltstone; bioturbated
30 cm siltstone; bioturbated
concretions, cL volcanics in burrows
well exposed
2 m poorly exposed siltstone
poorly exposed siltstone
20 cm vfM; well exposed
2.4 m poor exposure; siltstone with a few beds of vfM sandstone
1.4 m covered by vegetation
70 cm partially exposed; thin bedded vfL-M; fining upward to siltstone; horizontal lams.
1.9 m partially exposed; siltstone; bioturbated



Location: Tehoro Valley Overlap

Strat. Interval: Muddy Interval above CC4

Logged by: NC TA

Date(s): 2/19/13 Page 1 of 1

Notes

5 cm volcaniclastic mudstone

90 cm siltstone; bioturbated

1-2 cm mL-cL sandstone; volcaniclastic bearing volcaniclastic mudstone grading to volcaniclastic sandstone

98 cm siltstone; bioturbated

1-2 cm vfL-M sandstone

50 cm siltstone; bioturbated

1-2 cm vfL sandstone

17 cm vfL sandstone; few volcanics; burrowed, fines to siltstone

28 cm siltstone; bioturbated
1 cm vfL sandstone
10 cm siltstone; bioturbated
2-3 cm mU-cL; volcaniclastic

30 cm siltstone; bioturbated, lenses of vfL sandstone

10 cm vfL sandstone; silt bearing, well cemented, concretions

1.72 m siltstone; bioturbated

4-5 cm vfL-M sandstone; horizontal lamination

55 cm siltstone; bioturbated

1-2 cm vfL sandstone; bioturbated, wavy horizontal lams
13 cm siltstone; bioturbated
1-2 cm volcaniclastic mudstone; cL max

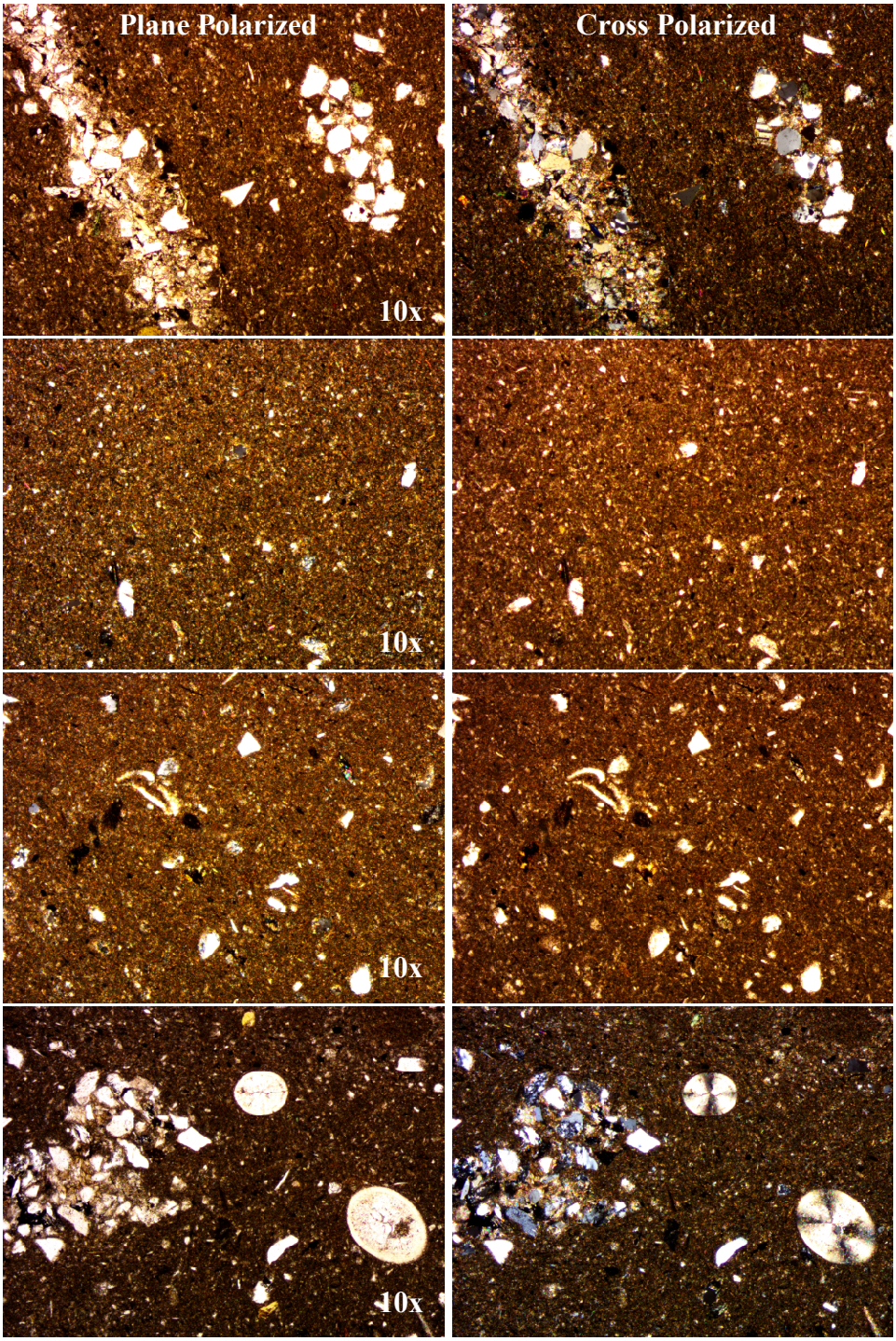
34 cm siltstone; bioturbated

1-2 cm vfL-M sandstone

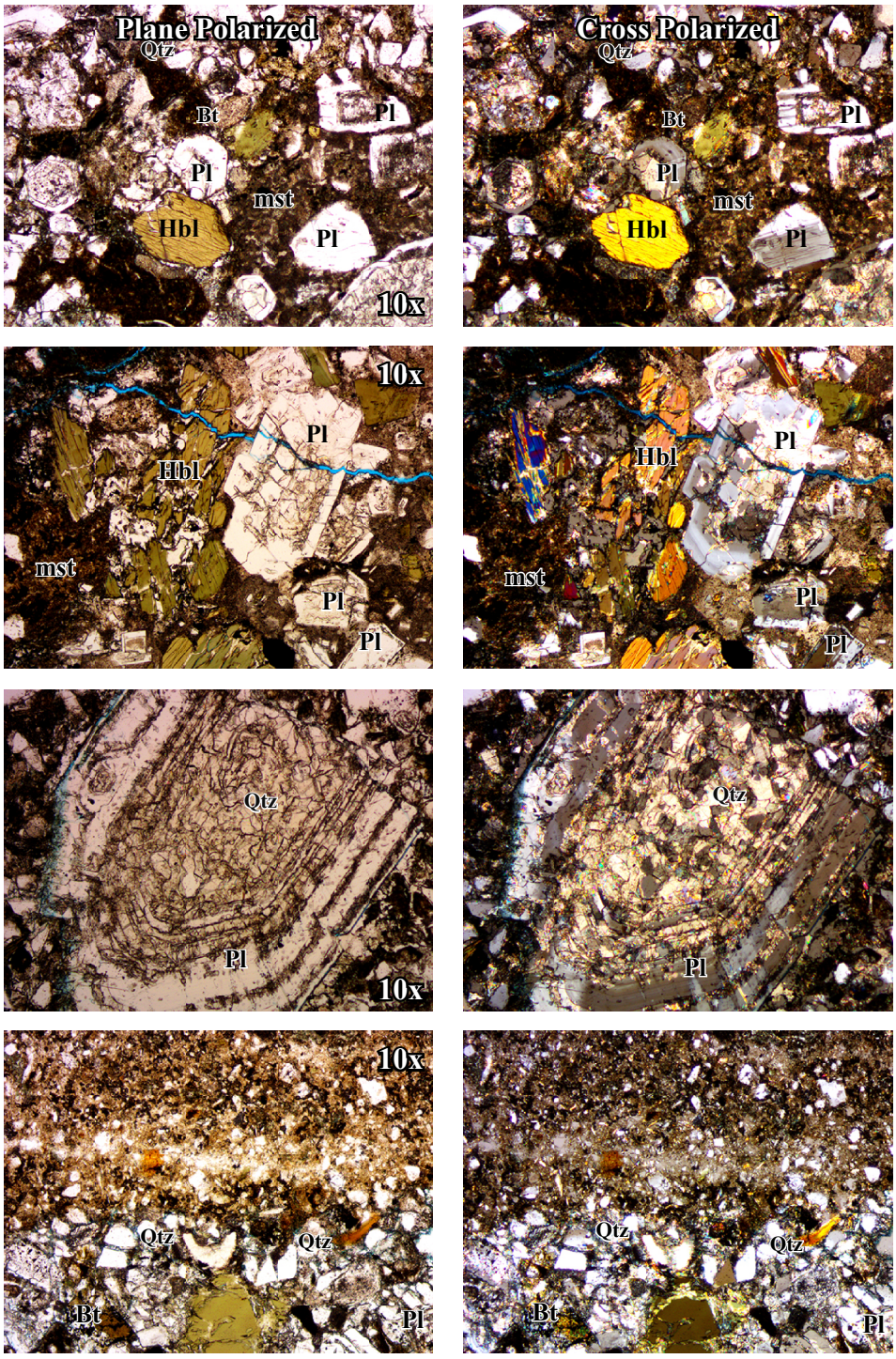
1.2 m siltstone; bioturbated

APPENDIX B

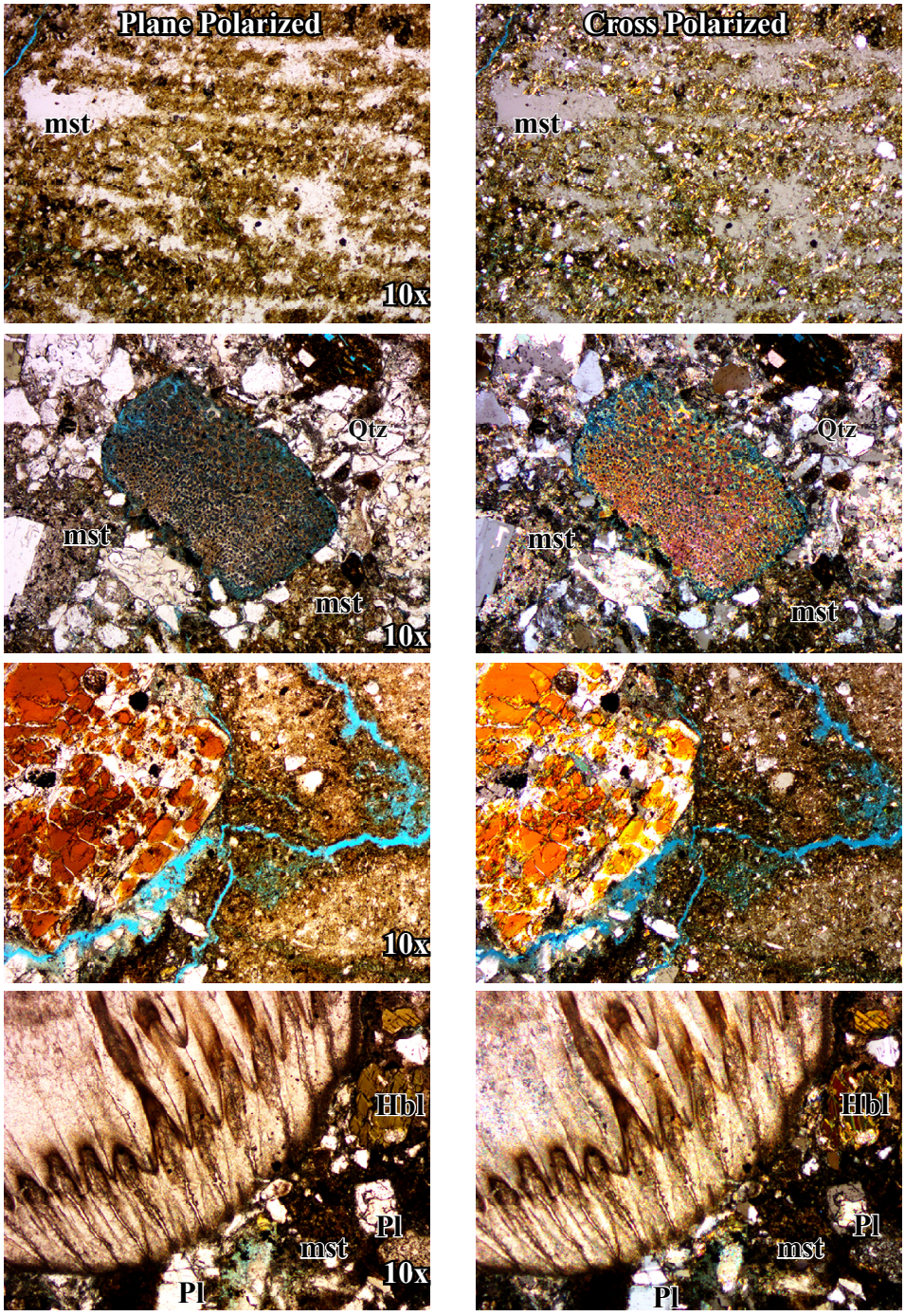
THIN SECTION ANALYSIS



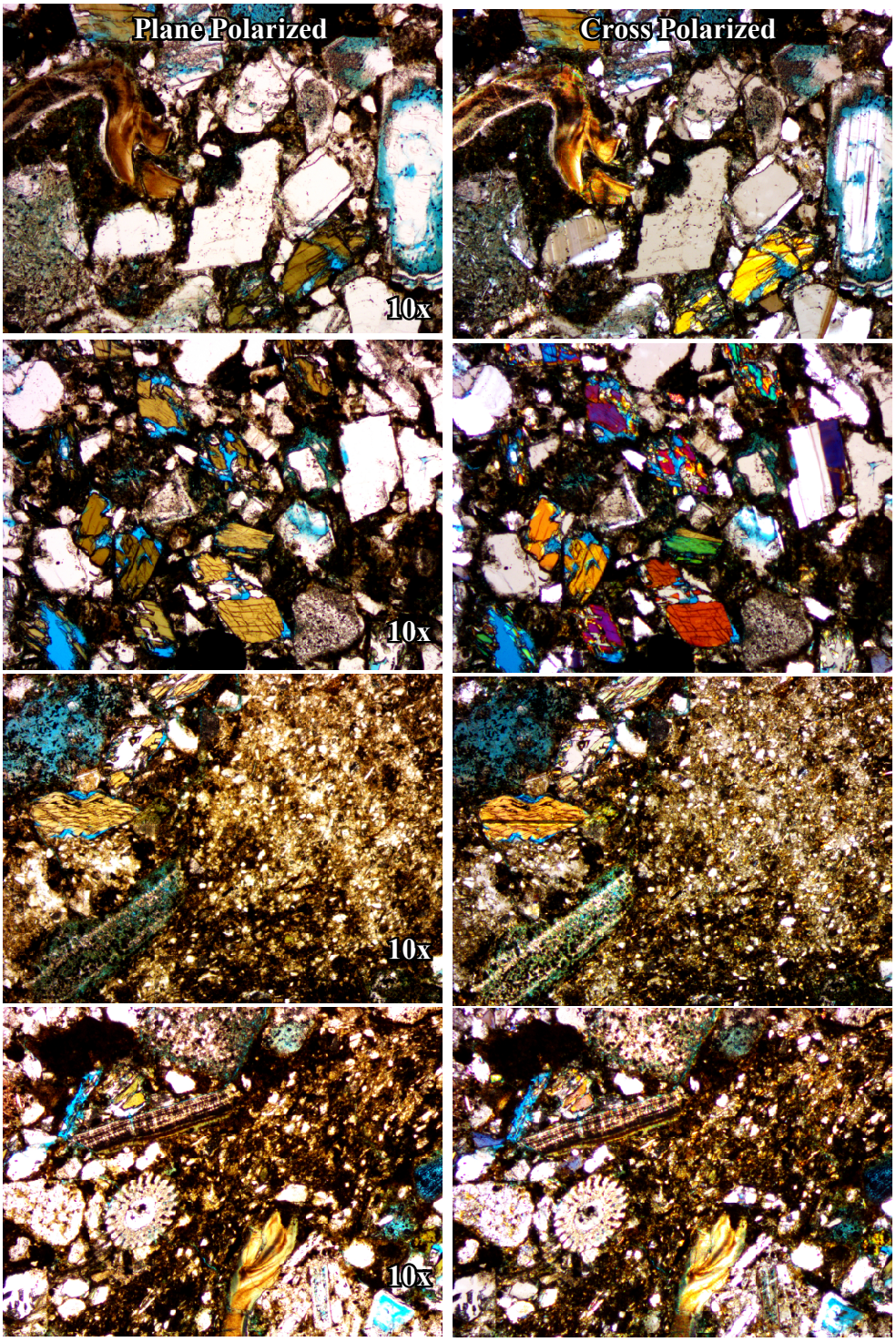
Thin Section sample 1. Sample 1 was collected from volcaniclastic siltstone at Locked Gate. It shows silt sized grains that dominate within a mudstone matrix. Small pockets of coarser grained volcaniclastic phenocrysts and fossils are also present. Phenocrysts consist primarily of quartz and plagioclase, although smaller amounts of biotite, hornblende, and oxides are present.



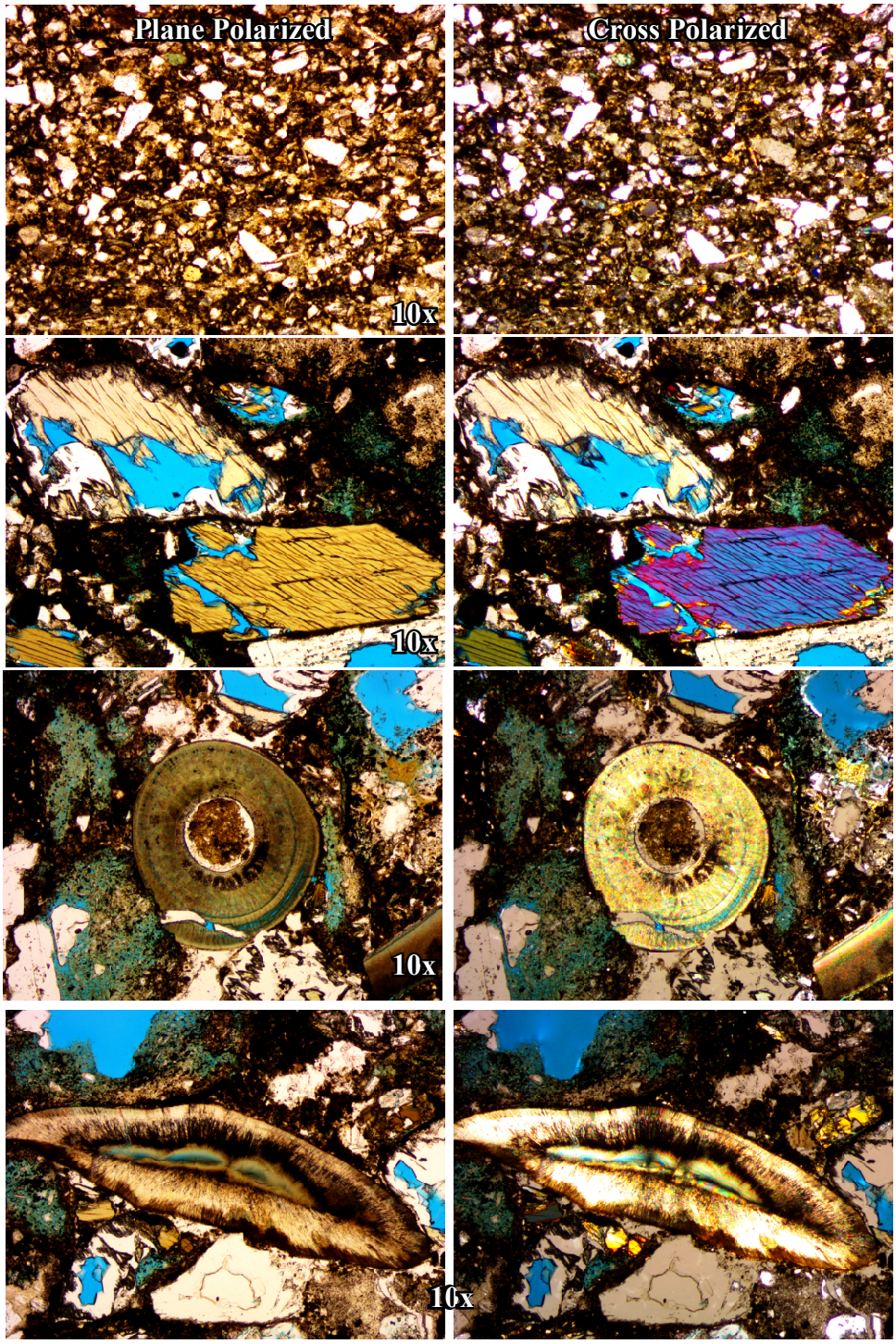
Thin Section sample 2. Sample 2 was collected within a bioclastic and volcaniclastic rich interval at Locked Gate within the upper composite of CC1B. It shows a wide range of grain size, mineralogy, and bioclastic input. Grain size varies from mudstone (mst) up to coarse-grained, and the presence of large fossils is common. Volcaniclastic phenocrysts consist of plagioclase (Pl), hornblende (Hbl), and oxides, as well as low percentages of clino- and orthopyroxene. Biotite mica (Bt) and quartz (Qtz) are also common throughout.



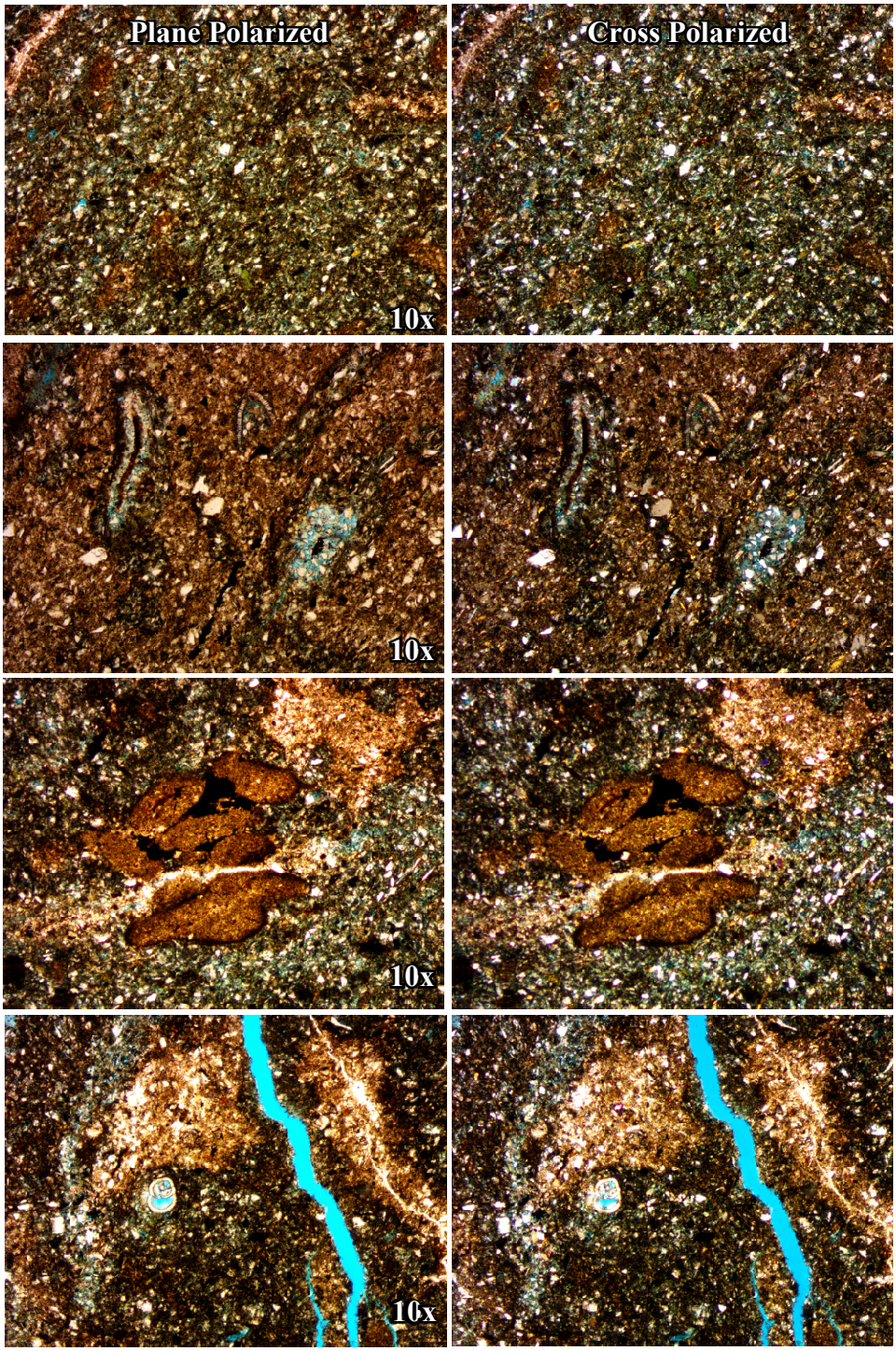
Thin Section sample 2 (continued). Sample 2 was collected within a bioclastic and volcaniclastic rich interval at Locked Gate within the upper composite of CC1B. It shows a wide range of grain size, mineralogy, and bioclastic input. Grain size varies from mudstone (mst) up to coarse-grained, and the presence of large fossils is common. Volcaniclastic phenocrysts consist of plagioclase (Pl), hornblende (Hbl), and oxides, as well as low percentages of clino- and orthopyroxene. Biotite mica (Bt) and quartz (Qtz) are also common throughout.



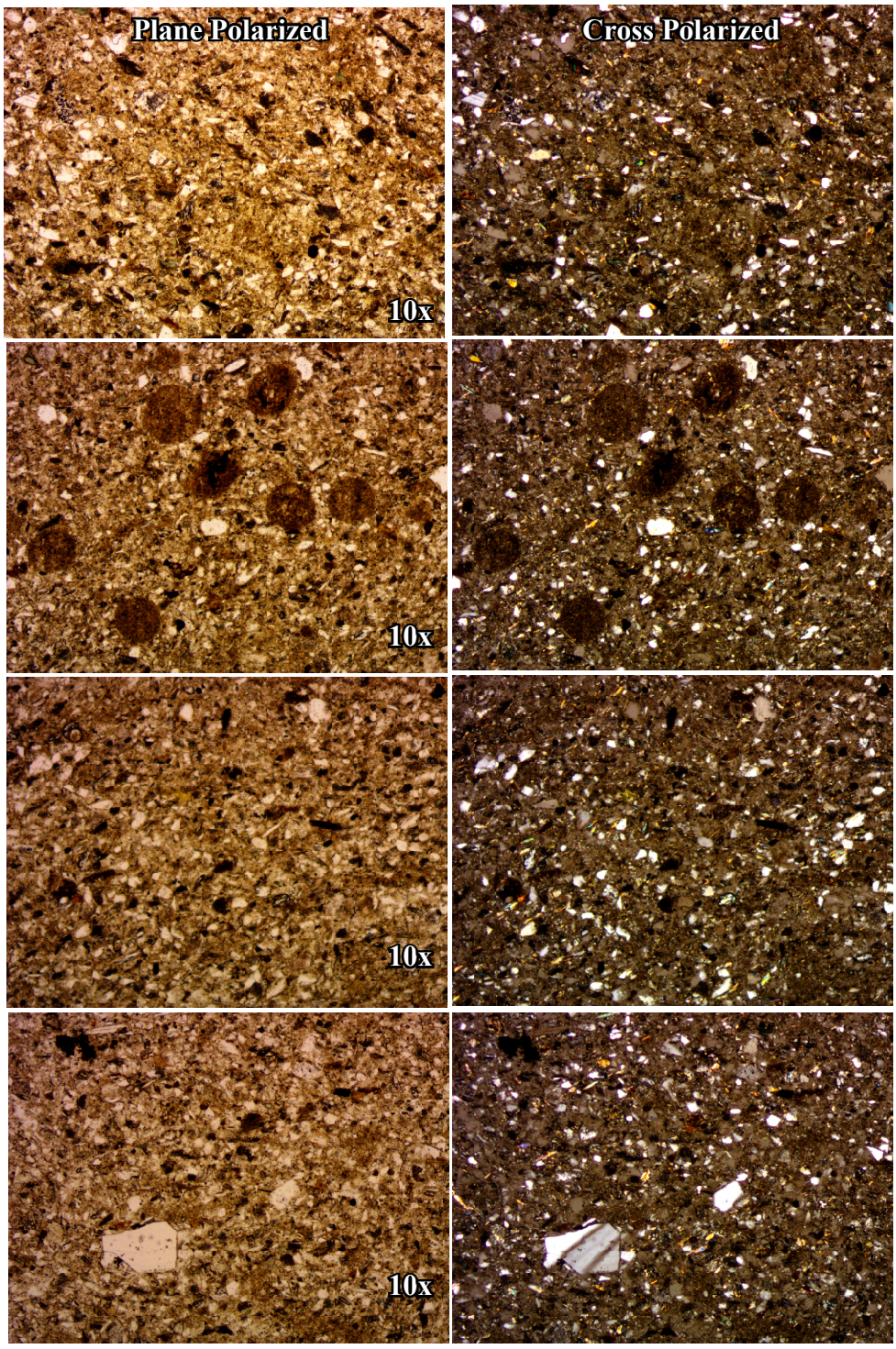
Thin Section sample 3. Sample 3 was collected north of Waikiekie Stream in a poorly-sorted mudstone-rich bed within CC1B. Grain size varies from mudstone up to fine- to medium-grained sandstone and coarse-grained volcaniclastic phenocrysts. Large fossils are common. Volcaniclastic phenocrysts consists of plagioclase, hornblende, and oxides, as well as low percentages of clino- and orthopyroxene.



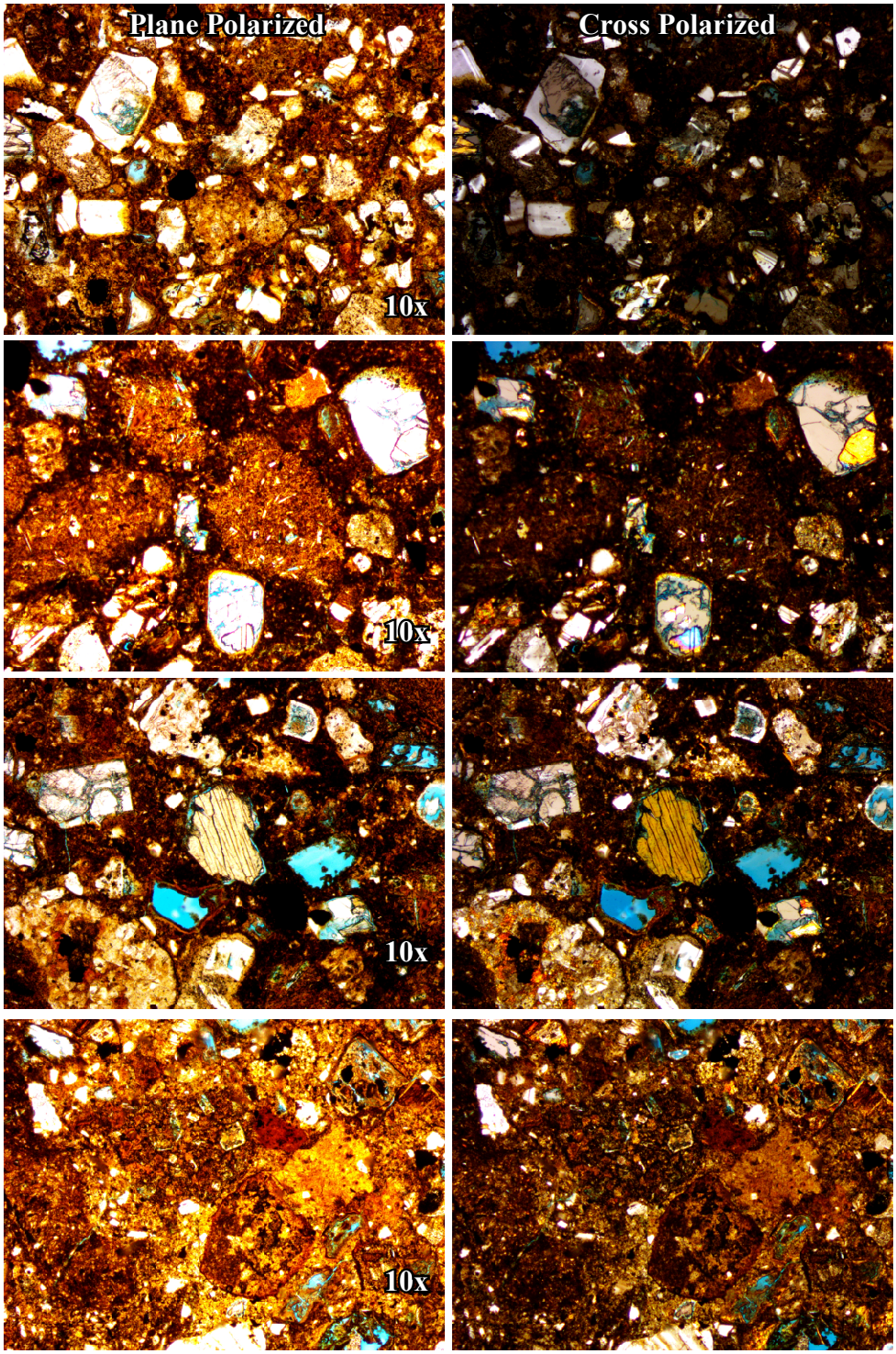
Thin Section sample 4. Sample 4 was collected north of Waikiekie Stream in a muddy sandstone within CC1B. Less mudstone is seen within this sample compared to sample 3. Grain size varies from fine-grained sandstone to very coarse-grained volcaniclastic phenocrysts. Large fossils are also present within this sample. Volcaniclastic phenocrysts consists of plagioclase, hornblende, and oxides, as well as low percentages of clino- and orthopyroxene.



Thin Section sample 5. Sample 5 was collected south of Waikiekie Stream in a siltstone dominated volcaniclastic mudstone. Silt size grains dominate within a mudstone matrix. Sharp and angular volcaniclastic silt size grains are inferred to represent volcaniclastic ash. Pockets of very fine-grained volcaniclastic phenocrysts and small fossils are also present.



Thin Section sample 6. Sample 6 was collected south of Waikiekie Stream within a siltstone bearing volcaniclastic sandstone with mudstone-clasts. The sample is poorly-sorted with grain size from mudstone up to fine- to medium-grained quartz and volcaniclastic phenocrysts. Volcaniclastic phenocrysts are angular to sharp, and quartz is sub-angular. Millimeter-scale mudstone-clasts that are well rounded show little to no shearing.



Thin Section sample 7. Sample 7 was collected below CC1B at Tutapuha Stream in an organic bearing volcaniclastic mudstone. Within the outcrop, this sample had a fully artic-ulated very small leaf fossil preserved. The sample is poorly-sorted with grain size from mudstone up to coarse-grained volcaniclastic phenocrysts. The sample shows high amounts of alteration, likely reflected by the precipitation of iron between grains.